Università degli Studi di Palermo
Dottorato di Ricerca in Scienze Chimiche
Dipartimento di Fisica e Chimica
S.S.D. - CHIM/06

Université de Namur
Doctorat en Sciences
Faculté des Sciences
Département de Chimie

ORGANIC-INORGANIC HYBRID CATALYSTS BASED ON IMIDAZOLIUM AND THIAZOLIUM SALTS

PhD STUDENT
LUCIA ANNA BIVONA

COORDINATOR
Prof. PAOLO LO MEO

TUTOR
Prof. MICHELANGELO GRUTTADAURIA

TUTOR
Prof. CARMELA APRILE

CICLO XXVI
2016

Thesis submitted for the achievement of the Philosophical Degree (PhD) in Chemistry

JURY

Prof. Michelangelo Gruttadauria (Unipa)

Prof. Antonino Martorana (Unipa, President)

Prof. Carmela Aprile (UNamur)

Dr. Luca Fusaro (UNamur, President)

Dr. Valeria La Parola (CNR, Palerme)

Try not to become a man of success,
but rather try to become a man of value.
(A. Einstein)

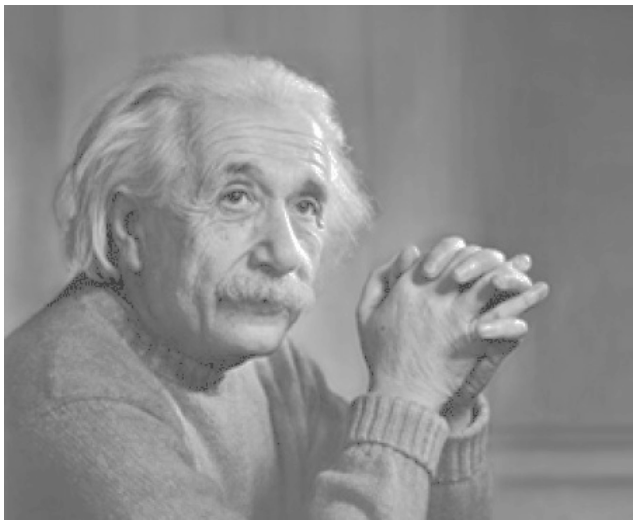

Acknowledgements

During the last three years I spent my life in two different countries, I met a lot of people that come from several parts of the Europe (and of the world) and before starting with the issue itself, I have the pleasure to thank everyone that I met since the beginning of my PhD thesis.

First of all I would like to express my sincere gratitude for my promoter at the University of Palermo, *Prof. Michelangelo Gruttadauria,* for the years spent together, he gave me the possibility, under his supervision, to develop some research projects. Thank you for helping me and for having always given the opportunity to express myself in the projects we developed.

I am sincerely grateful to my promoter at the University of Namur, *Prof. Carmela Aprile*, thank you for all the discussions (also during the lunch time!), thank you for infusing me enthusiasm, curiosity and criticism for chemistry. Thank you for always believing in me. Together with *Prof. Gruttadauria*, you taught me all the fundamental qualities to become a good researcher.

A special thank goes to my "comité d'accompagnement": *Prof. Davide Bonifazi*, *Prof. Bao-Lian Su* and *Dr. Leonarda Francesca Liotta*, for helping me during these years.

Many thanks go to *Dr. Francesco Giacalone*, for all the scientific (and not!) discussions. Thank you for the time that you invested in helping me, during which I adsorbed all of the passion for science.

Thanks to the group of Prof. Michelangelo Gruttadauria, in particular my PhD colleagues *Vincenzo* and *Hazi, Carla, Anna* and *Nino*, who shared with me this beautiful experience.

I am also grateful to *Prof. Giuseppe Lazzara* for the TGA experiments, to *Prof. Delia Chillura* for IR analyses, and to *Dr. Marco Cascino* for all the NMR analyses.

A special thank goes to *Dr. Mireia Buaki-Sogó* (Mi postdoc!) with whom I shared my experience in Namur. You are a very hard working person and it was great to collaborate with you. I will never forget all of the moments shared with you, in the lab and out of the lab! Thanks Miramiré! I wish you all of the best for your career.

Numerous thanks go to all of the members of CMA laboratory, first *Xavier,* then *Adrien*, *Alvise, Nicolas, Olivia, Farah*, my master students *François* (Life is for you!) and *Ornella.* Thank to my second favorite postdoc *Dr. Esther Carbonell-Llopis,* who shared with me "Lucia's Lab", thank you for your help when I was sick and for all the tortilla de patatas! Thanks also to CMI laboratory, especially for introducing me to many "Belgian" habits.

I am grateful to all of the members of the UNamur, in particular I would like to acknowledge *Guy Daelen* for NMR experiments, *Bernadette Norberg* for solving X-Ray spectra, *Corry Charlier* for all of the time spent to teach me the electronic microscopy, and finally *Pierre Louette* for all of the patience devoted to explain me the XPS spectroscopy.
I would like to thank *Dr. Luca Fusaro* for the many hours spent with me, with whom I shared interminable and innumerable discussions (still open!) on our projects and perspectives.

Many thanks go to all of the past and present members of the COMS, especially *Valentina* (thank you for all!), *Federica, Laura, Rosaria, Andrea, Rodolfo, Pietro, Lu, Jhonny, Florent, Davide, Francesco, Maria* (mi *Hermana*!), *Dario* and *Hamid.* Thanks to *Thanh Vy* for her infusion healing!

Thanks to the people that shared with me my "Belgium experience" since the beginning: *Silvia, Francesco, Giovanni, Nes*, *Irina, George, Marta* and the spanish people*,* my friends that come to visit me during this special adventure: *Giulia* (two times!), *Mariangela, Domenico, Maria Antonietta*, *Elisa, Piero* and *Salvatore*. Countless thanks to my friends, cousins and collegues that supported me also from far (*Annalisa*, *Dorella*, *Noemi*, *Angela*, *Carla, Rosanna,..*). Thanks *Virginia* for sharing the room with me!

Gauthier, thank you for always being there… no words can describe the gratitude and love for you. Thank you for who you are!

Finally, a special thank goes to my parents, thank you for your absolute and unconditional love and support. Thank you mum for coming in Belgium when I had the chickenpox! From near and far you gave me strength and energy, you always believed in me and always ready to help me, without asking anything back. This thesis is dedicated to you.

List of abbreviations

AAS	Atomic absorption spectroscopy
AIBN	2,2′-Azobis(2-methylpropionitrile)
Anal.	Combustion elemental analysis
BE	Binding energy
BET	Brunauer-Emmett-Teller
BJH	Barret, Joyner and Halanda
CNTs	Carbon nanotubes
Conv.	Conversion
CVD	Chemical vapor deposition
DLS	Dynamic light scattering
ECH	Epychlorohydrin
EDX	Energy-dispersive X-ray spectroscopy
FSM	Folded Sheets Mesoporous
GC-MS	Gas chromatography mass spectroscopy
GLY	Glycidol
HK	Horvath-Kawazoe
ILs	Ionic liquids
IR	Infrared spectroscopy
M.p.	Melting point
mlc-SILLP	multi-layer covalently supported ionic liquid like phase
M-NPs	Metal nanoparticles
MAS	Magic angle spinning
MO	Mobile corporation
MCM	Mobile composite of matter
MSU	Michigan State University
MWCNTs	Multi walled carbon nanotubes
NMR	Nuclear magnetic resonance
Prod	Productivity
PO	Propylene oxide
POSS	Polyhedral oligomeric silsesquioxane
PSD	Pore size distribution
PSILs	Polymer supported ionic liquids

RTILs	Room temperature ionic liquids
SBA	Santa Barbara Amorphous
SCILLs	Solid catalysts with ionic liquid layers
SEM	Scanning electron microscopy
SI	Supporting information
SILs	Supported ionic liquids
SILP	Supported ionic liquid phase
SILLP	Supported ionic liquid like phase
SILnPs	Supported ionic liquid nanoparticles
SO	Styrene oxide
SWCNTs	Single walled carbon nanotubes
TEM	Transmission electron microscopy
TEMPO	(2,2,6,6-Tetramethyl-piperidin-1-yl)oxyl
TEOS	Tetraethylorthosilicate
TON	Turnover number
TSILs	Task specific ionic liquids
XPS	X-ray photoelectron spectroscopy
XRD	X-ray diffraction
wt%	Weight %

TABLE OF CONTENTS

1. **Chapter 1** - General Introduction 1

1.1 Green chemistry and catalysis 2
1.2 Heterogeneization process and supports 3
1.3 Carbon Nanotubes 4
1.4 Ordered Mesoporous Silica 7
1.5 Ionic Liquids 10
1.6 Immobilized Ionic Liquids for catalysis 13
1.7 Immobilized Ionic Liquids for stabilization of metal nanoparticles 17
1.8 Polyhedral Oligomeric Silsesquioxanes 20
1.9 References 25

2. **Chapter 2** - Objectives 31

Objectives 32

Foreword chapters 3 to 5 34

3. **Chapter 3** - Thiazolium-based catalysts for the etherification of benzylic alcohols under solvent-free conditions 36

3.1 Introduction 37
3.2 Results and Discussion 39
3.3 Conclusions 50
3.4 References 51

4. **Chapter 4** - Cross-linked Thiazolidine network as support for palladium: a new catalyst for Suzuki and Heck reactions 53

4.1 Introduction 54
4.2 Results and Discussion 55
4.3 Conclusions 66
4.4 References 67

5. **Chapter 5** - Imidazolium functionalized carbon nanotubes for the synthesis of cyclic carbonates: bridging the gap between homogeneous and heterogeneous catalysis 69

5.1 Introduction 70
5.2 Results and Discussion 72
5.3 Conclusions 83
5.4 References 84

Foreword chapters 6 and 7 85

6. **Chapter 6** - Polyhedral oligomeric silsesquioxane based catalyst for the efficient synthesis of cyclic carbonates 88

6.1 Introduction 89
6.2 Results and Discussion 90
6.3 Conclusions 100
6.4 References 101

7. **Chapter 7** - Imidazolium polyhedral oligomeric silsesquioxane tetrachloropalladate: a new pre-catalyst for Suzuki coupling reactions 103

7.1 Introduction 104
7.2 Results and Discussion 106
7.3 Conclusions 113
7.4 References 115

8. Chapter 8 – Experimental Section 117

8.1 Experimental Section chapter 3 118
8.2 Experimental Section chapter 4 122
8.3 Experimental Section chapter 5 126
8.4 Experimental Section chapter 6 130
8.5 Experimental Section chapter 7 134

9. Chapter 9 – General conclusions and perspectives 138

9.1 General conclusions 139
9.2 Perspectives 141

Annexes 143

A Supporting informations 143

A.1 Supporting Information for the Chapter 3 144
A.2 Supporting Information for the Chapter 4 151
A.3 Supporting Information for the Chapter 6 152
A.4 Supporting Information for the Chapter 7 158

B List of publications and conferences 161

B.1 List of publications 162
B.2 List of conferences, congress and schools 164

Abstract

In the last years, great attention was focused on immobilized ionic liquids for their application in the field of catalysis. The main challenge is represented by the possibility of combining the benefits of the ionic liquids to that of the supports. In order to achieve this ambitious objective both the choice of the support and the functionalization strategy are of fundamental importance.

In this context, one of the aims of this doctoral project was to develop novel catalysts based on covalently mono- or multilayer imidazolium or thiazolium networks onto a high ordered mesoporous silica or carbon nanotubes materials. The second goal of this PhD thesis was to design novel imidazolium based catalysts using hybrid organic-inorganic compounds, known as POSS. All the compounds were extensively characterized using a broad series of characterization techniques in order to study their structure and to understand and justify their catalytic activity.

From a general point of view, the main interest of this thesis was to developed novel organic-inorganic hybrid systems that show improved catalytic performances in both terms of yield and selectivity compared to the existing catalysts. The imidazolium and thiazolium based solids have found applications for various reactions of relevant academic and industrial interest such as etherification reactions, the conversion of carbon dioxide, or as systems to stabilize palladium nanoparticles in order to catalyze C-C cross coupling reactions.

Chapter 1

General Introduction

Chapter 1

General Introduction

1.1 Green chemistry and catalysis

The term "Green Chemistry" was coined at the beginning of nineties at the US Environmental Protection Agency (EPA) and later by Anastas and Warner.[1-3] There are numerous and similar definitions of green chemistry, among them one proposed by Warner and Anastas was "*the design of chemical products and processes that reduce or eliminate the use and generation of hazardous substances*".[3] In other words, an ideal green chemical synthetic design should be based on the reduction of waste, energy consumption, risk and hazard, and on the use of renewable feedstock or raw materials. To better illustrate these ideas, Anastas suggested a series of principles called "Twelve Principles of Green Chemistry" where one of these is catalysis.[1]

The term "catalysis" was first proposed by Berzelius in 1836 in order to explain various decomposition and transformation reactions. The term catalysis is based on the use of a small amount of substance (catalyst) can speed up the rate of reaction without changing the thermodynamic balance and allowing the production of other compounds. Catalysts are used in the chemical industry and many processes (around 85%) require a catalyst, in particular in the production of polymers, fuels, pharmaceutical products and others.[4] In addition, the use of catalytic processes is an important technology from the environmental point of view, as it can reduce the energy consumption. Catalytic reactions are distinguished into two classes: homogeneous and heterogeneous catalysis.

The homogeneous catalysis implicates that all the components of the reaction are in the same phase (solid, liquid or gas), whereas in the case of heterogeneous catalysis the catalyst is not in the same phase of the other components.[5]

There are various homogeneous catalysts such as metal ions or complexes, organometallic complexes, organocatalysts, etc. They show many advantages related to the good dispersion of the catalytic active sites in the reaction medium, allowing excellent results in terms of yield and selectivity. However, these systems have some drawbacks mainly related to the difficulty of separating the catalyst from the reaction media because of the high solubility of these molecules, limiting then the possible applications in industrial field. On the other hand, the properties of heterogeneous catalysts make separation of these

substances from the reaction media easier. Nevertheless, the performance of the heterogeneous catalyst depends of the diffusion of the reactants and products from the surface of the catalyst. As consequence, it seems evident that finding a perfect equilibrium between homogeneous and heterogeneous systems is not exactly an easy task. Nevertheless, it is the heterogeneous catalysis that finds major applications in the field of the industry thanks to an easier recovery and reuse of the catalyst.

To avoid the problem linked to the separation of the catalyst from the reaction media, a homogeneous catalyst can be fixed onto a solid support (ex. amorphous and mesoporous silica-based support, active carbons, zeolites, carbon nanotubes, organic polymers, etc.) converting it into a heterogeneous one. This process is called heterogeneization,[6] and the details are discussed in the next paragraphs of this chapter.

1.2 Heterogeneization process and supports

The heterogeneization of catalysts can offer significant advantages in term of separation and reuse, thus simplifying the work-up of the reaction and limiting the production of waste, all in accord with the principles of Green Chemistry.

The performance of the heterogeneous catalysts is dependent by the method and the choice of support in which the catalytic active sites are immobilized. The strategies applied for the heterogeneization can be realized by a covalent or not-covalent immobilization of the homogeneous catalyst onto a support. In particular, the first one can be divided into two classes represented by the post-synthetic (or post-functionalization) and the co-synthesis approach.[6]

In this PhD thesis we followed the procedure to immobilize some homogeneous catalysts through the post-functionalization process. This approach implies the grafting of the catalytic active sites on a preformed support.

In order to obtain the final material, a linker between the homogeneous catalyst and the support is often needed. These types of molecules (usually organic compounds, as organosilanes) have a crucial importance, because they could have an influence on the performance of the catalyst.[7] In order to connect the active sites and the support, the linker has to have two different functionalizations, one active only with the support and the other with the catalyst (Scheme 1).

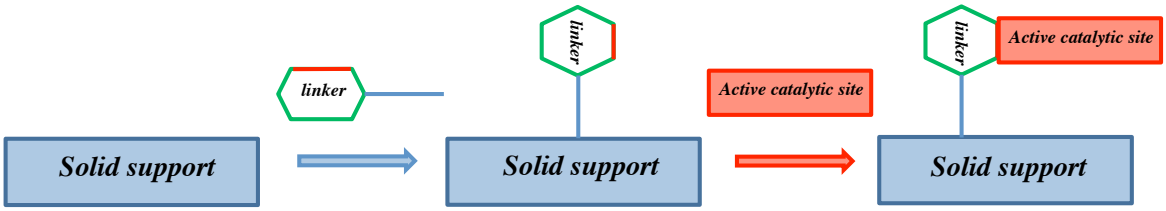

Scheme 1. Schematic representation of the covalent immobilization through a post-synthetic approach.

In catalysis, a successful support is a material that should have some characteristics, as:

- Chemical, mechanical, and thermal stability
- Large surface area
- Abundant surface functionalities
- Rapid mass transport of reactants and products to and from the active sites

For these reasons, and in addition to the low cost and availability of the material, the choice of the support has a significant importance. Some popular supports that satisfy the above mentioned criteria, are represented by the microporous materials, such as zeolite, alumina, mesoporous materials as SBA-15, MCM-41 or silica gel, and organic solids as carbon nanotubes.

In recent years, organic-inorganic hybrid compounds become a growing research area due to the various advantages such as thermal and mechanical stability of the inorganic substrate.

In this PhD thesis we focused our attention on two of these classes of solids reported before, the carbon nanotubes and the ordered mesoporous material SBA-15. In addition, we studied one class of hybrid organic-inorganic substrates, the polyhedral oligomeric sylsesquioxane, which will be discussed later.

1.3 Carbon Nanotubes

Since their discovery in 1991 by Iijima,[8] the industrial and academic interest in carbon nanotubes (CNTs) increased dramatically. Casually, Iijima observed some filaments of nanometric dimensions (carbon nanotubes) in a residue of soot produced by the vaporization of the graphite used for making fullerenes. In these compounds, called carbon nanotubes, one or more superimposed graphene sheets are folded to form an empty cylindrical structure, whose properties depend on the diameter and the length of the tubes. In particular, carbon nanotubes consist of one (single- walled) or more (multi- walled)

graphene sheets closed up into a cylindrical shape.[9] Single-walled CNTs (SWCNTs) may exhibit external diameters ranging from 0.4 to 4 nm, while in multi-walled CNTs (MWCNTs) the external diameters can reach 100 nm. Depending upon the method of synthesis, the length of CNTs could be in the size of micrometers. Concerning the single walled nanotubes, there are different angles and curvatures in which the graphene layers may be wrapped. Depending on the arrangement of the sp^2 carbon hexagons, the final tubes may have a "zigzag", "armchair" or "chiral" structure and different properties (metallic or semiconducting).[9] The Figure 1 shows three different ways for the SWCNTs in which the graphene sheets could close up.

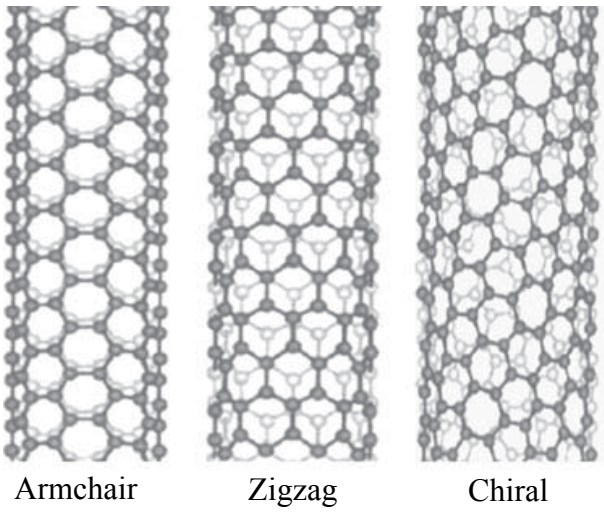

Figure 1. The different types of single walled carbon nanotubes (SWCNTs).[9b]

Concerning the synthesis, a large number of methods were proposed, although the most suitable are laser ablation, arc discharge, and chemical vapor deposition (CVD). In particular, laser ablation and arc discharge are based on the vaporization of carbon in an inert atmosphere from graphite heated by a laser or by an applied current, respectively. Instead, CVD method is based on the catalytic decomposition of a carbon-containing gas.[10] Because of their unique properties, such as high thermal stability and the metallic or semiconducting behavior, CNTs can be considered as attractive candidates in numerous applications, such as in nanoelectronics, nanotechnology, biomaterials and catalysis.[11]
However, their usage was limited because of the lack solubility and the difficult manipulation in any solvents. On the other hand, the size and the shape are the key parameters that have made these materials important for the interactions with several classes of compounds.[12] In the field of materials, carbon nanotubes are promising compounds. Different studies highlighted the porous nature of these materials and, in

general, the specific surface area of SWCNT is often larger than that of MWCNT. Usually, total surface area of as-grown SWCNT can reach 1000 $m^2 g^{-1}$ whereas, for as-produced MWCNT values ranging between 200 and 400 $m^2 g^{-1}$ are often described.[13] In particular, the presence of pores attracts increasing attention due the possibility to use these interesting materials for efficient gas storage.[14] In the case of SWCNT, the flexible rope-like network generates a not-ordered mesoporosity in these materials, preserving the microporosity of the tubes, but affecting the total specific surface area. In specific, the micropores consist of a pore size distribution < 2 nm, whereas the mesopores show a pore size in the range between 2 and 50 nm.

In the field of catalysis, CNTs offer important advantages such as an high catalytic activities resulting from the high activity/selectivity due to the possibility to work in the inner cavity of nanotubes.[15] In this context, in 2007 Pan *et al.* reported a study based on the catalytic activity of the Rhodium particles confined inside the nanotubes for the conversion of CO and H_2 to ethanol. For the first time, they observed that the formation rate of ethanol is higher inside the nanotubes than outside.[15b] Moreover, the combination of all of these characteristics, in addition to the high thermal stability, makes CNTs attractive and competitive materials in the application as support in catalysis. Concerning the functionalization, carbon nanotubes can be chemically modified following three different procedures (Figure 2):[9a,12b]

a) the covalent attachment of groups through reactions onto the π- systems of CNTs;

b, c) the non-covalent absorption of molecules (as π-π interactions or not-covalent wrapping);

d) the endohedral filling of the inner empty cavity of CNTs.

There are numerous reactions that follow the covalent approach, such as halogenation of CNTs, cycloadditions or radical additions, plasma activation, nucleophilic additions, etc.[9a] We focused our interest onto one of these methods, based on the grafting of catalytic active sites through radical reactions (“grafting from” method), taking advantage from the high reactivity of the CNTs C=C double bonds present on the nanotubes. This approach allows to not use any linker between the active sites and the nanotubes.

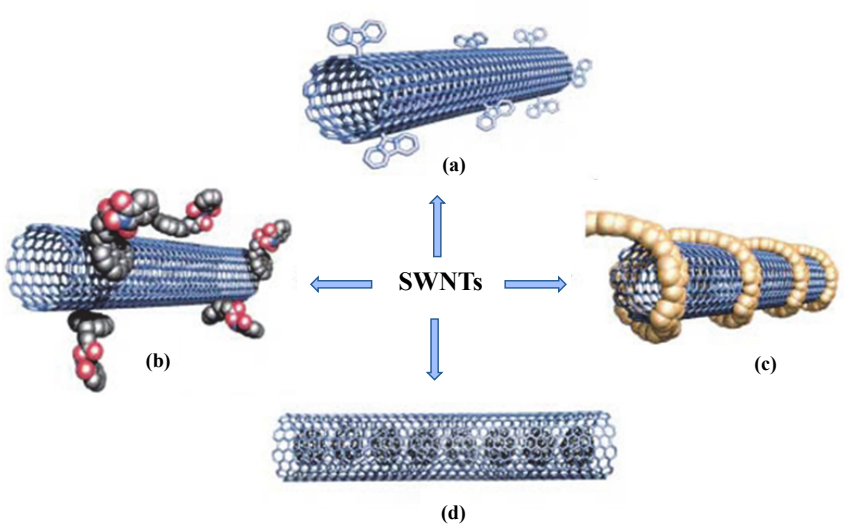

Figure 2. Functionalization possibilities for SWNTs: (a) covalent functionalization, (b) and (c) not-covalent functionalization, and (d) endohedral functionalization.[12b]

Another and attractive class of materials that could find applications in the field of catalysis is represented by the mesoporous silica materials, that are discussed in the next paragraph of this chapter.

1.4 Ordered Mesoporous Silica

In the last decades, the research was focused on the synthesis of materials that have an ordered structure with a pore size distribution larger than zeolites, which are crystalline aluminosilicates with specific internal micropores. This ambitious objective was reached by the Mobil Corporation (MC) in 1992. With the synthesis of M41S family, the researcher at MC gave a significant contribution to the development of the porous materials.[16] From a crystallographic point of view, these solids are amorphous and not ordered at atomic level, however the regular channels and pores are ordered at the nanometer level, for this reason they are so called crystalline mesoporous materials. Mesoporous silica materials have a narrow pore size distribution (pore size: 2-50 nm), a high surface area, generally equal to 1000 m^2g^{-1}, large pore volume (>1 cm^3g^{-1}) and a good thermal stability.[17] Thanks to the good properties, they found some industrial applications, for the elimination of SO_2 from gaseous systems,[18] in nanoelectronics[19] and drug-delivery systems.[20]

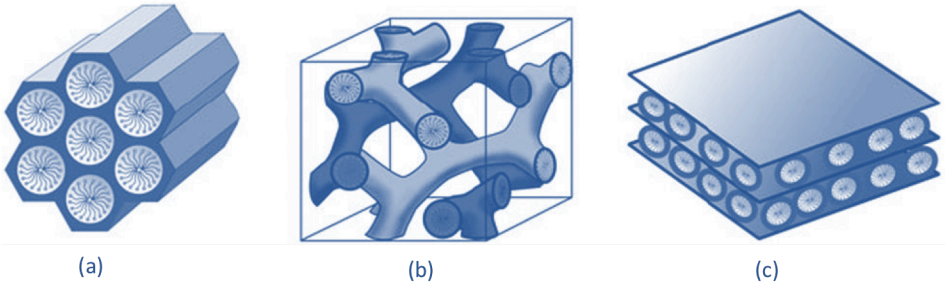

Figure 3. Structure of MCM-41 (a), MCM-48 (b) and MCM-50 (c).[17]

By utilizing various surfactants as structure-directing -agents and silica precursors, the researchers generated a series of MCM-type (the acronym for Mobile Composite of Matter) mesoporous silica structures with tunable pore size and morphology, as MCM-41, MCM-48 or MCM-50 silica consisting of hexagonal, cubic or lamellar structure, respectively (Figure 3). After some years, several other ordered mesoporous silica materials, such as SBA-,[21] MSU-,[22] FSM-[23] types have been developed.

In this context, in the late of 1990s the SBA family (the acronym for Santa Barbara Amorphous) emerged as new class of materials introduced by Stucky and co-workers.[24] A general feature of interest respect of the M41S materials is related to the thicker pore walls, which allow a greater thermal stability. Among the different materials, in this PhD thesis we focused our attention on the synthesis of one of the most attracting mesoporous solids: the SBA-15, which is characterized by a 2D hexagonal pore structure. Compared to other mesoporous materials, SBA-15 may have pores up to 30 nm and walls substantially thicker than other structured mesoporous materials.[17] Another important feature of the SBA-15 solids is the presence of a non-regular microposity and interconned mesopores. In general, we can consider the SBA-15 as a combination of micro- and mesoporosity. SBA-15 can be prepared including various amounts of micropores. The microporosity come from the block copolymer chains that can be occluded in the silica walls and, when removed, lead to the formation of micropores.[21,25] Such microporosity (between 0.5 and 2 nm in size) can be controlled systematically by changing the synthesis temperature or the ratio TEOS/surfactant. In particular, by increasing the temperature, the pore size increase and the thickness of the walls decrease.[26]

The typical synthesis of these structures is based on a surfactant micelle templating approach, as shown in Figure 4.

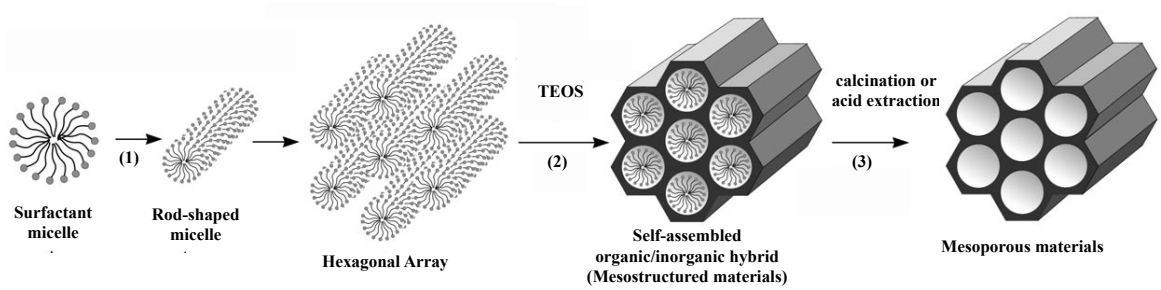

Figure 4. Formation mechanism of mesoporous silica materials.

Firstly, in an acidic aqueous solution, the not ionic surfactant triblock-copolymer poly(ethylene oxide)-poly(propylene-oxide)-poly(ethylene oxide) (PEO_x-PPO_y-PEO_x) forms self-assembled micelles. In these systems the micelles are positively charged and serve as structure-directing agents that can interact with the silica species positively charged as $-SiOH_2^+$ (denoted as I^+) *via* electrostatic interactions, assisted by the counterion of the acids (X^-). In other words, the interaction can be represented in this way: PEO_x-$_m$[EO-H_3O^+]m--mX^---I^+, in which the protonated unit of the copolymer (EO-H_3O^+) is assembled with the counterion X^- and the silica based cationic I^+. Then, the mesoporous material is formed through inorganic polymerization and condensation of the silica species. Finally, by calcination or acid extraction, the organic surfactants are removed, leaving an inorganic mesoporous silica framework. A schematic representation is reported in Figure 5.

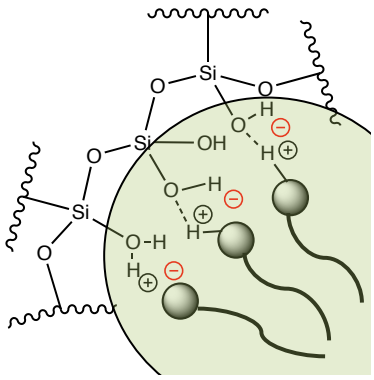

Figure 5. Schematic representation of silica-surfactant interface.

Many scientists have studied the functionalization of these materials in order to make them suitable for a waste range of applications such as adsorbents for metal ions or capture for carbon dioxide,[27] sensors,[28] carrier materials in drug-delivery sistems,[29] and in phocatalytic applications.[30] In the case of adsorbents, Shahbazi and co-workers reported a SBA-15 functionalized with amine and melamine for the adsorption of heavy metal ions, such as Pd (II), Cu (II) and Cd (II),[27b] whereas in 1996, Zhu *et al.* prepared a modified mesoporous

SBA-15 with tetraethylenepentamine (TEPA) which showed an high adsorption capacity for the CO_2.[27d] In biomedical field, SBA-15 was used in the separation and purification of molecules, including proteins[29a] and, in this context, Yilmaz reported a series of SBA-15 functionalized with alkoxysilanes in which they have incorporated different amounts of amoxicillin, dipending of the type of alkoxysilane grafted on the mesoporous silica.[29e]

There are a lot of examples reported in literature in which these materials are employed as support in catalysis.[31] Actually, the hexagonal mesoporous pure silica SBA-15 was used as support for preparing highly dispersed V-containing catalysts employed for the oxidation of methane,[31a] or, in another work, for the decomposition of the most stable chlorinated-alkane, such as dichloromethane.[31b] SBA-15 was also investigated as support for Platinum and Nickel catalysts for the synthesis of biodiesel.[31c] In 2010, Che and co-workers employed SBA-15 as support for organic molecules, such as terpyridine based catalyst, for oxidative C-C cross coupling reactions.[31d] Another example regarding its application as support in catalysis is related to its functionalization with TEMPO (the acronym of (2,2,6,6-Tetramethyl-piperidin-1-yl)oxyl) molecules for oxidation reactions.[31e]

Furthermore, it is important to note that the use of support could transform a homogeneous catalyst in heterogeneous one, obtaining then the advantages related to the heterogeneous systems.

In the next paragraph we will discuss about one class of organic green compounds, ionic liquids, which have been employed as catalysts during the development of this PhD thesis.

1.5 Ionic Liquids

Ionic liquids (ILs) become a topic of increasing interest in the last decade. The term ionic liquids (ILs) indicate ionic salts, constituted by positively and negatively charged ions, that melt below 100 degrees, in contrast to high-temperature molten salts (NaCl, NaBr…).[32] In particular, most of them remain liquids at room temperature, for this reason they are called "room temperature ionic liquids" (RTILs).[33]

Ionic liquids have a unique array of physicochemical properties, as low vapor pressure, that allow to eliminate the hazardous exposure and air contamination problems. Moreover, they can be not toxic and show low or reduced flammability hazards, they display an excellent chemical and thermal stability, and they are good conductors. Some of the physical properties distinguish them from other liquids systems, such as organic, or aqueous phase. Due to their stability, non-volatility, modifiable miscibility, and polarity, ILs may be used as ideal substitutes for conventional organic solvents.[34] Nonetheless, the

high viscosities of ILs are therefore one of the major limiting factors for their industrial use.[35]

As mentioned above, ionic liquids are constituted by cations and anions; in particular typical cations are imidazolium, pyridinium, thiazolium, ammonium, phosphonium derivatives. Among them, the most used is the imidazolium cation. Regarding the anions, they can be of organic or inorganic origin. The most employed as inorganic ions are halide, tetrafluoroborate or hexafluorophosphate, and the common organic ions are derivatives of sulfate and acetate[36] (some example are reported in Figure 6).

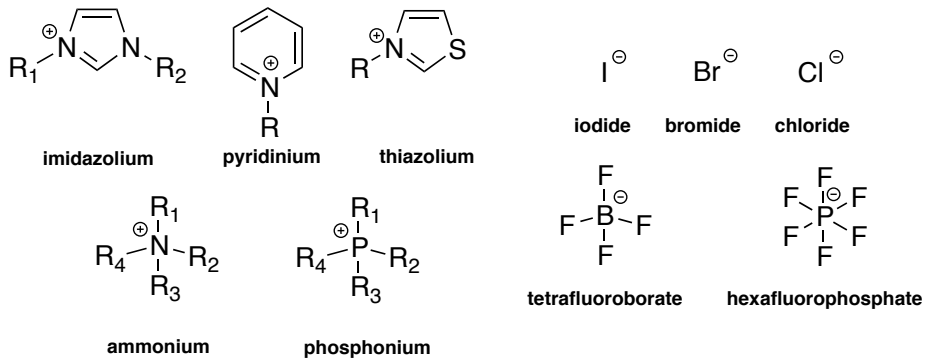

Figure 6. Some example of cations and anions in ionic liquids.

Usually, cations may display some substituents as alkyl chains or, more in general, functional groups, such as methoxy or hydroxyl groups. In particular, functionalized ionic liquids are designated as "task specific ionic liquids" (TSILs).[37] This term was coined by Davis for some ILs in which functional group is included in a part of the cation / or anion structure.[37e,f]

Some studies performed in the solid state by X-Ray diffraction demonstrated that in the ILs exist some weak interactions, in particular in the case of interactions between 1,3-dialkylimidazolium cations and not-coordinating anions such as PF_6 and BF_4, they show an extended network of hydrogen-bonded cations and anions in which one cation is enclosed by at least three anions and each anion is surrounded by at least three imidazolium cations, allowing a supramolecular structural organization and a high order system.[38] In particular, from studies performed in solution by ^1H NMR spectroscopy, conductivity and microcalorimetry, this supramolecular organization is preserved to a great range even in solutions, at least in solvents with a low dielectric costant.[38] In other words, ILs should be considered as supramolecular structures with a high degree of self-organization and weak interactions.

The good properties of ionic liquids, especially for RTILs, render them excellent candidates for several applications. As mentioned before, ILs can be used as alternative solvents because of their versatile properties.[39] In this context, Toma and co-workers reported for the first time an organocatalyzed aldol reaction of aromatic aldehydes with acetone, using ILs as solvent.[40] In 2002, Rogers *et al.* used a bmimPF_6 as solvent for radical polymerization of methyl methacrylate and styrene obtaining polymers with higher molecular weights compared to the same reaction developed in the traditional solvents, such as benzene.[41] Later, the same group reported the possibility to use ILs to solubilize cellulose without pretreatments.[42]

Anyway, they are not only used to replace numerous traditional organic solvents, but they are employed as systems for the capture and separation of some gas, such as CO_2,[43] as reagents,[44] in biodiesel production,[45] and in catalysis.[46] It was found that ILs were investigated as electrolytes for water oxydation.[47] Furthermore, ILs can be used as good electrolytes in lithium batteries,[48] in electroplating processes,[49] and solar cells.[50] In particular, the introduction of ILs as eco-friendly reaction media has opened new frontiers in the field of electrochemical energy storage. Very recently Scrosati *et al.* described the positive role of the ILs in the synthesis of supercapacitors, materials for batteries and green electrode processing.[51,52]

These are an extended range of examples of applications of ILs, and an overview is better represented in the Figure 7.

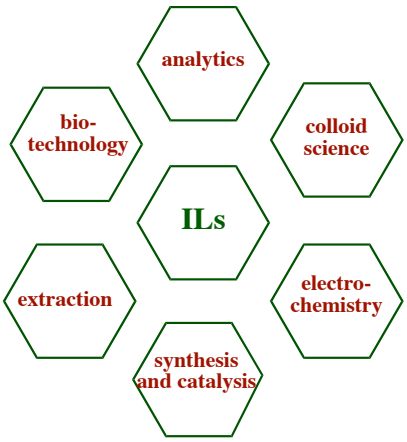

Figure 7. Major applications of ILs.

In the field of catalysis, there are continuous researches focusing on the use of ILs as solvent/catalyst/co-catalyst and significant improvement in term of product yield and reaction work-up was obtained.[39b] In this contest, one of the more interesting applications

of ILs is linked to their double function: they are able to both solubilize and stabilize a catalyst. In this sense, they can stabilize metal catalysts, without the need of expensive ligands. Thus, ILs can be used not only as catalysts but also as support for metal active sites. The aspect concerning their application in catalysis will be developed in the next section.

1.6 Immobilized Ionic Liquids for catalysis

In the last years, great attention was focused onto the catalytic applications of materials based on supported ionic liquids (in particular imidazolium salts), generally called SILs.[53] The general concept involves the immobilization of the ionic liquids onto a solid support, usually a highly porous material. One of the first examples reported in literature is related to immobilization of acidic chloroalluminate IL onto a inorganic silica material. This solid was used as catalyst for some alkylation reactions of aromatic compounds.[54] In 2002, Mehnert at ExxonMobil Research[55] developed an new approach allowing the synthesis of a multiple layer of supported ionic liquids via the initial formation of a covalently anchored monolayer followed by the adsorption of additional ionic liquid moieties. The final multilayer ionic liquid phase was successfully used to dissolve the catalyst for hydroformilation reaction. In addition, this catalyst displayed improved catalytic performances (in comparison with the biphasic system) due to the higher concentration of the active catalyst at the interface.

Until today, various novel systems of efficient heterogeneous catalytic systems based on ILs were developed. There are different methods that can be employed, such as the absorption or the covalent attachment[7] of the ionic liquids onto the support. One example of non-covalent anchoring consists in the solubilization of a homogeneous catalyst in a solvent in the presence of a solid support (usually silica gel) followed by removal of the solvent under reduced pressure. In this way the so-called SILP (Supported Ionic Liquid Phase) materials, in which the Ionic Liquid Phase is adsorbed, are obtained. On the other hand, the Ionic Liquid Phase can be covalently linked to the support and in this case the material can be called SILLP (Supported Ionic Liquid-Like Phase). Some examples of materials that can be good candidates as supports in catalysis are silica materials, polymers or carbon nanotubes, as mentioned above. Other examples of supported ionic liquids are solid catalysts with IL layers (SCILL), polymer supported ILs (PSILs),[56] and supported ionic liquid nanoparticles (SILnPs)[57] (Figure 8).

In the "solid catalyst with ionic liquid layers" (SCILL) a solid heterogeneous catalyst is coated with a thin film of IL, and in contrast with the SILP or SILLP, in this case the support material constitute the catalytically active phase and no additional homogeneous catalysts are involved.[58]

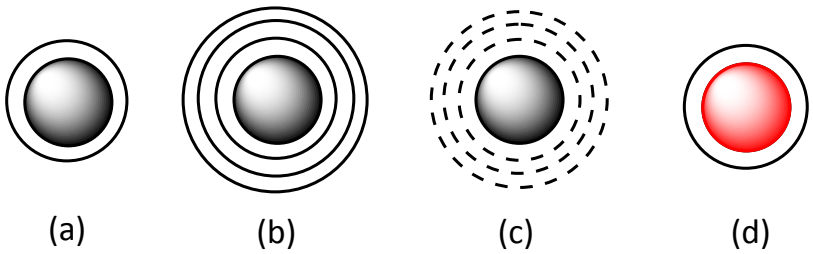

Figure 8. Schematic representation of (a) covalently attached monolayer of ionic liquid onto a solid support, (b) covalently attached multilayer of ionic liquid, (c) adsorbed multilayer of ionic liquid; (d) coated monolayer of ionic liquid onto a solid catalyst.

In this context, Kernchen and co-workers developed a novel material based on Ni catalyst coated with a bmim(-$nC_8H_{17}OSO_3$) for the hydrogenation of cyclooctadiene (COD) to cyclooctene (COE).[58a] They demonstrated that the coating of the surface with the ionic liquid strongly enhances the yield of the reaction, comparing with the uncoated catalyst. However, the research in the field of SCILL is at the beginning, and more experiments are needed to better understand the effects of these systems.

It should be pointed out that the process to transform a homogeneous catalyst in heterogeneous is important because it keeps the advantage of the heterogeneous systems and, thus, can be applied in continuous-flow operated fix bed processing. In comparison to the pure ionic liquids, immobilized ionic liquids offer the additional advantage of an easier recover of the catalyst from the reaction mixture.

In a recent publication, it was demonstrated that some physicochemical properties of the ionic liquids are maintained after the heterogeneization process.[59] Essentially, the aim of the immobilization process is to transfer the desired catalytic properties of the liquids to a solid catalyst. Moreover, in this case the immobilization could also present the advantage to reduce the high viscosity of the ILs. In other words, SILs catalysis combines the most attractive qualities of homogeneous catalysis like high activity and selectivity with the benefits of heterogeneous catalysts such as facility of product separation.

The problem linked to the immobilized heterogeneous catalysts could be the low loading amount of the immobilized catalytic active sites. This drawback can be circumvent by using larger amount of heterogeneous catalyst; however the application of vast amount

could have some drawbacks such as the larger amount of solvents required. Thus, the development of a simply strategy for the synthesis of high loading of catalytic sites is necessary. In order to reach this objective, in 2009 Wei and co-workers developed a SiO_2-supported diimidazolium ionic liquids (SILLPs) that shows two imidazolium moieties grafted onto a support that offers a higher amount of catalytic active centers than the supported-mono ILs (Figure 9).[60]

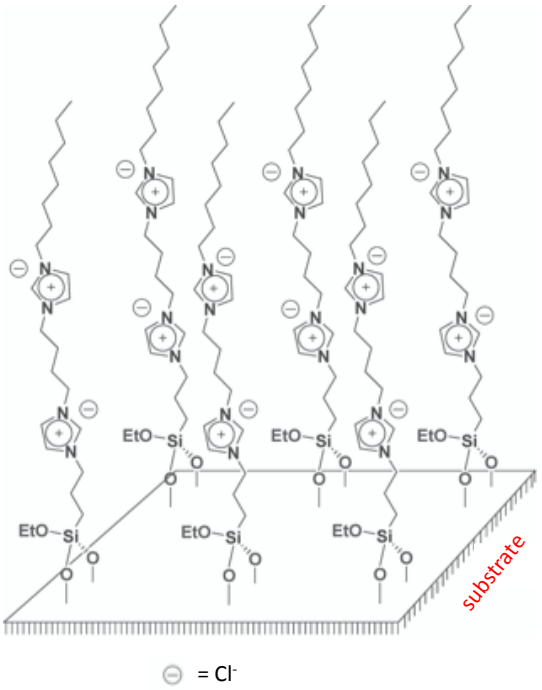

Figure 9. Supported diimidazolium ionic liquids (SILLPs).[60]

Recently, the group where I developed this PhD thesis has synthetized a new kind of materials constituted by highly cross-linked imidazolium network obtained through a radical polymerization of the bis-vinyl imidazolium salts on the mercapto-silica modified gel.

This materials, called "multilayer covalently Supported Ionic Liquid Like Phase" (mlc-SILLP) show a high loading of supported ionic liquids, keeping the catalytic behavior of the unsupported one[61] (Figure 8b), which could improve the catalytic performances of the materials.

In this context, very recently Pourjavadi *et al.* reported a novel magnetic heterogeneous catalyst based on magnetic nanoparticles (Fe_3O_4) coated by multi-layers of poly-(1-vinylimidazole), (Figure 10). This catalyst was tested for the synthesis of 4H-benzo*[b]*pyrans, with good results in term of yield of products. Because of the multi-layered form of polymer, the catalyst shows a very high loading of imidazole moieties and

it was employed in very low amounts, comparing with the substrates. In addition, the catalyst was magnetically separated from the reaction mixture and reused for 10 times without loss of catalytic activity. They also reported the catalytic tests in presence of 1-vinylimidazole as catalyst in order to highlight the improved catalytic performances of the poly(1-vinylimidazole) coated magnetic nanoparticles (MNP@PVIm).[62]

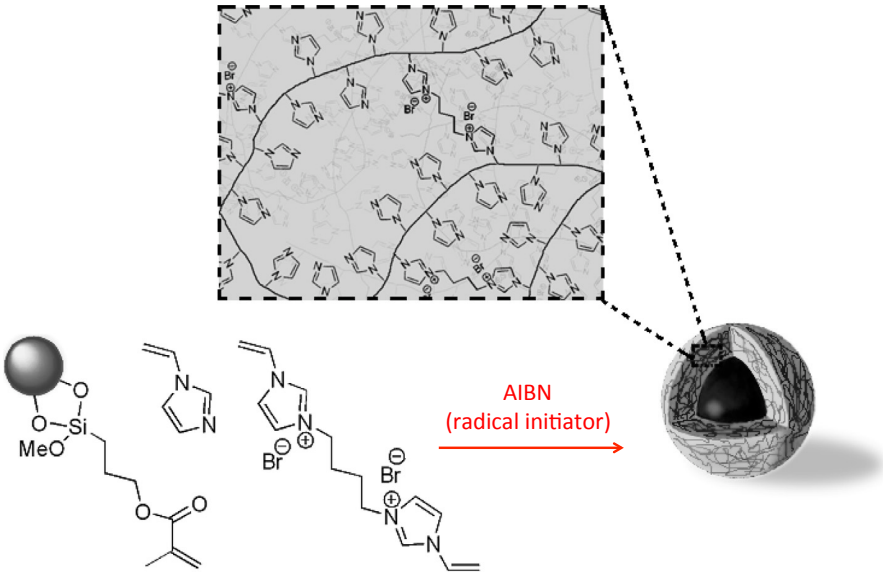

Figure 10. Synthesis of MNP@PVIm catalyst.[62]

Finally, as showed in the examples mentioned before, the supported ionic liquids have a considerable importance in the field of catalysis. However, the scientific research focused onto new material supports and functionalized ionic liquids in order to improve the performances of the final materials is in a continuous development.

1.7 Immobilized Ionic Liquids for stabilization of metal nanoparticles

A potential application of ILs is to be used as systems for stabilize some catalysts (Figure 11). In particular, due to their high polar nature, they can dissolve inorganic salts and stabilize metal catalysts.[63] Immobilized ionic liquids (SILP, SILLP, mlc-SILLP and others) found wide applications, combining the advantages of using ionic liquids that the ones related to the heterogeneous supported materials.[61,64]

Metal nanoparticles (M-NPs) have a significant interest for technological applications in several areas of industry and science, especially in catalysis due to their high activity. However, nanoparticles are often not stable and they can suffer of aggregation phenomena (inter-particle interaction) or sintering.

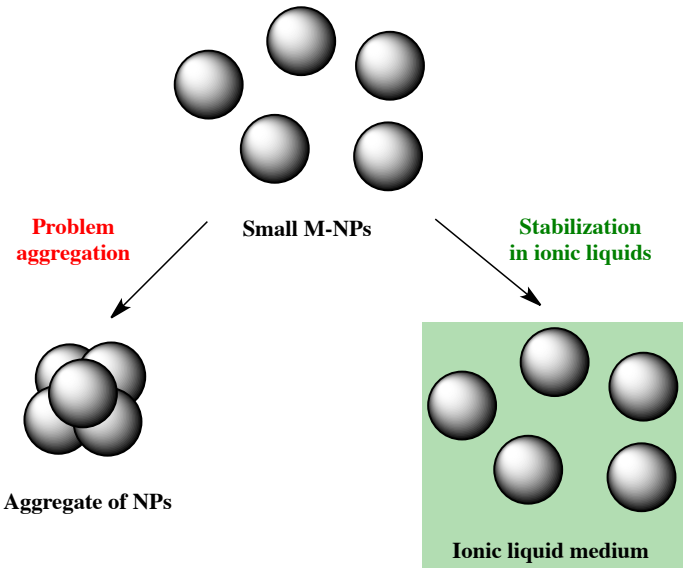

Figure 11. Stabilization of metal nanoparticles (M-NPs) using ILs.[65]

In order to avoid this aggregation, some studies reported that ILs can act to stabilize M-NPs, such as palladium or gold nanoparticles[63b,66]

In 2010, Dupont and co-workers reported the stabilization of NPs in the ionic liquids. The authors attribute the stabilization effect to a reorganization of the IL network with the generation of nanostructures with polar and non-polar regions, including the NPs. The ILs form a protective layer probably located around the nanoparticle surface, providing an electrostatic protection against the aggregation of the nanoparticles.[66a] However, these types of interactions are not very clear and the role of the ILs are currently matter of debate.[66b]

In 2008, Redel and co-workers evidenced the dependence of the stability of silver nanoparticles with the molecular volume of the IL counterion, suggesting that the thickness of the stabilizing shells around the nanoparticles depends on the anion IL volume.[67] In particular, AgNP size increases linearly with the molecular volume of the IL anion. In another work the same authors evidences the influence of the reaction conditions (thermal or photochemical decomposition) on the size of the Mo NPs, obtaining larger particles in the case of the photolytic route, because of the faster process.[68]

Nonetheless, in 2010 Morais and co-workers showed by in situ X-Ray photoelectron analysis the interaction between metal iridium nanoparticles and the surrounding imidazolium ionic liquid. By monitoring the C 1s signal of the ionic liquid (C2 carbon), they observed a shift of its binding energy (BE) in presence of the metal nanoparticles.

These results highlight the effective interaction of the cation ionic liquid with the metal NPs.[69]

It is interesting to note that recently Beer and co-workers reported in an article a collection of possible stabilization models for nanoparticles in imidazolium ionic liquids. They suggested that the stabilization of M-NPs could be through the formation of a coating layer of the anions on the surface of nanoparticles, which is surrounded by the cations, as a "core-shell system", providing the stabilization via Coulombic repulsions between NPs (Figure 12, a). A second model is designated by carbene NHC-(type) stabilization (Figure 12,b) or finally, through parallel coordination by the imidazolium cations (Figure 12,c).[63b,70]

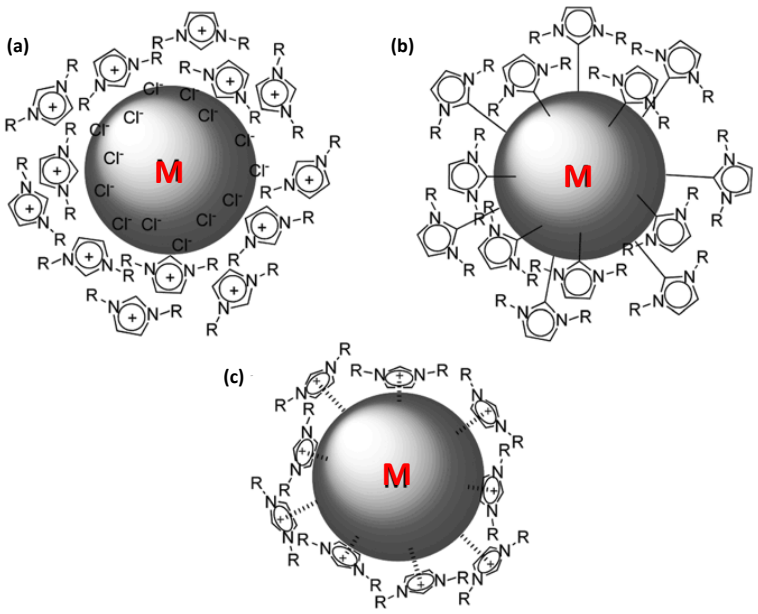

Figure 12. Possible stabilization models for M-NPs in ionic liquids.[63b]

Concerning the synthesis, M-NPs can be prepared in ILs mainly via chemical[71] or photochemical reduction[72] of the corresponding metal salts, and by decomposition of organometallic complexes, as metal carbonyls with zero valent metal atoms.[68] In the chemical reduction, hydrides (mainly $NaBH_4$) are the most used reducing agents for the generations of metal NPs. However the use of these agents, in presence of imidazolium salts, could deprotonate the imidazolium cation generating carbenes that might bind to metal surface. The advantage to use supported ILs instead of the corresponding un-supported analogous is related to the easily purification of the catalyst from the by-products generated from the reducing agent (such as Na or B compounds). In 2008, Redel and co-workers obtained chromium, molybdenum and tungsten nanoparticles through

thermal decomposition under argon from metal carbonyl precursors. It is worth to be mentioned that they employed very high temperature (230 °C) in order to obtain stable nanoparticles.

Sans and co-workers reported a new polymeric material based onto g-SILLPs (gel-Supported Ionic Liquid Like Phases) consisting in imidazolium salts anchored onto a polystyrene-divinyl benzene (PS-DVB) solid supports (Figure 13).[73] Its catalytic activity was tested for Heck reaction highlighting excellent performance in term of activity and recyclability. They obtained very good results in term of TON (turnover number) and TOF (turnover frequency) for the coupling of phenyliodide and methylacrylate.

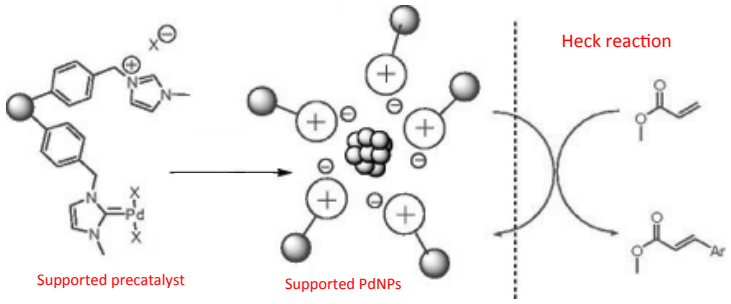

Figure 13. Supported Pd NPs catalyst for Heck reaction.[73]

In 2010, Karimi and co-workers prepared for the first time a high loading ionic liquids obtained by the synthesis of periodic mesoporous organosilica based on alkylimidazolium ionic liquids in which the imidazolium moiety is distributed in the silica network (Figure 14). This material was used as support for palladium NPs, which was demonstrated as efficient catalyst for Suzuki-Miyaura reaction in water. They showed that the catalyst was recovered and reused for four reaction cycles without significant loss of activity. However, the synthesis procedure of the catalyst required the use of toxic solvent, such as DMSO.[74]

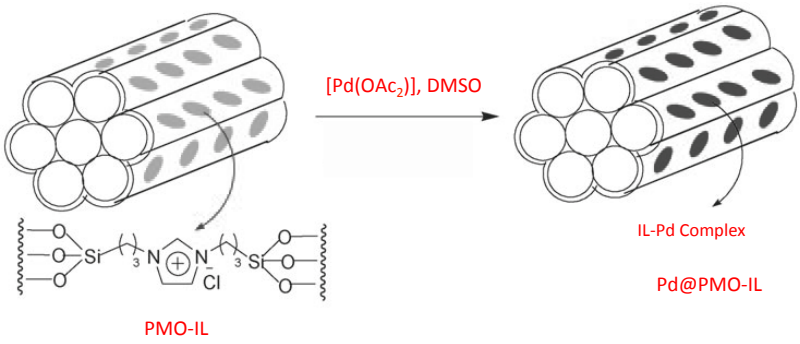

Figure 14. Synthesis of Pd-PMO-IL catalyst for Suzuki-Miyaura reaction.[74]

In general, supported ILs (SILs) are interesting systems that can play an essential role not

only in the stabilization of metal nanoparticles, but also in facilitating their separation from the reaction mixture. This has a crucial importance from an environmental and economic point of view. Additionally, these systems present the advantage linked to their potential application in continuous flow conditions.[75] Furthermore, the synthesis of a highly loaded supported ionic liquids allows stabilizing a very high amount of catalytic species.

1.8 Polyhedral Oligomeric Silsesquioxane (POSS)

In the last decades, silsesquioxanes represented a versatile class of organosilicon compounds with well-defined nanometrical dimensions. These hybrid organic-inorganic systems attracted considerable attention in both academic community and industrial field. Silsesquioaxane is the general name of a family of compounds with formula $(RSiO_{1.5})_a(H_2O)_{0.5b}$, where R can be an hydrogen or an organic groups, and *a* and *b* are integer numbers (a = 1,2,3,…; b = 0,1,2,3,...) with $a+b = 2n$, where n is integer (n = 1,2,3,…) and $b \leq a+2$.[76] Silsesquioxanes-based compounds are usually obtained by hydrolytic condensation reactions of trifunctional organosilanes ($RSiX_3$). Depending of the reaction conditions (concentration of $RSiX_3$, temperature, nature of R and X group, reaction time, solvent, pH, etc.) different structures of silsesquioxanes can be formed.[76]

As a consequence, these molecular systems can be divided into 4 groups: random structures, ladder polymers, completely condensed and incompletely condensed polyhedral silsesquioxanes (Figure 15).

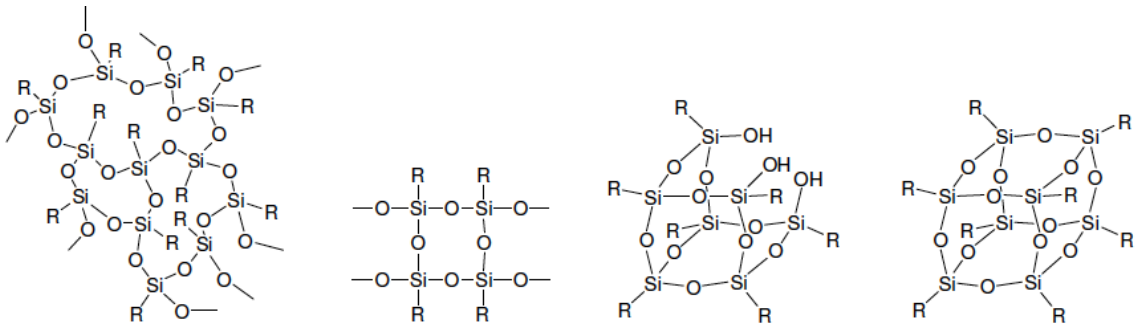

(a) (b) (c) (d)

Figure 15. Random structure (a), ladder polymers (b), incompletely (c) and completely condensed silsesquioxanes (d).

In particular, in the case of condensed structure *b* value corresponds to zero, the oxygen atoms act as a bridge between to silicon atoms and there are no OH-functionalities; on the other hand the *b* value is ≠ 0, and the incompletely silsesquioxane has silanol groups (Si-OH), showing a more complex formula and becoming an ideal compounds as ligand for

metal coordinate complexes.[77]

We focused our attention onto one class of these compounds, the completely condensed polyhedral silsesquioxane, called POSS (Figure 15.d). An easier notation to describe these hybrids systems is T_nR_m, where T represents silicon atoms and R the organic groups. These notations use letters to define the type of silicon atom in the silicon-oxygen frameworks. In other words, it suggests the number of oxygen atom bonded to silicon: an "M" unit has a silicon atom bound to one oxygen atom, "D" unit has a silicon atom bound to two oxygen atoms, "T" unit consist when it is bound to three oxygen atoms and finally, "Q" unit represents silicon that is bound to four oxygen atoms[78] (Figure 16).

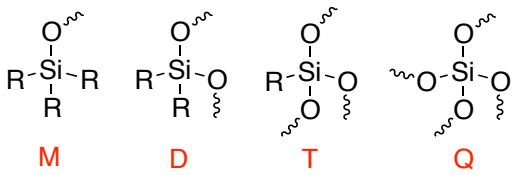

Figure 16. One example of silsesquioxane nomenclature.

There are multiple cage structures in the completely condensed polyhedral silsesquioxanes (T_8, T_{10}, T_{12},…) although one of the most investigated is the octameric structure, as $(RSiO_{1.5})_8$ or T_8R_8. Octameric silsesquioxanes molecules have a cage-shaped three dimensionals (3D) structure, and they consist of a rigid and inorganic silica cores (side length: 0.5-0.7 nm) surrounded by eight organic functional groups (Figure 17).

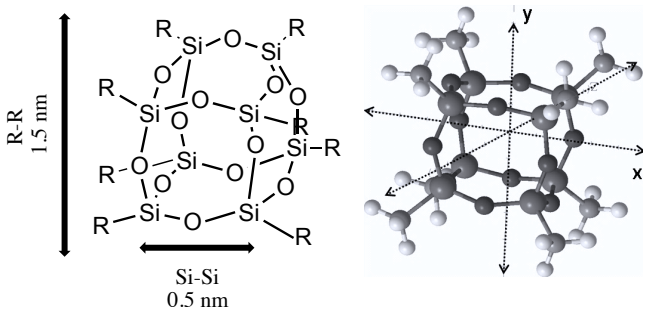

Figure 17. Typical size of octameric silsesquioxane (left); 3-D schematic drawing of octamethylsilsesquioxane (right).

In the proposed mechanism for the synthesis of completely silsesquioxane (T_8R_8) the reaction carried out firstly through the formation of the dimer, then of the cyclic tetramer and finally of the octameric silsesquioxane (Figure 17).[79]

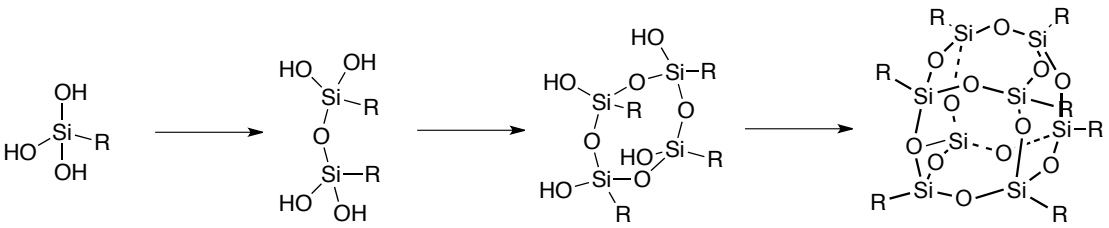

Figure 18. Proposed mechanism of formation for the completely condensed silsesquioxane T_8R_8.

The good performance of these systems come from the combination of the high rigidity and thermal stability provided by the inorganic silica nano-core, and the easily functionalization of the organic moieties. In other words, POSS embody both organic and inorganic characteristics and cage-like structures in one small nano-entity. In this context, the organic groups on the corner can be modified with several organic functionalizations through simple reactions,[80] providing unique properties to these nanocomposites. The growing interest of POSS could be highlighted in many applications, actually they were applied as biomaterials,[81] or for the development of hybrid electrochromic devices,[82] in solar cells,[83] as models compounds for silica supported catalyst,[84] or additives in synthesis of periodic mesoporous organisilicas[85] polymer nanocomposites,[86] in lithium-ion batteries,[87] and in the field of biomedicine as complexes with DNA.[88] One relevant application in the field of dye-sensitized solar cells (ssDSSC, Figure 19), was reported by Wang and co-workers. They described the use of an octa-POSS completely functionalized with imidazolium iodide salts, which act as iodide source, giving good conversions and long-term stability.[83a]

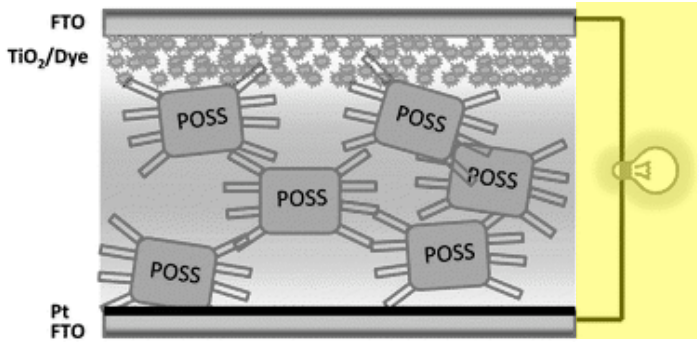

Figure 19. POSS with height imidazolium iodide as as solid-state electrolytes in solid-state dye-sensitized solar cells.[83a]

Very recently, Zhang and co-workers reported the preparation of octa-imidazolium based POSS with dodecyl sulfate as anions.[89] In both cases, the imidazolium POSS systems were characterized via the standard characterization techniques. However, concerning these systems, a depth characterization of the nanocage in order to well understand the

functionalization and the stability under different reaction conditions is not described.

Regarding the application in the field of catalysis, there are some examples reported in literature.[90] In this context, Nie and co-workers reported a POSS supported (S)-α,α-diphenylprolinol trimethylsilyl ether as catalyst for asymmetric Michael addition reactions of aldehydes and arylnitroalkenes.

Very recently, Leng and co-workers developed a new heterogeneous catalyst by bridging an oxo-molybdenum Schiff base on a polyhedral oligomeric silsesquioxane (POSS) via covalent functionalization (Figure 20) for the epoxydation of alkenes.[91] They highlighted a higher catalytic activity than the corresponding un-supported and homogeneous compound (with the same number of the active sites), suggesting a catalytically promotional role of the POSS for the epoxydation reaction. They attributed the enhanced catalytic performance to the hydrophobic property of the POSS monomer.

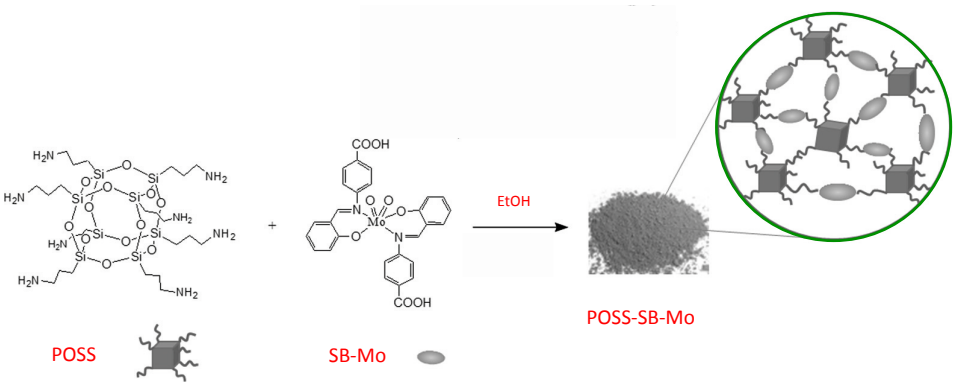

Figure 20. POSS-bridged oxo-molybdenum Schiff base catalyst.[91]

As mentioned above, because of the properties can be tuning in function of the organic moieties, POSS can be soluble in different reaction media. In particular, the same organic functions (such as imidazolium salts) could allow the solubility of the nano-systems in the reaction media and, on the other hand, could be catalytic active sites for reactions. This means that, in the field of catalysis, POSS may act as homogeneous macromolecular catalyst (general figure is reported in Figure 21).

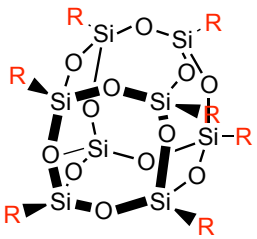

Figure 21. General representation of Octa-POSS with R functionalizations.

One of the main interests in this PhD thesis was to synthetize some materials based on supported ionic liquids (mono- and multi- layer) following the grafting process. In particular we focused our attention on two class of ionic liquids, imidazolium and thiazolium salts. In summary, there are large applications concerning the imidazolium salts because of their unique properties. The choice of imidazolium and thiazolium salts is related to their possible multifunctional applications, such as active species in catalysis, or as supported ionic liquids for stabilizing metal nanoparticles. Concerning the supports, we decide to investigate to different materials, such as a silica based materials (SBA-15), and carbon nanotubes (CNTs).

The catalytic activity of all the catalysts was tested for some reactions of relevant academic and industrial interest. One of these reactions is represented by the etherification reaction; actually we can found ethers in several compounds, as biologically active compounds, drugs, fragrances and in the diesel blends.

One of the most important reactions in industrial field is related to the conversion of carbon dioxide into useful products for industrial applications. To reach this objective, we investigated the catalytic performances of some of the compounds for the conversion of carbon dioxide with epoxide into the corresponding cyclic carbonates.

Then, we employed the organic-inorganic hybrid systems in order to stabilize palladium species which were consequently tested to catalyze C-C cross coupling reactions, such as Suzuki-Miyaura reactions and Heck reactions, which are useful transformations used for the synthesis of pharmaceutical or natural products or in the field of material chemistry.

1.9 References

1. J. Clark, D. Macquarrie, M. Gronnow, V. Budarin, Process Intensification for Green Chemistry, John Wiley & Sons, Ltd 2013, 33-58.
2. R. Höfer, M. Selig, Polymer Science: A Comprehensive Reference, ed. K. M. Möller, Elsevier 2012, 5-14.
3. P. T. Anastas, J. C. Warner, Green Chemistry: Theory and Practice, Oxford University, Press: New York 1998.
4. I. Chorkendorff, J. W. Niemantsverdriet, Concepts of modern catalysis and kinetics, John Wiley & Sons 2006.
5. a) S.-E. Park, E.-Y. Jeong, Bridging Heterogeneous and Homogeneous Catalysis: Concepts, Strategies, and Applications, Wiley-VCH 2014, 85-110; b) G. F. Swiegers, Mechanical Catalysis: Methods of Enzymatic, Homogeneous, and Heterogeneous Catalysis, John Wiley & Sons 2008, 37-54.
6. M. Gruttadauria, F. Giacalone, Catalytic methods in asymmetric synthesis: advanced materials, techniques and applications, Wiley 2011.
7. C. Baleizão, B. Gigante, H. Garcia, A. Corma, Journal of Catalysis 2003, 215, 199-207.
8. S. Iijima, Nature, 1991, 354, 56-58.
9. a) D. Tasis, N. Tagmatarchis, A. Bianco, M. Prato, Chemical Reviews 2006, 106, 1105-1136; b) K. Babooram, R. Narain, Chemistry of Bioconjugates: Synthesis, Characterization, and Biomedical Applications, First Edition, John Wiley & Sons, Inc. 2014, 239-252; c) M. Ghiazza, G. Vietti, I. Fenoglio, Carbon Nanotubes: properties, applications and toxicity 2014, 147-174.
10. G. D. Nessim, Nanoscale 2010, 2, 1306-1323.
11. a) R. H. Baughman, A. A. Zakhidov, W. A. de Heer, Science 2002, 297, 787; b) H. Ago, K. Petritsch, M. S. P. Shaffer, A. H. Windle, R. H. Friend, Advanced Materials 1999, 11, 1281-1285; c) A. Javey, J. Guo, Q. Wang, M. Lundstrom. H. J. Dai, Nature 2003, 424, 654-657; d) S. S. Fan, M. G. Chapline, N. R. Franklin, T. W. Tombler, A. M. Cassell, H. J. Dai, Science 1999, 283, 512-514; e) P. Serp, M. Corrias, P. Kalck, Applied Catalysis A: General 2003, 253, 337-358; f) P. Serp, E. Castillejos, ChemCatChem 2010, 2, 41-47.
12. a) L. Dai, A. W. H. Mau, Advanced Materials 2001, 13, 899-913; b) A. Hirsch, Angewandte Chemie International Edition 2002, 41, 1853-1859; c) J. L. Bahr, J. M. Tour, Journal of Materials Chemistry 2002, 12, 1952-1958; d) J. J. Davis, K. S. Coleman, B. R. Azamian, C. B. Bagshaw, M. L. H. Green, Chemistry - A European Journal 2003, 9, 3732-3739.
13. a) R. R. Bacsa, C. Laurent, A. Peigney, W. S. Bacsa, T. Vaugien, A. Rousset, Chemical Physics Letters 2000, 323, 566-571; b) F. Li, Y. Wang, D. Wang, F. Wei, Carbon 2004, 42, 2375-2383.
14. Y. Zhai, Y. Dou, D. Zhao, P. F. Fulvio, R. T. Maye, S. Dai, Advanced Materials 2011, 23, 4828-4850.
15. a) L. Rodríguez-Pérez, M. Teuma, A. Falqui, M. Gómez, P. Serp, Chemical Communications 2008, 4201-4203; b) X. Pan, Z. Fan, W. Chen, Y. Ding, H. Luo, X. Bao, Nature Materials 2007, 6, 507-511.
16. J. S. Beck, J. C. Vartuli, W. J. Roth, M. E. Leonowicz, C. T. Kresge, K. D. Schmitt, C. T.-W. Chu, D. H. Olson, E. W. Sheppard, S. B. McCullen, J. B. Higgins, J. L. Schlenker, Journal of the American Chemical Society 1992, 114, 10834-10843.
17. X. Ruren, P. Wenqin, Y. Jihong, H. Qisheng, C. Jiesheng, Chemistry of Zeolites and Related Porous Materials, Wiley 2007.
18. Y. Mathieu, M. Soulard, J. Patarin and M. Molière, Fuel Processing Technology

2012, 99, 35-42.
19. D. Wang, H. P. Jakobson, R. Kou, J. Tang, R. Z. Fineman, D. Yu, Y. Lu, Chemistry of Materials 2006, 18, 4231-4237.
20. a) C.-Y. Lai, B. G. Trewyn, D. M. Jeftinija, K. Jeftinija, S. Xu, S. Jeftinija, V. S.-Y. Lin, Journal of the American Chemical Society 2003, 125, 4451-4459; b) E. Climent, A. Bernardos, R. Martínez-Máñez, A. Maquieira, M. D. Marcos, N. Pastor-Navarro, R. Puchades, F. Sancenón, J. Soto, P. Amorós, Journal of the American Chemical Society 2009, 131, 14075-14080.
21. a) D. Zhao, J. Feng, Q. Huo, N. Melosh, G. H. Frederickson, B. F. Chmelka, G. D. Stucky, Science 1998, 279, 548-552; b) P. Llewellyn, Adsorption by Powders and Porous Solids, Elsevier Ltd 2014.
22. S. A. Bagshaw, E. Prouzet, T. J. Pinnavaia, Science 1995, 269, 1242-1244.
23. S. Inagaki, Studies in Surface Science and Catalysis 2004, 148, 109-132.
24. Q. Huo, D. I. Margolese, G. D. Stucky, Chemistry of Materials 1996, 8, 1147-1160.
25. a) A. Galarneau, H. Cambon, F. Di Renzo, F. Fajula, Langmuir 2001, 17, 8328-8335; b) A. Galarneau, N. Cambon, F. Di Renzo, R. Ryoo, M. Choi, F. Fajula, New Journal of Chemistry 2003, 27, 73-79.
26. K. Miyazawa, S. Inagak, Chemical Communication 2000, 2121-2122.
27. a) E. Da'na, N. De Silva, A. Sayari, Chemical Engineering Journal 2011, 166, 454-459; b) A. Shahbazi, H. Younesi, A. Badiei, Chemical Engineering Journal 2011, 168, 505-518; c) L. Hajiaghababaei, B. Ghasemi, A. Badiei, H. Goldooz, M. R. Ganjali, G. M. Ziarani, Journal of Environmental Sciences 2012, 24, 1347-1354; d) M. B. Yue, Y. Chun, Y. Cao, X. Dong, J. H. Zhu, Advanced Functional Materials 2006, 16, 1717-1722.
28. a) M. Hosseini, V. K. Gupta, M. R. Ganjali, Z. Rafiei-Sarmazdeh, F. Faridbod, H. Goldooz, A. R. Badiei, P. Norouzi, Analytica Chimica Acta 2012, 715, 80-85; b) M. R. Ganjali, V. K. Gupta, M. Hosseini, Z. Rafiei-Sarmazdeh, F. Faridbod, H. Goldooz, A. R. Badiei, P. Norouzi, Talanta 2012, 88, 684-688.
29. a) A. Katiyar, S. Yadav, P. G. Smirniotis, N. G. Pinto, Journal of Chromatography A 2006, 1122, 13-20; b) S. W. Song, K. Hidajat, S. Kawi, Langmuir 2005, 21, 9568-9575; c) E. Basaldella, M. Legnoverde, J. Sol-Gel Sci. Technol. 2010, 56, 191-196; d) H. H. P. Yiu, C. H. Botting, N. P. Botting, P. A. Wright, Physical Chemistry Chemical Physics 2001, 3, 2983-2985; e) F. Sevimli, A. Yılmaz, Microporous and Mesoporous Materials 2012, 158, 281-291; f) D. Hwang, D. Lee, H. Lee, D. Choe, S. Lee, K. Lee, Korean J. Chem. Eng. 2010, 27, 1087-1092.
30. S. Perathoner, P. Lanzafame, R. Passalacqua, G. Centi, R. Schlögl, D. S. Su, Microporous and Mesoporous Materials 2006, 90, 347-361.
31. a) V. Fornés, C. López, H. H. López, A. Martínez, Applied Catalysis A: General 2003, 249, 345-354; b) M. Piumetti, B. Bonelli, P. Massiani, S. Dzwigaj, I. Rossetti, S. Casale, M. Armandi, C. Thomas, E. Garrone, Catalysis Today 2012, 179, 140-148; c) A. E. Barrón Cruz, J. A. Melo Banda, H. Mendoza, C. E. Ramos-Galvan, M. A. Meraz Melo, D. Esquivel, Catalysis Today 2011, 166, 111-115; d) P. Liu, C.-Y. Zhou, S. Xiang, C.-M. Che, Chemical Communications 2010, 46, 2739-2741; e) B. Karimi, E. Badreh, Organic & Biomolecular Chemistry 2011, 9, 4194-4198; f) J. Moreno, J. Iglesias, J. A. Melero, D. C. Sherrington, Journal of Materials Chemistry 2011, 21, 6725-6735; g) Á. Reyes-Carmona, R. Moreno-Tost, J. Mérida-Robles, J. Santamaría-González, P. Maireles-Torres, A. Jiménez-López, E. Moretti, M. Lenarda, E. Rodríguez-Castellón, Adsorption 2011, 17, 527-538; h) J. Guan, B. Liu, X. Yang, J. Hu, C. Wang, Q. Kan, ACS Sustainable Chemistry & Engineering 2014, 2, 925-933; j) T. Joseph, S. S. Deshpande, S. B. Halligudi, A. Vinu, S. Ernst, M. Hartmann, Journal of Molecular Catalysis A: Chemical 2003,

206, 13-21; k) J. Zheng, H. Lin, X. Zheng, X. Duan, Y. Yuan, Catalysis Communications 2013, 40, 129-133; l) J. Bassil, A. AlBarazi, P. Da Costa, M. Boutros, Catalysis Today 2011, 176, 36-40; m) H. H. P. Yiu, P. A. Wright, N. P. Botting, Journal of Molecular Catalysis B: Enzymatic 2001, 15, 81-92.

32. a) A. De, M. Dewan, S. Mozumdar, Advanced Sensor and Detection Materials, Scrivener Publishing LLC 2014, 309-368; b) T. Welton, Coordination Chemistry Reviews 2004, 248, 2459-2477; c) B. Kirchner, Ionic Liquids, Springer 2009.
33. T. Welton, Chemical Reviews 1999, 99, 2071-2083.
34. H. Zhao, S. Xia, P. Ma, Journal of Chemical Technology and Biotechnology 2005, 80, 1089-1096.
35. P. Bonhôte, A.-P. Dias, N. Papageorgiou, K. Kalyanasundaram, M. Grätzel, Inorganic Chemistry 1996, 35, 1168-1178; b) H. Weingärtner, Angewandte Chemie International Edition 2007, 47, 654-670.
36. N. V. Plechkova, K. R. Seddon, Chemical Society Reviews 2008, 37, 123-150.
37. a) J. H. Davis Jr, Chemistry Letters 2004, 33, 1072-1077; b) R. Giernoth, Angewandte Chemie International Edition 2010, 49, 2834-2839; c) C. Chiappe, C. S. Pomelli, European Journal of Organic Chemistry 2014, 2014, 6120-6139; d) S.-G. Lee, Chemical Communications 2006, 1049-1063; e) J. H. Davis Jr, K. J. Forrester, Tetrahedron Letters 1999, 40, 1621-1622; f) J. H. Davis Jr, K. J. Forrester, T. Merrigan, Tetrahedron Letters, 1998, 39, 8955-8958.
38. a) C. S. Consorti, P. A. Z. Suarez, R. F. de Souza, R. A. Burrow, D. H. Farrar, A. J. Lough, W. Loh, L. H. M. da Silva, J. Dupont, The Journal of Physical Chemistry B 2005, 109, 4341.
39. a) R. Sheldon, Chemical Communications 2001, 2399-2407; b) J. Dupont, R. F. de Souza, P. A. Z. Suarez, Chemical Reviews 2002, 102, 3667-3692; c) N. Jain, A. Kumar, S. Chauhan, S. M. S. Chauhan, Tetrahedron 2005, 61, 1015-1060; d) Š. Toma, R. Šebesta, in Ionic Liquids in Biotransformations and Organocatalysis, John Wiley & Sons, Inc., 2012, 331-359; e) K. Vijayakrishna, K. Manojkumar, A. Sivaramakrishna, in Applications of Ionic Liquids in Polymer Science and Technology, Springer Berlin Heidelberg, 2015, 355-387; f) A. K. Prasad, V. Kumar, S. Malhotra, V. T. Ravikumar, Y. S. Sanghvi, V. S. Parmar, Bioorganic & Medicinal Chemistry 2005, 13, 4467-4472. g) K. Kumari, P. Singh, G. K. Mehrotra, International Journal of Green Nanotechnology 2012, 4, 262-276; h) J. Muzart, Advanced Synthesis & Catalysis 2006, 348, 275-295.
40. P. Kotrusz, I. Kmentova, B. Gotov, S. Toma, E. Solcaniova, Chemical Communications 2002, 2510-2511.
41. K. Hong, H. Zhang, J. W. Mays, A. E. Visser, C. S. Brazel, J. D. Holbrey, W. M. Reichert, R. D. Rogers, Chemical Communications 2002, 1368-1369.
42. R. P. Swatloski, S. K. Spear, J. D. Holbrey, R. D. Rogers, Journal of the American Chemical Society 2002, 124, 4974-4975.
43. a) J. Blatha, N. Deubler, T. Hirtha, T. Schiestel, Chemical Engineering Journal 2012, 181, 152-158; b) E. D. Bates, R. D. Mayton, I. Ntai, J. H. Davis, Journal of the American Chemical Society, 2002, 124, 926-927.
44. N. Iranpoor, H. Firouzabadi, R. Azadi, Tetrahedron Letters 2006, 47, 5531-5534.
45. N. Muhammad, Y. A. Elsheikh, M. I. A. Mutalib, A. A. Bazmi, R. A. Khan, H. Khan, S. Rafiq, Z. Man, I. khan, Journal of Industrial and Engineering Chemistry 2015, 21, 1-10.
46. a) R. Ratti, Advances in Chemistry 2014, 2014, 16; b) A. K. Chakraborti, S. R. Roy, Journal of the American Chemical Society 2009, 131, 6902-6903; c) X. Li, D. Zhao, Z. Fei, L. Wang, Science in China series B: Chemistry 2006, 49, 385-401; d) D. Zhao, M. Wu, Y. Kou, E. Min, Catalysis Today 2002, 74, 157-189; e) V. I.

Pârvulescu, C. Hardacre, Chemical Reviews 2007, 107, 2615-2665.
47. F. Zhou, A. Izgorodin, R. K. Hocking, L. Spiccia, D. R. MacFarlane, Advanced Energy Materials 2012, 2, 1013-1021.
48. a) N. Byrne, P. C. Howlett, D. R. MacFarlane, M. Forsyth, Advanced Materials 2005, 17, 2497-2501; b) S. Seki, Y. Kobayashi, H. Miyashiro, Y. Ohno, A. Usami, Y. Mita, M. Watanabe, N. Terada, Chemical Communications 2006, 5, 544-545.
49. W. Yang, H. Cang, Y. Tang, J. Wang, Y. Shi, Journal of Applied Electrochemistry 2008, 38, 537-542.
50. a) Y. Cao, J. Zhang, Y. Bai, R. Li, S. M. Zakeeruddin, M. Grätzel, P. Wang, The Journal of Physical Chemistry C 2008, 112, 13775-13781; b) D. Kuang, S. Uchida, R. Humphry-Baker, S. M. Zakeeruddin, M. Grätzel, Angewandte Chemie International Edition 2008, 47, 1923-1927; c) P. Wang, S. M. Zakeeruddin, J.-E. Moser, M. Grätzel, The Journal of Physical Chemistry B 2003, 107, 13280-13285.
51. G. Gebresilassie Eshetu, M. Armand, B. Scrosati, S. Passerini, Angewandte Chemie International Edition 2014, 53, 13342-13359.
52. M. Armand, F. Endres, D. R. MacFarlane, H. Ohno, B. Scrosati, Nat Mater 2009, 8, 621-629.
53. a) J. Scholz, M. Haumann, Nanomaterials in Catalysis, Wiley-VCH Verlag GmbH & Co. KGaA 2013, 251-280; b) B. Xin, J. Hao, Chemical Society Reviews 2014, 43, 7171-7187; c) C. P. Mehnert, Chemistry - A European Journal 2005, 11, 50-56.
54. C. De Castro, E. Sauvage, M. H. Valkenberg, W. F. Hölderich, Journal of Catalysis 2000, 196, 86-94.
55. C. P. Mehnert, R. A. Cook, N. C. Dispenziere, M. Afeworki, Journal of the American Chemical Society 2002, 124, 12932-12933.
56. a) D. W. Kim, D. Y. Chi, Angewandte Chemie International Edition 2004, 43, 483-485; b) W. Chen, Y. Zhang, L. Zhu, J. Lan, R. Xie, J. You, Journal of the American Chemical Society 2007, 129, 13879-13886.
57. K. B. Sidhpuria, A. L. Daniel-da-Silva, T. Trindade, J. A. P. Coutinho, Green Chemistry 2011, 13, 340-349.
58. a) U. Kernchen, B. Etzold, W. Korth, A. Jess, Chemical Engineering & Technology 2007, 30, 985-994; b) J. Arras, E. Paki, C. Roth, J. Radnik, M. Lucas, P. Claus, The Journal of Physical Chemistry C 2010, 114, 10520-10526; c) J. Arras, M. Steffan, Y. Shayeghi, D. Ruppert, P. Claus, Green Chemistry 2009, 11, 716-723.
59. V. Sans, N. Karbass, M. I. Burguete, V. Compañ, E. García-Verdugo, S. V. Luis, M. Pawlak, Chemistry - A European Journal 2011, 17, 1894-1906.
60. J.-F. Wei, J. Jiao, J.-J. Feng, J. Lv, X.-R. Zhang, X.-Y. Shi, Z.-G. Chen, The Journal of Organic Chemistry 2009, 74, 6283-6286.
61. a) M. Gruttadauria, L. F. Liotta, A. M. P. Salvo, F. Giacalone, V. La Parola, C. Aprile, R. Noto, Advanced Synthesis & Catalysis 2011, 353, 2119-2130; b) C. Pavia, E. Ballerini, L. A. Bivona, F. Giacalone, C. Aprile, L. Vaccaro, M. Gruttadauria, Advanced Synthesis & Catalysis 2013, 355, 2007-2018; c) C. Pavia, F. Giacalone, L. A. Bivona, A. M. P. Salvo, C. Petrucci, G. Strappaveccia, L. Vaccaro, C. Aprile, M. Gruttadauria, Journal of Molecular Catalysis A: Chemical 2014, 387, 57-62.
62. A. Pourjavadi, S. H. Hosseini, S. S. Amin, Chemical Engineering Journal 2014, 247, 85-92.
63. a) P. Migowski, J. Dupont, Chemistry European Journal 2007, 13, 32-39; b) C. J. Serpell, J. Cookson, A. L. Thompson, C. M. Brown, P. D. Beer, Dalton Transactions 2013, 42, 1385-1383.
64. H. Hagiwara, Synlett 2012, 23, 837-850.
65. C. Vollmer, C. Janiak, Coordination Chemistry Reviews 2011, 255, 2039-2057.

66. a) J. Dupont, J. D. Scholten, Chemical Society Reviews 2010, 39, 1780-1804; b) M.-A. Neouze, Journal of Materials Chemistry 2010, 20, 9593-9607.
67. E. Redel, R. Thomann, C. Janiak, Inorganic Chemistry 2008, 47, 14-16.
68. E. Redel, R. Thomann, C. Janiak, Chemical Communications 2008, 1789-1791.
69. F. Bernardi, J. D. Scholten, G. H. Fecher, J. Dupont, J. Morais, Chemical Physics Letters 2009, 479, 113-116.
70. a) H. S. Schrekker, M. A. Gelesky, M. P. Stracke, C. M. L. Schrekker, G. Machado, S. R. Teixeira, J. C. Rubim, J. Dupont, Journal of Colloid and Interface Science 2007, 316, 189-195; b) L. S. Ott, M. L. Cline, M. Deetlefs, K. R. Seddon, R. G. Finke, Journal of the American Chemical Society 2005, 127, 5758-5759; c) S. Özkar, R. G. Finke, Journal of the American Chemical Society, 2002, 124, 5796-5810.
71. Z. Li, A. Friedrich, A. Taubert, Journal of Materials Chemistry 2008, 18, 1008-1014.
72. M. A. Firestone, M. L. Dietz, S. Seifert, S. Trasobares, D. J. Miller, N. J. Zaluzec, Small 2005, 1, 754-760.
73. M. I. Burguete, E. García-Verdugo, I. Garcia-Villar, F. Gelat, P. Licence, S. V. Luis, V. Sans, Journal of Catalysis 2010, 269, 150-160.
74. B. Karimi, D. Elhamifar, J. H. Clark, A. J. Hunt, Chemistry – A European Journal 2010, 16, 8047-8053.
75. A. Kirschning, W. Solodenko, K. Mennecke, Chemistry - A European Journal 2006, 12, 5972-5990.
76. P. P. Pescarmona, T. Maschmeyer, Australian Journal of Chemistry 2001, 54, 583-596.
77. a) O. I. Shchegolikhina, Y. A. Pozdnyakova, Y. A. Molodtsova, S. D. Korkin, S.S. Bukalov, L. A. Leites, K. A. Lyssenko, A. S. Peregudov, N. Auner, D. E. Katsoulis, Inorganic Chemistry 2002, 41, 6892; b) C. Zucchi, M. Mattioli, A. Cornia, A. C. Fabretti, G. Gavioli, M. Pizzardi, R. Ugo, O. I. Shchegolikhina, A. A. Zhdanov, G. Palyi, Inorganica Chimica Acta 1998, 280, 282.
78. R. H. Baney, M. Itoh, A. Sakakibara, T. Suzuki, Chemical Reviews 1995, 95, 1409-1430.
79. P. P. Pescarmona, C. Aprile, S. Swaminathan, in New and Future Developments in Catalysis (Ed.: S. L. Suib), Elsevier, Amsterdam, 2013, 385-422.
80. a) A. Provatas, M. Luft, J. C. Mu, A. H. White, J. G. Matisons, B. W. Skelton, Journal of Organometallic Chemistry 1998, 565, 159-164; b) G. Li, L. Wang, H. Ni, C. U. Pittman, Journal of Inorganic and Organometallic Polymers 2001, 11, 123-151; c) R. M. Laine, Journal of Materials Chemistry 2005, 15, 3725-3744; d) P. D. Lickiss, F. Rataboul, Advances in Organometallic Chemistry 2008, 57, 1-116; e) D. B. Cordes, P. D. Lickiss, F. Rataboul, Chemical Reviews 2010, 10, 2081-2173; f) S. H. Phillips, T. S. Haddad, S. J. Tomczak, Current Opinion in Solid State and Materials Science 2004, 8, 21-29.
81. a) K. Tanaka, Y. Chujo, Bulletin of the Chemical Society of Japan 2013, 86, 1231-1239; b) M. Lo Conte, S. Staderini, A. Chambery, N. Berthet, P. Dumy, O. Renaudet, A. Marra, A. Dondoni, Organic & Biomolecular Chemistry 2012, 10, 3269; c) J. Wu, P. T. Mather, Polymer Reviews, 2009, 49, 25-63.
82. M. Čolović, I. Jerman, M. Gaberšček, B. Orel, Solar energy materials & Solar Cells 2011, 95, 3472-3481.
83. a) W. Zhang, J. Li, S. Jiang, Z.-S. Wang, Chemical Communications 2014, 50, 1685-1687; b) W. Zhang, Z.-S. Wang, ACS Applied Materials & Interfaces 2014, 6, 10714-10721.

84. B. J. Hendan, H. C. Marsmann, Applied Organometallic Chemistry 1999, 13, 287-294.
85. M. Seino, W. Wang, J. E. Lofgreen, D. P. Puzzo, T. Manabe, G. A. Ozin, Journal of the American Chemical Society 2011, 133, 18082-18085.
86. a) Y.-C. Sheen, C.-H. Lu, C.-F. Huang, S.-W. Kuo, F.-C. Chang, Polymer 2008, 49, 4017-4024; b) S.-W. Kuo, F.-C. Chang, Progress in Polymer Science 2011, 36, 1649-1696.
87. B. Liang, Y. P. Liu, S. Q. Tang, Y. Q. Lai, Y. X. Liu, Zhongguo Youse Jinshu Xuebao/Chinese Journal of Nonferrous Metals 2013, 23, 2851-2862.
88. L. Cui, D. Chen, L. Zhu, ACS Nano 2008, 2, 921-927.
89. J. Tan, D. Ma, X. Sun, S. Feng, C. Zhang, Dalton Transactions 2013, 42, 4337-4339.
90. a) S. Sakugawa, K. Wada, M. Inoue, Journal of Catalysis 2010, 275, 280-287; b) E. S. Cozza, V. Bruzzo, F. Carniato, E. Marsano, O. Monticelli, ACS Applied Materials & Interfaces 2012, 4, 604-607; c) M. Janssen, J. Wilting, C. Müller, D. Vogt, Angewandte Chemie International Edition 2010, 49, 7738-7741; d) S. Tang, R. Jin, H. Zhang, H. Yao, J. Zhuang, G. Liu, H. Li, Chemical Communications 2012, 48, 6286-6288; e) Y. Leng, J. Liu, C. Zhang, P. Jiang, Catalysis Science & Technology 2014, 4, 997-1004; f) C.-H. Lu, F.-C. Chang, ACS Catalysis 2011, 1, 481-488; g) Y. Leng, J. Liu, P. Jiang, J. Wang, ACS Sustainable Chemistry & Engineering 2015, 3, 170-176; h) W. Zheng, C. Lu, G. Yang, Z. Chen, J. Nie, Catalysis Communications 2015, 62, 34-38.
91. Y. Leng, J. Liu, C. Zhang, P. Jiang, Catalysis Science & Technology 2014, 4, 997-1004.

Chapter 2

Objectives

Chapter 2

Objectives

The main objective of this PhD thesis is focused on the synthesis of hybrid organic-inorganic catalysts based on imidazolium and thiazolium salts. We focused our attention on the development and the study of new materials and compounds which could act as catalysts for some interesting reactions, such as etherification reactions and the conversion of carbon dioxide. In addition, some of these materials can be employed as supports for metal catalysts and tested for some C-C bond forming reactions (Suzuki-Miyaura and Mizoroki-Heck reactions).
During this thesis, all the catalysts were extensively characterized in order to well understand their structure and then, to explain their catalytic behaviour.
Concerning the catalytic applications, this PhD thesis can be divided into two parts: the first one related to the application of the catalysts in heterogeneous conditions (Chapters 3, 4 and 5), whereas the second one is associated to the application of the catalysts in homogeneous phase (Chapters 6 and 7).

The catalysts involved in the heterogeneous reactions (first section) are constituted by multilayered covalently supported thiazolium or imidazolium based mesoporous materials (**SBA-15-Thia** and **SBA-15-Imi**, Chapter 3), palladium supported highly loaded thiazolidine based on mesostructured silica materials (**SBA-15-Thiazolidine-Pd**, Chapter 4) and mono- or multi- layer imidazolium functionalized carbon nanotubes (**S-Imi-NT** and **bV-Imi-NT**, Chapter 5). A graphical illustration of these catalysts is reported in the Figure 1.

The following part is focused on the application of some hybrid organic-inorganic compounds in homogeneous conditions. These systems are represented by the polyhedral oligomeric silsesquioxane (POSS) functionalized with imidazolium units, with chloride (**POSS-Imi**, Chapter 6) or tetrachloropalladate (**POSS-Imi-PdCl$_4$**, Chapter 7) as anions, in function of their application (Figure 2).

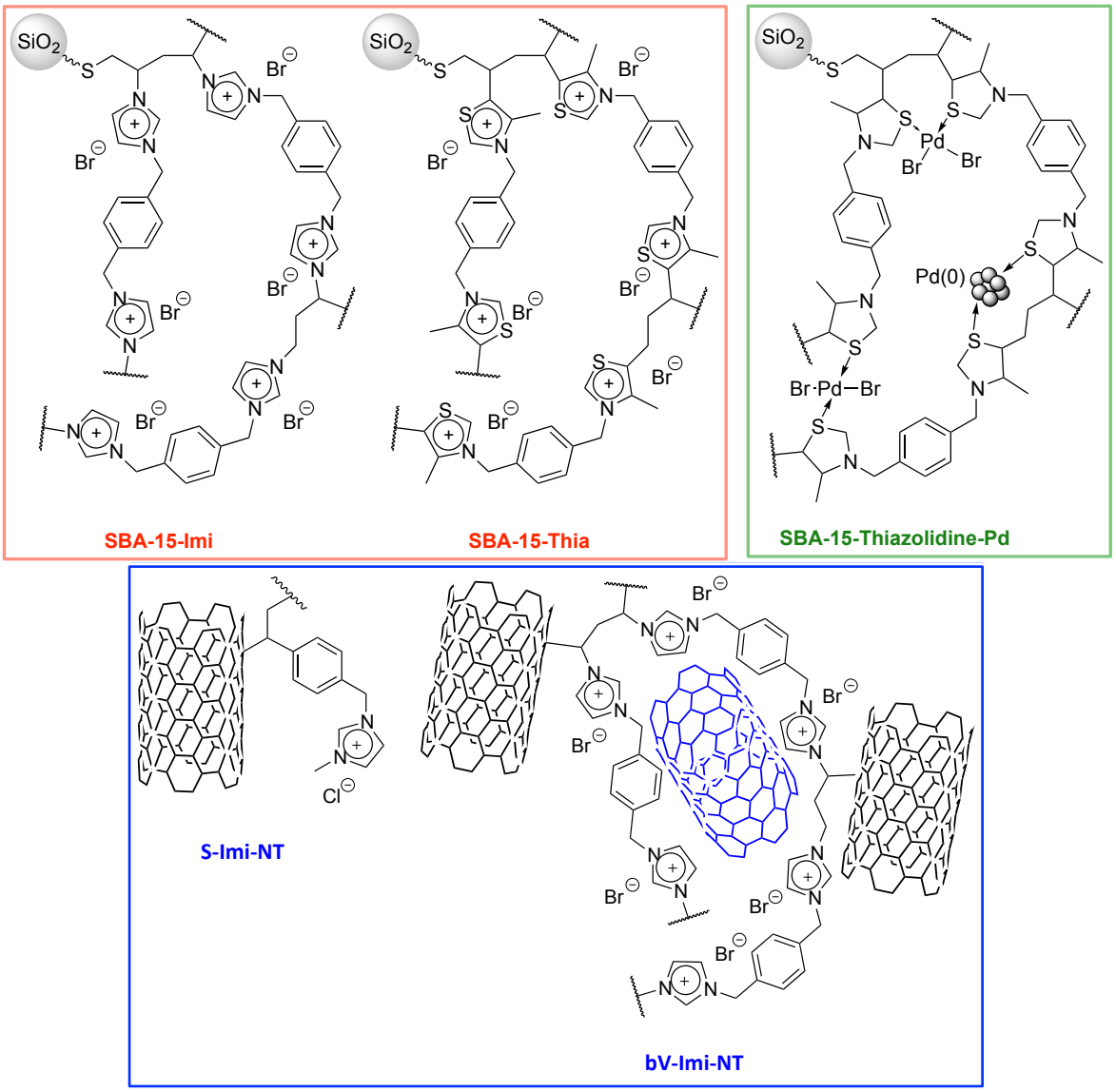

Figure 1. Schematic representation of the catalysts for heterogeneous reactions.

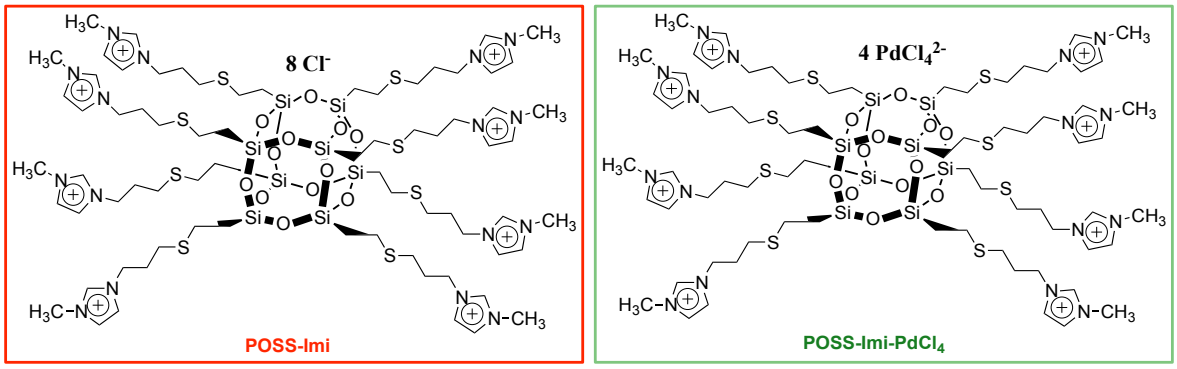

Figure 2. Schematic representation of the catalysts for homogeneous reactions.

Chapters 3 to 5

Foreword

Chapters 3 to 5

Foreword

Supported ionic liquids have found important applications in the field of catalysis. The advantage of the heterogeneized catalytic systems based on supported ionic liquids, compared to the corresponding homogeneous analogous, is mainly related to the easily separation from the reaction mixture, and as well as to the possibility to use them in fixed bed reactors.

In the first three chapters of the results and discussion, the synthesis and the catalytic applications of novel thiazolium and imidazolium salts based materials is presented. The difference in the three sections is represented by nature of the heteroaromatic salts (imidazolium or thiazolium) or by the selected support as well as by their applications.
In specific, high loaded imidazolium and thiazolium based mesoporous materials (**SBA-15-Thia** and **SBA-15-Imi**) were tested for etherification reactions, moreover the thiazolium SBA-15 mesostructured material was not only used as catalyst but also to form a new highly loaded thiazolidine based material employed as support for palladium catalysts (**SBA-15-Thiazolidine-Pd**) for Suzuki-Miyaura and Heck reactions.
Another and interesting material used as support in catalysis is represented by carbon nanotubes. These materials can be functionalized with imidazolium salts forming a mono- or multilayer of imidazolium networks around the nanotubes (**S-Imi-NT** and **bV-Imi-NT**). The last catalysts were tested for one attractive reaction: the conversion of carbon dioxide.

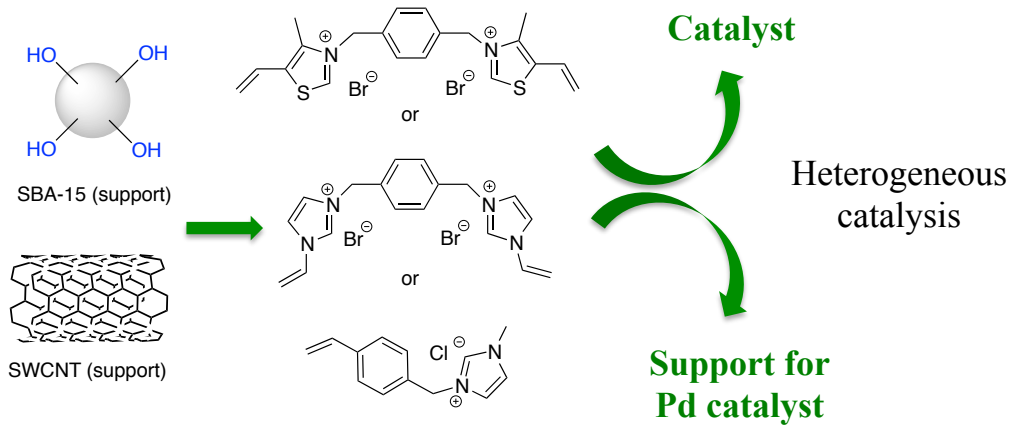

Figure 1. Schematic representation of the catalysts for applications in heterogeneous reactions.

Chapter 3

Thiazolium-based catalysts for the etherification of benzylic alcohols under solvent-free conditions

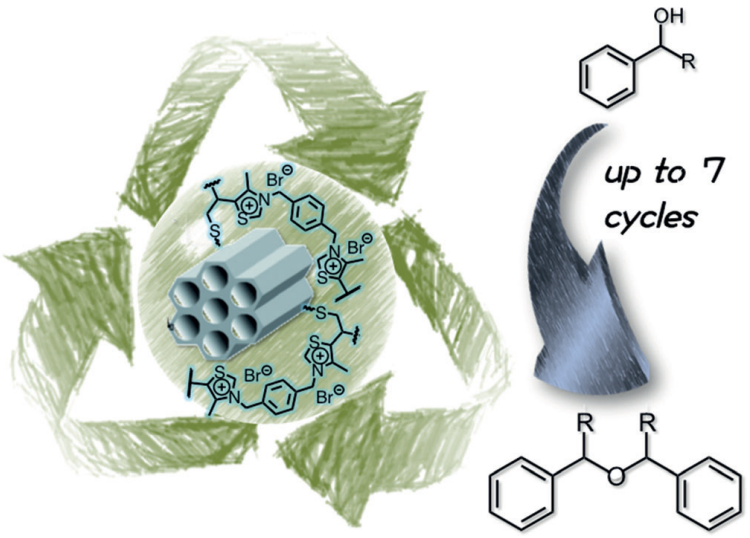

Chapter 3

This chapter is based on: L. A. Bivona, F. Quertinmont, H. A. Beejapur, F. Giacalone, M. Buaki-Sogo, M. Gruttadauria, C. Aprile, Advanced Synthesis & Catalysis, 2015, 357, 800-810.

Thiazolium-based catalysts for the etherification of benzylic alcohols under solvent-free conditions

3.1 Introduction

The development of innovative and efficient active materials plays a central role in the field of catalysis. The design of an ideal heterogeneous catalyst should fulfill a series of requirements such as high surface area, good amount of accessible active sites, no or low diffusion limitation of reactants and products, thermal and chemical stability at selected reaction conditions. Among all the existing catalytic processes, carbon-oxygen bond forming reaction is one of the most important transformations at both laboratory and industrial scale. Ethers are largely employed as biologically active compounds and drugs,[1] fragrances[2] and solvents. Moreover, they can find application in gasoline and diesel blends.[3,4] One of the most commonly used approach for the preparation of ethers, the Williamson reaction,[5] presents as major drawback the use of hard bases that can lead to the formations of salts as by-products and restrict the applicability to selected class of ethers non containing base sensitive functionalities.[5-7] An alternative methodology is represented by the use of Lewis acid catalysts.[8-10] The principal limitation of this synthesis protocol is represented by the decomposition of the Lewis acid caused by the water generated during the reaction. Recently, Firouzabadi and co-workers reported the etherification of different classes of alcohols using catalytic amounts of the heteropolyacid $AlPW_{12}O_{40}$.[11] Even though this catalyst is water tolerant, it was used in addition to organic toxic solvents such as the 1,2-dichloroethane. Reductive etherification from carbonyl compounds can be achieved using organosilanes and Lewis acid catalysts such as $BiCl_3$[12] or $FeCl_3$.[13] Also in this case, a large amount of acid catalyst is required due to its partial decomposition during the reaction. Very recently, Roth *et al.* reported a direct reductive synthesis of several ethers through a combination of organosilanes and triflic acid.[14] Although these methods are efficient, the use of silanes is not considered a valid alternative since some of them can

release toxic SiH_4 gas.[15] Alternative route have been investigated, e.g. the use of UV irradiation,[16] dimethyl sulfoxide,[17] and phase-transfer catalyst.[18-21] Elegant catalytic methods for etherification reactions are represented by the use of transition metals.[22-26] In addition, Argouarch and co-workers reported a reductive etherification of aldehydes photocatalyzed by iron complexes.[27] Abu-Omar *et al.* demonstrated a direct method to prepare symmetric and asymmetric ethers under mild homogeneous conditions employing palladium (II) catalysts. Complexes of this metal show a high selectivity for etherification of secondary alcohols, although they are used in combination with silver triflate.[28] Pale and co-workers investigated a series of transition metals for the formation of biphenyl methyl ethers, [29,30] using $PdCl_2$, AuCl, $CuCl_2$, $NaAuCl_4$.[31] In most of cases, the methods based on transition metal catalysts display good performances, however the homogeneous conditions used and the elevate price of the metals limit their large scale applications. From what reported, it appears evident that the development of new methods to obtain a large variety of ethers, or the improvement of the existing strategies in order to increase the yield and selectivity, is still of major interest. Ionic liquids recently emerged as a novel class of compounds with multiple possible uses from alternative "green" reaction media to active molecules in catalytic reactions.[32] Supported ionic liquid phase (SILP) or supported ionic liquid-like phase (SILLP) are a class of materials that have interesting applications. These systems compared to corresponding homogeneous ionic liquid phase show the general advantages of the easy separation, recyclability, and can be potentially applied in continuous processes.[33-35] It is worth to note that immobilized ionic liquids can be considered as an advanced class of heterogeneous catalysts since they combine some of the properties of the pure ionic liquids to the characteristics of a solid support. Herein, we investigate the use of supported imidazolium and thiazolium salts as catalysts for the etherification of benzylic alcohols. Recently, we have reported the synthesis and use of a new kind of SILLP materials, the multilayered covalently linked imidazolium salts on silica gel (mlc-SILLP). These materials were employed as catalysts [36,37] or as supports for catalysts.[38-41] In the present work, we have used such approach in order to prepare two different materials based on multilayered covalently-linked imidazolium or thiazolium salts on SBA-15 mesostructured silica. The two materials were prepared in order to study the influence of the N-heterocyclic moiety on the reaction. To the best of our knowledge, this is the first time that a multilayered covalently supported imidazolium or thiazolium-based material has been reported as catalyst for the synthesis of ethers. In particular, the use of thiazolium-based catalyst represents a novelty for the target reaction.

3.2 Results and Discussion

In order to study the influence of the N-heterocyclic moiety, two different materials were synthesized (Scheme 1). The syntheses of the heterogeneous organocatalysts bearing either imidazolium or thiazolium active sites (**SBA-15-Imi** and **SBA-15-Thia**, respectively) were successfully accomplished by grafting the corresponding bis-vinyl salts (**bV-Imi** or **bV-Thia**) on a thiol-functionalized SBA-15 silica (Scheme 1). The presence of the bis-vinyl functionalities allows the formation of the multilayer cross-linked organic shell *via* a well-established synthetic mechanism: one of the double bonds reacts through a thiol-ene coupling with the thiol group of the mesoporous support ensuring the covalent anchoring, and the other may undergo self-addition reactions generating the oligomeric/polymeric network. This second process is favored by the large excess of the imidazolium or thiazolium salt in the reaction mixture. The two materials were extensively characterized by N_2 physisorption, transmission electron microscopy, X-ray diffraction, ^{29}Si and ^{13}C magic angle spinning (MAS)-NMR.

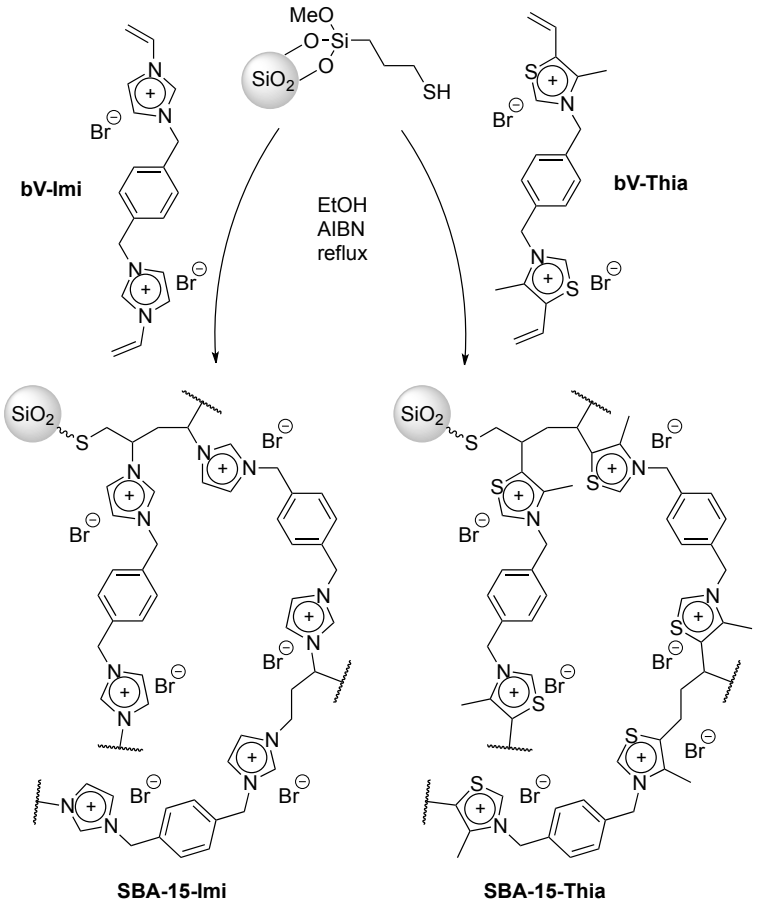

Scheme 1. Synthesis of of **SBA-15-Imi** and **SBA-15-Thia**.

Table 1. BET specific surface area and cumulative pore volume of supports.

Entry	Support	BET surface area [$m^2\ g^{-1}$]	Cumulative pore volume [$cm^3\ g^{-1}$]	Loading of Thia or Imi [mmol g^{-1}][a]
1	**SBA-15**	911	1.18	-
2	**SBA-15-SH**	675	0.86	-
3	**SBA-15-Thia**	129	0.17	2.46
4	**SBA-15-Imi**	145	0.18	2.32

[a] Loading of Thia or Imi: loading of thiazolium or imidazolium moiety, calculated by nitrogen data in elemental analysis.

Nitrogen adsorption/desorption measurements, performed on all samples (Supporting Information, section A.1, Figures S1 to S4) evidenced a progressive decrease of the surface area with the functionalization (see Table 1), accompanied by a reduction of the pore volume. This expected behavior can be ascribed to the coating of the silica support by the polymeric matrix and the partial filling of the mesopores. The unreacted monomers or oligomers eventually adsorbed on the surface were removed by consecutive washing with hot methanol and soxhlet extraction of the final solids.

The transmission electron microscopy (TEM) investigation evidenced the presence of the typical mesoporous structure in the SBA-15 as well as the formation of a polymeric shell covering the particles in the final solid (Figure 1).

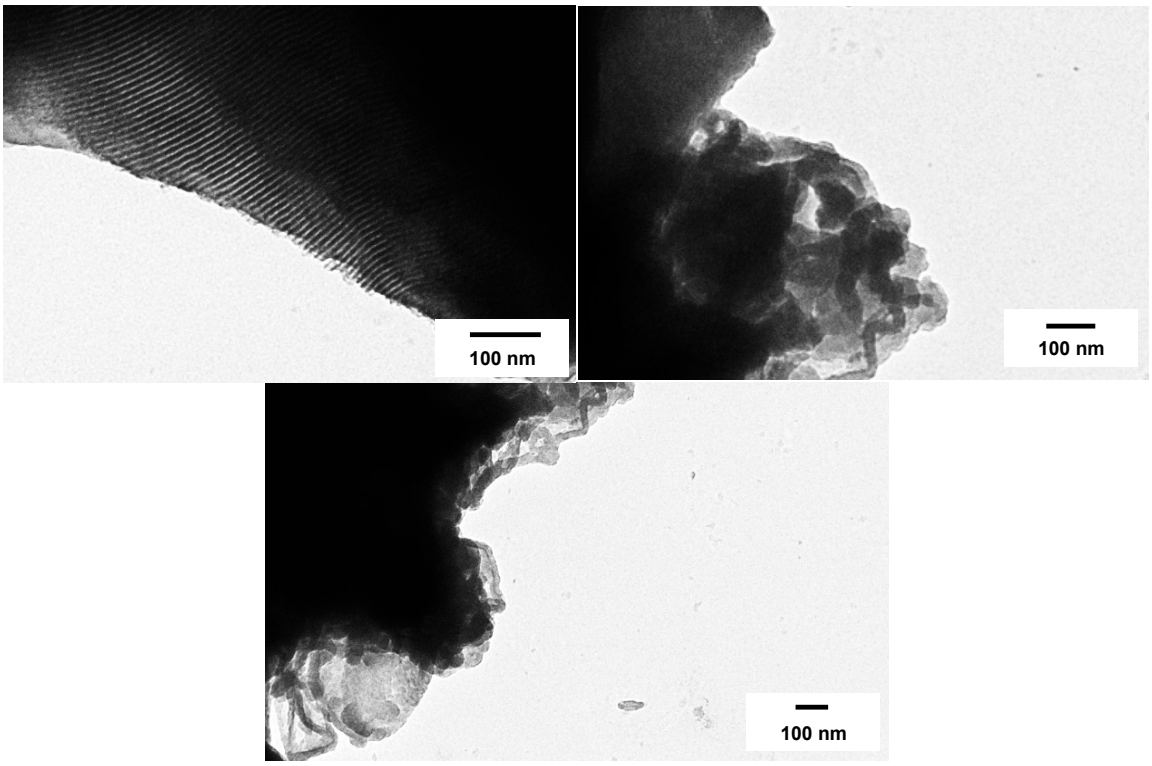

Figure 1. Transmission electron microscopy of **SBA-15-Thia**.

Solid state ^{29}Si MAS-NMR characterization confirmed the good degree of condensation leading to the formation of Si-O-Si bonds in the SBA-15 material as well as the covalent anchoring of the 3-mercaptopropyltrimethoxysilane with the appearance of T2 and T1 signals (Figure 2a).

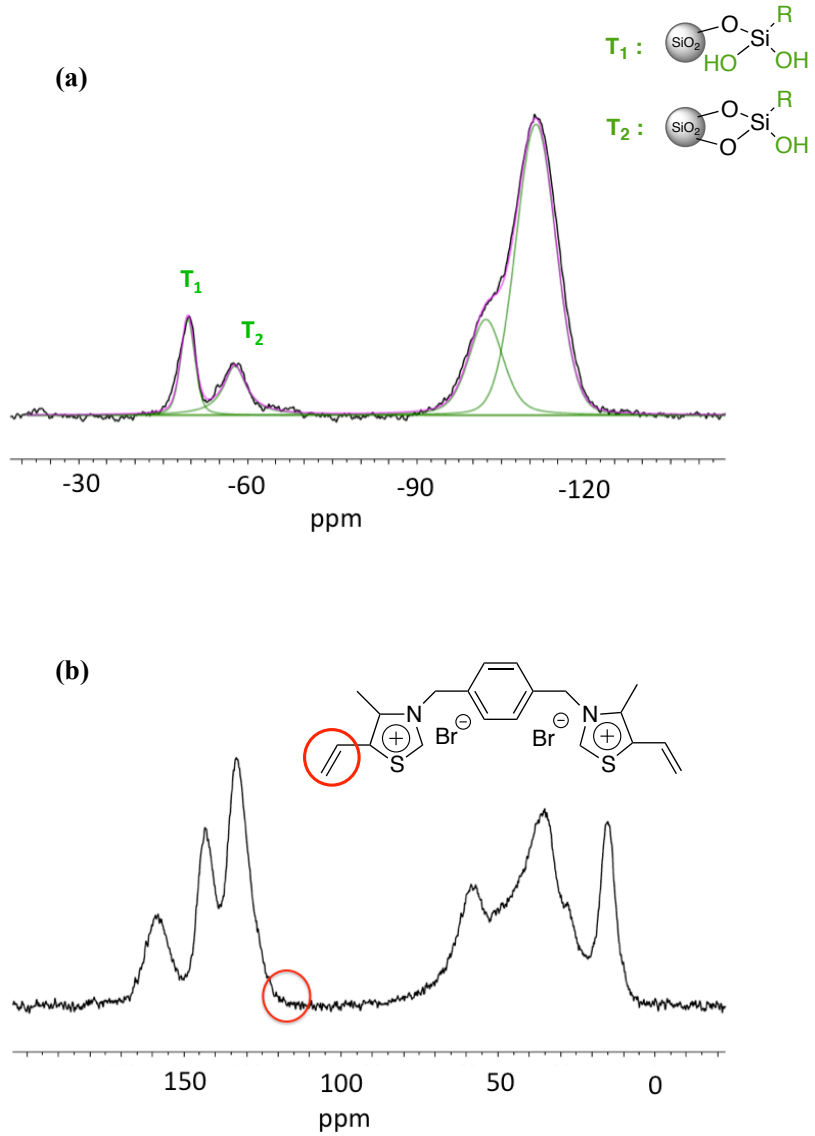

Figure 2. a) Solid state ^{29}Si MAS NMR spectrum (99 MHz) of **SBA-15-SH**; b) Solid state ^{13}C MAS NMR spectrum (125 MHz) of **SBA-15-Thia**.

The relative contribution of Q4/Q3 and T2/T1 species was estimated via deconvolution (Figure 2a, green line) of the original NMR signal. ^{13}C MAS-NMR spectra displayed the pattern of the imidazolium or thiazolium species. The disappearance of the signals corresponding to the terminal vinyl carbons further confirmed the absence of unreacted bisvinyl precursors in the supported solids, although the presence of traces of adsorbed oligomers cannot be completely excluded (Figure 2b, red circle and Supporting Information, section A.1, Figures S5 to S7).

Table 2. 1-Phenylethanol etherification catalyzed by **SBA-15-Thia** or **SBA-15-Imi** materials.[a]

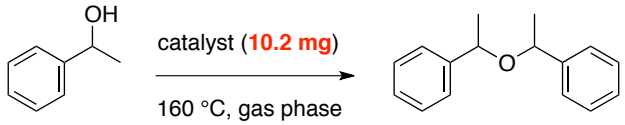

Entry	Support	Time [h]	Gas phase	Conv.[%][b]	Selectivity [%][c]
1	**SBA-15-Thia**	24	O_2	93	73
2	**SBA-15-Thia**	24	Air	93	86
3	**SBA-15-Thia**	24	N_2	55	93
4	**SBA-15-Thia**	24	Ar	57	91
5	**SBA-15-Imi**	24	O_2	73	38[d]
6	**SBA-15-Imi**	24	Air	48	70
7	**SBA-15-Thia**	7	O_2	92	75
8	**SBA-15-Thia**	7	Air	78	88

[a] Reaction conditions: 1-phenylethanol (5.4 g, 44.2 mmol), **SBA-15-Thia** or **SBA-15-Imi** (10.2 mg), 160 °C, under stirring. [b] Conversion determined by ^{1}H NMR. [c] Selectivity toward ether. [d] Main by-product: acetophenone.

All these findings, combined with the exceptionally high degree of organic functionalization, quantified through combustion chemical analysis (see the Experimental Section, Chapter 8, section 8.1), allow an assumption of the presence of a multilayered matrix. The two solids, **SBA-15-Imi** and **SBA-15-Thia**, display good specific surface area and high percentage of active sites, which are promising features for catalytic applications.

In order to explore their activity, 1-phenylethanol was selected as model compound for the industrially relevant etherification reaction. To investigate the possible formation of oxidation by-products, the etherification reaction was initially performed in the presence of different gas phases (oxygen, air, nitrogen and argon) for 24 h. The results of these preliminary catalytic tests are reported in Table 2. It is worthy of note that challenging conditions in terms of substrate to catalyst weight ratio (mg alcohol/mg catalyst = 540) were used.

After 24 h an almost quantitative conversion was observed using the **SBA-15-Thia** catalyst in both oxygen and air (entries 1 and 2). The selectivity toward ether was lower (73 %) when the reaction was carried out under an oxygen atmosphere, acetophenone then being the main by-product. In order to understand the effect of the gas phase, the etherification was performed under an inert atmosphere. Under a nitrogen or argon atmosphere, the conversion was much lower and an increased selectivity was observed (entries 3 and 4 in Table 2). Interestingly, the analogous imidazolium-based material displayed a lower conversion and poorer selectivity evidencing that the nature of the N-heterocyclic ring has a determinant impact on the performances of the reaction (entries 1 and 2 vs. 5 and 6 in

Table 2). In all these reactions, the main by-product was represented by acetophenone and, in some cases, by styrene, which was found in the reaction mixture in lower amounts.

It is known that yield and selectivity of the etherification reaction are strongly influenced by the textural properties of the heterogeneous catalysts as well as by the nature and strength of the acid sites.[42] In our case, the distinct catalytic behavior of imidazolium and thiazolium-based materials cannot be ascribed to relevant differences in terms of surface area, accessibility or acidity of the two solids, but rather to a different reactivity of the two heterocyclic systems.

Since the conversion under oxygen or air after 24 h was high, the reaction was monitored at a shorter reaction time (entries 7 and 8 in Table 2). As expected, the selectivity increases by decreasing the percentage of oxygen in the reaction mixture. Interestingly a lower conversion was also observed under air suggesting that the presence of oxygen has a global beneficial influence on the reaction. This trend is even more evident in Figure 3 in which are highlighted the decrease of the conversion (blue) and the parallel increase of the selectivity (green) upon lowering the initial oxygen concentration after 7 h of reaction time. A blank experiment performed in the absence of catalyst, under the same reaction conditions, revealed an extremely low conversion (6%) after 7 h with acetophenone as main product and traces of the etherification compound. Similar results were found when non-functionalized SBA-15 was used as catalyst. The kinetic profiles of the etherification under O_2, air and N_2 are shown in Figure 4.

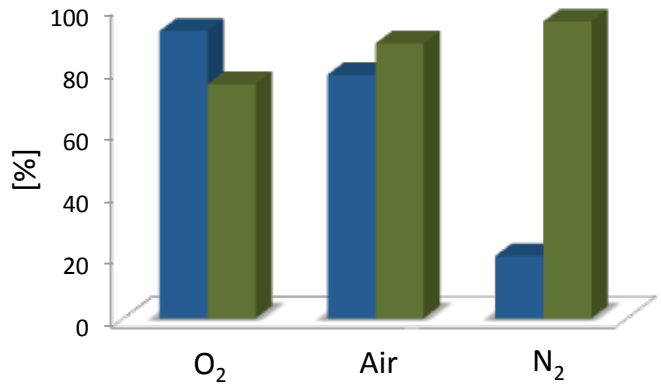

Figure 3. Conversion (blue) and selectivity (green) in the etherification reaction of 1-phenylethanol mediated by **SBA-15-Thia** after 7h.

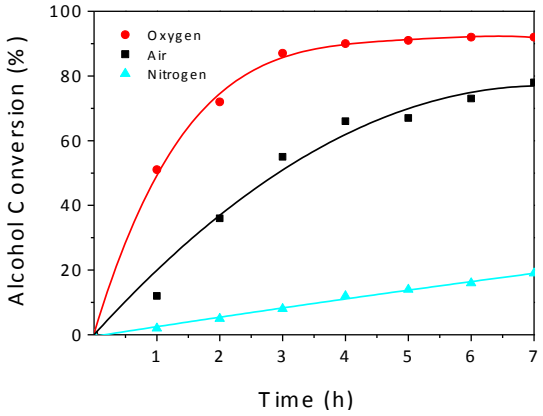

Figure 4. Conversion of 1-phenylethanol with **SBA-15-Thia** as function of the time under oxygen, air or nitrogen atmosphere.

Interestingly under O_2 an almost conversion is reached after 3 h. In the presence of air and nitrogen the reaction displayed a slower kinetic profile with a plateau that is attained after 6 h in the first case, and a linear slow increase of 1-phenylethanol conversion over time in the second. These results clearly evidenced an oxygen-dependent behavior of the **SBA-15-Thia** -catalyzed reaction.

Since the O_2 favors the formation of acetophenone, in order to exclude an active role of the oxidation byproduct in the synthesis of the ether, the reaction was performed using an equimolecular mixture of 1-phenylethanol and deuterated acetophenone as starting materials. The presence of a partially deuterated bis (α-methylbenzyl) ether in the final products would represent evidence of the role of acetophenone as synthesis intermediate. The analysis of the mixture after 7 h reaction showed the presence of the etherification product. However, GC-MS analysis did not evidence any partially deuterated compound in the reaction mixture. This test allows us to exclude an active participation of the acetophenone in the reaction mechanism. To completely clarify the mechanism an additional test using deuterated styrene as starting materials was also performed with similar results. These findings confirmed that the three reaction products (acetophenone, ether and styrene) are formed through independent reaction routes. Motivated by the excellent catalytic results and aiming to a thorough understanding of the novel thiazolium-catalyzed reaction, we investigated the role of the hydrogen at the C-2 position. For this mechanistic study, two easily accessible thiazolium-based catalysts, to be used under homogeneous conditions, were prepared. The two salts reported in Figure 5 differ only in the presence of hydrogen (**Homo-Thia-H**) or a methyl group (**Homo-Thia-Me**) at C-2 and were prepared with the objective to simulate the proximity of the active sites in the supported heterogeneous catalyst.

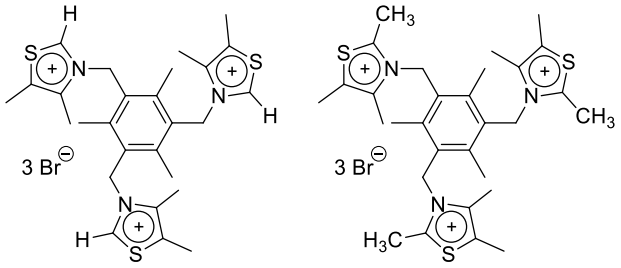

Figure 5. Structure of catalysts **Homo-Thia-H** and **Homo-Thia-Me**.

The two novel homogeneous organocatalysts (**Homo-Thia-H** and **Homo-Thia-Me**) can be prepared in high yield via a one-step procedure starting from the 2,4,6-tris(bromomethyl)mesitylene and the 4,5-dimethyl- or 2,4,5-trimethylthiazole, respectively (see Experimental Section for more details and Supporting Information, section A.1, Figures S8 to S11). The salts were tested under the previously reported reaction conditions in both oxygen and air atmospheres (Table 3). The results of this study revealed that the methyl group has a detrimental effect on the etherification reaction. In the presence of oxygen or air the conversion of the reaction catalyzed by the **Homo-Thia-H** reach the 92% after 7 h (entries 1 and 2 in Table 3) while under the same condition the **Homo-Thia-Me** catalyst gave 80% and 24% conversion, respectively (entries 3 and 4 in Table 3). A lower selectivity was observed when the reaction was performed in oxygen (entry 3), acetophenone being the main by-product. The differences between the catalysts in terms of both yield and selectivity toward the etherification product are even more evident under air and a shorter reaction time, highlighting once more the positive influence of the high O_2 concentration (entries 5-8).

Table 3. 1-Phenylethanol etherification catalyzed by **Homo-Thia-H** or **Homo-Thia-Me**.[a]

Entry	Catalyst	Time [h]	Gas phase	Conv. [%][b]	Selectivity [%][c]
1	**Homo-Thia-H**	7	O_2	92	72
2	**Homo-Thia-H**	7	Air	92	72
3	**Homo-Thia-Me**	7	O_2	80	56
4	**Homo-Thia-Me**	7	Air	24	73
5	**Homo-Thia-H**	4	O_2	81	74
6	**Homo-Thia-H**	4	Air	63	82
7	**Homo-Thia-Me**	4	O_2	67	51
8	**Homo-Thia-Me**	4	Air	14	71

[a] Reaction conditions: 1-phenylethanol (5.4 g, 44.2 mmol), **Homo-Thia-H** or **Homo-Thia-Me** (10.15 mg), 160 °C. [b] Conversion determined by ^{1}H NMR. [c] Selectivity toward ether.

After 4 h only 14% of conversion is obtained in the presence of the **Homo-Thia-Me** catalyst with a corresponding selectivity of 71% (entry 8) while a higher conversion and lower selectivity are obtained under oxygen (entry 7) where the remaining product is mainly represented by the acetophenone. These results show the key role of C-2 in the catalytic mechanism. The reduced performance of **Homo-Thia-Me** could be attributed to a negative combination of steric and electronic effects. The kinetic profiles of the reactions performed in both air and oxygen with an analysis of the composition of the reaction mixture over time are reported in Figure 6 and Figure 7. Finally, we performed the etherification reaction of (S)-1-phenylethanol under oxygen for 4 h (Scheme 2).

The ^{1}H NMR spectrum showed a 60/40 ratio of the two diastereomeric ether products indicating that the reaction follows mainly an SN_1 pathway. Based on these results, a possible explanation can be found in the reactivity of the C-2 as proposed in the mechanism depicted in Scheme 3.

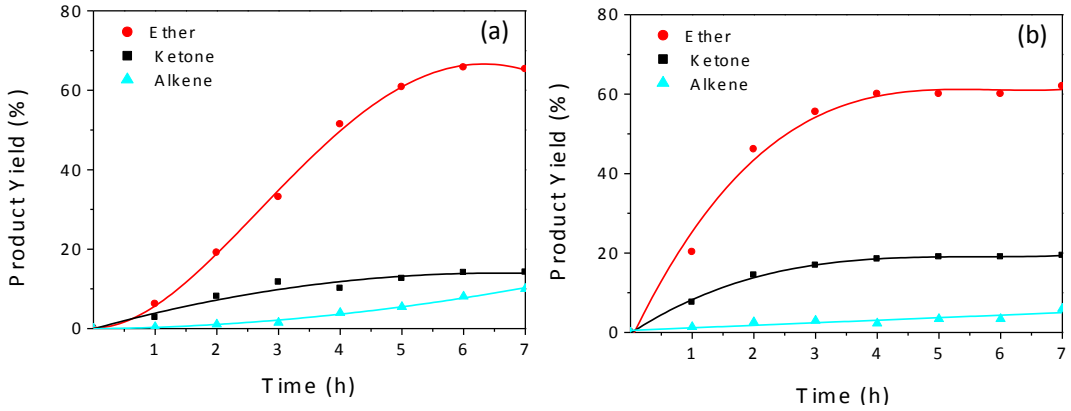

Figure 6. Kinetic profile of the reaction of 1-phenylethanol catalyzed by **Homo-Thia-H** under a) an air and b) an oxygen atmosphere.

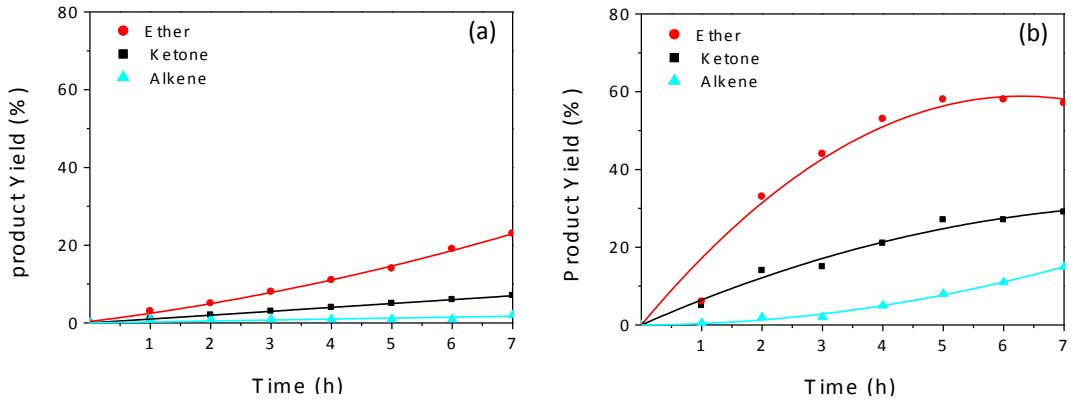

Figure 7. Kinetic profile of the reaction of 1-phenylethanol catalyzed by a) **Homo-Thia-Me** under an air and b) an oxygen atmosphere.

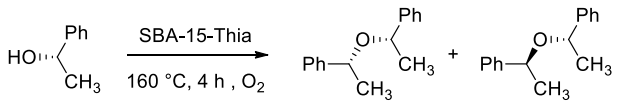

Scheme 2. Etherification reaction of (S)-1-phenylethanol.

This reaction mechanism allows us to explain the key role of the organocatalyst in the alcohol to ether transformation. It is known that the electrophilic C-2 atom may react with nucleophiles such as the hydroxide ion, amines or carbenes.[43] In our case, the nucleophilic attack of the alcohol gives the intermediate species **1**, which undergoes a nucleophilic attack by another alcohol molecule mainly via an S_N1 pathway. The different reactivity observed with the imidazolium-based catalyst can be ascribed to the different reactivity of C-2 and different ability as leaving group in the etherification cycle. Formation of by-products could be also explained through the intermediate **1**.

Acetophenone (**2**) could be generated via the oxidation cycle through a pathway which resembles the oxoammonium-based mechanism.[44] On the other side, the presence of styrene (**3**), may be justified by the elimination cycle. It is worthy of note that oxygen emerges as a fundamental element of the catalytic mechanism in both heterogeneous and homogeneous conditions. To justify its undeniable role, we envisaged a possible dual mechanism, similar to the one proposed by Corma and Garcia[45,46] for oxidation reactions in aerobic conditions.

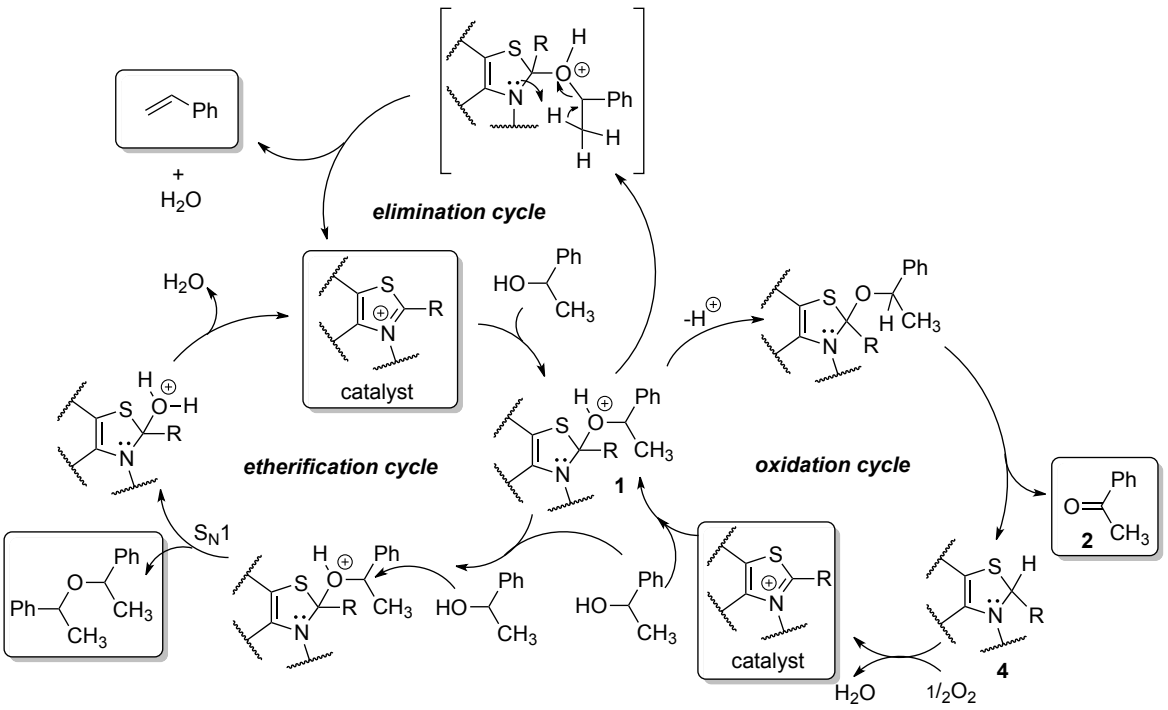

Scheme 3. Proposed etherification catalytic cycles in the presence of thiazolium-based catalyst.

The O_2 could promote the elimination of hydrogen forming water and regenerating the active site of the catalyst, which is engaged in the oxidation cycle and thus would be blocked for the etherification cycle otherwise. In other words it promotes the oxidation of the 2,3-dihydrothiazole ring (**4**) regenerating the thiazolium catalyst and improving, as consequence, the overall performances of the catalyst. An alternative reaction route that could allow an explanation of the formation of acetophenone as by-product would envisage a mechanism similar to the NAD^+/NADH cycle with the thiazolium moiety playing the role of the pyridinium moiety of NAD^+ and acting as a biomimetic oxidizing/reducing agent (Scheme 4). The analysis of the results obtained with the homogenous and heterogeneous thiazolium-based catalysts (compare entry 7 in Table 2 and entry 1 in Table 3) highlight the good performances of **SBA-15-Thia** for etherification reactions. Due to the differences in the reaction conditions in terms of temperature, reaction time, nature and amount of active sites, a comparison with literature data is difficult.

However, we can state that the productivity of the **SBA-15-Thia** catalyst (defined as: productivity = amount in gram of product/ total amount in gram of catalyst) is one of the highest reported in the literature with a similar value after 7 h, of 338 g ether /g catalyst for the reaction performed under oxygen and 337 g ether /g catalyst under an air atmosphere.

In order to have a deeper understanding of the mechanism one additional catalyst, constituted by a single thiazolium unit, was prepared (Figure 8 and Supporting Information, section A.1, Figures S12 and S13). The **Mono-Thia** was tested in the etherification of 1-phenylethanol under air. After 7 h reaction a conversion of 68 % was obtained. This result further proves the activity of the thiazolium moiety and evidence that **Mono-Thia** displays an intermediate catalytic behavior compared to **Homo-Thia-H** and **Homo-Thia-Me**.

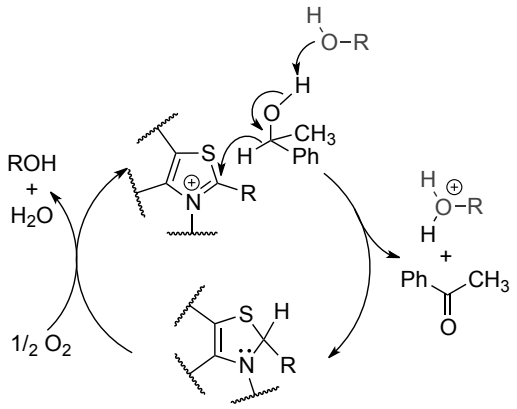

Scheme 4. Oxidation of 1-phenylethanol via the thiazolium / thiazoline system.

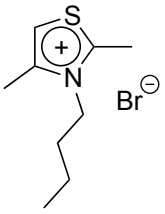

Mono-Thia

Figure 8. Structure of catalyst **Mono-Thia**.

This finding suggests that the lower catalytic activity of the trimer catalyst (**Homo-Thia-Me**), ascribed to the presence of the methyl group at C-2, could be balanced by other effects such as the higher accessibility of the same carbon atom in the monomeric catalyst.

In the evaluation of a heterogeneous catalyst, the catalytic performances related to activity or selectivity is not the only parameter that should be taken into account. The stability under the reaction conditions should also be tested. Recycle experiments performed with the **SBA-15-Thia** highlight that the excellent catalytic performances are preserved in multiple catalytic runs (Figure 9). In order to confirm the activity of the **SBA-15-Thia**, additional catalytic test using a primary alcohol and a more hindered secondary alcohol were performed as well (Figure 10). The etherification compounds are known products and the references are included in the Experimental Section, Chapter 8 (section 8.1). It is worthy to underline that the etherification reaction and recycle experiments were performed under solvent-free conditions. Catalytic experiments performed with non-benzylic alcohols such as 2-phenylethanol and 1-decanol gave poor conversion thus confirming that the reaction mainly proceeds through an S_N1 mechanism. The excellent catalytic performances and the stability of the material in consecutive catalytic cycles together with the straightforward preparation of the solid render **SBA-15-Thia** an extremely promising catalyst also for other possible applications.

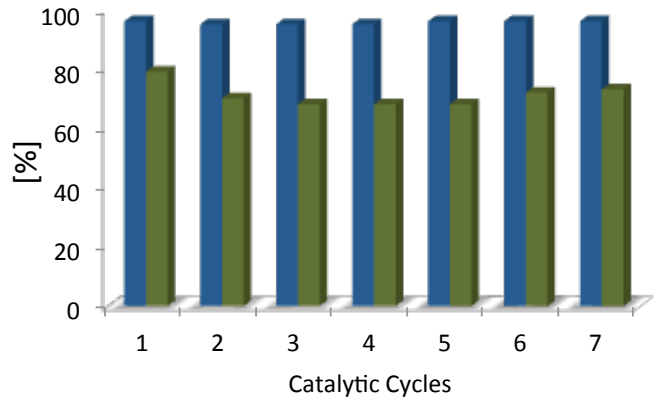

Figure 9. Conversion (blue) and selectivity (green) in multiple catalytic runs of the etherification reaction of 1-phenylethanol promoted by **SBA-15-Thia**.

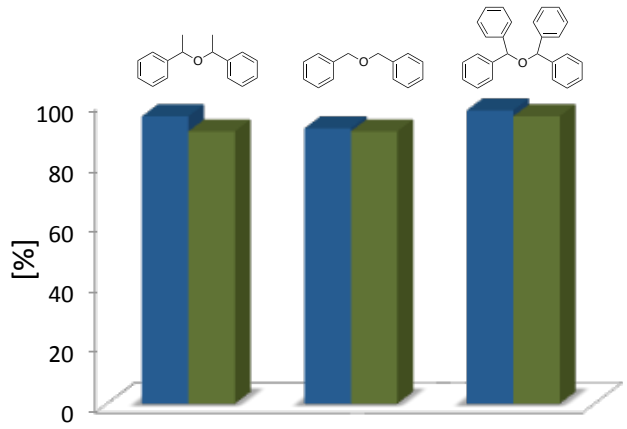

Figure 10. Conversion (blue) and selectivity (green) in the etherification reaction of 1-phenylethanol, benzyl alcohol and diphenylmethanol.

3.3 Conclusions

Multilayered covalently supported ionic liquid-like phases were prepared through a straightforward approach. The two solids bearing an imidazolium or a thiazolium active site were extensively characterized and tested as catalysts for the etherification of 1-phenylethanol. The thiazolium-based heterogeneous catalyst displayed good catalytic performance in the etherification of benzylic alcohols with an excellent productivity (P= 392 $g_{ether}/g_{catalyst}$) after 24 h under air. The catalyst exhibits similar productivity in the reaction performed using either benzylic alcohol or diphenylmethanol as starting material (P= 390-394 $g_{ether}/g_{catalyst}$). Moreover, the solid preserves its activity in consecutive catalytic cycles. The reaction mechanism was investigated using two unsupported thiazolium-based salts. This study allowed us to prove that oxygen plays an active role in the reaction, probably regenerating the catalysts. A possible triple reaction pathway was proposed to explain the formation of the etherification compound as well as the presence of the two by-products. Moreover, an additional test in the presence of enantiopure 1-phenylethanol demonstrated that the reaction follows mainly an S_N1 pathway. This study represents the first use of thiazolium-based compounds as catalysts for the etherification reaction of alcohols.

3.4 References

1. J. Buckingham, in: Dictionary of Natural Products on DVD, CRC Press, Taylor & Francis Group, London, 2013.
2. W. H. Miles, K. B. Connell, Journal of Chemical Education 2006, 83, 285-286.
3. M. Pagliaro, R. Ciriminna, H. Kimura, M. Rossi, C. Della Pina, Angewandte Chemie International Edition 2007, 119, 4516-4522; Angewandte Chemie International Edition 2007, 46, 4434-4440.
4. K. F. Yee, A. R. Mohamed, S. H. Tan, Renewable and Sustainable Energy Reviews 2013, 22, 604-620.
5. A.W. Williamson, J. Chem. Soc. 1852, 4, 229-239.
6. M. B. Smith, J. March, March's Advanced Organic Chemistry: Reactions Mechanisms and Structure, 7th edn., Wiley, Hoboken, 2013.
7. C. H. Jin, H. Y. Lee, S. H. Lee, I. S. Kim, Y. H. Jung, Synlett 2007, 2695-2698.
8. S. Kim, K. N. Chung, S. Yang, J. Org. Chem. 1987, 52, 3917-3919.
9. A. De Mico, R. Margarita, G. Piancatelli, Tetrahedron Letters 1995, 36, 2679-2680.
10. T. Ooi, H. Ichikawa, Y. Itagaki, K. Maruoka, Heterocycles 2000, 52, 575-578.
11. H. Firouzabadi, N. Iranpoor, A. A. Jafari, Journal of Molecular Catalysis A: Chemical 2005, 227, 97-100.
12. M. Wada, S. Nagayama, K. Mizutani, R. Hiroi, N. Miyoshi, Chemistry Letters 2002, 248-249.
13. K. Iwanami, K. Yano, T. Oriyama, Chemistry Letters 2007, 36, 38-39.
14. B. A. Gellert, N. Kahlcke, M. Feurer, S. Roth, Chemistry - A European Journal 2011, 17, 12203-12209.
15. S. C. Berk, S. L. Buchwald, J. Org. Chem. 1992, 57, 3751-3753.
16. R. E. Balsells, A. R. Frasca, Tetrahedron 1982, 38, 2525-2538.
17. J. Emert, M. Goldenberg, G. L. Chiu, A. Valeri, J. Org. Chem. 1977, 42, 2012-2013.
18. S. N. Tan, R. A. Dryfe, H. H. Girault, Helvetica Chimica Acta 1994, 77, 231-242.
19. J. Alvarez-Builla, J. J. Vaquero, J. L. Garcia Navio, J. F. Cabello, C. Sunkel, M. Fau de Casa-Juana, F. Dorrego, L. Santos, Tetrahedron 1990, 46, 967-978.
20. C. J. Thoman, T. D. Habeeb, M. Huhn, M. Korpusik, D. F. Slish, J. Org. Chem. 1989, 54, 4476-4478.
21. J. Bender, D. Jepkens, H. Husken, Organic Process Research & Development 2010, 14, 716-721.
22. P. Salehi, N. Iranpoor, F. K. Behbahani, Tetrahedron 1998, 54, 943-948.
23. G. V. M. Sharma, A. K. Mahalingam, J. Org. Chem. 1999, 64, 8943-8944.
24. A. Kawada, K. Yasuda, H. Abe, T. Harayama, Chem. Pharm. Bull. 2002, 50, 380-383.
25. M. I. Burguete, E. García-Verdugo, I. Garcia-Villar, F. Gelat, P. Licence, S. V. Luis, V. Sans, Journal of Catalysis 2010, 269, 150-160.
26. Y.-J. Zhang, W. Dayoub, G.-R. Chen, M. Lemaire, Tetrahedron 2012, 68, 7400-7407.
27. G. Argouarch, G. Grelaud, T. Roisnel, M. G. Humphrey, F. Paul, Tetrahedron Letters 2012, 53, 5015-5018.
28. K. J. Miller, M. M. Abu-Omar, Eur. J. Org. Chem. 2003, 1294-1299.
29. Y. Bikard, J.-M. Weibel, C. Sirlin, L. Dupuis, J.-P. Loeffler, P. Pale, Tetrahedron Letters 2007, 48, 8895-8899.
30. R. Mezaache, Y. A. Dembelé, Y. Bikard, J.-M. Weibel, A. Blanc, P. Pale, Tetrahedron Letters 2009, 50, 7322-7326.
31. A. B. Cuenca, G. Mancha, G. Asensio, M. Medio-Simón, Chemistry - A European

Journal 2008, 14, 1518-1523.
32. J. P. Hallett, T. Welton, Chemical Reviews 2011, 111, 3508-3576.
33. M. Gruttadauria, F. Giacalone, P. Agrigento, R. Noto, in: Ionic Liquids in Biotransformations and Organocatalysis, John Wiley & Sons, Inc., Hoboken, 2012, 361-417.
34. J. Scholz, M. Haumann, in: Nanomaterials in Catalysis, Wiley-VCH, Weinheim, 2013, 251-280.
35. T. Selvam, A. Machoke, W. Schwieger, Applied Catalysis A: General 2012, 445-446, 92-101.
36. C. Aprile, F. Giacalone, P. Agrigento, L. F. Liotta, J. A. Martens, P. P. Pescarmona, M. Gruttadauria, ChemSusChem 2011, 4, 1830-1837.
37. P. Agrigento, S. M. Al-Amsyar, B. Soree, M. Taherimehr, M. Gruttadauria, C. Aprile, P. P. Pescarmona, Catalysis Science & Technology 2014, 4, 1598-1607.
38. M. Gruttadauria, L. F. Liotta, A. M. P. Salvo, F. Giacalone, V. La Parola, C. Aprile, R. Noto, Advanced Synthesis & Catalysis 2011, 353, 2119-2130.
39. C. Pavia, E. Ballerini, L. A. Bivona, F. Giacalone, C. Aprile, L. Vaccaro, M. Gruttadauria, Advanced Synthesis & Catalysis 2013, 355, 2007-2018.
40. Pavia, F. Giacalone, L. A. Bivona, A. M. P. Salvo, C. Petrucci, G. Strappaveccia, L. Vaccaro, C. Aprile, M. Gruttadauria, Journal of Molecular Catalysis A: Chemical 2014, 387, 57-62.
41. E. Montroni, M. Lombardo, A. Quintavalla, C. Trombini, M. Gruttadauria, F. Giacalone, ChemCatChem 2012, 4, 1000-1006.
42. N. M. Bertero, A. F. Trasarti, C. R. Apesteguía, A. J. Marchi, Applied Catalysis A: General 2013, 458, 28-38.
43. F. G. Bordwell, A. V. Satish, Journal of the American Chemical Society 1991, 113, 985-990.
44. G. Tojo, M. Fernández, in: Oxidation of Primary Alcohols to Carboxylic Acids, Springer, New York, 2007, 79-103.
45. A. Abad, P. Concepción, A. Corma, H. García, Angewandte Chemie International Edition 2005, 117, 4134-4137; Angewandte Chemie International Edition 2005, 44, 4066-4069.
46. A. Abad, A. Corma, H. García, Chem. Eur. J. 2008, 14, 212-222.

Chapter 4

Cross-linked Thiazolidine network as support for palladium: a new catalyst for Suzuki and Heck reactions

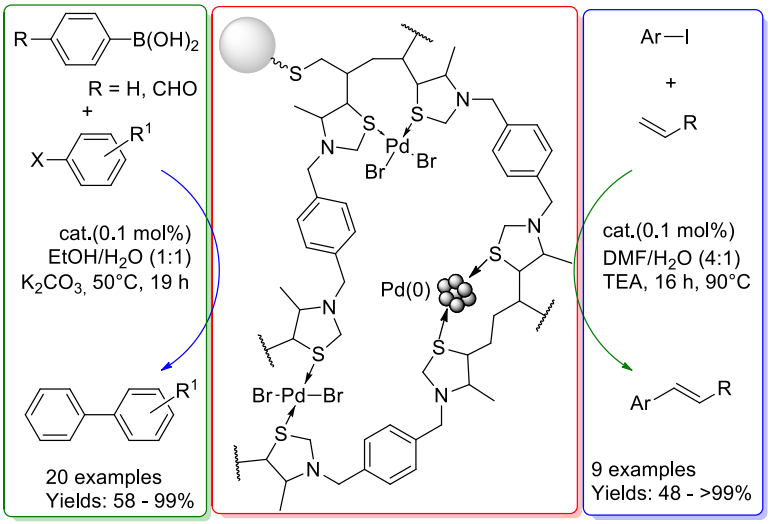

Chapter 4

This chapter is based on: L. A. Bivona, F. Giacalone, L. Vaccaro, C. Aprile, M. Gruttadauria, ChemCatChem 2015, 7, 2526-2533.

Cross-linked Thiazolidine network as support for palladium: a new catalyst for Suzuki and Heck reactions

4.1 Introduction

Carbon-carbon bond forming reactions, such as Suzuki-Miyaura and Mizoroki-Heck reactions, catalyzed by palladium compounds are nowadays of great interest from both academic and industrial points of view.[1] These important and useful transformations are widely employed in synthetic organic chemistry for the synthesis of pharmaceuticals and natural products,[2] but also in the field of materials chemistry for the preparation of conjugated polymers.[3] The rush towards the development of more active, selective, and recyclable catalysts has led to the use of a plethora of different palladium-based catalytic systems.[4] Nevertheless, in order to limit problems related to separation of homogeneous catalysts from reaction crude and, with the aim of costs abatement, in recent years a lot of efforts have been devoted to the preparation and application of recyclable supported palladium catalysts. These catalysts have been immobilized on various supports such as silica, alumina, zeolites, organic polymers, magnetic nanoparticles, and dendrimers.[5] However, although the literature is full of C-, N-, S-, and P-based ligands for the immobilization of Pd^{II} species and palladium nanoparticles, there are very few examples in which these species are stabilized and/or anchored by employing SN ligands.[6] The knowledge of oxygen and moisture stability of Pd^{II} complexes with a thiazolidine derivative obtained from thiamine dates back to 1981,[7] and the first example of a Heck reaction promoted by $Pd(OAc)_2$ immobilized onto a polystyrene resin through a SN ligand has been reported in 1987.[8] However, very recently a 4-amino-5-methyl-3-thio-1,2,4 triazole-functionalized polystyrene resin supported Pd^{II} complex has been successfully employed in the Suzuki, Heck, and copper-free Sonogashira reactions,[9] whilst the complex between palladium and 1-benzyl-4-phenylthiomethyl-1H-1,2,3-triazole promoted C-C coupling processes in 0.01 mol% loadings by forming *in-situ* Pd nanoparticles that were stabilized by the ligand.[10] Oxazolidine-thioether and thiazolidine–alcohol palladium

complexes were used in the asymmetric palladium-catalyzed allylic alkylation.[11] These few data indicated that there is still a lot of room to explore the use of SN ligands for the immobilization of Pd nanoparticles. Recently, we have developed a new concept of heterogeneous materials based on highly cross-linked imidazolium salts supported on silica gel for the immobilization of palladium nanoparticles in high loadings. Such kind of supported ionic liquid-like phase (SILLPs) resulted to be highly efficient, recoverable, and reusable in the Suzuki-Miyaura and in Heck reactions both under batch[12] and flow conditions.[13] Interestingly, these materials are also able to effectively promote the synthesis of cyclic carbonates,[14] ethers,[15] or even to act as palladium scavengers.[14a,16] Finally, these SILLPs found application as non-covalent supports for the reversible immobilization of ionic liquid tag-endowed organocatalysts[17] working under a "release and catch" regime.[18] Such highly cross-linked imidazolium networks are obtained by radical oligomerization of bis-vinylimidazolium salts on the surface of mercaptopropyl-modified amorphous silica gel or ordered mesoporous silica SBA-15 giving a multilayered ionic liquid-like material.[12-17] The advantage of such highly loaded SILLP material arise from the possibility that are able to stabilize high amounts of catalytically active Pd species. Indeed, it has been possible to immobilize up to 10 wt% of palladium on such materials. Whereas imidazolium-based ionic liquids as well as imidazolium-based supports have been largely used as homogeneous and heterogeneous supports for Pd-based catalysts, sulfur-nitrogen ligands such as the thiazolidine ring has been very scarcely used as ligands for palladium[7] and thiazolidine-based supports have not been previously reported or used for such scope. Taking advantage of our synthetic methodology for the preparation of highly loaded imidazolium-based silica, we envisaged a new approach for the palladium immobilization based on a highly loaded thiazolidine-functionalized silica support. Herein we describe the synthesis, characterization and uses of a new palladium catalyst immobilized on a cross-linked thiazolidine-modified mesoporous silica gel.

4.2 Results and Discussion

The first step was the synthesis of the thiazolium-based SBA-15 material, **SBA-15-Thia** (Scheme 1). This material was prepared by reaction between the mercaptopropyl-modified silica SBA-15 and the bisvinylthiazolium salt (**bV-Thia**) as reported in the Chapter 3 (see Experimental Section, Chapter 8, and Supporting Information, section A.1).[15] **SBA-15-Thia** has a specific Brunauer-Emmett-Teller (BET) surface area of 116 m^2g^{-1} and a cumulative pore volume of 0.14 cm^3g^{-1}.

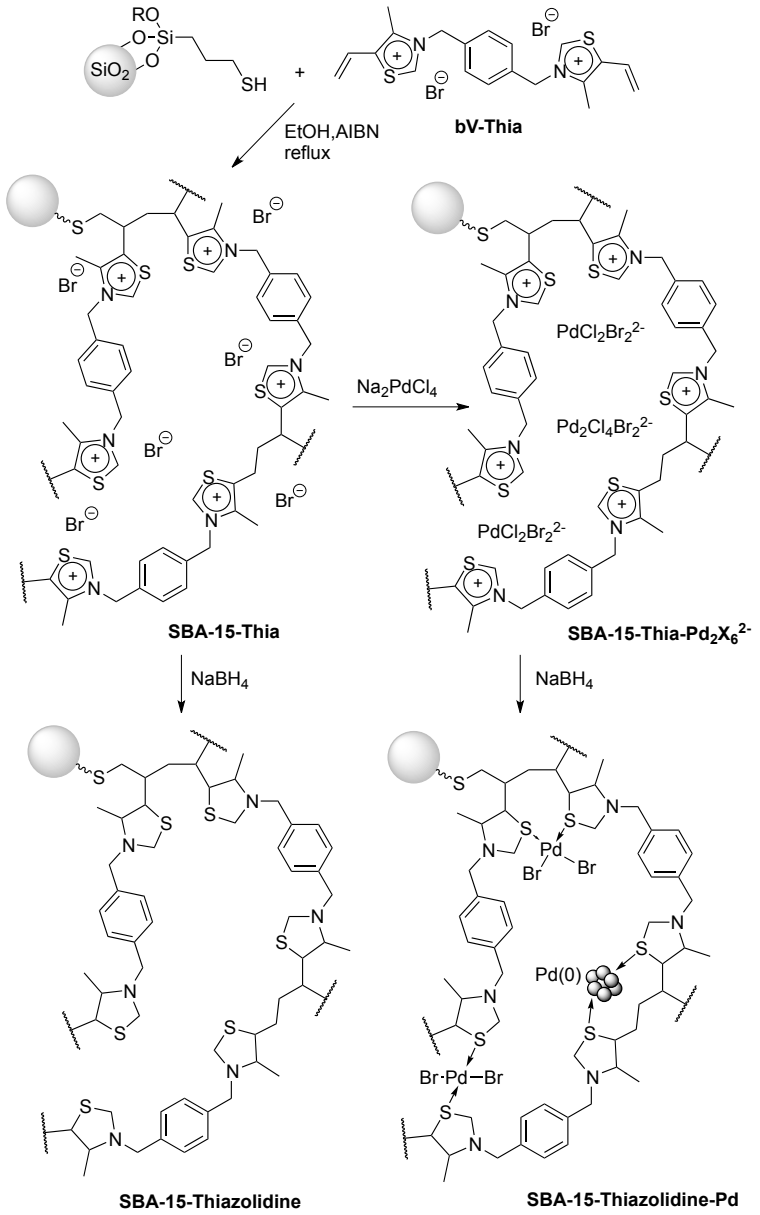

Scheme 1. Synthesis of thiazolidine-based materials.

Transmission electron microscopy investigation (Chapter 3, Figure 1) allows evidencing the presence of the typical structure of the SBA-15 solid as well as of the polymeric network. Elemental analysis gave a thiazolium loading of 2.28 mmol g^{-1}. These data are comparable with those of a previous synthesis of the same material reported in the Chapter 3 of this thesis.[15] In addition, the ^{13}C magic angle spinning (MAS) NMR spectroscopy data of the freshly prepared material was superimposable to that of a previous preparation.[15] These results demonstrate the reproducibility of our synthesis methodology. The thiazolium-based SBA-15 material was stirred with an aqueous solution of sodium tetrachloropalladate (Na_2PdCl_4). Then, the material was recovered by filtration and no palladium was found in the filtrate (Scheme 1).

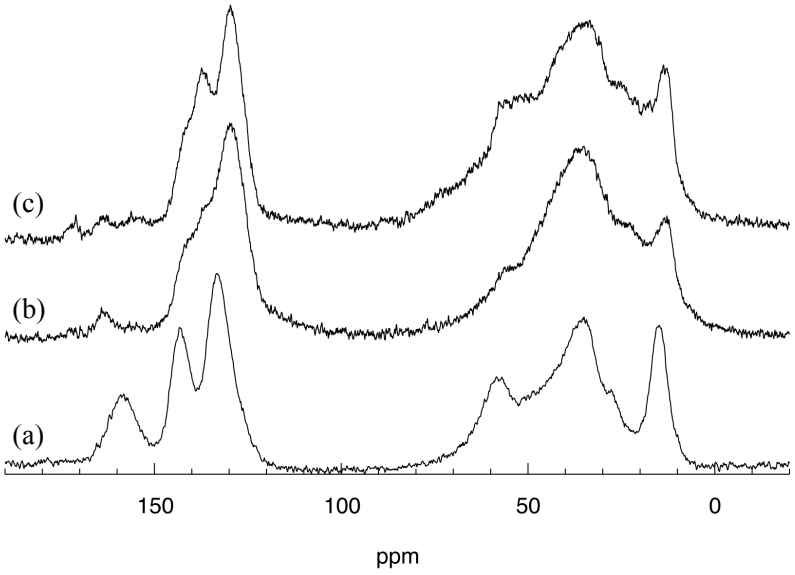

Figure 1. Solid state ^{13}C CP-MAS NMR (125 MHz) spectra of: a) **SBA-15-Thia;** b) **SBA-15-Thiazolidine-Pd**; c) **SBA-15-Thiazolidine.**

The material **SBA-15-Thia-$Pd_2X_6^{2-}$** was treated with $NaBH_4$ in ethanol and the final Pd loading was determined by atomic absorption spectroscopy (AAS) with a graphite furnace on the final material **SBA-Thiazolidine-Pd**. It is known that the thiazolium ring is reduced to thiazolidine if treated with sodium borohydride in methanol[19] or water.[20] In addition, such treatment causes partial palladium reduction.

To confirm the formation of the thiazolidine network, the thiazolium-based material was treated with $NaBH_4$ to give the **SBA-15-Thiazolidine**. Solid-state ^{13}C MAS NMR spectra of the final materials were recorded (Figure 1b and 1c). ^{13}C NMR spectrum of **SBA-15-Thia** (Figure 1a) shows the signal at approximately 155 ppm, which is ascribed to C-2 of the thiazolium ring. In Figure 1c the ^{13}C NMR spectrum of **SBA-15-Thiazolidine** is shown. The disappearance of the signal at 155 ppm and the increase of signals in the aliphatic region could be explained with the formation of the thiazolidine network. An almost identical spectrum is obtained in the case of **SBA-15-Thiazolidine-Pd** (Figure 1b). This last material was further characterized by transmission electron microscopy (TEM) and X-ray photoelectron spectroscopy (XPS). TEM analysis does not show traces of ionic liquid polymer as a separate domain.

Palladium nanoparticles are not clearly visible (Figure 2a) or are completely absent (Figure 2b) suggesting a low percentage of Pd^0 in the sample with the formation of clusters or small nanoparticles with a narrow particle size distribution.

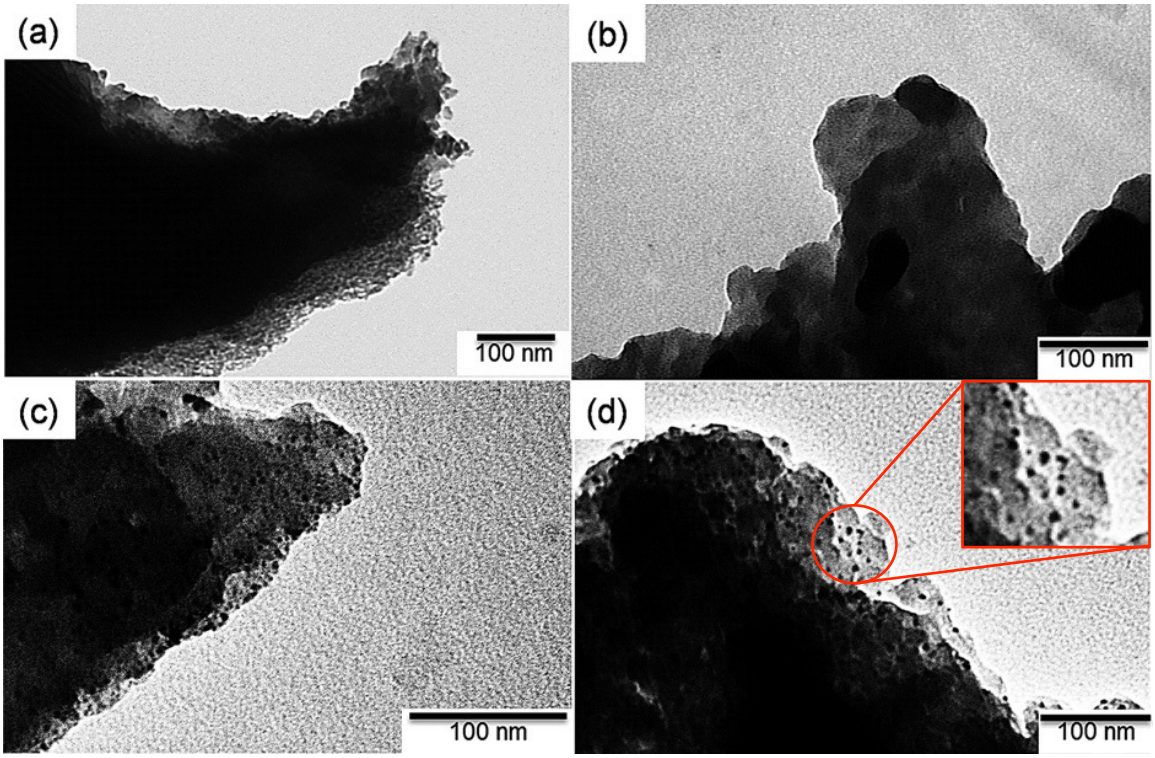

Figure 2. TEM images of: a), b) fresh **SBA-15-Thiazolidine-Pd**; c), d) reused **SBA-15-Thiazolidine-Pd** after 3 cycles.

Information on the chemical state and the surface chemical composition of the fresh and used catalyst were obtained by XPS (Table 1 and Figure 3). As expected, the fresh sample exhibited a higher percentage of Pd^{II} (85 %; binding energy, BE, 337.0 eV) with respect to metallic Pd (15 %; BE 335.4 eV) indicating that the treatment with $NaBH_4$ was not able to completely reduce palladium and confirming the previous observation by electron microscopy investigation.

The low amount of Pd^0 found in fresh catalyst could be ascribed to the stabilization of Pd^{II} species by the thiazolidine ligands.

Table 1. XPS Pd $3d_{5/2}$ binding energies (eV), Pd(0) [%] of prepared and used catalyst.

Entry	**SBA-15-Thiazolidine-Pd**	Pd $3d_{5/2}$ eV $[Pd^{2+}]^{[a]}$	Pd $3d_{5/2}$ eV $[Pd^0]^{[a]}$	Pd^0 [%]	Pd/C
1	fresh	337.0	335.4	15	0.02
2	after 1 cycle	337.0	335.2	20	0.02
3	after 3 cycles	337.0	335.1	32	0.02
4[b]	after 3 cycles	336.9	335.1	28	0.02

[a] The reference signal C 1s was fixed at 284.6 eV. [b] Repeated cycles.

XPS and energy-dispersive X-ray (EDX) analysis of **SBA-15-Thiazolidine-Pd** indicated the presence of bromo and absence of chloro atoms. The absence of chloro atoms could be a consequence of anion exchange process in which the labile tetrachloropalladate has reacted with bromide anions giving mononuclear $PdCl_2Br_2^{2-}$ and/or dinuclear bromide bridged Pd^{II} species $Pd_2X_6^{2-}$ (X=Cl, Br).[21]

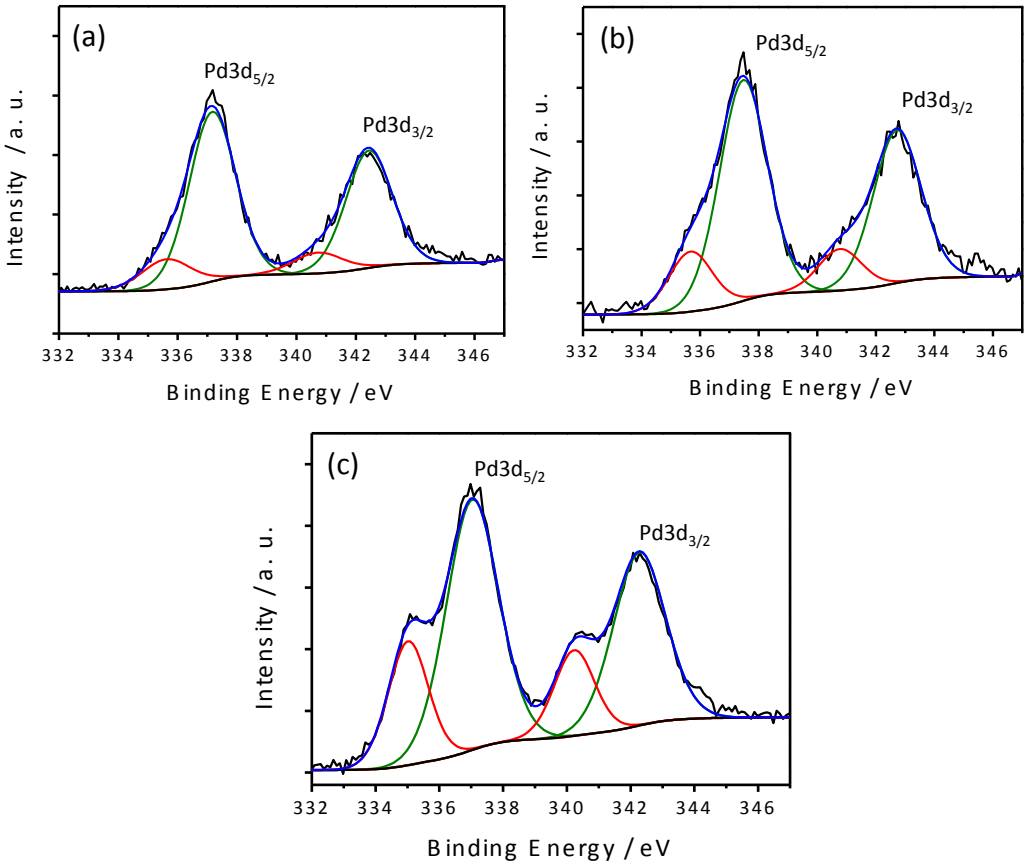

Figure 3. XPS core Pd 3d spectra of: a) **SBA-15-Thiazolidine-Pd**; b) reused **SBA-15-Thiazolidine-Pd** after 1 cycle; c) reused **SBA-15-Thiazolidine-Pd** after 3 cycles.

In Scheme 1 is reported a tentative picture of the obtained material. Very likely, Pd species can be stabilized through the sulfur atoms of the heterocyclic ligand to give complexes of type PdL_2Br_2.[22]

Table 2. XPS S $2p_{3/2}$ and S $2p_{1/2}$ binding energies (eV), of **SBA-15-Thiazolidine-Pd**.[a]

Entry	S $2p_{3/2}$ eV[a]	S $2p_{1/2}$ eV[a]
1	162.1	163.2
2	164.4	165.6
3	167.3	168.7

[a] The reference signal C 1s was fixed at 284.6 eV.

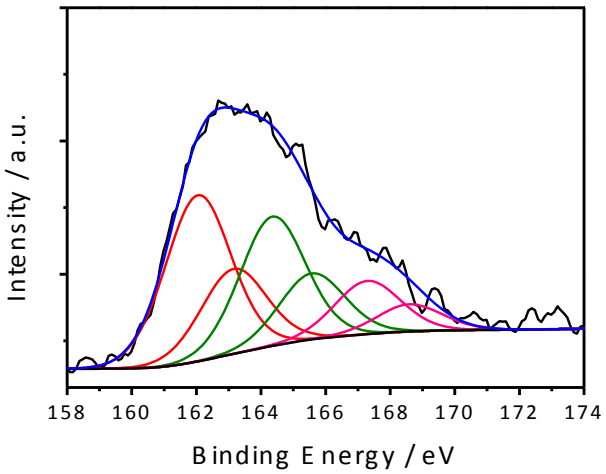

Figure 4. XPS core S 2p spectrum of **SBA-15-Thiazolidine-Pd**.

The high-resolution S2p core-level XPS spectrum of **SBA-15-Thiazolidine-Pd** (Figure 4) shows the presence of a broad peak indicating the presence of different sulfur moieties. Three different doublets (attributable to $S2p_{3/2}$ and $S2p_{1/2}$ components originating from the spin orbit splitting- effect contributions, Table 2 and Figure 4) can be thus resolved. The peak at 162.1 eV can be ascribed to the presence of C-S→Pd interaction, as previously reported.[23] The other two peaks at 164.4 and 167.3 eV can be assigned to the sulfur of free thiazolidine in its reduced and oxidized form, respectively. The oxidation of sulfur after exposure to air is a known process that may take place in the presence of palladium.[23b]

The catalyst **SBA-15-Thiazolidine-Pd** was used in the Suzuki-Miyaura reaction between phenylboronic acid or 4-formylphenylboronic acid and a set of aryl bromides (or iodides) in ethanol/water at 50 °C in the presence of K_2CO_3 as base under an open atmosphere (Table 3). All the reactions were run for 19 h. All of the products reported in the Table 3 are known compounds and the references can be found in the Experimental Section, part 8.2. The catalyst was used in 0.1 mol % loading. Reaction with 4-bromobenzaldehyde and phenylboronic acid was quantitative (entry 1). This reaction was selected for recycling studies of the catalyst (entries 2-4). Recycling reactions were performed on a larger scale (10 mmol of 4-bromobenzaldehyde) and the catalyst was recovered by filtration. No decrease in its activity was observed. These recycling experiments were duplicated, giving identical results. The catalyst was analyzed by XPS after the first reuse and after the third reuse. As can be clearly observed in Table 1 the materials display the same Pd/C ratio thus proving that no substantial modification of Pd loading is occurring at the surface of the sample. Analysis performed with AAS after the first cycle confirmed that the total Pd loading remains constant within the experimental error.

Table 3. Suzuki-Miyaura reactions between phenylboronic acid and aryl halides in the presence of the catalyst **SBA-15-Thiazolidine-Pd**.[a]

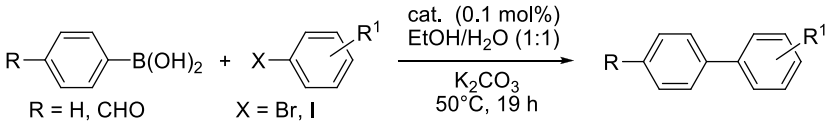

Entry	R	X	Product	Conv. [%][b]	Yield [%][c]	TON [d]
1	H	Br	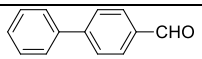	> 95	99	1053
2[e]	H	Br	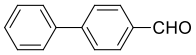	> 95	99	1053
3[f] II cycle	H	Br	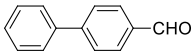	> 95	98	1043
4[f] III cycle	H	Br	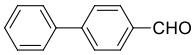	> 95	98	1043
5	H	Br	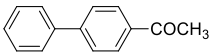	> 95	98	1043
6	H	Br	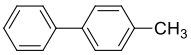	> 95	99	1053
7	H	Br	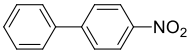	> 95	97	1032
8	H	Br	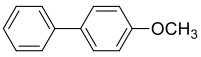	> 95	98	1043
9	CHO	Br	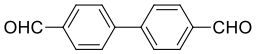	> 95	97	1032
10	H	Br	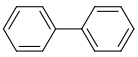	> 95 [g]	95	1011
11	H	Br		95[f]	95	1011
12	H	Br	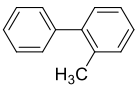	89	88	936
13	H	Br	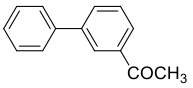	88	85	904
14	CHO	Br	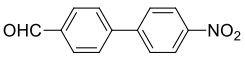	60	58	617
15[h]	H	I	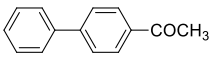	> 95	99	1053
16	H	I	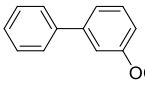	90	90	957
17	H	I	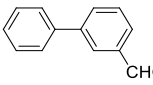	> 95	99	1053
18	CHO	I	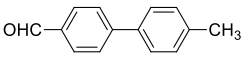	> 95	92	979
19	CHO	I	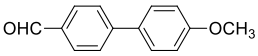	89	88	936
20[i]	H	Br	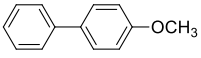	48	47	500

21[i]	H	Br	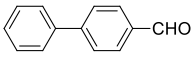	77	76	809
22[i]	H	Br	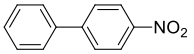	89	87	926
23[i]	H	Br	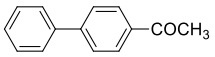	85	85	905

[a] Reaction conditions: aryl halide (1.0 mmol), phenylboronic acid or 4-formilphenylboronic acid (1.1 mmol), K_2CO_3 (1.2 mmol), EtOH (1.2 mL), H_2O (1.2 mL), catalyst **SBA-15-Thiazolidine-Pd** (0.1 mol%, 1 mg). [b] Conversion determined by ^{1}H NMR on isolated reaction mixture. [c] Calculated on isolated products or from the reaction mixture. [d] TON (*turnover number* calculated as: moles of product/moles of active sites). [e] Reaction on 10 mmol; duplicated experiment. [f] In each cycle the amount of reagents were scaled in function of the amount of catalyst recovered. Duplicated experiment. [g] Determined by GC. [h] Reaction time: 5 h and 45 min. [i] Reaction carried out in ethanol.

To further support our findings, EDX microanalysis realized with scanning electron microscopy (SEM) was performed as well. This analysis allowed confirming the previous observation by XPS. The averaged values of Pd/(C+N) of the materials **SBA-Thiazolidine-Pd** before and after the catalytic cycles were constant and equal to 0.03. The difference in the relative values (Pd/C=0.02 by XPS and Pd/(C+N)=0.03 by EDX) can be ascribed to the different distribution of Pd species at the surface and in the core of the multilayered thiazolidine network (Figure 4 and 5).

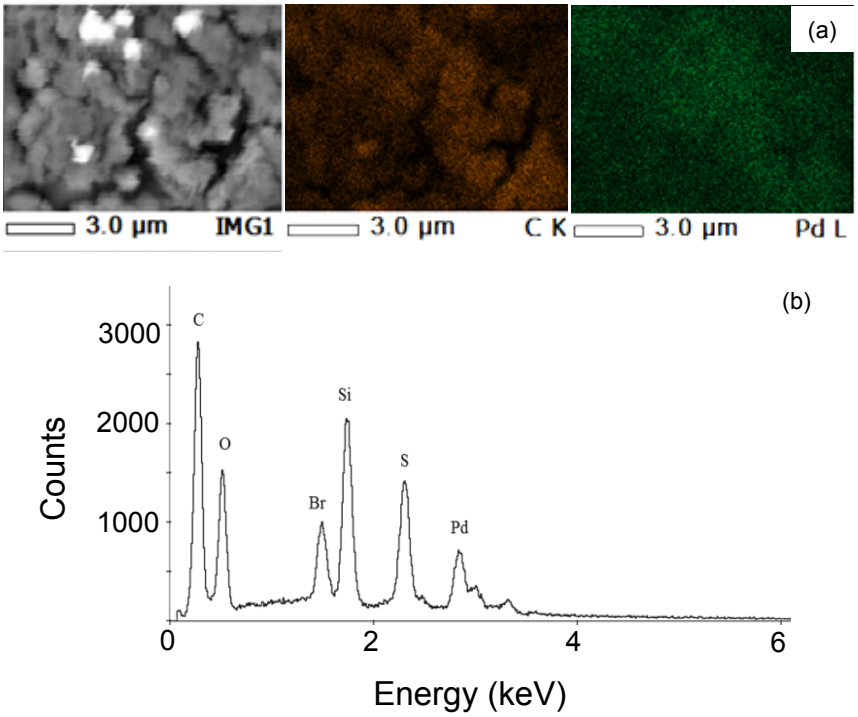

Figure 4. SEM image and EDX mapping of C and Pd for the catalyst **SBA-15-Thiazolidine-Pd** (a), and EDX spectrum of the same material (b). For the EDX spectrum the N signal is overlapping with the C, for this reason the ratio Pd/(C+N) was calculated.

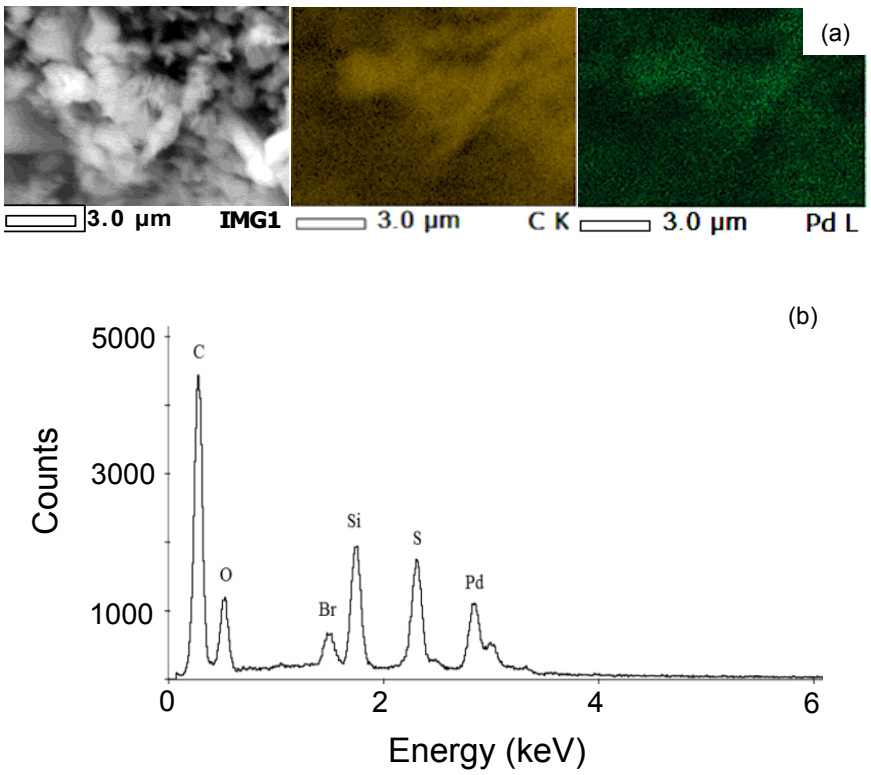

Figure 5. SEM image and EDX mapping of C and Pd for the catalyst **SBA-15-Thiazolidine-Pd** after reuse (a), and EDX spectrum of the same material (b). For the EDX spectrum the N signal is overlapping with the C, for this reason the ratio Pd/(C+N) was calculated.

XPS analysis revealed an increased amount of Pd^0 after reuse (Table 1; Figure 3b and 3c) that can be attributed to the *in-situ* reduction likely caused by the solvent under basic conditions.[12b, 13a, 24] Solid state ^{13}C NMR spectrum was also recorded in the case of reused catalyst **SBA-15-Thiazolidine-Pd** (after 3 cycles) and no changes were observed (Figure 6).

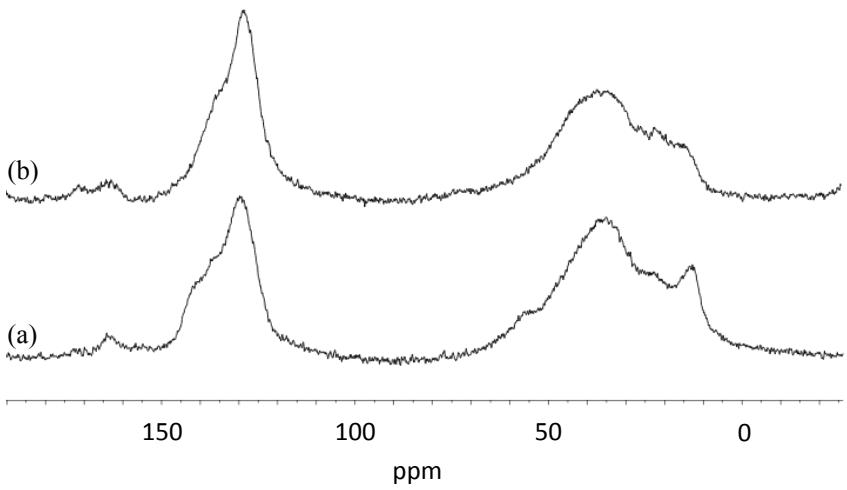

Figure 6. ^{13}C CP MAS NMR of the material **SBA-15-Thiazolidine-Pd** fresh catalyst (a) and of the material **SBA-15-Thiazolidine-Pd** after three consecutive cycles (b).

Interestingly, TEM investigation revealed the presence of metallic nanoparticles on the entire sample with an average particle size distribution centered at 3 nm (Figure 1c, 1d and in Supporting Information, Section A.2, Figure S1). Moreover, no traces of separate domains of silica and polymeric material were found further confirming the stability of the solid in consecutive catalytic cycles. Excellent conversions were observed in the case of 4-substituted aryl bromides, bromobenzene and 1-bromonaphthalene (Table 3, entries 5-11). High conversions were also observed with 2- and 3-substituted aryl bromides (entries 12, 13) whereas a lower conversion was obtained with 4-formylphenylboronic acid and 4-bromonitrobenzene (entry 14). As expected, the use of aryl iodides gave also high to excellent conversions (Table 3, entries 15-19). On the other hand, the use of the less reactive aryl chloride 1-chloro-4-nitrobenzene was unsuccessful. A certain conversion (≈6 %) was achieved by increasing the amount of catalyst to 1 mol%. As we have previously[13] demonstrated that the Suzuki-Miyaura reaction can be successfully performed under flow condition using ethanol as the sole solvent, we have also shortly investigated the Suzuki-Miyaura reaction in this solvent. Although conversions were not quantitative, the reactions were very clean (entries 20-23). To investigate if any "release and catch" mechanism[18] is occurring, the reaction between phenylboronic acid and 3-bromoacetophenone in ethanol/water at 50 °C was analyzed in more in details.

Three parallel experiments were performed, the first one was stopped and analyzed after 4 h (Table 4, entry 1), the second one was filtered at 50 °C after 4 h and the filtrate left to react up to 19 h (entry 2).

Table 4. Suzuki-Miyaura reactions between phenylboronic acid and 3-bromoacetophenone in the presence of the catalyst **SBA-15-Thiazolidine-Pd**.[a]

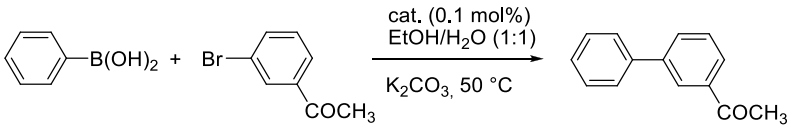

Entry	Total reaction time [h]	Procedure	Conv. [%] [b]
1	4	No filtration	14
2	19	Filtration after 4 h at 50 °C	58
3	19	Filtration after 4 h at r.t.	11

[a] Reaction conditions: 3-bromoacetophenone (1.0 mmol), phenylboronic acid (1.1 mmol), K_2CO_3 (1.2 mmol), EtOH (1.2 mL), H_2O (1.2 mL) catalyst **SBA-15-Thiazolidine-Pd** (0.1 mol%, 1 mg). [b] Conversion determined by ^1H NMR.

The third reaction was filtered after 4 h, but the filtration was performed at room temperature, and the filtrate left to react up 19 h at 50 °C (entry 3, and in Supporting Information, section A.2, Figure S2).

The reaction filtered after 4 h at 50 °C and left to react gave a higher conversion than both the reaction stopped after 4 h and the reaction filtered after 4 h at room temperature and left to react up to 19 h. It seems that the palladium leaching is operative at 50 °C whereas palladium seems to be recaptured at lower temperature.

Table 5. Heck reaction between methyl acrylate or styrenes and aryl iodides in the presence of the catalyst **SBA-15-Thiazolidine-Pd**. [a]

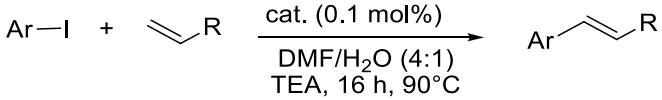

Entry	Ar	R	Product	Yield [%][b]	TON[c]
1	4-NO_2-C_6H_4	CO_2Me	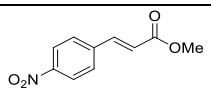	99	1053
2	Ph	CO_2Me	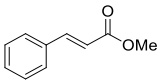	85	904
3	4-CH_3O-C_6H_4	CO_2Me	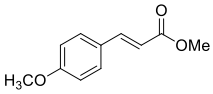	99	1053
4	3-CH_3O-C_6H_4	CO_2Me	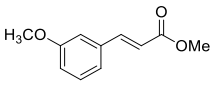	89	947
5	3-Br-C_6H_4	CO_2Me	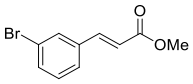	91	968
6	4-Br-C_6H_4	CO_2Me	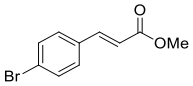	99[d]	1053
7	2-thienyl	CO_2Me	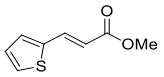	48	511
8	4-CH_3O-C_6H_4	Ph	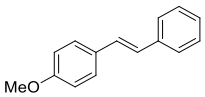	76[e]	809
9[f]	4-CH_3O-C_6H_4	4-Cl-C_6H_4	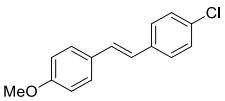	94[g]	1000

[a] Reaction conditions: acrylate or styrene (1.5 mmol), aryl iodide (1 mmol), TEA (2 mmol), catalyst **SBA-15-Thiazolidine-Pd** (0.1 mol% 1 mg), 90 °C, 16 h. [b] Calculated on isolated products. [c] TON (*turnover number* calculated as: moles of product/moles of active sites). [d] Conversion. Mixture (92/8) of monoacrylate/ bisacrylate.[12c] [e] Conversion. Mixture (86/14) of *trans*-styrene/*gem*-styrene.[12c] [f] Reaction time: 21 h. [g] Conversion. Mixture (94/6) of *trans*-styrene/*gem*-styrene.[12c]

Finally, to further explore the versatility of the catalyst it was also used in the Heck reaction between aryl iodides and methyl acrylate or styrenes (Table 5). Yields were high or excellent (entries 1-6), except in the reaction between 2-iodothiophene and methyl acrylate (entry 7). Good conversions were also observed with styrene derivatives (entries 8, 9). All the compounds are known and the references are reported in the Experimental Section, Chapter 8, section 8.2.

4.3 Conclusions

For the first time, a thiazolidine-based mesoporous silica gel was synthesized and used as a new support for palladium immobilization. The synthesis of the support was accomplished by reaction of a highly cross-linked thiazolium-modified mesoporous silica gel, having a high thiazolium loading (2.28 mmol g^{-1}), with sodium borohydride as reducing agent. Indeed, the preparation of a high-loaded thiazolidine-based support allowed the preparation of a high-loaded palladium catalyst (10 wt%). The catalytic material was used in the Suzuki-Miyaura and in the Heck reactions allowing the synthesis of several biphenyl and alkene compounds in high yields working with only 0.1 mol% of catalyst (1 mg of catalyst per mmol of reagent). Recycling (3 times) in the Suzuki-Miyaura reaction showed no decrease in activity. The catalytic material was characterized before and after reuse by solid state ^{13}C NMR spectroscopy, X-ray photoelectron spectroscopy, energy-dispersive X-ray spectroscopy, and transmission electron microscopy. Having demonstrated the usefulness of such catalyst under batch condition, our next goal will be the development of an efficient flow approach for Pd-catalyzed C-C coupling reactions using such catalytic material.

4.4 References

1. a) A. De Meijere, F. Diederich, Metal-Catalyzed Cross-Coupling Reactions 2004; b) E. Negishi, Handbook of Organopalladium Chemistry for Organic Synthesis 2002; c) K. C. Nicolaou, P. G. Bulger, D. Sarlah, Angewandte Chemie International Edition 2005, 44, 4442-4489; d) N. T. S. Phan, M. Van Der Sluys, C. W. Jones, Advanced Synthesis & Catalysis 2006, 348, 609-679; e) A. Zapf, M. Beller, Chemical Communications 2005, 431-440; f) I. P. Beletskaya, A. V. Cheprakov, Chemical Reviews 2000, 100, 3009-3066; g) N. J. Whitcombe, K. K. Hii, S. E. Gibson, Tetrahedron 2001, 57, 7449-7476.
2. a) J. G. De Vries, Canadian Journal of Chemistry 2001, 79, 1086-1092; b) C. Torborg, M. Beller, Advanced Synthesis & Catalysis 2009, 351, 3027-3043.
3. a) Z. Peng, A. R. Gharavi, L. Yu, Journal of the American Chemical Society 1997, 119, 4622-4632; b) F. Babudri, G. M. Farinola, F. Naso, Journal of Materials Chemistry 2004, 14, 11-34; c) Y. Lim, Y. S. Park, Y. Kang, D. Y. Jang, J. H. Kim, J. J. Kim, A. Sellinger, D. Y. Yoon, Journal of the American Chemical Society 2011, 133, 1375-1382; d) A. D. Schlüter, Journal of Polymer Science Part A: Polymer Chemistry 2001, 39, 1533-1556; e) J. Sakamoto, M. Rehahn, G. Wegner, A. D. Schlüter, Macromolecular Rapid Communications 2009, 30, 653-687.
4. a) Á. Molnár, Palladium-Catalyzed Coupling Reactions: Practical Aspects and Future Developments, 2013; b) A. Molnár, Chemical Reviews 2011, 111, 2251-2320; c) N. Marion, S. P. Nolan, Accounts of Chemical Research 2008, 41, 1440-1449; d) V. Farina, Advanced Synthesis & Catalysis 2004, 346, 1553-1582; e) R. B. Bedford, C. S. J. Cazin, D. Holder, Coordination Chemistry Reviews 2004, 248, 2283-2321.
5. a) V. Polshettiwar, C. Len, A. Fihri, Coordination Chemistry Reviews 2009, 253, 2599-2626; b) Y. M. A. Yamada, S. M. Sarkar, Y. Uozumi, Journal of the American Chemical Society 2012, 134, 3190-3198; c) A. Fihri, M. Bouhrara, B. Nekoueishahraki, J. M. Basset, V. Polshettiwar, Chemical Society Reviews 2011, 40, 5181-5203; d) M. Lamblin, L. Nassar-Hardy, J. C. Hierso, E. Fouquet, F. X. Felpin, Advanced Synthesis & Catalysis 2010, 352, 33-79; e) M. Weck, C. W. Jones, Inorganic Chemistry 2007, 46, 1865-1875; f) R. Andrés, E. De Jesús, J. C. Flores, New Journal of Chemistry 2007, 31, 1161-1191; g) D. A. Pears, S. C. Smith, Aldrichimica Acta 2005, 38.
6. A. Kumar, G. K. Rao, S. Kumar, A. K. Singh, Organometallics 2013, 33, 2921-2943.
7. N. Hadjiliadis, J. Markopoulos, Journal of the Chemical Society, Dalton Transactions 1981, 1635-1644.
8. X. Li, H. Liu, Y. Jiang, Journal of Molecular Catalysis A: Chemical 1987, 39, 55-62.
9. M. Bakherad, A. Keivanloo, B. Bahramian, S. Jajarmi, Journal of Organometallic Chemistry 2013, 724, 206-212.
10. F. Saleem, G. K. Rao, A. Kumar, S. Kumar, M. P. Singh, A. K. Singh, RSC Advances 2014, 4, 56102-56111.
11. A. L. Braga, C. C. Silveira, M. W. G. de Bolster, H. S. Schrekker, L. A. Wessjohann, P. H. Schneider, Journal of Molecular Catalysis A: Chemical 2005, 239, 235-238.
12. a) M. Gruttadauria, L. A. Bivona, P. Lo Meo, S. Riela, R. Noto, Eur. J. Org. Chem. 2012, 2635-2642; b) M. Gruttadauria, L. F. Liotta, A. M. P. Salvo, F. Giacalone, V. La Parola, C. Aprile, R. Noto, Advanced Synthesis & Catalysis 2011, 353, 2119-2130; c) C. Pavia, F. Giacalone, L. A. Bivona, A. M. P. Salvo, C. Petrucci, G.

Strappaveccia, L. Vaccaro, C. Aprile, M. Gruttadauria, Journal of Molecular Catalysis A: Chemical 2014, 387, 57-62.
13. a) C. Pavia, E. Ballerini, L. A. Bivona, F. Giacalone, C. Aprile, L. Vaccaro, M. Gruttadauria, Advanced Synthesis & Catalysis 2013, 355, 2007-2018; b) C. Petrucci, G. Strappaveccia, F. Giacalone, M. Gruttadauria, F. Pizzo, L. Vaccaro, ACS Sustainable Chemistry & Engineering 2014, 2, 2813-2819.
14. a) C. Aprile, F. Giacalone, P. Agrigento, L. F. Liotta, J. A. Martens, P. P. Pescarmona, M. Gruttadauria, ChemSusChem 2011, 4, 1830-1837; b) P. Agrigento, M. J. Beier, J. T. N. Knijnenburg, A. Baiker, M. Gruttadauria, Journal of Materials Chemistry 2012, 22, 20728-20735.
15. L. A. Bivona, F. Quertinmont, H. A. Beejapur, F. Giacalone, M. Buaki-Sogo, M. Gruttadauria, C. Aprile, Advanced Synthesis & Catalysis 2015, 357, 800-810.
16. R. Buscemi, F. Giacalone, S. Orecchio, M. Gruttadauria, ChemPlusChem 2014, 79, 421-426.
17. a) H. A. Beejapur, V. Campisciano, F. Giacalone, M. Gruttadauria, Advanced Synthesis & Catalysis 2014, 357, 51-58; b) H. A. Beejapur, F. Giacalone, R. Noto, P. Franchi, M. Lucarini, M. Gruttadauria, ChemCatChem 2013, 5, 2991-2999; c) E. Montroni, M. Lombardo, A. Quintavalla, C. Trombini, M. Gruttadauria, F. Giacalone, ChemCatChem 2012, 4, 1000-1006.
18. M. Gruttadauria, F. Giacalone, R. Noto, Green Chemistry 2013, 15, 2608-2618.
19. a) A. Dondoni, G. Fantin, M. Fogagnolo, A. Medici, P. Pedrini, J. Org. Chem. 1989, 54, 693-702; b) A. Dondoni, Synthesis 1998, 1998, 1681-1706; c) A. V. Denisenko, A. V. Tverdokhlebov, A. A. Tolmachev, Y. M. Volovenko, S. V. Shishkina, O. V. Shishkin, Synthesis 2011, 2011, 251-256.
20. a) G. E. Bonvicino, D. J. Hennessy, Journal of the American Chemical Society 1957, 79, 6325-6328; b) G. M. Clarke, P. Sykes, Journal of the Chemical Society C 1967, 1411-1414.
21. C. J. Serpell, J. Cookson, A. L. Thompson, C. M. Brown, P. D. Beer, Dalton Transactions 2013, 42, 1385-1393
22. S. Nadeem, M. K. Rauf, M. Bolte, S. Ahmad, S. A. Tirmizi, M. Asma, A. Hameed, Transition Metal Chemistry 2010, 35, 555-561.
23. a) J. C. Love, D. B. Wolfe, M. L. Chabinyc, K. E. Paul, G. M. Whitesides, Journal of the American Chemical Society 2002, 124, 1576–1577; b) J. C. Love, D. B. Wolfe, R. Haasch, M. L. Chabinyc, K. E. Paul, G. M. Whitesides, R. G. Nuzzo, Journal of the American Chemical Society 2003, 125, 2597-2609; c) S. Santra, K. Dhara, P. Ranjan, P. Bera, J. Dash, S. K. Mandal, Green Chemistry 2011, 13, 3238-3247.
24. A. R. Siamaki, A. E. R. S. Khder, V. Abdelsayed, M. S. El-Shall, B. F. Gupton, Journal of Catalysis 2011, 279, 1-11.

Chapter 5

Imidazolium functionalized carbon nanotubes for the synthesis of cyclic carbonates: bridging the gap between homogeneous and heterogeneous catalysis

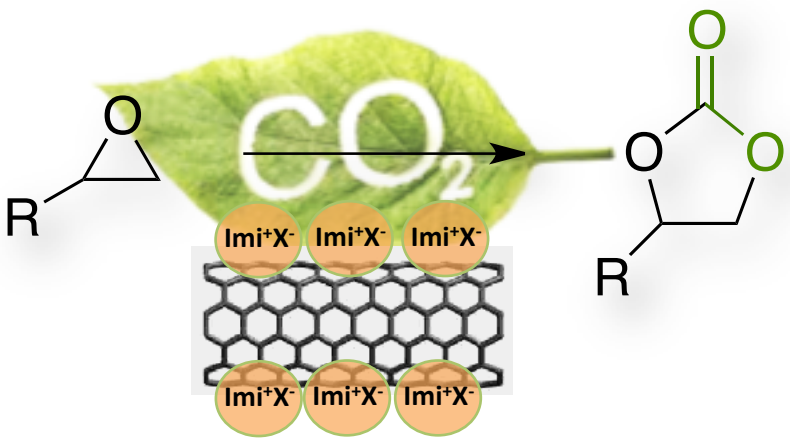

Chapter 5

This chapter is based on: M. Buaki-Sogó, A. Vivian, L. A. Bivona, H. García, M. Gruttadauria, C. Aprile, article in preparation.

Imidazolium functionalized carbon nanotubes for the synthesis of cyclic carbonates: bridging the gap between homogeneous and heterogeneous catalysis

5.1 Introduction

In recent years, the synthesis of cyclic carbonates attracted a growing interest in the scientific community due to their application in various industrial processes. These high-added value products are widely employed as polar aprotic solvents, precursor of pharmaceuticals and as intermediates in the synthesis of polycarbonates. The synthesis approach involving the use of CO_2 and epoxides as starting materials is receiving a particular deal of interest due to the possibility of transforming CO_2, an abundant, renewable and easily available reagent, into useful products.[1] Moreover the use of CO_2 and epoxides represents a sustainable alternative to the conventional route requiring the use of toxic reactants such as phosgene.[2,3]

The main drawback related to the conversion of carbon dioxide come from its high thermodynamic and kinetic stability.[3] The problem of the elevated energy input required for CO_2 transformation may be partially solved selecting high energy starting materials, like epoxides, and low energy products as carbonates. Moreover, the design of a catalyst able to promote the reaction in an efficient way is of fundamental importance.[4] Among the many species able to catalyze the transformation of CO_2 and epoxides into cyclic carbonates imidazolium based ionic liquids displayed an excellent catalytic activity.[5]

There is a large number of reports describing the use of imidazolium based catalytic systems under homogeneous conditions.[6] These systems usually display high efficiencies in terms of yield and selectivity, however catalyst recovery for subsequent reuse is not always feasible. In contrast, heterogeneous catalysts can be easily recovered from the reaction mixture but they often present lower catalytic performances if compared with their homogeneous analogous. The ideal catalyst should be able to combine the excellent

activity of homogeneous systems with the easier recovery of the heterogeneous ones. One of the most used techniques for the synthesis of highly efficient heterogeneous catalysts consists in the "heterogeneization" of the active species.[4]

Among the different solid supports already reported for "heterogeneization"[4] carbon nanotubes (CNTs) emerged as attractive materials due to their unique chemical and physical properties. Owing to their large specific surface area, high electrical conductivity and chemical and thermal stability, CNTs are one of the most employed material in nanoscience and nanotechnology.[7] The above mentioned characteristics represent also interesting features for catalytic applications. The main strategies employed for the functionalization of CNTs can be classified in two categories: non-covalent functionalization (e.g. through Van der Waals or π-π interactions)[8] and covalent functionalization.[8] The last strategy would be preferable in view of possible catalytic applications implying the reusability of the "heterogenized" material. However, it is known that low loading of organic species is usually achieved *via* functionalization of nanotubes at the tips or on the walls.

An interesting alternative is represented by the possible covalent grafting of long polymeric chains via radical promoted reaction of properly functionalized styrene derivatives with the double bonds available on the nanotubes walls followed by self-condensation of the organic moieties. This synthesis strategy would allow having a high loading of polymerized organic species covalently attached to the SWCNT.

Herein, imidazolium functionalized SWCNTs were synthesized in a one-pot procedure *via* self-assembly and polymerization of vinyl substituted imidazolium monomers. Two different synthesis strategies were selected and the materials extensively characterized via transmission electron microscopy (TEM), Raman spectroscopy, N_2 physisorption, Infrared (IR) spectroscopy and combustion chemical analysis. The solids resulted to be active for the reaction of CO_2 and various epoxides to produce cyclic carbonates. The excellent catalyst performances were highlighted by the elevated turnover number and productivities in absence of co-catalyst.

The best catalyst was used in multiple catalytic cycles without loss of activity. Moreover, the materials displayed excellent dispersion ability in the reaction media as well as in different organic solvents producing suspensions that resulted to be stables for weeks. (This behaviour could open the door also to other possible applications in nanotechnology).

5.2 Results and Discussion

Imidazolium functionalized SWCNTs were synthesized starting from raw nanotubes and two different imidazolium based salts. In a first attempt a styrene derivative of the imidazolium salt was employed (**S-Imi**) while a second strategy involved the use of a salt bearing bis-vinyl functionality (**bV-Imi**). In both cases a covalent functionalization of the carbon nanostructures together with the generation of a polymeric chain was envisaged. It is known that long charged polymeric chain may help the dispersion of carbon nanotubes in various solvents.[8] Moreover, the positive effect of the non-covalent interaction of imidazolium based surfactants on the disaggregation of SWNT was recently reported.[9] The design of SWNT decorated with imidazolium based polymers was expected combing an improved dispersion of the carbon nanotubes with a high degree of catalytic active species obtained *via* covalent immobilization/polymerization of the monomeric precursors.

The 1-methyl-3-(4-vinylbenzyl)-1H-imidazol-3-ium salt (**S-Imi**) was synthesized starting from 1-methyl imidazole and 4-vinylbenzyl chloride. The second imidazolium salt 3,3'-(1,4-phenylenebis(methylene))bis(1-vinyl-1H-imidazol-3-ium) derivative (**bV-Imi**) was prepared reacting 1,4-dibromo-*p*-xylene with 1-vinylimidazole. Both imidazolium salts were characterized by ^{1}H NMR, ^{13}C NMR, IR and combustion chemical analysis (Figure 1).[10,11]

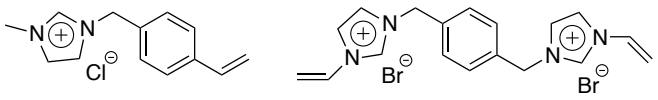

S-Imi **bV-Imi**

Figure 1. Ionic liquids **S-Imi** (a) and **bV-Imi** (b).

After characterization, **S-Imi** and **bV-Imi** were used for the preparation of imidazolium based polymeric chains via *in-situ* radical polymerization. The covalent grafting was achieved by taking advantage from the high reactivity of the SWCNT C=C double bonds present on the nanotube. The **S-Imi** was, hence, expected to react with the SWCNT surface as well as with the monomers present in solution via self-condensation generating polymeric or oligomeric chains covalently anchored to the walls at least at one of their extremities. The presence of the bis-vinyl functionality in the **bV-Imi** would favour the formation of an imidazolium cross-linked porous network with the dual effect of anchoring and trapping the carbon nanostructures (Scheme 1).

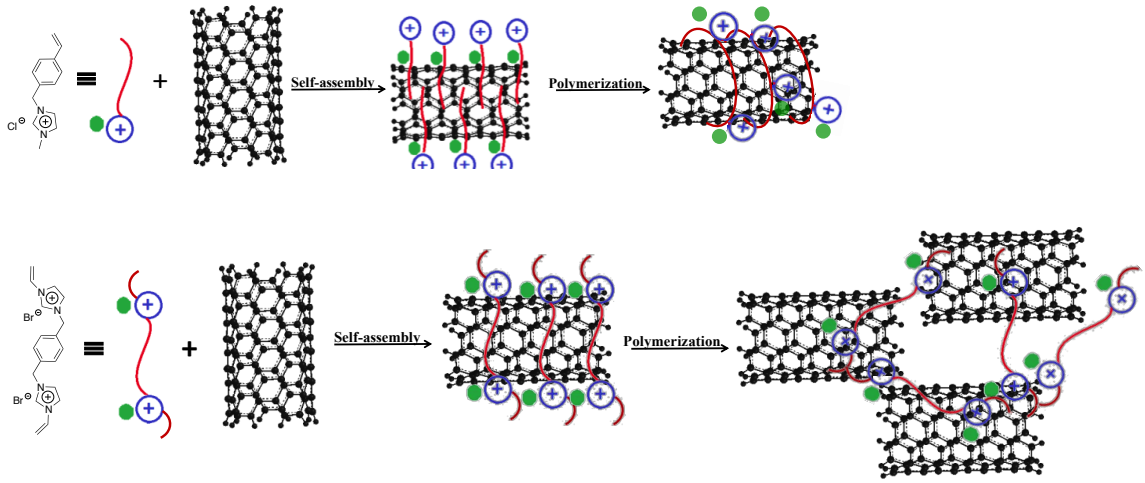

Scheme 1. Self-assembly and polymerization of **S-Imi** (a) and **bV-Imi** (b) in the presence of SWCNTs.

Two different approaches were selected for the preparation of imidazolium supported nanotubes. The first approach was inspired to the work of Ford and co-workers reported in 2004 for the synthesis of poly-styrenesulfonate functionalized SWCNT.[12] The amphiphilic character of ionic liquids **S-Imi** and **bV-Imi** in water solutions was used to favour the interaction with the nanotube wall prior to the polymerization. It is known that ammonium based ionic liquids self-organize around the SWCNT in a kind of tubular micellar shape favouring their dispersion in polar solvents. The hydrophilic imidazolium head is expected to face the water phase, while the hydrophobic styrene moiety would interact with the nanotube surface most probably by π-stacking interactions. After simple stirring in water, the mixture of **S-Imi** (or **bV-Imi**) and SWCNT appears as a homogeneous black suspension evidencing the increased dispersion properties of the nanotube. In absence of imidazolium salts the carbon nanotubes were visible in water as black aggregates. The addition of the radical source was performed after the formation of this homogeneous dispersion. After reaction, the imidazolium functionalized SWCNT (named **S-Imi-NT-1** and **bV-Imi-NT-1** where 1 stands for first synthesis procedure) were collected, filtered and washed with milliQ water and methanol.

In the second approach, bis-vinyl imidazolium salt **bV-Imi** was employed to generate a cross-linked polymeric network around the carbon nanotube framework. After stirring of the bis-vinyl imidazolium salt and the raw SWCNT in absolute ethanol, the anchoring/polymerization reaction was initiated using AIBN (2,2′-Azobis(2-methylpropionitrile)) as the radical source.

As in the previous case, the SWCNTs form a uniform dispersion during the pre-polymerization treatment with imidazolium monomers and this second batch of functionalized SWCNTs (**bV-Imi-NT-2**) was also collected by filtration and washed with

hot methanol. All the samples of functionalized carbon nanotubes were characterized by TEM, Raman spectroscopy and N_2 physisorption. The degree of functionalization was evaluated by combustion chemical analysis.

From a macroscopic point of view both **S-Imi-NT-1** and **bV-Imi-NT-2** form stable dispersions in organic solvents as ethanol, methanol and dichloromethane confirming the positive effect of the imidazolium moieties was preserved after the reaction. Moreover, they behave in a similar way in presence of different epoxides used as target starting materials for the chemical fixation of carbon dioxide indicating that their properties can be advantageous also from a catalytic point of view. Figure 2 displays the comparison between functionalized **bV-Imi-NT-2** (a) and pristine nanotubes (b) in water. In the same figure, samples c and d show the dispersion of **bV-Imi-NT-2** in styrene oxide and ethanol respectively. Interestingly, **bV-Imi-NT-1** displayed a different behaviour more similar to the pristine nanotubes, suggesting that a lower degree of imidazolium functionalization occurred.

From combustion chemical analysis emerged that **S-Imi-NT-1** present an imidazolium loading corresponding to 19 wt% while **bV-Imi-NT-1** displayed a very low nitrogen loading (≈ 5 wt%) indicating that the first synthesis approach, in which potassium persulfate was used as radical source, was not appropriate for the formation of the cross-linked polymeric network. On the other hand, elemental analysis of **bV-Imi-NT-2** prepared *via* the AIBN induced polymerization revealed an exceptionally high imidazolium loading (55 wt%).

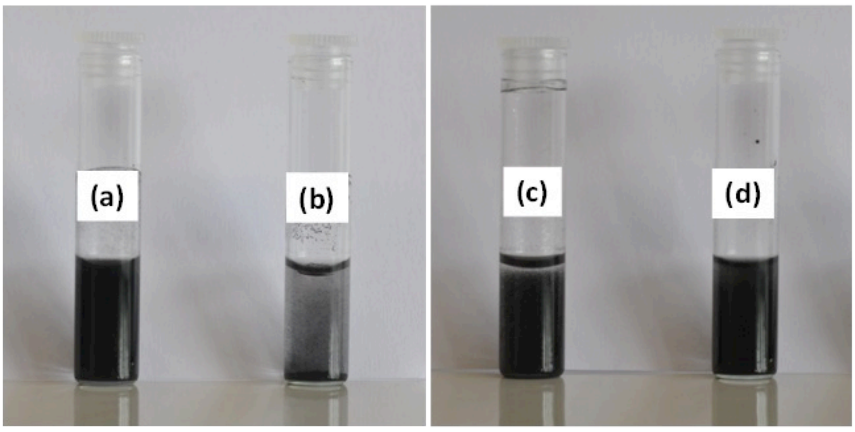

Figure 2. Suspensions formed in water with functionalized **bV-Imi-NT-2** (a) and pristine nanotubes (b); (c) and (d) correspond to **bV-Imi-NT-2** in styrene oxide and ethanol, respectively.

From this preliminary investigation, **S-Imi-NT-1** and **bV-Imi-NT-2** clearly represent the most promising materials for catalytic applications. Therefore, only the full characterization of these two nanostructures will be discussed herein.

Transmission electron microscopy investigation allows highlighting major differences between the **S-Imi-NT-1** and **bV-Imi-NT-2** (TEM images of the pristine nanotubes are reported in Figure 3a). In both cases the typical 1D structure of single walled carbon nanotube can be observed indicating that the nanostructure was not strongly affected by the chemical treatment. However, as can be clearly observed in Figure 3b **S-Imi-NT-1** present a larger tube diameter compared with the original SWNT and some spiral like structures can be tentatively identified at higher magnifications suggesting a preference of the imidazolium decorated polystyrene to enrobes the carbon nanotubes. It deserves to be mentioned that thin layers or filaments of polymeric organic species look usually transparent to the transmitted electron beam and are difficult to observe in TEM measurements. The **bV-Imi-NT-2** solid mainly displayed a standard nanotube diameter and various regions in which de-bundled tubes can be observed (Figure 3c).

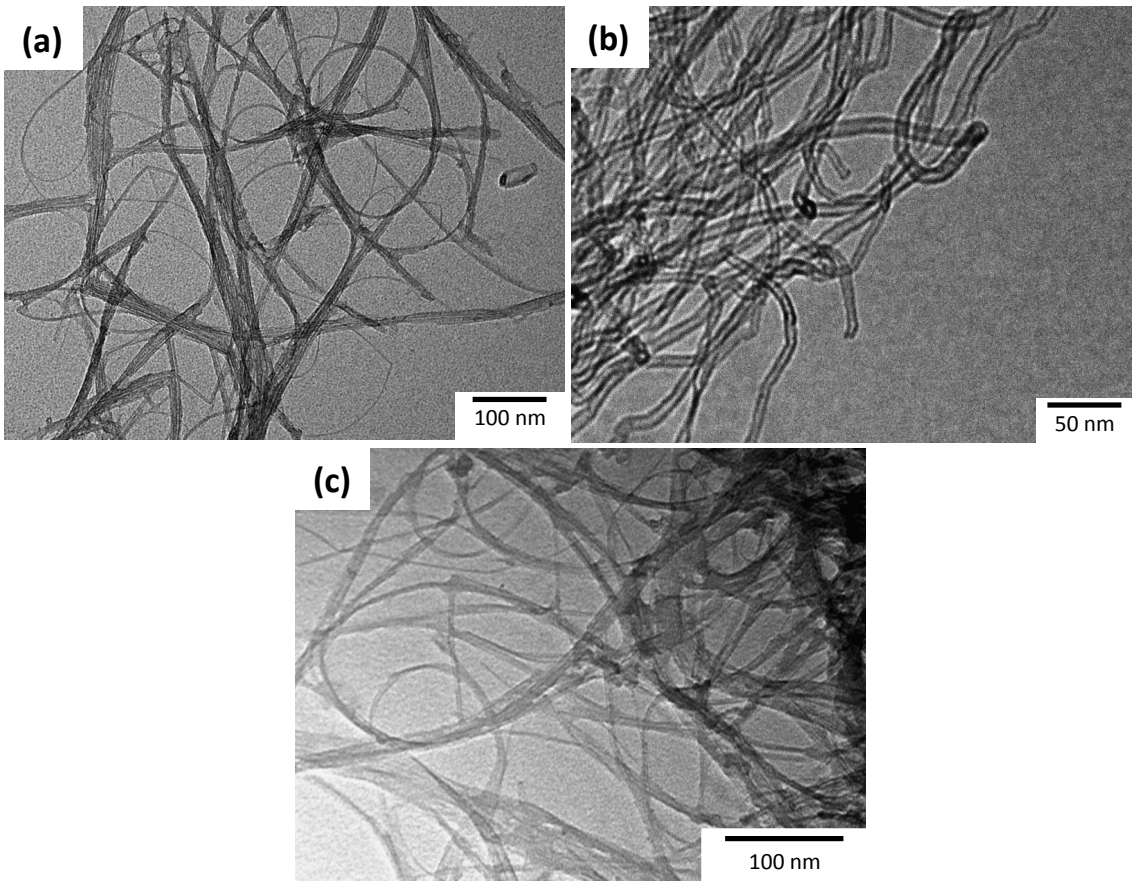

Figure 3. TEM images of raw SWCNT (a), **S-Imi-NT-1** (b) and **bV-Imi-NT-2** (c).

In addition to transmission electron microscopy, Raman spectroscopy is one of the most powerful techniques to investigate the nanotube structures. Comparing the Raman spectra of the non-functionalized SWCNT with the **S-Imi-NT-1** and **bV-Imi-NT-2**, we observed an evident variation of the region between 1300 and 1600 cm^{-1}. The D band (at 1346 cm^{-1} in Figure 4) is usually associated with defects and amorphous carbon while the G band ("graphitic" band) centred at 1592 cm^{-1} is attributed to the ordered sp^2 carbon network.[13] As can be clearly seen in the figure a small decrease in the intensity of the tangential vibration of the graphene wall at 1590 cm^{-1} and a more evident increase of a broad unresolved band at about 1380 can be detected for both samples, **S-Imi-NT-1** (Figure 4b) and **bV-Imi-NT-2** (Figure 4c), indicating that a certain degree of covalent functionalization occurred. The relative ratio between the areas of the two bands (I_D/I_G) was calculated as well. In the case of **S-Imi-NT-1** an increase in the I_D/I_G ratio from 0.085 (for the raw SWCNT) to 0.32 was observed while **bV-Imi-NT-2** displayed an I_D/I_G ratio of 0.14 suggesting a preference of the self-polymerization rather than covalent functionalization of the bis-vinyl-imidazolium precursor.

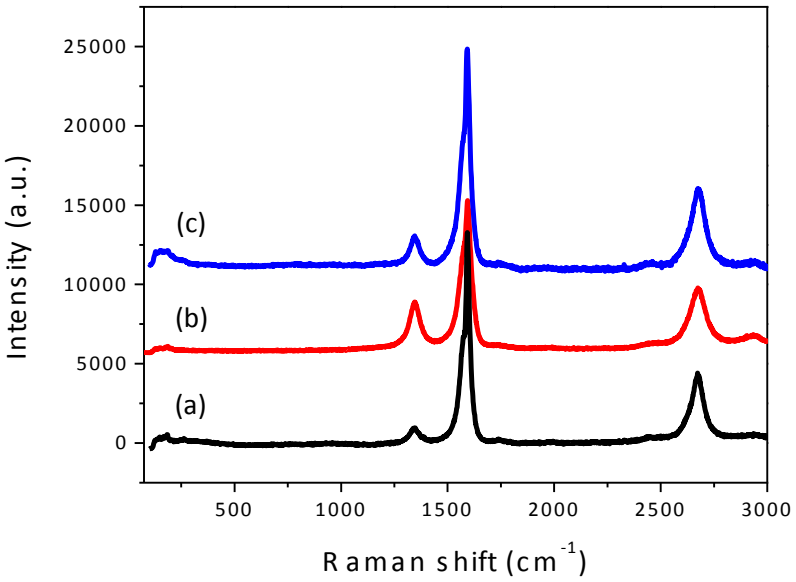

Figure 4. Raman spectra of raw SWCNT (a), **S-Imi-NT-1** (b) and **bV-Imi-NT-2** (c).

Nitrogen adsorption-desorption isotherms of the non-functionalized and functionalized nanotubes are shown in Figure 5. The high specific surface area estimated via the Brunauer, Emmett and Teller (BET) method for the non-functionalized nanotubes (1000 m^2/g) is in agreement with the literature.[14] As expected, the functionalization decreased the BET values to 360 m^2/g and 100 m^2/g for **S-Imi-NT-1** and **bV-Imi-NT-2** respectively. The lower surface area of the **bV-Imi-NT-2** can be attributed to exceptional high imidazolium

loading. A similar trend was observed for silica supported cross-linked polymeric network whose catalytic behavior was not affected by the surface area indicating that a disordered but accessible porous organization was obtained.[11,15] The evident hysteresis loop observed in all the samples may be ascribed to the large and non-ordered mesoporosity generated by the flexible rope-like network of the SWCNT and to a combination of the previously mentioned behavior of the nanotubes with the polymeric organization in the case of **S-Imi-NT-1** (Figure 5b) and **bV-Imi-NT-2** (Figure 5c). The pore size distribution of all the solids was evaluated via the standard Barrett-Joyner-Halenda (BJH) method and the results are shown in the insets reported in Figure 5. As can be observed, the pore size distribution (PSD) of SWNT (inset of Figure 5a) obtained via the BJH displays two maxima, one in the microporous region corresponding to the diameter of the carbon nanotubes (1.53 nm) and the other, less defined, in the mesoporous region attributed to the slits between the bundles of nanotubes.[16] **S-Imi-NT-1** (inset in Figure 5b) shows a similar behavior indicating that the polymerization occurs only on the external surface of nanotubes while for **bV-Imi-NT-2** (inset of Figure 5c) only the mesoporous organization due to the presence of the cross-linked network trapping the nanotube is observed. This expected behavior can be attributed (once more) to the high loading of organic functionalization in the case of **bV-Imi-NT-2**. The PSD calculated via the BJH method represents a good approximation of the nanotubes distribution. However, as reported by Wang and co-workers,[16] a more correct interpretation should involve a different treatment of the two part of the desorption isotherm. Following the work of Wang, the first section (corresponding to a PSD <2 nm) was also analyzed using the Horvath-Kawazoe (HK) method while the application of the BJH method was restricted to the second section (PSD > 2nm). The PSD calculated with the HK method and applying a cylindrical pore model gave a value of 1.35 nm, slightly smaller than the distribution obtained *via* the BJH analysis of the samples and in agreement with literature data.

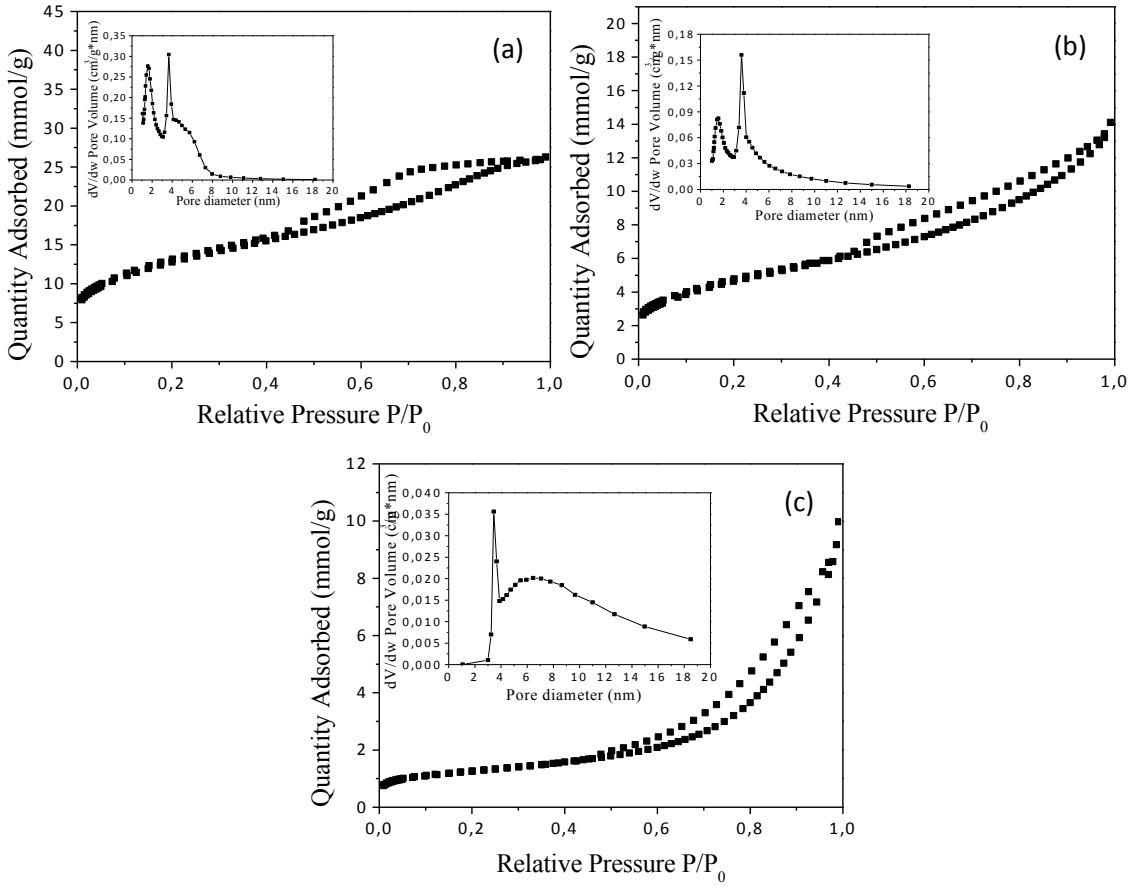

Figure 5. Nitrogen adsorption-desorption isotherms of raw SWCNT (a), **S-Imi-NT-1** (b) and **bV-Imi-NT-2** (c) catalyst (the insets correspond to the PSD obtained from the BJH desorption data).

Both imidazolium-based SWCNT presented interesting features for catalytic applications: good surface area, high degree of functionalization and excellent dispersion in the reaction medium also at room temperature. **S-Imi-NT-1** and **bV-Imi-NT-2** were, hence, tested as catalyst in the transformation of CO_2 and epoxides into cyclic carbonates. The broadly accepted reaction mechanism for this reaction is described in the following Scheme (Scheme 2).[17] In general, the reaction mechanism involves the epoxide opening by the nucleophile with consequent generation of negatively charged oxygen, which attacts CO_2 to give the carbonate anion. Then the carbonate anion, through a S_N2 reaction, forms the five-membered ring, rigenerating simultaneously the nucleophile.

The chemical fixation of CO_2 onto epoxides was performed in a batch reactor ready to work at high pressures and with individual temperature control (a picture of the reactor is reported in the Experimental Section, Chapter 8, section 8.3). The reaction was carried out under solvent-free conditions and the reaction time was set to 3 hours for all the tests.

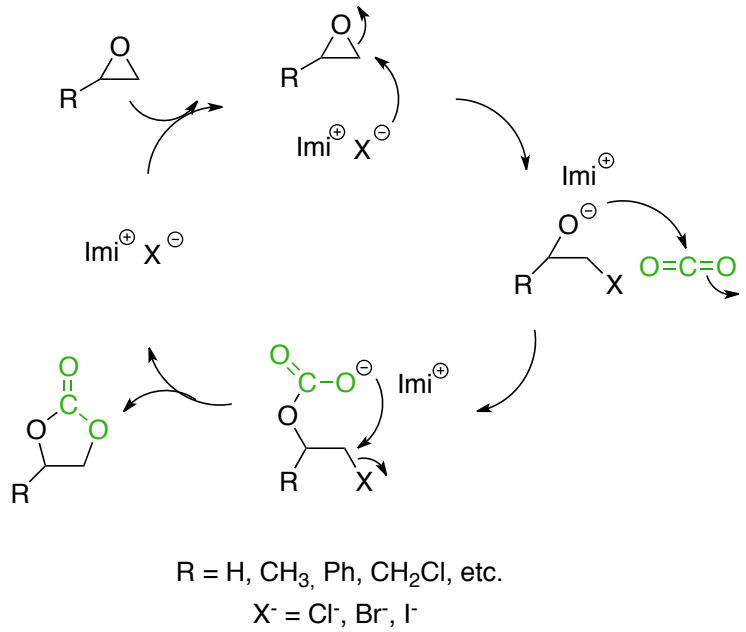

Scheme 2. Proposed mechanism for the chemical conversion of carbon dioxide with epoxides into cyclic carbonates catalysed by imidazolium salts; the cation is a common imidazolium and the anion is a generic halogen.

Owing to the industrial importance of epichlorohydrin carbonate, epichlorohydrin was used as target starting material and challenging conditions in terms of substrate to catalyst ratio were used (100 mg of catalyst for 24 mL of epoxide). Moreover, a screening of pressure, temperature and substrate was performed as well.

Due to the different imidazolium loading and in order to allow a meaningful comparison with literature data, the results obtained are discussed in terms of turnover number (TON, calculated as *moles converted/moles of imidazolium active sites*) and productivity (Prod, defined as *g converted/g of catalyst*).

Table 1. Catalyic tests performed in supercritical CO_2 with **S-Imi-NT-1** and **bV-Imi-NT-2** catalysts.[a]

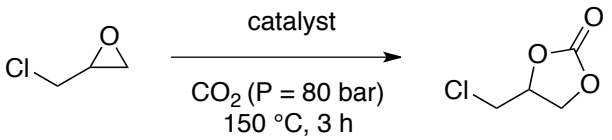

Entry	Catalyst	Conversion [%][b]	Selectivity [%][c]	TON[d]	Prod.[e]
1	**S-Imi-NT-1**	30	> 95	1091	125
2	**bV-Imi-NT-2**	81	> 95	1000	338

[a] Reaction conditions: epichlorohydrin (ECH = 24 mL, 0.306 mol); 100 mg of catalyst; T = 150 °C; P = 80 bar, 3 h. [b] Conversion and carbonate yield determined by ^{1}H NMR. [c] Selectivity toward cyclic carbonate. [d] TON (*turnover number* calculated as*: moles converted/moles of imidazolium active sites*). [e] Prod. (Productivity calculated as: *g converted*/total *g of catalyst*).

From a first comparison of the catalytic behaviour of **S-Imi-NT-1** and **bV-Imi-NT-2** appeared evident that the carbon nanotubes embedded in the cross linked polymeric network (**bV-Imi-NT-2**) displayed improved performances. Excellent selectivity was achieved with both catalysts (Table 1). However, under the same reaction conditions (compare entry 1 and 2 in Table 1) the conversion obtained with **bV-Imi-NT-2** was higher than the conversion obtained when **S-Imi-NT-1** was used as catalyst. It is worth to underline the extremely high turnover number obtained in both cases. Despite the similar TON (due to the different loading of active sites) it is clear that from a more applied point of view the total amount of catalyst employed represents a key factor.

To achieve the same conversion almost 300 mg of **S-Imi-NT-1** should be used. The advantage of the polymeric cross-linked network results more evident when comparing the productivity values obtained with both catalysts.

In light of this evidence, further catalytic investigation was performed with the best **bV-Imi-NT-2** solid. Carbon dioxide pressure screening (see entries 1-3 in Table 2) evidenced that the catalytic performances of **bV-Imi-NT-2** were not strongly affected by the decrease of the pressure indicating that milder reaction conditions (e.g. 40 bar) can be used without decreasing the catalytic activity. Additional catalytic experiences allow evidencing that the temperature play a key role on the catalyst performances (see entries 4 and 5): at 125 °C a decrease in the conversion was already observed with a consequent drop in TON values from 1058 to 398 (compare entries 3 and 4), a further decrease of the temperature caused a drastic reduction of the catalytic performances. It is worth to underline that when imidazolium or ammonium catalyst are used without addition of any co-catalyst with Lewis acid properties, high temperatures (superior to 125 °C) are usually required.[18]

Table 2. Pressure and temperature screening for CO_2 reaction with epichlorohydrin using **bV-Imi-NT-2** catalyst.[a]

Entry	Temperature [°C]	Pressure CO_2 [bar]	Conversion [%][b]	Selectivity [%][c]	TON[d]	Prod.[e]
1	150	80	81	> 95	1000	338
2	150	60	82	> 95	962	343
3	150	40	83	> 95	1058	347
4	125	40	34	> 95	398	142
5	100	40	9	> 95	107	38

[a] Reaction conditions: epichlorohydrin (ECH = 24 mL, 0.306 mol); 100 mg of **bV-Imi-NT-2** catalyst, 3 h. [b] Conversion and carbonate yiled determined by ^{1}H NMR. [c] Selectivity toward cyclic carbonate. [d] TON (*turnover number* calculated as*: moles converted/moles of imidazolium active sites*). [e] Prod. (Productivity calculated as: *g converted*/total *g of catalyst*).

In any case the high TON values and productivity obtained with the **bV-Imi-NT-2** catalyst allow highlighting the positive role of the polymeric cross-linked network that presents a double advantage: an increased imidazolium loading and an enhanced contact between reagents due to the good solubility of CO_2 in the ionic liquid-like phase.[11,19]

In order to have a better understanding of the catalytic behavior of the **bV-Imi-NT-2** the use of a challenging substrate like styrene oxide (SO) was investigated as well. Table 3 shows the conversion obtained with SO and under the same reaction condition used for ECH (150 °C and 100 mg of catalyst).

The results allow confirming the low influence of the pressure on the catalyst performances. In all the tests a high selectivity was obtained while, as expected, a lower conversion was achieved. However, when 200 mg of **bV-Imi-NT-2** were used (compare entries 4 and 5 in Table 3) a proportional increase of the conversion was observed. Once more, the good turnover number and the high productivity represent a proof of the good performance of the catalyst. In the catalytic evaluation of a heterogeneous catalyst, the high activity is not the only parameter that should be considered. Its stability under the reaction conditions with the consequent possibility of reuse in consecutive runs should be tested as well.

Table 3. Pressure and temperature screening for the reaction of CO_2 with styrene oxide using **bV-Imi-NT-2** catalyst.[a]

Entry	Mass Cat. [mg]	Pressure CO_2 [bar]	Conversion [%][b]	Selectivity [%][c]	TON[d]	Prod.[e]
1	100	80	11	> 95	103	38
2	100	60	11	> 95	91	38
3	100	50	11	> 95	105	38
4	100	40	11	> 95	105	38
5	200	40	22	> 95	109	38

[a] Reaction conditions: styrene oxide (SO = 24 mL, 0.210 mol), **bV-IMI-NT-2** as catalyst, biphenyl as internal standard, 150 °C, 3 h. [b] Conversion and carbonate yield determined by ^{1}H NMR. [c] Selectivity toward cyclic carbonate. [d] TON (*turnover number* calculated as*: moles converted/moles of imidazolium active sites*). [e] Prod. (Productivity calculated as: *g converted*/total *g of catalyst*).

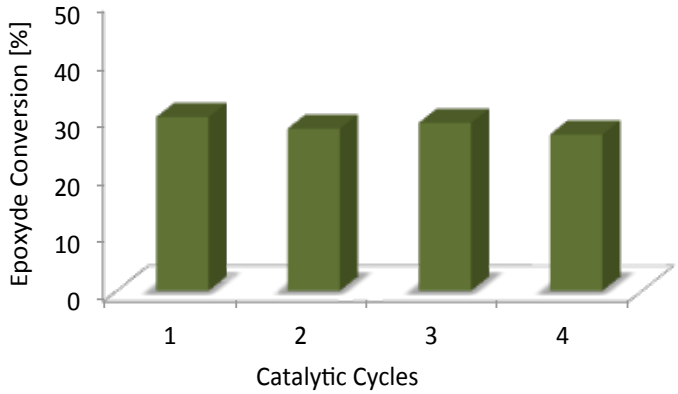

Figure 6. Recycling experiments for styrene oxide (SO = 24 mL, 0.210 mol) conversion using **bV-Imi-NT-2** catalyst (250 mg).

Recycling experiments were, hence, performed with the **bV-Imi-NT-2** using styrene oxide as target reagent (Figure 6). As can be clearly seen from the Figure 6 the catalyst can be reused in multiple catalytic cycles without loss of activity. After each cycle, the catalyst was recovered from the reaction mixture by centrifugation, washed with toluene and methanol and then dried in an oven at 80 °C (see Experimental Section for more details, Chapter 8). No additional treatment was needed in order to restore the activity.

In order to better highlight the difference between the two different synthesis approaches, recycling experiments in presence of **S-Imi-NT-1** and under the same reaction conditions used for **bV-Imi-NT-2** were performed as well. This investigation allow proving that **S-Imi-NT-1** suffered of an important leaching of organic active species in the reaction mixture as evidenced by the dramatic drop in the epoxide conversion during the second cycle. This hypothesis was confirmed via characterization of the sample after the use by means of combustion chemical analysis.

Table 4. Epoxide screening for **bV-Imi-NT-2** catalyst.[a]

Entry	Epoxyde	Temperature [°C]	Conversion [%][b]	Selectivity [%][c]	TON[d]	Prod.[e]
1	ECH	150	83	> 95	1058	347
2	PO	150	20	> 95	279	71
3	GLY	100	85	> 95	1184	307

[a] Reaction conditions: epoxide (0.306 mol); 100 mg of **bV-Imi-NT-2** catalyst; P = 40 bar, 3 h. [b] Conversion determined by ^{1}H NMR. [c] Selectivity toward cyclic carbonate. [d] TON (*turnover number* calculated as*: moles converted/moles of imidazolium active sites*). [e] Prod. (Productivity calculated as: *g converted*/total *g of catalyst*).

Finally, in order to prove versatility of the **bV-Imi-NT-2** solid, two additional epoxides were also testes. Propylene oxide (PO) and glycidol (GLY) in addition to the already tested styrene oxide (SO) and epichlorohydrin (ECH) were selected as target substrates and the results obtained in the reaction with CO_2 are shown in Table 4. The **bV-Imi-NT-2** catalyst displayed good catalytic activity with high carbonate yields and TONs for all the epoxides. With the highly reactive glycidol excellent conversion and selectivity were obtained also at the temperature of 100 °C (see entry 3). With this epoxide, temperatures higher that 100 °C were detrimental for the selectivity of the reaction. This behaviour was previously observed in the literature and can be probably ascribed to possible *inter- and intramolecular ring-opening reactions* leading to the formation of dendritic polymers and/or macromolecular cycles.[20]

5.3 Conclusions

Imidazolium-functionalized single-walled carbon nanotubes materials were synthesized using an *in-situ* radical polymerization process to covalently anchor two different imidazolium salts, both bearing vinyl functionalities, to the π-skeleton of nanotubes (**S-Imi-NT-1** and **bV-Imi-NT-2**). The characterization of the prepared materials proved the successful grafting of the imidazolium salts for **S-Imi-NT-1** and **bV-Imi-NT-2**, in particular a high imidazolium loading for the material **bV-Imi-NT-2**. Both materials were tested for the conversion of carbon dioxide with epoxydes into the corrisponding cyclic carbonates, without the use of any co-catalysts. From the results of a preliminary tests with epichlorohydrin, both catalysts displayed excellent activity in the conversion of the epoxide, with a very high selectivity towards the cyclic carbonate product. However, in terms of catalytic performance (productivity), the highly functionalized **bV-Imi-NT-2** was the most active, revealing the effectiveness of the cross-linked polymeric network obtained supporting the bis-vinylimidazolium salt. In light of this evidence, further studies were performed on **bV-Imi-NT-2** and the optimization of the reaction conditions was carried out, obtaining high turnover numbers, especially with epychloridrin as substrate. Moreover, it was easily recovered and reused in consecutive catalytic runs with only negligible loss of activity. Furthermore, it proved to be versatile in the conversion of CO_2 with other epoxydes.

5.4 References

1. a) W.-L. Dai, S.-L. Luo, S.-F. Yin, C.-T. Au, Applied Cat. A: General 2009, 366, 2-12; b) J. H. Clements, Ind. Eng. Chem. Res. 2003, 42, 663-674; c) S. Uhm, Y. D. Kim, Current Applied Physics 2014, 14, 672-679; d) C. Maeda, Y. Miyazaki, T. Ema, Catalysis Science & Technology 2014, 4, 1482-1497; e) H. Li, J. C. Liao, Energy & Environmental Science 2013, 6, 2892-2899; f) M. Aresta, A. Dibenedetto, in Catalytic Process Development for Renewable Materials, Wiley-VCH Verlag GmbH & Co. KGaA, 2013, 355-385; g) M. Aresta, A. Dibenedetto, Dalton Transactions 2007, 2975-2992.
2. S. Fukuoka, M. Kawamura, K. Komiya, M. Tojo, H. Hachiya, K. Hasegawa, M. Aminaka, H. Okamoto, I. Fukawa, S. Konno, Green Chemistry 2003, 5, 497-507.
3. T. Sakakura, J.-C. Choi, H. Yasuda, Chemical Reviews 2007, 107, 2365-2387.
4. M. Gruttadauria, F. Giacalone, Catalytic methods in asymmetric synthesis: advanced materials, techniques and applications, Wiley 2011.
5. a) L. A. Blanchard, D. Hancu, E. J. Beckman, J. F. Brennecke, Nature 1999, 399, 28-29.
6. a) M. North, R. Pasquale, C. Young, Green Chemistry 2010, 12, 1514-1539; b) A.-L. Girard, N. Simon, M. Zanatta, S. Marmitt, P. Goncalves, J. Dupont, Green Chemistry 2014, 16, 2815-2825; c) S. Zhang, Y. Chen, F. Li, X. Lu, W. Dai, R. Mori, Catalysis Today 2006, 115, 61-69; d) S. N. V. K. Aki, B. R. Mellein, E. M. Saurer, J. F. Brennecke, The Journal of Physical Chemistry B 2004, 108, 20355-20365.
7. a) A. Krueger, in Carbon Materials and Nanotechnology, Wiley-VCH Verlag GmbH & Co. KGaA, 2010, 123-281; b) C. Binns, in Introduction to Nanoscience and Nanotechnology, John Wiley & Sons, Inc., 2010, 53-95; c) K. Tanaka, S. Iijima, Carbon Nanotubes and Graphene: Edition 2, 2014.
8. D. Tasis, N. Tagmatarchis, A. Bianco, M. Prato, Chemical Reviews 2006, 106, 1105-1136.
9. A. Di Crescenzo, D. Demurtas, A. Renzetti, G. Siani, P. De Maria, M. Meneghetti, M. Prato, A. Fontana, Soft Matter 2009, 5, 62-66.
10. B. Huber, L. Rossrucker, J. Sundermeyer, B. Roling, Solid State Ionics 2013, 247-248, 15-21.
11. C. Aprile, F. Giacalone, P. Agrigento, L. F. Liotta, J. A. Martens, P. P. Pescarmona, M. Gruttadauria, ChemSusChem 2011, 4, 1830-1837.
12. S. Qin, D. Qin, W. T. Ford, J. E. Herrera, D. E. Resasco, S. M. Bachilo, R. B. Weisman, Macromolecules 2004, 37, 3965-3967.
13. S. A. Hodge, M. K. Bayazit, K. S. Coleman, M. S. P. Shaffer, Chemical Society Reviews 2012, 41, 4409-4429.
14. R. R. Bacsa, C. Laurent, A. Peigney, W. S. Bacsa, T. Vaugien, A. Rousset, Chemical Physics Letters 2000, 323, 566-571.
15. a) C. Pavia, E. Ballerini, L. A. Bivona, F. Giacalone, C. Aprile, L. Vaccaro, M. Gruttadauria, Advanced Synthesis & Catalysis 2013, 355, 2007-2018; b) L. A. Bivona, F. Quertinmont, H. A. Beejapur, F. Giacalone, M. Buaki-Sogo, M. Gruttadauria, C. Aprile, Advanced Synthesis & Catalysis 2015, 357, 800-810.
16. F. Li, Y. Wang, D. Wang, F. Wei, Carbon 2004, 42, 2375-2383.
17. a) V. Caló, A. Nacci, A. Monopoli, A. Fanizzi, Organic Letters 2002, 4, 2561-2563; b) M. North, R. Pasquale, Angewandte Chemie International Edition 2009, 48, 2946-2948.
18. a) M. H. Anthofer, M. E. Wilhelm, M. Cokoja, I. E. Markovits, A. Pöthig, J. Mink, W. A. Herrman, F. E. Kühn, Catalysis Science & Technology 2014, 4, 1749-1758;

b) M. Buaki-Sogo, H. Garcia, C. Aprile, Catalysis Science & Technology 2015, 5, 1220-1230; c) H. Sun, D. Zhang, Journal of Physical Chemistry A 2007, 111, 8036-8043.

19. a) S. Baj, T. Krawczyk, K. Jasiak, A. Siewniak, M. Pawlyta, Applied Catalysis A: General 2014, 488, 96-102.
20. M. E. R. Weiss, F. Paulus, D. Steinhilber, A. N. Nikitin, R. Haag, C. Schütte, Macromolecular Theory and Simulations 2012, 21, 470-481.

Chapters 6 and 7

Foreword

Chapters 6 and 7

Foreword

During the last decades, organic-inorganic hybrid compounds have become research area of growing interest. This increased deal of attention is due to the combination of advantages such as the high thermal and mechanical stability of the inorganic part together with the possibility to functionalize the organic part allowing a facile tuning of their properties. In this context, Polyhedral oligomeric silsesquioxane (POSS) emerged as a novel class of organic-inorganic hybrids that may find a wide range of applications in several fields. In particular, the functionalization of the organic peripheries allows modifying their properties in terms of solubility, thermal stability and reactivity. All these parameters are extremely important for catalytic applications.

In the Chapters 6 and 7, two silsesquioxanes based nanostructure functionalized with imidazolium chloride (**POSS-Imi**) or tetrachloropalladate (**POSS-Imi-PdCl$_4$**) peripheries are presented.

In particular, in the Chapter 6 of this PhD thesis, we reported for the first time the imidazolium chloride substituted nanocage (**POSS-Imi**) as catalyst for the conversion of carbon dioxide. In the following chapter, we propose the use imidazolium POSS chloride as precursor and, taking the advantage of the presence of chloride as anions, we synthetized a new catalyst based on imidazolium functionalized POSS tetrachloropalladate salts (**POSS-Imi-PdCl$_4$**), which is employed as pre-catalyst for Suzuki-Miyaura reactions, avoiding then the use of reducing agents.

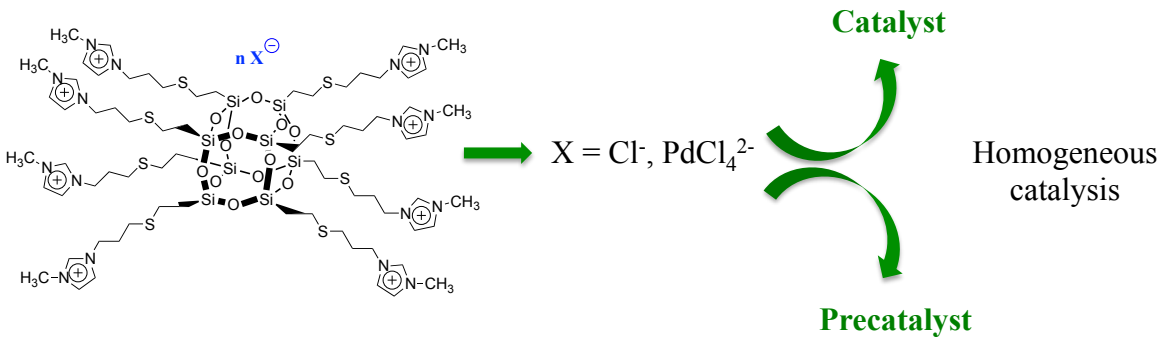

Figure 1: Schematic representation of the catalysts for applications in homogeneous reactions.

Chapter 6

Polyhedral oligomeric silsesquioxane based catalyst for the efficient synthesis of cyclic carbonates

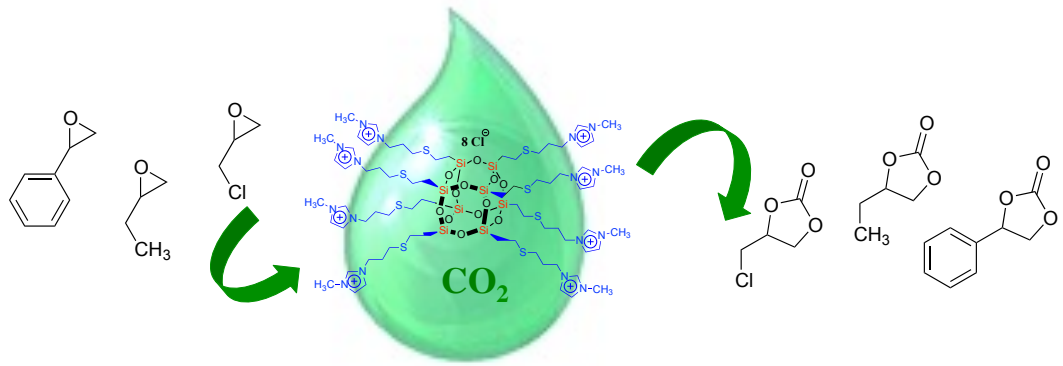

Chapter 6

This chapter is based on: L. A. Bivona, O. Fichera, L. Fusaro, F. Giacalone, M. Buaki-Sogo, M. Gruttadauria, C. Aprile, Catalysis Science & Technology, 2015, 5, 5000-5007.

Polyhedral oligomeric silsesquioxane based catalyst for the efficient synthesis of cyclic carbonates

6.1 Introduction

In recent years, the use of CO_2 as feedstock in chemical processes has attracted a considerable attention from the scientific community.[1,2] Its low toxicity, along with its abundance and availability make of CO_2 an interesting molecule for sustainable applications. Carbon dioxide has been employed in different synthesis procedures as reagent, solvent and/or as extracting agent in purification processes.[2-5] One of the most studied reactions involving the use of CO_2 is represented by its fixation onto epoxides to produce cyclic carbonates and/or polycarbonates. Both classes of compounds are considered high added-value products widely used for different industrial and chemical applications.[2,6-10] Among the possible active species able to catalyze the synthesis of cyclic carbonates,[6] imidazolium ionic liquids have shown excellent performances acting as catalysts or co-catalysts, for the latter usually in combination with organometallic complexes with Lewis acid properties.[11-19] When used as the sole catalysts, imidazolium salts display good catalytic performances in function of the selected counterion, however high temperatures (usually 150 °C) are required.[20-22] It is worth to be mentioned that, as highlighted by Sakakura,[3] a temperature of 150 °C does not represent necessarily a drawback in industrial applications. In particular, since the synthesis of cyclic carbonates from CO_2 and epoxides is an exothermic reaction, an efficient heat removal should be envisaged in large-scale applications in order to optimize the energy consumption. A reaction temperature of about 150 °C would allow recovering the reaction heat as steam. Different parameters including the working pressure or the presence of a co-solvent may greatly influence the performance of the selected catalyst. It is known that the close proximity of the reactants, achievable using various strategies, plays a positive effect on the catalytic activity.[11] Improved carbonate yield can be obtained in absence of solvent[11,23,24] or when the reaction takes place in a confined space or in a particular phase

rich in catalytically active species.[21,25,26] Due to their excellent performances various imidazolium based catalysts working under both homogeneous and heterogeneous conditions have been proposed. However, the design of a catalyst displaying a perfect compromise between the excellent conversion and selectivity achieved with the homogeneous catalysts and the easy recovery of the heterogeneous ones, still represents a challenging objective. Polyhedral oligomeric Silsesquioxanes (POSS) is a family of organic-inorganic hybrids compounds characterized by an O/Si molar ratio of 1.5. Their structure can be expressed by the general formula T_nR_m, where T represent the number of Si and R the organic functionalities.[27-29] The most common of these compounds (T_8R_8) is the totally condensed POSS displaying an almost cubic structure. POSS nanostructures have attracted a growing interest during last decades due to their unique properties. Silsesquioxanes exhibit both organic and inorganic characteristics and a rigid cage-like core whose presence provides a high thermal and mechanical stability. Moreover, the organic peripheries can be easily functionalized allowing a facile tuning of the silsesquioxanes properties.[28,30-33] Therefore, they have been widely used in different applications as the development of bio-inspired materials[34] and optic devices,[35,36] as solid electrolytes,[37] additives in synthesis of periodic mesoporous organosilicas[38,39] and composites,[40] and more recently in (photo)catalysis.[39,41-47] Herein, we present a silsesquioxane based nanostructure functionalized with imidazolium chloride peripheries as efficient catalyst for the chemical fixation of carbon dioxide. Although similar POSS structures have already been reported,[31,36] here we report a novel synthesis protocol. Moreover, to the best of our knowledge this is the first time that imidazolium substituted silsesquioxanes (**POSS-Imi**) have been used as catalysts for the synthesis of cyclic carbonates starting from CO_2 and epoxides. An in-depth investigation of the **POSS-Imi** nanocage via ^{29}Si NMR, never reported earlier, was also performed. The anchoring of the imidazolium moieties to the POSS nanocage produced a substantial improvement of the catalytic performances thus proving the importance of the silsesquioxane core.

6.2 Results and Discussion

Polyhedral oligomeric silsesquioxane functionalized with imidazolium moieties was synthesized in a two steps procedure starting from the commercially available T_8R_8 octavinyl- substituted silsesquioxane (**POSS-vinyl**, Scheme 1). The **POSS-vinyl** was reacted with 3-chloro-1-propanethiol through a thiol-ene reaction in presence of 2,2-azobisisobutyronitrile (AIBN) as radical source to give the **POSS-Cl** (Scheme 1). The

good performance of the thiol-ene reaction was confirmed by following, *via* ^{1}H NMR spectroscopy, the disappearance of the vinyl signals in the region between 5.5 and 6.5 ppm (Supporting Information, section A.3, Figure S1). After purification, the product was also characterized by ^{13}C NMR and FT-IR spectroscopy as well as by combustion chemical analysis (see Experimental Section, Chapter 8, part 8.3 and Supporting Information Figures S2 and S3). The integrity of the nanocage was confirmed by the presence of only one signal in the ^{29}Si NMR spectrum typical of a T_8R_8 structure, corresponding to the T^3 silicon units (Figure 1b).

For comparison, the ^{29}Si NMR spectrum of the **POSS-vinyl** is shown in Figure 1a. The **POSS-Cl** was used as starting material in the reaction with the 1-methylimidazole to produce the desired imidazolium functionalized silsesquioxane (**POSS-Imi**, Scheme 1). Different parameters, in terms of amount of 1-methylimidazole and reaction time, were tested in order to improve the yield of the target product. After optimization of the reaction conditions, the **POSS-Imi** was obtained in relatively high yield (85 %) *via* an easy purification from the unreacted precursors by precipitation and washing.

The imidazolium based organocatalyst was exhaustively characterized by ^{1}H-NMR, ^{13}C-NMR, ^{29}Si-MAS-CP-NMR and FT-IR spectroscopy (reported in the Supporting Information, section A.3, Figures S4 to S6).

The degree of functionalization was proved by combustion chemical analysis, which revealed a high but not total degree of functionalization with a percentage of nitrogen corresponding to an average value of 7.2 imidazolium units per silsesquioxane nanocage and an amount of imidazolium unit of 39 wt%.

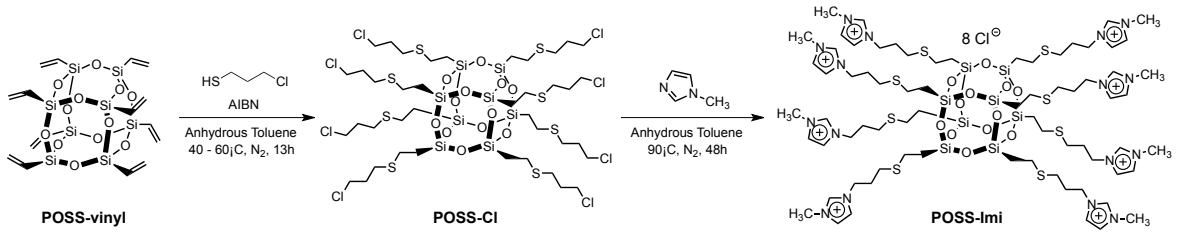

Scheme 1. Synthesis of the **POSS-Imi** catalyst.

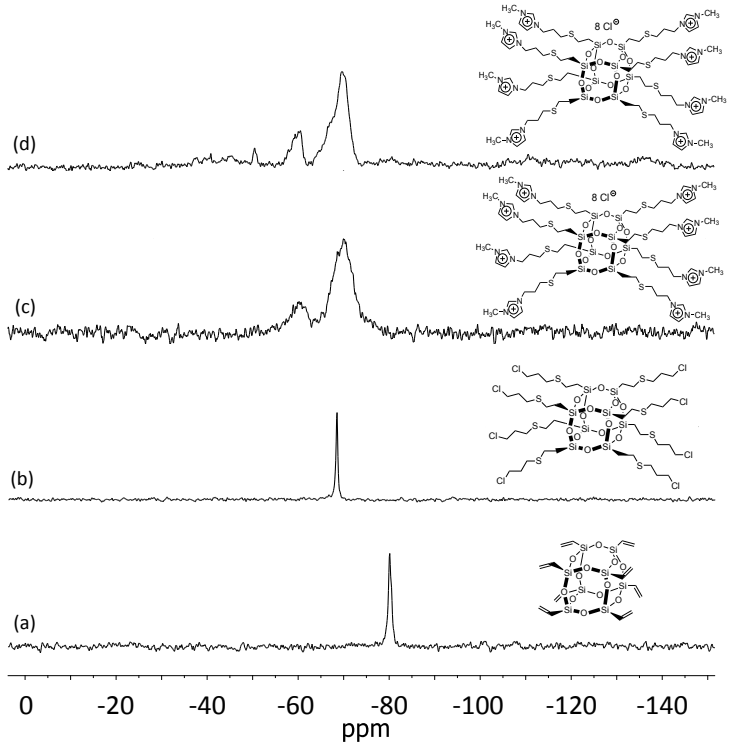

Figure 1. Liquid state ^{29}Si NMR spectra of the **POSS-vinyl** in deuterated toluene (a), **POSS-Cl** in deuterated toluene (b), **POSS-Imi** in deuterated water (d) and solid state ^{29}Si MAS NMR of the **POSS-Imi** (c).

In the ^{13}C NMR of the **POSS-Imi** a small signal at 43 ppm, corresponding to the unreacted chloropropyl branches can be also observed (Supporting Information, section A.3, Figure S5). The synthesis was repeated four times with highly reproducible results (%N = 9.15-9.35). Interestingly, solid state ^{29}Si-MAS-NMR (Figure 1c) performed on the **POSS-Imi** displayed two different bands, the most intense located at -70 ppm can be attributed to the T^3 silicon units (compare Figures 1b and 1c) while the second at -60 ppm could be a consequence of a partial opening of the silsesquioxane nanocage via corner cleavage. Liquid state ^{29}Si NMR (Figure 1d) exhibited an even more complex pattern with the presence of one additional contribution (at -50 ppm) of minor but still appreciable relevance. The difference between solid and liquid state ^{29}Si NMR can be attributed to the better signal to noise ratio usually obtained in liquid state nuclear magnetic resonance experiments. Surprisingly, the liquid state spectrum of **POSS-Imi** still displayed the broad bands typical of the solid state patterns indicating that the broadening of the signals can not be completely attributed to the effect of chemical shift anisotropy or heteronuclear dipolar coupling. The presence of these large bands could be the consequence of various contributions due to silicon units with similar chemical environment. In order to understand the origin of these additional contributions an in-depth study on the stability

and reactivity of the silsesquioxane nanocage through liquid state ^{29}Si NMR spectroscopy was performed.

All the experiments described below were carried out in a NMR tube and repeated twice. Control experiments in a round-bottom flask and under magnetic stirring were performed as well, and the NMR spectra, recorded for comparison at the final time (48 h), displayed similar results. Since the synthesis of the imidazolium derivative was performed in toluene, the stability of the **POSS-Cl** was tested by dissolving the solid in deuterated toluene in a NMR tube at 90° C and by following the evolution of the ^{29}Si NMR spectrum in time (Figure 2). A special NMR tube (see experimental) was used in order to avoid solvent evaporation. Firstly, the ^{29}Si NMR spectrum of the **POSS-Cl** in deuterated toluene is reported in Figure 2a. The final ^{29}Si NMR recorded after 48 h, did not show substantial differences proving that the selected silsesquioxane was stable under the reaction conditions (Figure 2 b). In order to simulate the possible influence of moisture a small amount of water (10 μL) was also added. The NMR spectrum is shown in Figure 2c. These experiments allow excluding the eventual partial decomposition of the **POSS-Cl** as consequence of the solvent and/or of the temperature. The presence of the additional bands in the ^{29}Si NMR of the **POSS-Imi** could be hence attributed to the reaction with the imidazole unit or to the presence of the imidazolium chloride salt.

To exclude the possible interaction of imidazole and/or imidazolium with the silsesquioxane nanocage and remove any possible interference coming from other reactive groups, a silsesquioxane similar to **POSS-Cl** but bearing a terminal methyl group (**POSS-Me**) was synthesized (Figure 3).

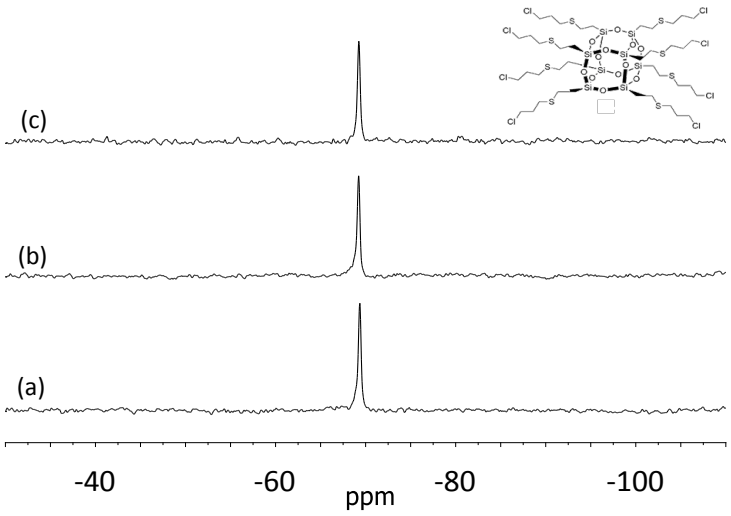

Figure 2. Liquid state ^{29}Si NMR spectra of the **POSS-Cl** in deuterated toluene (a), **POSS-Cl** in deuterated toluene after 48 h at 90 °C (b), **POSS-Cl** in deuterated toluene + 10 μL of H_2O after 48 h a 90 °C (c).

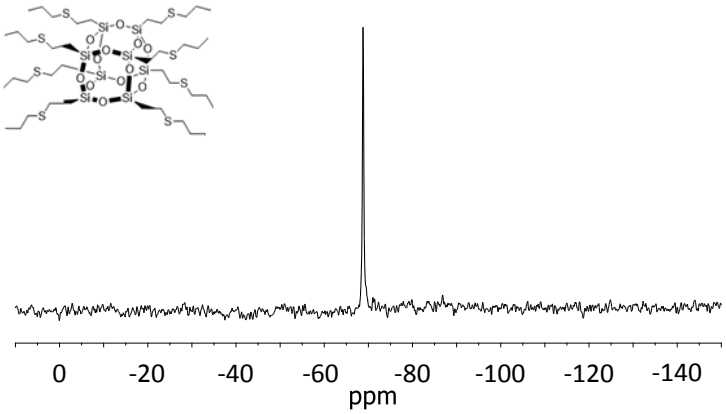

Figure 3. Liquid state ^{29}Si NMR spectrum of the **POSS-Me**.

The ^{29}Si NMR of the fresh catalyst is reported in Figure 3 while the ^{1}H and ^{13}C NMR as well as the IR spectra were included in the Supporting Information material (section A.3, Figures S7 to S9). The **POSS-Me** was reacted in presence of 1-Me-imidazole or 1-butyl-3-methylimidazolium chloride under the reaction conditions previously selected for the **POSS-Cl**. The final spectra after 48 h displayed in both cases only one signal corresponding to the T^3 units (see Supporting Information, Figure S10).

These experiments evidenced the absence of any detrimental effect of the reaction conditions as well as of the presence of the imidazolium chloride on the stability of the POSS nanocage. From the analysis of these data, the presence of the additional signals can not be clearly attributed to possible T^2, T^1 silicon units generated as consequence of the partial opening of silsesquioxane structure. The additional bands may be tentatively ascribed to the sensitivity of the ^{29}Si NMR chemical shift to the T-O-T angle. A total condensed and octa-functionalized silsesquioxane possesses a highly symmetric structure, which explains that the ^{29}Si NMR consists of a sole peak. On the other side, in hepta-functionalized nanocages the silicon atoms could not be chemically equivalent despite the similarity of the functional groups.[37] In the literature, difference in chemical shift of 10 ppm can be found only for POSS with T_8R_7R' structures where the R and R' have a very different nature (e.g. R = isobutyl and R' = vinyl [48]; R= cyclopentyl and R'= H [49]). In the present case the **POSS-Imi** is mainly a hepta-substituted silsesquioxane with similar R and R' functionalities, however the ionic nature and the aromatic character of the imidazolium moieties should not be underestimated. The interaction between the imidazolium functionalities could cause important distortions in the partially functionalized silica nanocage, which may display different O-Si-C angles. The polyhedral oligomeric

silsesquioxane with its small silica unit surrounded by imidazolium peripheries represents a promising catalyst for the conversion of CO_2 and epoxides into cyclic carbonates. The broadly accepted reaction mechanism for this reaction is reported in the previous chapter (Chapter 5, Scheme 3).[50,51]

The presence of the functionalized nanocage could create an increased local concentration of catalytic active species where the CO_2 migrates preferentially due to the affinity and high solubility of this small molecule in imidazolium ionic liquids phases. Since the opening of the three membered ring is catalyzed by the imidazolium counterion, the close proximity of the CO_2 is expected to bring improved carbonate yield.[11]

In order to test the catalytic performances of the **POSS-Imi**, styrene oxide was selected as target starting material as well as solvent for the reaction. All the catalytic tests were performed in presence of a small amount of co-solvent (1.5 mL per 24 mL of styrene oxide) in order to favor a homogeneous dispersion of the **POSS-Imi** in the reaction mixture. In absence of an appropriate co-solvent the **POSS-Imi** macromolecules tend to assembly forming large visible aggregates probably as consequence of the inter-molecular interaction between the imidazolium moieties. Different parameters including the nature of the solvent, pressure and relative amount of catalyst were studied.

Due to the absence of additional co-catalysts with Lewis acid properties the selected range of studied temperature was maintained between 100 °C and 150 °C (with the more reactive epoxides). It is known [21,22] that without "co-activation", good conversions at temperatures lower than 100 °C are difficult to achieve.

In a first attempt, the reaction of CO_2 with styrene oxide was conducted at the fixed temperature of 125 °C and in presence of water as co-solvent. The effect of different working pressures was studied and the results are summarized in Table 1 (entries 1- 5). At low pressures (Table 1, entries 1 and 2) a relatively low epoxide conversion was obtained with a corresponding TON (calculated as *moles converted/moles of imidazolium active sites*) of 70 and 102.

An increase in the working pressure to 40 bar led to enhanced conversion (Table 1, entry 3) while a further increase resulted in a slight reduction of the catalyst performance with a clear drop of the catalytic activity (Table 1, entry 5) under supercritical conditions. A similar trend was previously observed, in particular when heterogeneous catalysts with a multilayered ionic liquid like phase were used.[26]

Table 1. Catalytic tests performed with **POSS-Imi** with different working pressures.[a]

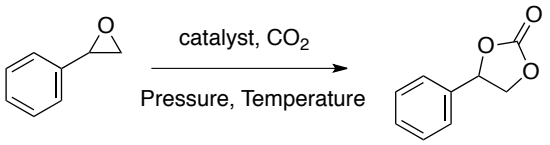

Entry	Pressure [bar]	Temperature [°C]	Conversion [%][b]	TON[c]
1	20	125	24	70
2	30	125	35	102
3	40	125	49	143
4	60	125	44	128
5	80	125	37	108
6	40	150	92	268

[a] Reaction conditions: 220 mg (0.10 mmol) of **POSS-Imi** (which corresponds to 0.72 mmol of Imi active sites), 24 mL (210 mmol) styrene oxide, 3 h and 1.5 mL of H_2O. [b] Conversion determined by ^{1}H NMR. [c] TON (*turnover number* calculated as*: moles converted/moles of imidazolium active sites*).

As expected, the increase of the temperature at 150 °C while keeping constant the pressure at 40 bar (Table 1, entry 6) caused a substantial improvement in the conversion (92 %) with a corresponding TON of 268. The influence of the catalyst amount was also evaluated (Table 2). It was observed that the decrease of the catalyst amount to 110 mg did not strongly affected the performances of the **POSS-Imi** (Table 2, entries 1 and 2) suggesting that, at higher silsesquioxane concentration and despite the presence of co-solvent, small aggregates probably non completely accessible are still present in the reaction mixture. A further decrease to 55 mg (Table 2 entry 3) caused a substantial decrease in the epoxide conversion indicating that a good balance between catalyst loading and dispersion was already obtained in the previous essay.

Table 2. Catalytic tests performed with **POSS-Imi** varying the catalyst amount.[a]

Entry	Catalyst [mg]	Catalyst [mmol]	Active sites [mmol]	Conversion [%][b]	TON[c]
1	220	0.100	0.72	92	268
2	110	0.050	0.36	71	414
3	55	0.025	0.18	47	548

[a] Reaction conditions: 40 bar, 150 °C, 24 mL (210 mmol) styrene oxide, 3 h and 1.5 mL of H_2O. [b] Conversion determined by ^{1}H NMR. [c] TON (*turnover number* calculated as*: moles converted/moles of imidazolium active sites*).

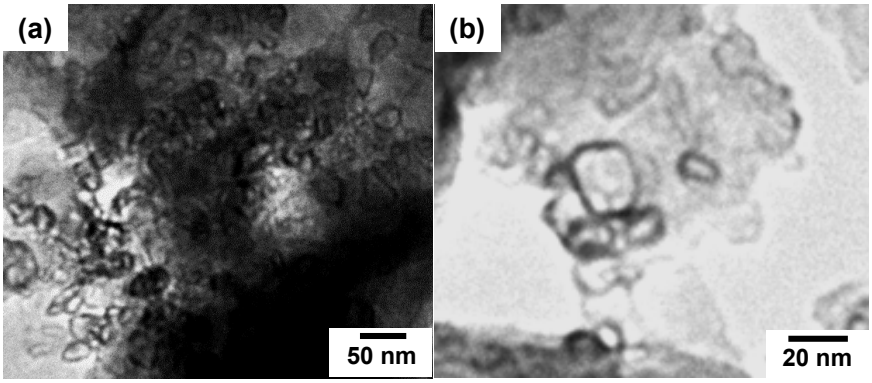

Figure 4. TEM images of **POSS-Imi**.

Transmission electron microscopy (TEM) investigation on the silsesquioxane based solid was performed as well. An aqueous solution of catalyst, with the same concentration of **POSS-Imi** used in the CO_2 conversion, was stirred for 1 h and analyzed by TEM. The analysis of the sample revealed the presence of nano-organizations with distorted spherical shape (Figure 4).

These irregular organizations may explain the trend observed in Table 2 thus confirming the previous hypothesis based on the formation of nanometric aggregates even if a possible role of the solvent evaporation can not be completely excluded.

It should be noticed that in the previous analysis of catalyst performances, the selectivity through the synthesis of cyclic carbonates was not considered.

The choice of water as co-solvent was dictated by the objective to maintain a higher sustainability of the catalytic process, moreover its use as efficient medium for the synthesis of cyclic carbonate was already reported.[52] Some of the most used co-solvents for the target reaction (eg: acetonitrile, dichloromethane, dioxane)[11,12] are not recommendable from an environmental point of view.[53] However, the use of water as co-solvent, caused a lowering of the selectivity due to the formation of styrene glycol as main by-product. Separation of the products from the reaction mixture allowed the isolation and complete characterization of the by-product (Supporting Information, section A.3, Figures S11 and S12).

A blank test performed in absence of catalyst and with the corresponding amount of water produces styrene glycol as the sole product.

In order to improve the selectivity, the best conditions in terms of epoxide conversion where selected and the effect of different co-solvents (always considering their environmental impact) was studied.

Table 3. Catalytic tests performed with different co-solvents.[a]

Entry	Catalyst	Co-solvent	Conv. [%][b]	Carbonate yield [%]	Selectivity [%][c]	TON[d]
1	**POSS-Imi**	H_2O	71	51	72	410
2	**POSS-Imi**	MeOH	73	69	95	429
3	**POSS-Imi**	EtOH	85	81	95	499
4	**POSS-Imi**	^{i}PrOH	94	94	> 95	553
5[e]	**BMim**	^{i}PrOH	98	98	> 95	326
6	**POSS-Imi**	EtOH(abs)	84	84	> 95	490

[a] Reaction conditions: 110 mg of catalyst (which corresponds to 0.36 mmol of imidazolium active sites in **POSS-Imi**), 40 bar, 150 °C, 24 mL (210 mmol) styrene oxide, 3 h and 1.5 mL of solvent were used in all tests. [b] Conversion determined by ^{1}H NMR. [c] Selectivity toward cyclic carbonate. [d] TON (*turnover number* calculated as*: moles converted/moles of imidazolium active sites*). [e] **BMim**, 0.63 mmol.

A first screening of different polar solvents allows identifying the alcohols as the most suitable class of solvents. The evolution of TON and selectivity in function of methanol (MeOH), ethanol (EtOH) and isopropanol (^{i}PrOH) are shown in Table 3 (entries 1-4). The reactions performed in both EtOH and ^{i}PrOH displayed improved conversions with respect to the analogous test conducted in presence of water while similar results were obtained in MeOH (compare entries 1 to 4 in Table 3). An increased selectivity was observed with all the alcohols. The best co-solvent was clearly represented by the ^{i}PrOH, which exhibited an almost total conversion (94%) and complete selectivity. It is worth to underline the exceptionally high TON obtained under this reaction conditions (entry 4).

The increased conversions in the series ^{i}PrOH>EtOH>MeOH≈H_2O can be related to the higher solvation of the chloride ions in water with respect to alcohols, especially ^{i}PrOH, that cause a decreased nucleophilicity. On the other hand, the lower reactivity of the chloride ions in water led to a lower selectivity because of the higher nucleophilicity of water. When the amount of water was decreased (entries 2-4) the selectivity was higher.

In order to highlight the importance of the silsesquioxane nanocage, an analogous catalytic test performed using the commercially available 1-butyl-3-methylimidazolium chloride (**BMIm**) in presence of isopropanol was performed as well. In order to allow a meaningful comparison and avoid the possible differences linked to the dispersion of the catalysts in the reaction mixture, the experiments were performed maintaining constant the amount of catalyst and comparing the results in terms of TON. The lower TON obtained in presence of **BMIm** (Table 3, entries 5) allows evidencing the positive role of the silsesquioxane. As previously described, the enhanced activity was ascribed to the proximity effect generated by the increased local concentration of imidazolium species surrounding the inorganic silsesquioxane core.

In an attempt to completely clarify the role of water in the formation of the by-product, absolute ethanol was also employed for the catalytic tests (Table 3, entry 6). This test allows proving that an exceptional selectivity (> 99%) can be achieved in absence of water (compare entries 3 and 6 in Table 3). The high selectivity represented an advantage not only from the point of view of the catalytic performances, but also because in absence of by-products the recovery of the catalyst after reaction was also accomplished by simple precipitation of the reaction mixture. The ^{29}Si NMR spectrum of the recovered **POSS-Imi** catalyst is shown in Figure 5.

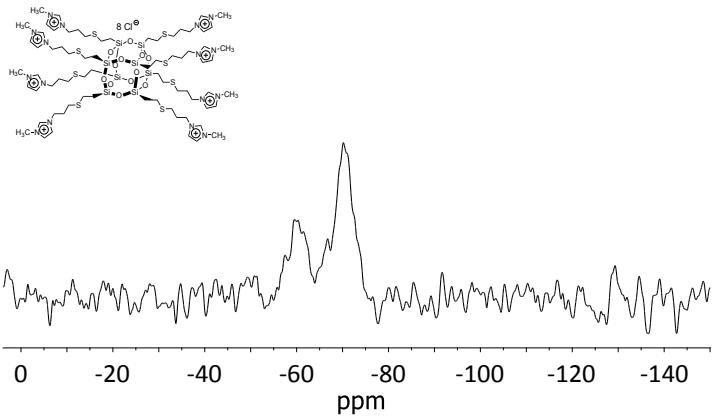

Figure 5. Solid state ^{29}Si MAS NMR spectrum of the **POSS-Imi** catalyst after its use in catalysis.

As can be clearly seen no major differences can be observed from the comparison of the ^{29}Si NMR before and after reaction proving that the **POSS-Imi** was stable under the reaction conditions.

From all these results emerged that **POSS-Imi** is a very promising catalyst, especially if we take into account that chloride is present as nucleophile and no additional expensive activating agents (e. g. Lewis acids) were added to the reaction mixture. In order to study the versatility of the catalyst, two aliphatic epoxides were also investigated and the results are collected in Table 4. Good conversion and selectivity were obtained in presence of 1-butene oxide (entry 2). With the more reactive epichlorohydrin a total conversion was obtained after 1h at 150 °C (entry 3). The decrease of the temperature at 125°C did not show substantial differences (compare entries 3 and 4) and an excellent conversion was also achieved at the challenging temperature of 100 °C (Table 4, entry 5).

Table 4. Catalytic tests performed with different substrates.[a]

Entry	Catalyst	Epoxide	Temperature [°C]	Reaction time [h]	Conv. [%][b]	Selectivity [%][c]	TON[d]
1	**POSS-Imi**	Styrene oxide	150	3	88	> 95	513
2	**POSS-Imi**	1-butene oxide	150	3	60	> 95	416
3	**POSS-Imi**	Epychlorohydrin	150	1	>95	> 95	722
4	**POSS-Imi**	Epychlorohydrin	125	1	93	> 95	706
5	**POSS-Imi**	Epychlorohydrin	100	3	63	> 95	479
6[e]	**Bmim**	Epychlorohydrin	100	3	79	> 95	342

[a] Reaction conditions: Imi active sites catalyst to epoxide molar ratio = 0.15%, 40 bar, 1.5 mL of absolute ethanol were used in all tests. [b] Conversion determined by ^{1}H NMR. [c] Selectivity toward cyclic carbonate. [d] Imi active sites catalyst to epoxide molar ratio = 0.23%. [e] TON (*turnover number* calculated as*: moles converted/moles of imidazolium active sites*).

A further comparison with **BMim** at the temperature of 100 °C while keeping constant the amount of catalyst was performed as well (Table 4, entry 6). The lower TON obtained with unsupported imidazolium salt allows further highlighting the positive effect of the inorganic core.

6.3 Conclusions

The synthesis of imidazolium functionalized polyhedral oligomeric silsesquioxanes was successfully achieved. The **POSS-Imi** nanostructure was extensively characterized in particular *via* ^{29}Si NMR spectroscopy and used as catalyst for the chemical fixation of carbon dioxide onto epoxides to give the corresponding cyclic carbonates. Different reaction conditions in terms of working pressure, temperature, amount of catalyst and nature of co-solvent were investigated. No additional co-catalyst with Lewis acid properties was added to the reaction mixture. The **POSS-Imi** showed excellent catalytic performances in the synthesis of styrene carbonate. Under the best reactions conditions, using isopropanol as co-solvent, an almost total conversion and complete selectivity was obtained. Moreover the catalyst was recovered by simple precipitation from the reaction mixture. The **POSS-Imi** displayed excellent performances also in presence of aliphatic epoxides. With the more reactive epichlorohydrin a remarkable TON of 479 was achieved at the challenging temperature of 100 °C. Comparison with unsupported 1-butyl-3-methylimidazolium chloride allows highlighting the positive effect of the silsesquioxane core on the catalytic activity.

6.4 References

1. G. Centi, E. A. Quadrelli, S. Perathoner, Energy and Environmental Science 2013, 6, 1711-1731.
2. A. M. Chapman, C. Keyworth, M. R. Kember, A. J. J. Lennox, C. K. Williams, ACS Catalysis 2015, 5, 1581-1588.
3. T. Sakakura, J.-C. Choi, H. Yasuda, Chemical Reviews 2007, 107, 2365-2387.
4. F. Jutz, J. Andanson, A. Baiker, Chemical Reviews 2011, 111, 322-353.
5. S. Hokenek, J. N. Kuhn, ACS Catalysis 2012, 2, 1013-1019.
6. P. P. Pescarmona, M. Taherimehr, Catalysis Science & Technology 2012, 2, 2169-2187.
7. M. North, R. Pasquale, C. Young, Green Chemistry 2010, 12, 1524-1539.
8. M. Kember, A. Buchard, C. K. Williams, Chemical Communications 2011, 47, 141-163.
9. D. J. Darensbourg, W.-C. Chung, K. Wang, H.-C. Zhou, ACS Catalysis 2014, 4, 1511-1515.
10. D. J. Darensbourg, W.-C. Chung, S. J. Wilson, ACS Catalysis 2013, 3, 3050-3057.
11. M. Taherimehr, A. Decortes, S. M. Al-Amsyhar, W. Lueangchaichaweng, C. Whiteoak, E. C. Escudero-Adán, A. W. Kleij, P. P. Pescarmona, Catalysis Science & Technology 2012, 2, 2231-2237.
12. A. Decortes, A. W. Kleij, ChemCatChem 2011, 3, 831-834.
13. N. Zhao, N. Yu, J. Wang, D. Zhuang, Y. Ding, R. Tan, D. Yin, Microporous Mesoporous Materials 2009, 122, 240-246.
14. M. Alvaro, C. Baleizao, D. Das, E. Carbonell, H. Garcia, Jouranl of Catalysis 2004, 228, 254-258.
15. X. Xu, C. Wang, H. Li, Y. Wang, S. Weilin, Z. Shen, Polymer 2007, 48, 3921-3924.
16. F. Castro-Gómez, G. Salassa, A. W. Kleij, C. Bo, Chemistry - A European Journal 2013, 19, 6289-6298.
17. C. M. Miralda, E. E. Macias, M. Zhu, P. Ratnasamy, A. Carreon, ACS Catalysis 2012, 2, 180-183.
18. D. Tian, B. Liu, Q. Gan, H. Li, D. J. Darensbourg, ACS Catalysis 2012, 2, 2029-2035.
19. C. Martín, G. Fiorani, A. W. Kleij, ACS Catalysis 2015, 5, 1353-1370.
20. M. H. Anthofer, M. E. Wilhelm, M. Cokoja, I. E. Markovits, A. Pöthig, J. Mink, W. A. Herrman, F. E. Kühn, Catalysis Science & Technology 2014, 4, 1749-1758.
21. M. Buaki-Sogo, H. Garcia, C. Aprile, Catalysis Science & Technology 2015, 5, 1220-1230.
22. H. Sun, D. Zhang, Journal of Physical Chemistry A 2007, 111, 8036-8043.
23. X. Zhang, D. Wang, N. Zhao, A. S. N. Al-Arifi, T. Aouak, Z. A. Al-Othman, W. Wei, Y. Sun, Catalysis Communications 2009, 11, 43-46.
24. J. Q. Wang, X. D. Yue, C. Fei, L. N. He, Catalysis Communications 2007, 8, 167-172.
25. P. Agrigento, S. M. Al-Amsyhar, B. Sorée, M. Taherimehr, M. Gruttadauria, C. Aprile, P. P. Pescarmona, Catalysis Science & Technology 2014, 4, 1598-1607.
26. C. Aprile, F. Giacalone, P. Agrigento, L. F. Liotta, J. A. Martens, P. P. Pescarmona, M. Gruttadauria, ChemSusChem 2011, 4, 1830-1837.
27. P. Pescarmona, T. Maschmeyer, Australian Journal of Chemistry 2001, 54, 583-596.
28. D. B. Cordes, P. D. Lickiss, F. Rataboul, Chemical Reviews 2010, 110, 2081-2173.
29. H. Mori, International Journal of Polymer Science 2012, 2012, 1-17.

30. K. Rózga-Wijas, J. Chojnowski, Journal of Inorganic Organometallic Polymers 2012, 22, 588-594.
31. J. Tan, D. Ma, X. Sun, S. Feng, C. Zhang, Dalton Transactions 2013, 42, 4337-4337.
32. M. Janeta, L. John, J. Ejfler, S. Szafert, Chem. Eur. J. 2014, 20, 15966-15974.
33. K. Tanaka, F. Ishiguro, Y. Chujo, Polymer Journal 2011, 43, 708-713.
34. K. Tanaka, W. Chujo, Bulletin of the Chemical Society of Japan 2013, 86, 1231-1239.
35. M. A. Castriciano, N. Leone, P. Cardiano, S. Manickam, L. M. Scolaro, S. Lo Schiavo, Journal of Materials Chemistry C 2013, 1, 4746-4753.
36. W. Zhang, J. Li, S. Jiang, Z.-S. Wang, Chemical Communications 2012, 50, 1685-1687.
37. M. Colovic, I. Jerman, M. Gaberscek, B. Orel, Solar Energy Materials & Solar Cells 2011, 95, 3472-3481.
38. M. Seino, W. Wang, J. E. Lofgreen, D. P. Puzzo, T. Manabe, G. A. Ozin, Journal of the American Chemical Society 2011, 133, 18082-18085.
39. S. Sakugawa, K. Wada, M. Inoue, Journal of Catalysis 2010, 275, 280-287.
40. E. Ayandele, B. Sarkar, P. Alexandridis, Nanomaterials 2012, 2, 445-475.
41. E. S. Cozza, V. Bruzzo, F. Carniato, E. Marsano, O. Monticelli, ACS Applied Materials & Interfaces 2012, 4, 604-607.
42. M. Janssen, J. Wilting, C. Müller, D. Vogt, Angewandte Chemie International Edition 2010, 49, 7738-7741.
43. S. Tang, R. Jin, H. Zhang, H. Yao, J. Zhuang, G. Liu, H. Li, Chemical Communications 2012, 48, 6286-6288.
44. S. E. Létant, J. Herberg, L. N. Dinh, R. S. Maxwell, R. L. Simpson, A. P. Saab, Catalysis Communications 2007, 8, 2137-2142.
45. H. M. Cho, H. Weissman, S. R. Wilson, J. S. Moore, Journal of the American Chemical Society 2006, 128, 14742-14743.
46. Y. Leng, J. Liu, C. Zhang, P. Jiang, Catalysis Science & Technology 2014, 4, 997-1004.
47. L. Zhang, H. C. L. Abbenhuis, G. Gerritsen, N. N. Bhriain, P. C. M. M. Magusin, B. Mezari, W. Han, R. A. van Santen, Q. Yang, C. Li, Chemistry - A European Journal 2007, 13, 1210-1221.
48. P. Zak, C. Pietraszuk, B. Marciniec, G. Spólnik, W. Danikiewicz, Advanced Synthesis & Catalysis 2009, 351, 2675-2682.
49. S. Randriamahefa, C. Lorthioir, P. Guégan, J. Penelle, Polymer 2009, 50, 3887-3894.
50. V. Caló, A. Nacci, A. Monopoli, A. Fanizzi, Organic Letters 2002, 4, 2561-2563.
51. M. North, R. Pasquale, Angewandte Chemie International Edition 2009, 48, 2946-2948.
52. J. Sun, J. Ren, S. Zhang, W. Cheng, Tetrahedron Letters 2009, 50, 423-426.
53. C. Christian, U. Fischer, K. Hungerbühler, Green Chemistry 2007, 9, 927-934.

Chapter 7

Proximity effect in a nanocage structure: Polyhedral oligomeric silsesquioxanes-imidazolium tetrachloropalladate salt as pre-catalyst for the Suzuki-Miyaura reaction in water

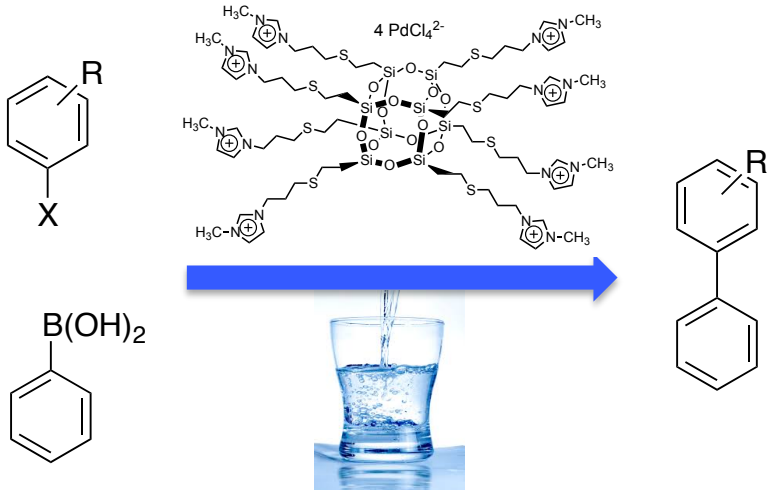

Chapter 7

This chapter is based on: L. A. Bivona, F. Giacalone, E. Carbonell-Llopis, M. Gruttadauria, C. Aprile, manuscript in preparation.

Proximity effect in a nanocage structure: Polyhedral oligomeric silsesquioxanes-imidazolium tetrachloropalladate salt as pre-catalyst for the Suzuki-Miyaura reaction in water

7.1 Introduction

The palladium-catalysed Suzuki-Miyaura cross-coupling reaction has emerged as an important and efficient tool in organic synthesis because it is one of the most convenient and modern methods for C-C bond formation.[1] The main advantages of this process are represented by the mild reaction conditions employed[2] and the tolerance toward a wide range of functional groups. In particular, this reaction is an important strategy of synthesis for the production of polymers, but also in the field of pharmaceutical and natural products.[3]

Traditionally, Suzuki-Miyaura reaction proceeds using palladium complexes with N- and P-ligands. It has been well established that ionic liquids (ILs) are interesting solvents and/or ligands in which to conduct Suzuki-Miyaura reaction with palladium salts under "ligand-free" conditions. This process allows achieving the advantages of the elimination of toxic solvents and the expensive P-ligands. Moreover, in ILs it is possible the use of Pd(II) as pre-catalyst for C-C coupling reaction, avoiding the use of reducing reagents.[4] In order to obtain greener conditions, a special attention has been paid to the use of eco-friendly and cheap solvents or co-solvents as water.[5] A useful Pd pre-catalyst have been tetrachloropalladate salts. Imidazolium tetrachloropalladate salts where employed as pre-catalyst in 1 mol% loading in Suzuki-Miyaura reactions in [Emim][NTf_2] at 100 °C, resulting in high conversions.[6] Other imidazolium tetrachloropalladate salts of the type $[IL]_2[PdX_4]$ (IL – imidazolium cation, X = Cl, Br) were used as catalyst precursors in 1 mol% loading in the Suzuki-Miyaura reaction in iPrOH or iPrOH/H_2O 1:1 at 40 °C.[7] In situ ESI-MS experiments showed evidences of $[(IL)_xPd_3]$ clusters formation when complexes of the type $[IL]_2[PdX_4]$ were used as catalyst precursors.[8] Other anionic palladium complexes of the type $[IL]_2[PdX_4]$ have been reported and used as pre-catalyst

in the Suzuki-Miyaura[9] reaction, in the oxidative Heck reaction[10] or for other catalytic applications.[11]

Recently, inorganic-organic hybrid materials have attracted great interest thanks to their better performance in term of thermal and mechanical stability. Nanostructured Polyhedral oligomeric silsesquioxanes (POSS) are a class of organic-inorganic hybrid compounds, with the general formula $(RSiO_{3/2})_n$, and consisting on inorganic silica-like core surrounded by organic groups.[12] In general, their structure can be expressed by the formula T_nR_m, where T indicates the number of Si atoms and R denotes the organic substituents. Typical POSS derivatives have a cube-octameric structure (T_8R_8). In the last years, the increased interest in POSS nanostructures have been attributed to their high performances, which come from the combination of inorganic and organic characteristics. Since the organic peripheries can be easily functionalized, POSS can be designed for a multi-functional nanocomposite. To date, they have been widely applied in many materials, as in biomaterials,[13] or for the development of hybrid electrochromic devices,[14] in solar cells,[15] as models of silica supported catalyst,[16] or additives in synthesis of periodic mesoporous organisilicas,[17] polymer nanocomposites[18] and in catalysis.[19] In particular, there are very few examples of POSS-stabilized Pd nanoparticles used as catalysts.[20]

In the last years, we have been involved in investigations on the development of new palladium-based catalysts[21] and, in addition, we have presented a silsesquioxane based nanostructure functionalized with imidazolium chloride (**POSS-Imi**) as efficient catalyst for chemical fixation of carbon dioxide.[22] In this case, the catalyst displayed improved catalytic performance with respect to unsupported 1-butyl-3-methylimidazolium chloride and such enhanced activity was ascribed to the proximity effect generated by the increased local concentration of imidazolium species surrounding the inorganic silsesquioxane core.

Since imidazolium-based ionic liquids have been employed as homogeneous supports for Pd based catalysts and, taking advantage of our synthetic strategy for the synthesis of **POSS-Imi**, we envisaged a new approach for the palladium based POSS imidazolium salts as pre-catalyst for Suzuki-Miyaura reactions. In this chapter, we describe the synthesis of a new imidazolium tetrachloropalladate salt immobilized on a POSS nanocage and its use as pre-catalyst in low catalytic loading in the Suzuki-Miyaura reaction in water, describing also an improved catalytic performance with respect to unsupported corresponding pre-catalyst.

7.2 Results and Discussion

Polyhedral oligomeric silsesquioxane functionalized with imidazolium moieties (**POSS-Imi**) was synthesized in a two steps procedure following a synthetic approach well explained in the previous chapter reported in this thesis (Chapter 6, Scheme 1 and for more details see Experimental Section, Chapter 8, part 8.5).

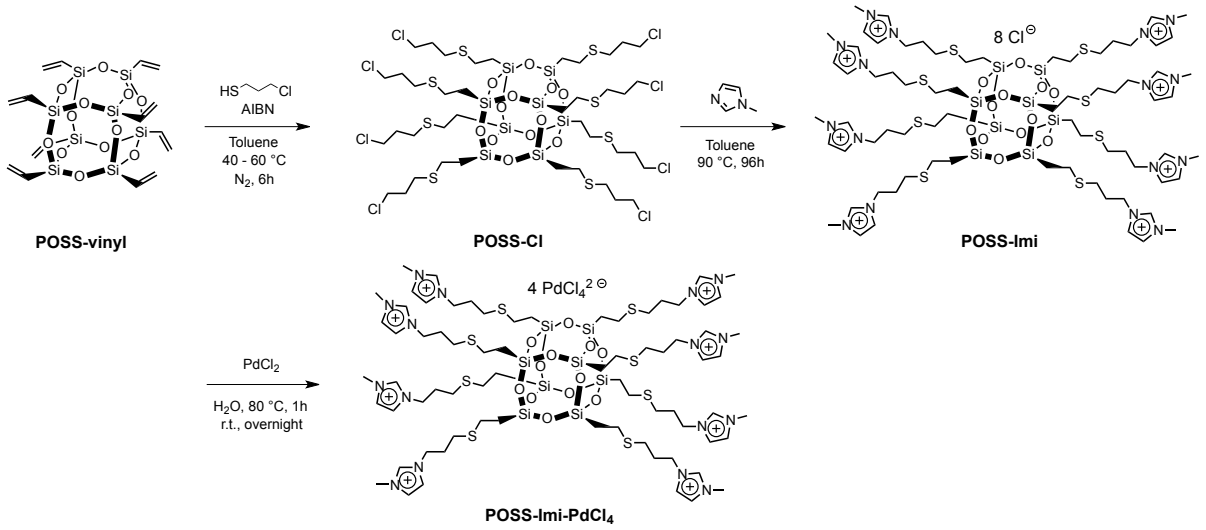

Scheme 1. Synthesis of the **POSS-Imi-PdCl$_4$** catalyst.

The desired **POSS-Imi-PdCl$_4$** was synthesized by treatment of **POSS-Imi** with $PdCl_2$ in water. Tetrachloropalladate-based ionic liquids can be synthesized by treatment of the proper imidazolium salt with $PdCl_2$, or with $PdCl_2$(cod), in acetonitrile.[11c] However, because of the low solubility of **POSS-Imi** in acetonitrile, the reaction was performed in water.

The final product was characterized by elemental analysis, ^{1}H and ^{13}C NMR, TEM, TGA and XPS (*vide infra*) (see Experimental Section, Chapter 8, section 8.5 and Supporting Information, section A.4). The ^{1}H and ^{13}C NMR spectra in D_2O, although not resolved as the precursor **POSS-Imi** (see SI, Figures S1 and S2), showed all the expected signals, however the aliphatic region is complicated to be well analyzed. Moreover, an NMR analysis at variable temperature, up to 95 °C, did not show any significant modification of the **POSS-Imi-PdCl$_4$** structure. This result highlights the stability of the catalyst at high temperature and in presence of palladium as counter anion.

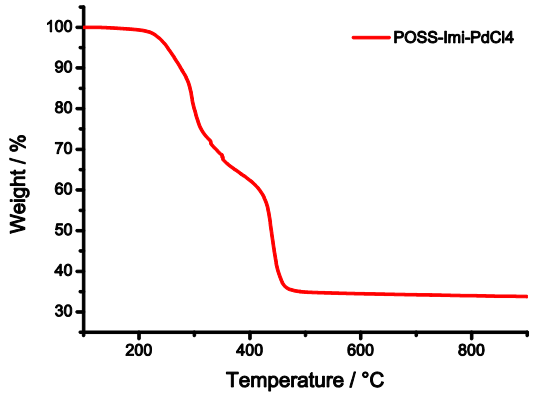

Figure 1. TGA of **POSS-Imi-PdCl$_4$** under oxygen flow.

Thermogravimetric analysis (TGA) was performed under oxygen flow up to 900 °C with a heating rate of 10°C min^{-1} (Figure 1). Under this condition, the residue is constituted by SiO_2 and Pd(0) and the result is in excellent agreement with the structure of **POSS-Imi-PdCl$_4$**.

POSS-Imi-PdCl$_4$ was then used as catalyst for the Suzuki-Miyaura reaction between phenylboronic acid and a set of aryl bromides. Reactions were carried out in water at 100°C for 4 h using K_2CO_3 as base in the presence of 0.16 mol% of catalyst (Table 1). All the biphenyls were obtained with high or excellent yields. Reactions can be carried out even at lower temperature (50 °C) as demonstrated by the quantitative yield obtained in the case of 4-bromobenzaldehyde and the high yield (85%) obtained with 4-bromoanisole (entries 11 and 12). All the products of the Suzuki reaction are known compounds and the references are reported in the Experimental Section, Chapter 8, section 8.5.

In order to investigate the role of the silsesquioxane nanocage, additional catalytic tests by using the corresponding imidazolium-based catalyst without the silsesquioxane nanocage were performed (i.e., 1-butyl-3-methylimidazolium tetrachloropalladate, **bmim$_2$PdCl$_4$**, Figure S4 to S6) (Table 2). These catalytic tests were carried out using different aryl bromide and two catalytic loadings (0.16 and 0.08 mol%). First, the two catalysts were employed in 0.16 mol% loading in the reaction with 4-bromoanisole (entries 1-2).

Table 1. Suzuki-Miyaura reactions between phenylboronic acid and aryl bromides catalyzed by POSS-Imi-$PdCl_4$.[a]

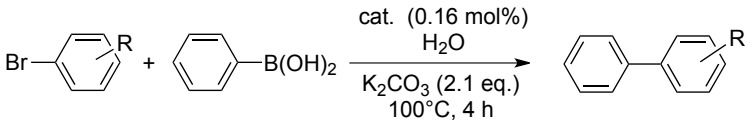

Entry	Product	Conv. [%][b]	Yield [%][c]	TON[d]
1	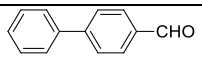	> 95	97	606
2	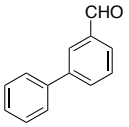	> 95	99	619
3	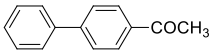	> 95	99	619
4	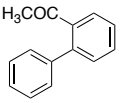	80	76	475
5	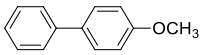	95	95	594
6	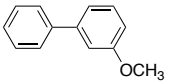	93	88	550
7	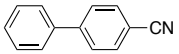	> 95	99	619
8	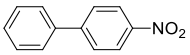	> 95	99	619
9	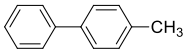	87	79	494
10	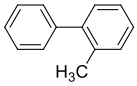	77	69	431
11[e]	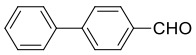	> 95	99	619
12[e]	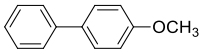	85	85	531

[a] Reaction conditions: aryl halide (1.0 mmol), phenylboronic acid (1.1 mmol), K_2CO_3 (2.1 mmol), H_2O (1.0 mL), catalyst **POSS-Imi-$PdCl_4$** (0.16 mol%, 1.2 mg). [b] Conversion determined by ^1H NMR. [c] Calculated after passing the residue on a short pad of silica gel. [d] TON (*turnover number* calculated as: *mmoles product*/*mmoles of catalytic active sites*). [e] Reaction carried out at 50 °C.

Conversion and yield drastically decreased when the reaction was performed in presence of **bmim$_2$PdCl$_4$** (compare entries 1 and 2, Table 2). Working at a catalyst loading of 0.08 mol% the difference between the POSS-based catalyst and the no POSS-based one was even more evident (entries 3-4). A similar behaviour was observed when 4-bromotoluene was used (entries 5-8). Indeed, the role of the POSS-based catalyst was still evident, particularly when the reaction was carried out with a catalyst loading of 0.08 mol%.

Table 2. Suzuki-Miyaura reactions between phenylboronic acid and aryl bromides in the presence of different amount and type of catalyst.[a]

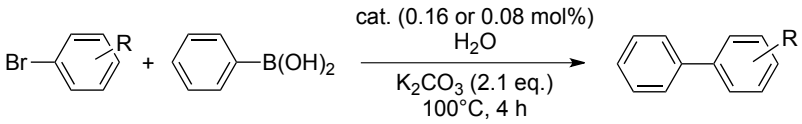

Entry	Catalyst	Catalyst [mol%]	Product	Conv. [%][b]	Yield [%][c]	TON[d]
1	**POSS-Imi-PdCl$_4$**	0.16	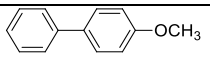	95	95	594
2	**bmim$_2$PdCl$_4$**	0.16	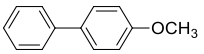	57	57	356
3	**POSS-Imi-PdCl$_4$**	0.08	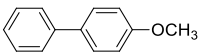	90	88	1100
4	**bmim$_2$PdCl$_4$**	0.08	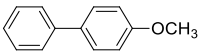	45	40	500
5	**POSS-Imi-PdCl$_4$**	0.16	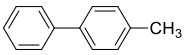	88	79	494
6	**bmim$_2$PdCl$_4$**	0.16	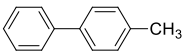	64	58	363
7	**POSS-Imi-PdCl$_4$**	0.08	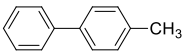	72	64	800
8	**bmim$_2$PdCl$_4$**	0.08	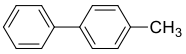	26	15	188

[a] Reaction conditions: aryl halide (1.0 mmol), phenylboronic acid (1.1 mmol), K_2CO_3 (2.1 mmol), H_2O (1.0 mL), catalyst (0.16 or 0.08 mol%). [b] Conversion determined by ^{1}H NMR. [c] Calculated after passing the residue on a short pad of silica gel. [d] TON (*turnover number* calculated as: *mmoles product/mmoles of catalytic active sites*).

Moreover, it is worth noting that the **POSS-Imi-PdCl$_4$** catalyst worked well even at 0.08 mol% loading, a catalytic loading much lower than other $[IL]_2[PdCl_4]$ catalytic systems reported in the literature.[6-8]

The two catalysts (**POSS-Imi-PdCl$_4$** and **bmim$_2$PdCl$_4$**) were characterized by X-ray photoelectron spectroscopy (XPS) before and after the Suzuki reaction (see Figures 2-3 and Table 3). As expected, the fresh catalysts showed the presence of Pd(II) species, although, in the case of **POSS-Imi-PdCl$_4$**, a small amount of Pd(0) was observed (entries 1 and 2, Figure 2). On the other hand, after reaction, both catalysts showed practically the same amount of Pd (0) (entries 3 and 4, Figure 3). In order to disclose if the presence of Pd(0) is imputable only to the C-C coupling reaction mechanism, the **bmim$_2$PdCl$_4$** catalyst was heated at 100 °C in water for 4 h. About a 30% of the Pd(0) species was observed (entry 5, Figure 4). Such reduced species could be ascribed to the thermal decomposition of tetrachloropalladate anion that takes place under the reaction condition independently from the Suzuki-Miyaura catalytic cycle.[23]

Table 3. XPS values of the **POSS-Imi-PdCl$_4$** and **bmim$_2$PdCl$_4$** catalysts before and after the Suzuki-Miyaura reaction.[a]

Entry	Catalyst	Pd 3d$_{5/2}$ eV [Pd^{2+}][a]	Pd 3d$_{5/2}$ eV [Pd^0][a]	Pd^{II} [%]	Pd^0 [%]
1	**POSS-Imi-PdCl$_4$** (fresh)	337.4	335.7	93	7
2	**bmim$_2$PdCl$_4$** (fresh)	337.2	-	99	Trace
3	**POSS-Imi-PdCl$_4$** (after reaction)	336.8	334.6	13	87
4	**bmim$_2$PdCl$_4$** (after reaction)	336.9	334.9	12	88
5[b]	**bmim$_2$PdCl$_4$** (after heating)	336.9	334.6	71	29

[a] C 1s is the reference peak that it is set at 284.6 eV. FWHM fit parameters are fixed between 0.5 and 3.5 eV for all of the signals. [b] After heating at 100 °C in water for 4 h.

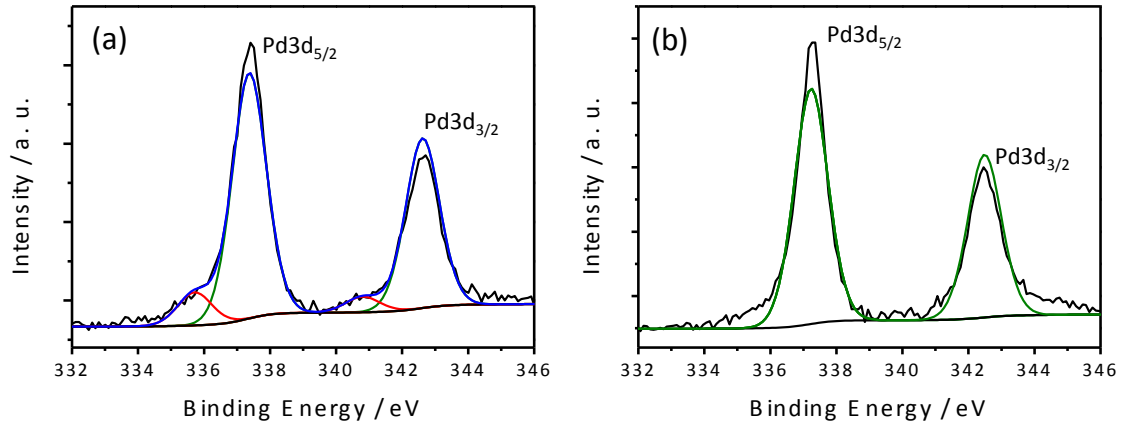

Figure 2. Pd 3d core level XPS spectra of fresh **POSS-Imi-PdCl$_4$** (a) and **bmim$_2$PdCl$_4$** (b).

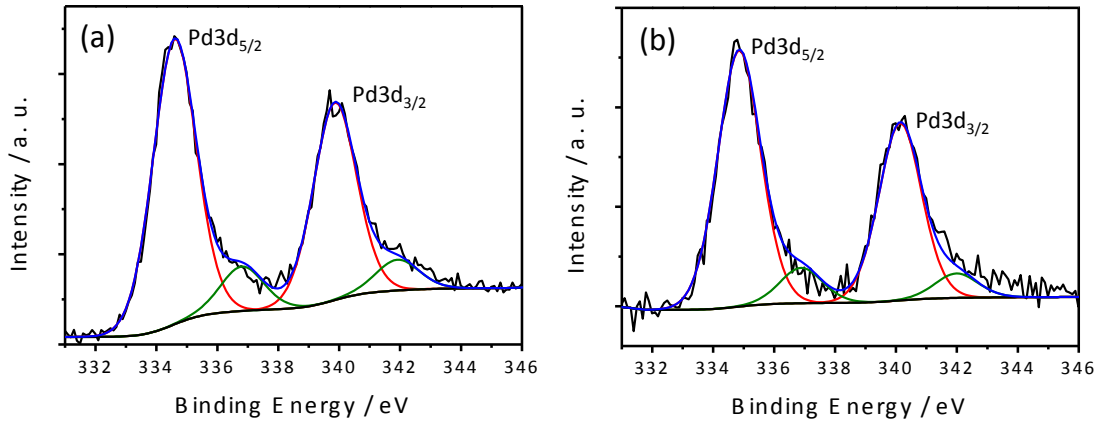

Figure 3. Pd 3d core level XPS spectra of **POSS-Imi-PdCl$_4$** (a) and **bmim$_2$PdCl$_4$** (b) after Suzuki-Miyaura reaction.

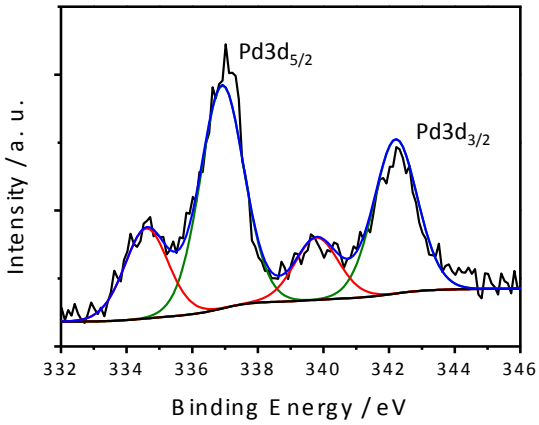

Figure 4. Pd 3d core level XPS spectrum of **bmim$_2$PdCl$_4$** after heating at 100 °C for 4 h.

We wondered also if the presence of sulfur atoms in the alkyl chains in the POSS nanocage may have a role in the stabilization of the Pd species. To shed some light on this question, high-resolution S 2p core-level XPS spectrum of **POSS-Imi-PdCl$_4$** was analysed. In order to make a comparison, we prepared the **POSS-Me-PdCl$_2$** compound (Scheme 2, for the synthesis see Experimental Part, section 8.4 and 8.5), which lacks the imidazolium units and XPS analysis was carried out (Figure 5).

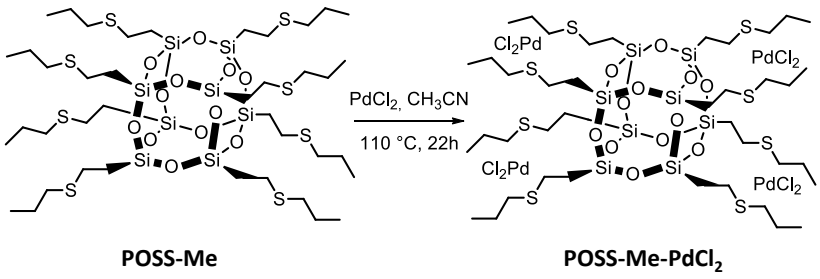

Scheme 2. POSS-Me and POSS-Me-PdCl$_2$ structures.

S 2p core-level XPS spectrum of **POSS-Imi-PdCl$_4$** (Figure 5a) can be resolved in doublet (due to S2p$_{3/2}$ and S2p$_{1/2}$ components originating from the spin–orbit splitting effect contributions). On the other hand, Figure 5b shows the presence of different sulfur moieties in **POSS-Me-PdCl$_2$**. At least two different doublets can be thus resolved. The peak at 161.9 eV (16 %), can be ascribed to the presence of S→Pd interaction, as previously reported.[24] This interaction is absent in **POSS-Imi-PdCl$_4$** indicating that, in this case, the sulfur atom plays a minor role in stabilizing Pd species.

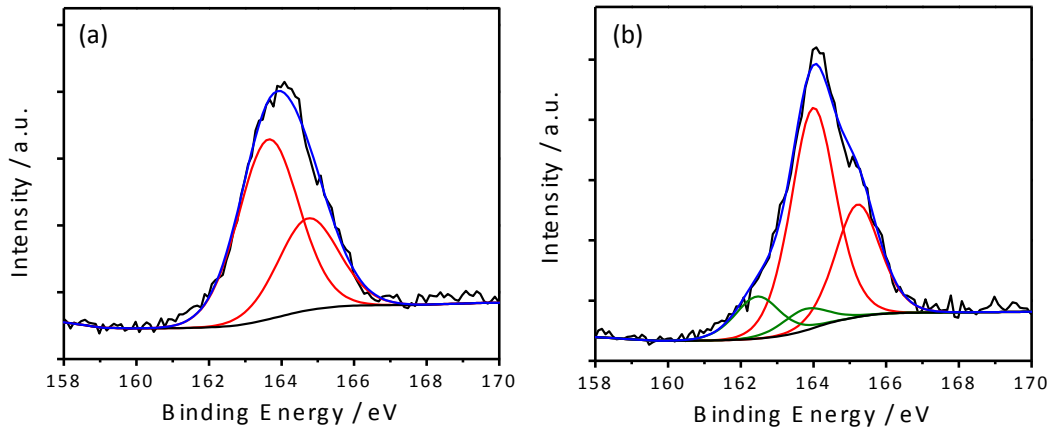

Figure 5. Sulfur 2p core level XPS spectra of **POSS-Imi-PdCl$_4$** (a) and **POSS-Me-PdCl$_2$** (b).

Transmission electron microscopy (TEM) investigation on the silsesquioxane-based catalyst before and after Suzuki-Miyaura reaction was performed as well (Figure 6).

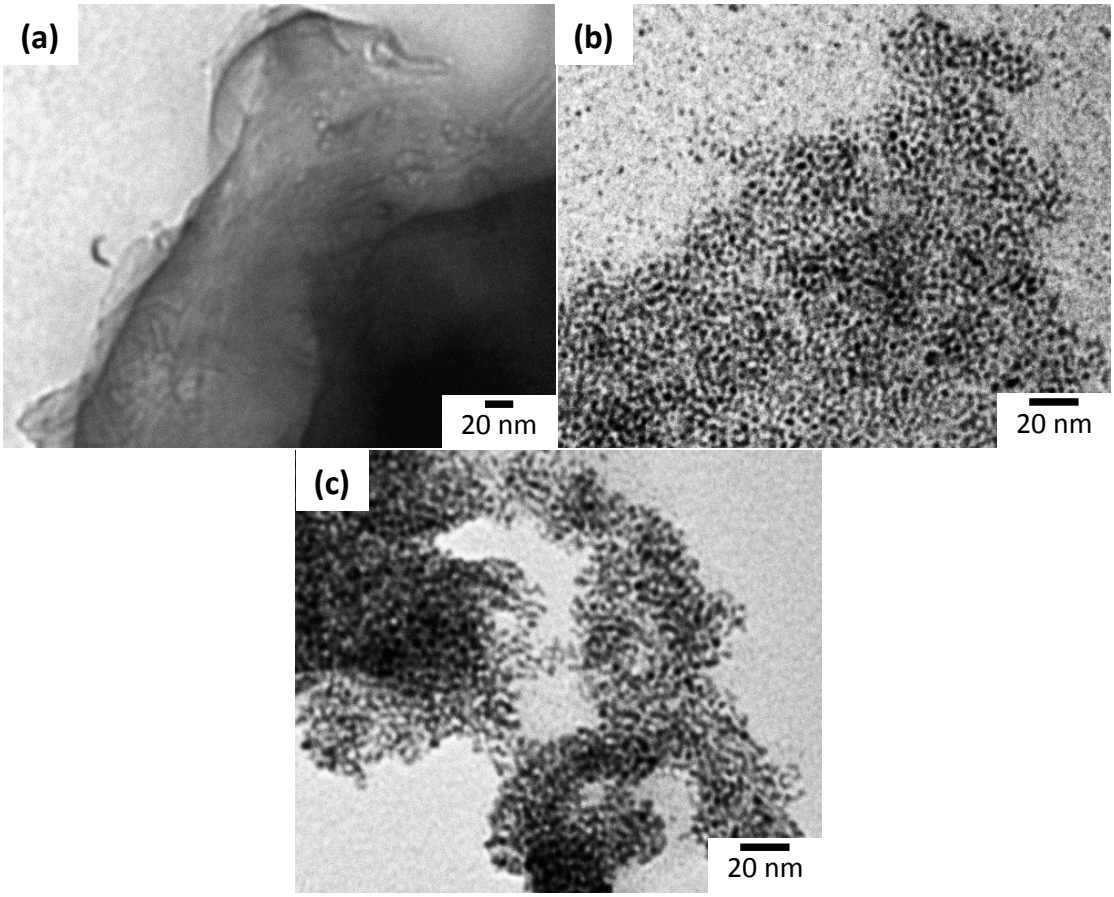

Figure 6. TEM images of fresh catalyst **POSS-Imi-PdCl$_4$** (a); (b) and (c) correspond to **POSS-Imi-PdCl$_4$** and **bmim$_2$PdCl$_4$** after Suzuki reaction between 4-bromotoluene and phenylboronic acid, respectively.

TEM analysis after Suzuki-Miyaura reaction confirmed the presence of Pd(0). Palladium nanoparticles appear well distributed and with an average dimension of 3 nm. TEM analysis, after the same Suzuki-Miyaura reaction carried out in the presence of **$bmim_2PdCl_4$**, shows also palladium nanoparticles with an average dimension of 3 nm. The only difference between the two catalysts could be ascribed to a slightly better dispersion of the Pd nanoparticles in the POSS-based compound.

Both TEM and XPS analyses do not provide a clear explanation of the improved (or enhanced) catalytic performance of **POSS-Imi-$PdCl_4$** compared to **$bmim_2PdCl_4$**. Such higher catalytic activity could be ascribed to a proximity effect played by former catalyst (Figure 7a).[25]

Nevertheless, it cannot be ruled out a sort of phase transfer catalysis played by imidazolium units linked to the silica nanocage, that could create a local environment in which the reactants are better dissolved with respect to the aqueous phase. Indeed, ILs containing imidazolium, phosphonium, ammonium, and pyridinium cations have been shown to act as phase transfers catalysts for fluorination, nucleophilic substitutions, etherification, and benzoin condensation reactions.[26] In selected cases, phase transfer catalytic activity has been observed also on supported ILs.[27] The above effects cannot be operative when the $bmim_2PdCl_4$ catalyst is used, because of the absence of the nanocage (Figure 7b).

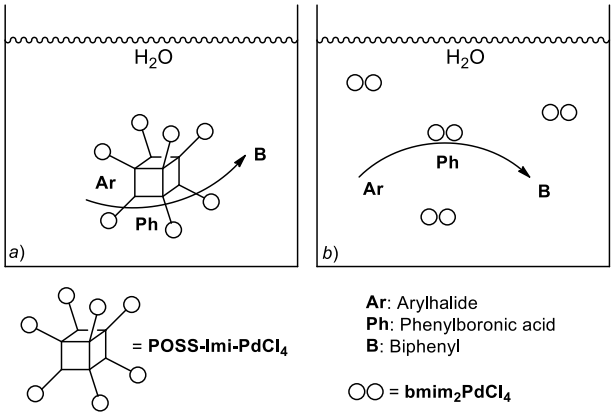

Figure 7. Schematic representation of Suzuki-Miyaura reaction in water catalysed by **POSS-Imi-$PdCl_4$** (a) and **$bmim_2PdCl_4$** (b).

7.3 Conclusions

In conclusion, for the first time a proximity effect has been observed in the Suzuki-Miyaura reaction between arylbromides and phenylboronic acid in water in the presence of a polyhedral oligomeric silsesquioxanes-imidazolium tetrachloropalladate salt (**POSS-Imi-**

$PdCl_4$) as pre-catalyst. **POSS-Imi-$PdCl_4$** was prepared by reaction of a POSS-imidazolium chloride salt (**POSS-Imi**) with $PdCl_2$ and used in water at 100 °C in low loading (0.08-0.16 mol%).

The catalytic activity of such pre-catalyst was compared with that of the corresponding pre-catalyst without the nanocage structure (**$bmim_2PdCl_4$**). XPS and TEM analyses did not evidence any particular stabilizing role of the POSS structure, then, the enhanced catalytic activity has been ascribed to a proximity effect played by the nanocage structure.

7.4 References

1. N. T. S. Phan, M. Van Der Sluys, C. W. Jones, Advanced Synthesis & Catalysis 2006, 348, 609-679. b) A. Zapf, M. Beller, Chemical Communications 2005, 431-440.
2. K. W. Anderson, S. L. Buchwald, Angewandte Chemie International Edition 2005, 44, 6173-6177.
3. a) C. Torborg, M. Beller, Advanced Synthesis & Catalysis 2009, 351, 3027-3043; b) F. Babudri, G. M. Farinola, F. Naso, Journal of Materials Chemistry 2004, 14, 11-34; c) Z. Peng, A. R. Gharavi, L. Yu, Journal of the American Chemical Society 1997, 119, 4622-4632; d) J. Sakamoto, M. Rehahn, G. Wegner, A. D. Schluter, Macromolecular Rapid Communications 2009, 30, 653-687.
4. a) J. Durand, E. Teuma, F. Malbosc, Y. kihn, M. Gòmez, Catalysis Communications 2008, 9, 273-275; b) D. Zhao, Z. Fei, R. Scopelliti, P. J. Dyson, Inorganic Chemistry 2004, 43, 2197-2205; c) F. McLachlan, C. J. Mathews, P. J. Smith, T. Welton, Organometallics 2003, 22, 5350-5357; d) V. Calò, A. Nacci, A. Monopoli, European Journal of Organic Chemistry 2006, 3791-3802; e) S. Navalon, M. Alvaro, H. Garcia, ChemCatChem 2013, 5, 3460-3480.
5. a) D. N. Korolev, N. A. Bumagin, Tetrahedron Letters 2006, 47, 4225-4229; b) D. Badone, M. Baroni, R. Cardamone, A. Ielmini, U. Guzzi, J. Org. Chem. 1997, 62, 7170-7173; c) N. E. Leadbeater, M. Marco, Organic Letters 2002, 4, 17, 2973-2976; d) G. A. Molander, B. Biolatto, J. Org. Chem. 2003, 68, 4302-4314.
6. H. Song, N. Yan, Z. Fei, K. J. Kilpin, R. Scopelliti, X. Li, P. J. Dyson, Catalysis Today 2012, 183, 172-177.
7. E. Silarska, A. M. Trzeciak, J. Pernak, A. Skrzypczak, Applied Catalysis A: general 2013, 466, 216-223.
8. W. Zawartka, A. Gniewek, A. M. Trzeciak, J. J. Ziółkowski, J. Pernak, Journal of Molecular Catalysis A: Chemical 2009, 304, 8-15.
9. X. Yang, Z. Fei, T. J. Geldbach, A. D. Phillips, C. G. Hartinger, Y. Li, P. J. Dyson, Organometallics 2008, 27, 3971-3977.
10. E. Silarska, A. M. Trzeciak, Journal of Molecular Catalysis A: Chemical 2015, 408, 1-11.
11. a) J. E. L. Dullius, P. A. Z. Suarez, S. Einloft, R. F. de Souza, J. Dupont, J. Fischer, A. De Cian, Organometallics 1998, 17, 815-819; b) C. K. Lee, H. H. Peng, I. J. B. Lin, Chemistry of Materials 2004, 16, 530-536; c) W. Zawartka, A. M. Trzeciak, J. J. Ziółkowski, T. Lis, Z. Ciunik, J. Pernak, Advanced Synthesis & Catalysis 2006, 348, 1689-1698; d) C.-M. Zhong, Y.-J. Zuo, H.-S. Jin, T.-C. Wang, S.-Q. Liu, Acta Crystallographica Section E 2006, 62, m2281-m2283.
12. a) P. Pescarmona, T. Maschmeyer, Australian Journal of Chemistry 2001, 54, 583-596, b) D. B. Cordes, P. D. Lickiss, F. Rataboul, Chemical Reviews 2010, 110, 2081-2173.
13. a) K. Tanaka, W. Chujo, Bulletin of the Chemical Society of Japan 2013, 86, 1231-1239; b) M. Lo Conte, S. Staderini, A. Chambery, N. Berthet, P. Dumy, O. Renaudet, A. Marra, A. Dondoni, Organic & Biomolecular Chemistry 2012, 10, 3269.
14. M. Colovic, I. Jerman, M. Gaberscek, B. Orel, Solar energy materials & Solar Cells 2011, 95, 3472-3481.
15. W. Zang, J. Li, S. Jiang, Z.-S. Wang, Chemical Communications 2014, 50, 1685-1687.
16. B. J. Hendan, H. C. Marsmann, Applied Organometallic Chemistry 1999, 13, 287-294.
17. M. Seino, W. Wang, J. E. Lofgreen, D. P. Puzzo, T. Manabe, G. A. Ozin, Journal of the American Chemical Society 2011, 133, 18082-18085.
18. a) E. Ayandele, B. Sarkar, P. Alexandridis, Nanomaterials, 2012, 2, 445-475; b) Y.- C. Sheen, C.-H. Lu, C.-F. Huang, S.-W. Kuo, F.-C. Chang, Polymer 2008, 49, 4017-4024.

19. a) S. Sakugawa, K. Wada, M. Inoue, J. Catal. 2010, 275, 280-287; b) E. S. Cozza, V. Bruzzo, F. Carniato, E. Marsano, O. Monticelli, ACS Applied Materials & Interfaces 2012, 4, 604-607; c) M. Janssen, J. Wilting, C. Müller, D. Vogt, Angewandte Chemie International Edition 2010, 49, 7738-7741; d) S. Tang, R. Jin, H. Zhang, H. Yao, J. Zhuang, G. Liu, H. Li, Chemical Communications 2012, 48, 6286-6288; e) Y. Leng, J. Liu, C. Zhang, P. Jiang, Catalysis Science & Technology 2014, 4, 997-1004.
20. a) C.-H. Lu, F.-C. Chang, ACS Catalysis 2011, 1, 481-488; b) S. E. Létant, J. Herberg, L. N. Dinh, R. S. Maxwell, R. L. Simpson, A. P. Saab, Catalysis Communications 2007, 8, 2137-2142.
21. a) V. Campisciano, V. La Parola, L. F. Liotta, F. Giacalone, M. Gruttadauria, Chemistry – A European Journal 2015, 21, 3327-3334; b) L. A. Bivona, F. Giacalone, L. Vaccaro, C. Aprile, M. Gruttadauria, ChemCatChem 2015, 7, 2526-2533; c) C. Petrucci, G. Strappaveccia, F. Giacalone, M. Gruttadauria, F. Pizzo, L. Vaccaro, ACS Sustainable Chemistry & Engineering 2014, 2, 2813-2819; d) M. Massaro, S. Riela, G. Lazzara, M. Gruttadauria, S. Milioto, R. Noto, Applied Organometallic Chemistry 2014, 28, 234-238; e) C. Pavia, F. Giacalone, L. A. Bivona, A. M. P. Salvo, C. Petrucci, G. Strappaveccia, L. Vaccaro, C. Aprile, M. Gruttadauria, Journal of Molecular Catalysis A: Chemical 2014, 387, 57-62; f) C. Pavia, E. Ballerini, L. A. Bivona, F. Giacalone, C. Aprile, L. Vaccaro, M. Gruttadauria, Advanced Synthesis & Catalysis 2013, 355, 2007-2018; g) M. Gruttadauria, L. F. Liotta, A. M. P. Salvo, F. Giacalone, V. La Parola, C. Aprile, R. Noto, Advanced Synthesis & Catalysis 2011, 353, 2119-2130.
22. L. A. Bivona, O. Fichera, L. Fusaro, F. Giacalone, M. Buaki-Sogo, M. Gruttadauria, C. Aprile, Catalysis Science & Technology 2015, 5, 5000-5007.
23. K. Okitsu, Y. Mizukoshi, H. Bandow, T. A. Yamamoto, Y. Nagata, Y. Maeda, The Journal of Physical Chemistry B 1997, 101, 5470-5472.
24. a) J. C. Love, D. B. Wolfe, M. L. Chabinyc, K. E. Paul, G. M. Whitesides, Journal of the American Chemical Society 2002, 124, 1576-1577; b) J. C. Love, D. B. Wolfe, R. Haasch, M. L. Chabinyc, K. E. Paul, G. M. Whitesides, R. G. Nuzzo, Journal of the American Chemical Society 2003, 125, 2597-2609; c) S. Santra, K. Dhara, P. Ranjan, P. Bera, J. Dash, S. K. Mandal, Green Chemistry 2011, 13, 3238-3247.
25. a) A. Dahan, M. Portnoy, Journal of the American Chemical Society 2007, 129, 5860-5869; b) T. Okano, M. Iwahara, J. Kiji, Synlett 1998, 09, 243-244.
26. a) V. Kumar, I. Jamie Talisman, O. Bukhari, J. Razzaghy, S. V. Malhotra, RSC Advances 2011, 1, 1721-1727; b) S. S. Shinde, H. M. Chi, B. S. Lee, D. Y. Chi, Tetrahedron Letters 2009, 50, 6654-6657; c) J. Bender, D. Jepkens, H. Hüsken, Organic Process Research & Development 2010, 14, 716-721; d) A. Perosa, P. Tundo, M. Selva, S. Zinovyev, A. Testa, Organic & Biomolecular Chemistry 2004, 2, 2249-2252; e) G. D. Yadav, S. P. Tekale, Organic Process Research & Development 2010, 14, 722-727; f) N. M. T. Lourenço, C. A. M. Afonso, Tetrahedron 2003, 59, 789-794; g) L.-W. Xu, Y. Gao, J.-J. Yin, L. Li, C.-G. Xia, Tetrahedron Letters 2005, 46, 5317-5320; h) D. W. Kim, C. E. Song, D. Y. Chi, Journal of the American Chemical Society 2002, 124, 10278-10279.
27. a) D. W. Kim, D. Y. Chi, Angewandte Chemie International Edition 2004, 43, 483-485; b) D. W. Kim, D. J. Hong, K. S. Jang, D. Y. Chi, Advanced Synthesis & Catalysis 2006, 348, 1719-1727; c) D. W. Kim, H.-J. Jeong, S. T. Lim, M.-H. Sohn, D. Y. Chi, Tetrahedron 2008, 64, 4209-4214; d) S. S. Shinde, B. S. Lee, D. Y. Chi, Tetrahedron Letters 2008, 49, 4245-4248.

Chapter 8

Experimental Section

8.1 Experimental Section Chapter 3

8.1.1 Materials and methods

1-Phenylethanol, benzyl alcohol, diphenylmethanol, 2-phenylethanol and 1-decanol were purchased from Sigma Aldrich and used without further purification. Liquid state ^{1}H NMR and ^{13}C NMR spectroscopy were performed with JEOL 400 spectrometer. The chemical shift for ^{1}H and ^{13}C are given in ppm relative to the residual signal of the solvent. Solid state of the ^{13}C CP MAS NMR spectra of the **SBA-15-Thia** and **SBA-15-Imi** were performed with a Bruker 500 spectrometer. ^{29}Si MAS NMR spectrum of the **SBA-15-SH** was recorded on a Bruker 500 spectrometer in the solid state, using a Chemagnetics 3.2 mm probe equipped with standard wall rotors spinning at a frequency of 5.5 kHz. All of the liquid ans solid-state experiments were recorded at room temperature. Combustion chemical analysis (C, H, N) was performed on a Thermo Finnigan-FlashEA 1112 apparatus. Transmission electron microscopy images were taken with a Philips TECNAI 10 instrument at 80 kV. XRD patterns were collected with a PANalytical X'pert diffractometer with Cu Ka radiation (k = 1.54178 Å). Isothermal nitrogen adsorption was carried out with at 77 K with a volumetric adsorption analyzer (Micromeritics Tristar 3000) with a prior sample drying under vacuum at 120 °C.

8.1.2 Synthetic procedures

The synthetic procedure of **1,4-bis(1-vinyl-imidazolium-1-methylbenzene) bromide** (**bV-Imi**) is similar to that described in literature.[1]

General procedure for the Synthesis of 1,4-Bis(5-methyl-4-vinyl-thiazolium-1-methylbenzene) Bromide (bV-Thia): In a two-necked round-bottom flask 1,4-bis-bromomethylbenzene (1.182 g, 4.48 mmol) and chloroform (3 mL) were placed. The solution was heated in an oil bath at 70 °C with magnetic stirring, under argon. A solution of 4-methyl-5-vinylthiazole (1 mL, 8.86 mmol, 2 equiv.) in chloroform (2 mL) was added drop-wise over 30 min. After 24 h, the reaction mixture was cooled down, filtered and washed several times with diethyl ether. The solid product was dried overnight in an oven at 60 °C.

1,4-Bis(5-methyl-4-vinyl-thiazolium-1-methylbenzene) bromide: Pale yellow powder. Yield: 96%; mp > 250 °C. ^{1}H NMR (400 MHz, D_2O): δ (ppm) = 2.42 (s, 6H, $-CH_3$), 5.63 (d, 2H, J=11 Hz, cis $CH=CH_2$), 5.67 (s, 4H, Ar-CH_2-N), 5.89 (d, 2H, J=17.2 Hz, trans

$CH=CH_2$), 6.87 (dd, 2H, J=17.4 and 11.2 Hz, $CH=CH_2$), 7.38 (4H, s, Ar-H), 9.67 (s, 2H, SCH= N); ^{13}C NMR (100 MHz, D_2O): δ (ppm) = 11.2, 56.3, 121.9, 123.8, 129.2, 132.9, 136.5, 142.3, 155.3; IR: ῡ max= 2985, 1103, 1566, 1455, 672 cm^{-1}. Anal. found for $C_{20}H_{22}Br_2N_2S_2$ (%): C 44.40, H 4.29, N 5.08, S 12.44; calcd. (%): C 46.70, H 4.31, N 5.45, S 12.47.

General procedure for the Synthesis of SBA-15: Mesoporous silica material SBA-15 was prepared starting from tetraethylorthosilicate (TEOS) as the silica source and by using the triblock copolymer poly(ethylene oxide)-poly(-propylene oxide)-poly(ethylene oxide) ($EO_{20}PO_{70}EO_{20}$, Pluronic P123) as template.

In a typical procedure, Pluronic P123 (11.0 g) was dissolved in an acid solution of HCl (5.99 g in 200.0 g of water). The solution was stirred overnight at 35 °C in a 500 mL closed polypropylene bottle. Afterwards, TEOS (21.80 g) was added to this solution and the mixture was stirred at the same temperature for 24 h. The milky suspension was heated to 100 °C for 24 h. The solid product was filtered off and washed with a solution of HCl (5% vol). The white solid was calcined at 550 °C for 5 h in air.

General procedure for the Synthesis of Modified Silica SBA-15 (SBA-SH): In a round-bottom flask SBA-15 (2.0 g), 3-(mercaptopropyl)trimethoxysilane (3.0 mL, 0.016 mol) and toluene (15 mL) were placed. The suspension was heated under reflux conditions for 24 h. After this time, the suspension was cooled to room temperature, filtered and washed with methanol. The white powder was dried in an oven at 80 °C overnight.

General procedure for the Synthesis of Material SBA-15-Thia: In a two-necked round-bottom flask 3-mercaptopropylmodified SBA-15 (200 mg, SH loading 0.9 mmol g^{-1}, 0.18 mmol), bis-vinylthiazolium or -imidazolium salt (3.69 equiv.), ethanol (5.6 mL) and AIBN were placed. The suspension was degassed by bubbling argon for 30 min. The reaction mixture was heated in an oil bath at 78 °C under argon, and stirred for 20 h. After cooling to room temperature, the mixture was filtered and the solid washed with methanol in a Soxhlet system for 48 h. Then, the obtained material was dried in an oven at 40 °C overnight. Anal. found for **SBA-15-Thia** (%): N 3.45, C 30.23, H 4.06, S 8.01.

General procedure for the Synthesis of Homo-Thia-H, Homo-Thia-Me and Mono-Thia

Homo-Thia-H: To a solution of 1,3,5-tris(bromomethyl)- 2,4,6-trimethylbenzene (0.98

mmol, 400 mg, 98%) in chloroform (11.7 mL), 4,5-dimethylthiazole (3.21 mmol, 340 µL, 97%) was added and the mixture was stirred at 60 °C for 17 h. After the solvent had been evaporated the resulting residue was washed with diethyl ether (3 x 20 mL) and dried under reduced pressure. Yield: 60%. ^{1}H NMR (400 MHz, D_2O): δ (ppm) = 2.1 (s, 9H, CH_3), 2.42 (s, 9H, CH_3), 2.5 (s, 9H, CH_3), 5.52 (s, 6H, CH_2), 8.86 (s, 3H); ^{13}C NMR (100 MHz, D_2O): δ (ppm) = 11.1, 11.9, 15.4, 128.8, 134.8, 142.2, 143.4, 151.7, 170.8. IR (powder): $\tilde{\upsilon}_{max}$ = 3391, 2972, 2050, 1591, 1440, 1356, 1314, 1221, 1050, 931, 820, 719, 517 cm^{-1}. Anal. found for $C_{27}H_{36}Br_3N_3S_3$ (%): C 45.01, H 5.02, N 5.48, S 13.32; calcd. (%): C 43.91, H 4.91, N 5.69, S 13.03.

Homo-Thia-Me: To a solution of 1,3,5-tris(bromomethyl)-2,4,6-trimethylbenzene (1.25 mmol, 500 mg) in chloroform (14.6 mL), 2,4,5-trimethylthiazole (4.087 mmol, 513 µL) was added and the mixture was stirred at 60 °C for 17 h. After the solvent was evaporated and the resulting residue was washed with diethyl ether (3 x 20 mL), and ethyl acetate (3 x 40 mL), then dried under reduced pressure. Yield: 70%. ^{1}H NMR (400 MHz, D_2O): δ (ppm) = 2.08 (s, 9H, -CH_3), 2.22 (s, 9H, -CH_3), 2.41 (s, 9H, -CH_3), 2.62 (s, 9H, -CH_3), 5.77 (s, 6H, -CH_2-); ^{13}C NMR (100 MHz, D_2O): δ (ppm) = 11.2, 12.3, 16.4, 16.6, 51.7, 130.2, 130.5, 139.1, 142.6, 168.1; IR (powder): $\tilde{\upsilon}_{max}$ = 3288, 2918, 2495, 2015, 1598, 1439, 1336, 1268, 1026, 928, 823, 743, 528 cm^{-1}. Anal. found for $C_{30}H_{42}Br_3N_3S_3$ (%): C 46.86, H 5.11, N 5.18, S 12.00; calcd. (%): C 46.16, H 5.42, N 5.38, S 12.32.

Mono-Thia: In a two-necked round-bottom flask 1-bromobutane (960 mL, 8.85 mmol, 99%) and chloroform (1.5 mL) were placed. The solution was heated in an oil bath at 70 °C with magnetic stirring, under nitrogen. A solution of 2,4-dimethylthiazole (1.0 mL, 8.86 mmol, 95%,) in chloroform (1.0 mL) was added dropwise during 10 min. After 43 h, the reaction mixture was cooled down, dried and washed with diethyl ether (3 x 20 mL). Then, the solid product was dried under reduced pressure. ^{1}H NMR (400 MHz, D_2O): δ (ppm) = 0.94 (t, 3H, -CH_3), 1.42 (m, 2H, -CH_2-CH_3), 1.77 (m, 2H,-CH_2-CH_2-CH3), 2.53 (s, 3H, -CH_3), 2.92 (s, 3H,-CH_3), 4.31 (t, 2H, N-CH_2-), 7.53 (s, 1H, =CH-); ^{13}C NMR (100 MHz, D_2O): δ (ppm) = 12.7, 13.3, 15.6, 19.3, 30.1, 49.9, 116.8, 146.3, 170.8; IR (powder): $\tilde{\upsilon}_{max}$ = 3370, 2956, 2836, 1583, 1488, 1361, 1265, 1136, 928, 846, 741, 543 cm^{-1}. Anal. found for $C_9H_{16}BrNS$: C 39.19, H 6.67, N 4.99, S 11.07; calcd. (%): C 43.21, H 6.45, N 5.60, S 12.81.

Catalytic tests

General procedure for the Etherification Reaction: The reaction was conducted in a two-necked round-bottom flask. Alcohol (44.2 mmol) and catalyst (10.2 mg) were stirred for 24 h at 160 °C. The suspension was then cooled down at room temperature and filtered to recover the catalyst. The mixture was analyzed by ^{1}H NMR to determine the conversion and purified by column chromatography (hexane/ethyl acetate 5:1).

Bis-methylbenzyl ether[2]: oil; ^{1}H NMR (400 MHz, $CDCl_3$): δ (ppm) = 1.40 (d, 6H, J=6.8 Hz, one diastereoisomer), 1.48 (d, 6H, J=6.4 Hz, one diastereoisomer), 4.26 (q, 2H, J=6.8 Hz, one diastereoisomer), 4.54 (q, 2H, J=6.4 Hz, one diastereoisomer), 7.39-7.22 (m, 10H, two diastereoisomers); ^{13}C NMR (100 MHz, $CDCl_3$, two diastereoisomers): δ (ppm) = 23.3, 25.0, 74.6, 74.9, 126.4, 126.6, 127.4, 127.6, 128.5, 128.7, 144.4, 144.5.

Bis-benzyl ether[3]: oil; ^{1}H NMR (400 MHz, $CDCl_3$): δ (ppm) = 4.61 (s, 4H), 7.32-7.43 (m, 10H); ^{13}C NMR (100 MHz, $CDCl_3$): δ (ppm) = 72.0, 127.6, 127.7, 128.3, 138.3.

Bis(diphenyl)methyl ether[4]: oil; ^{1}H NMR (400 MHz, $CDCl_3$): δ (ppm) = 5.42 (s, 2H), 7.25-7.40 (m, 20H); ^{13}C NMR (100 MHz, $CDCl_3$): δ (ppm) = 79.9, 127.1, 127.3, 128.2, 142.0.

8.1.3 References

1. C. Aprile, F. Giacalone, P. Agrigento, L. F. Liotta, J. A. Martens, P. P. Pescarmona, M. Gruttadauria, ChemSusChem 2011, 4, 1830-1837.
2. C. H. Jin, H. Y. Lee, S. H. Lee, I. S. Kim, Y. H. Jung, Synlett 2007, 2695-2698.
3. B. A. Gellert, N. Kahlcke, M. Feurer, S. Roth, Chem. Eur. J. 2011, 17, 12203-12209.
4. K. J. Miller, M. M. Abu-Omar, Eur. J. Org. Chem. 2003, 1294-1299.

8.2 Experimental Section Chapter 4

8.2.1 Materials and methods

Liquid state ^{1}H NMR and ^{13}C NMR spectroscopy were performed with a JEOL 400 spectrometer. ^{29}Si MAS NMR and ^{13}C cross-polarization MAS NMR spectra were recorded with a Bruker 500 spectrometer in the solid state, using a Chemagnetics 3.2 mm probe equipped with thin or standard wall rotors spinning at 12 kHz. Combustion chemical analyses (C, H, N) were performed on a Thermo Finnigan- FlashEA 1112 apparatus. TEM images were taken with a PHILIPS TECNAI 10 instrument at 80 kV. Samples were dispersed in ethanol and deposited on a carbon-coated copper grid. EDX measurements were performed with a JEOL JED2200 with an emission current equal to 15 eV. Isothermal nitrogen adsorption was performed with at 77 K with a volumetric adsorption analyzer (Micromeritics Tristar 3000) with a prior sample drying under vacuum at 120 °C. The XPS analyses were performed with a Thermo Scientific K-Alpha Surface Analysis spectrometer, equipped with a monochromatized Al anode (1486.6 eV). The spot size of the X-ray source on the sample was 200 μm, and the analyzer was operated with a pass energy equal to 200 eV for survey spectra, and 50 eV for high-resolution core-level spectra. A flood gun (electrons and Ar ions at very low energy) was used to avoid possible charging effects. Pressure in the chamber was in the range of 10^{-7} mbar. The BE of core levels was calibrated against the C1s BE set at 284.6 eV. Analyses of the peaks were performed with the software Thermo Avantage, based on nonlinear leastsquares fitting program using a weighted sum of Lorentzian and Gaussian component curves after background subtraction according to Shirley and Sherwood. AAS analyses were performed with a Perkin-Elmer using an electrothermal atomizers (graphite furnace Model HGA 600) and a lamp of palladium (λ = 247.6 nm). All the biphenyl, acrylate and styrene compounds synthesized are known molecules.[1,2]

8.2.2 Synthetic procedures

The synthesis of **1,4-Bis(5-methyl-4-vinyl-thiazolium-1-methylbenzene) Bromide** (**bV-Thia**), **SBA-15** and modified **SBA-15-SH** are obtained following the same procedure reported in the Experimental Section of the Chapter 3 (section 8.1.2).

The strategy employed for the experimental part concerning the synthesis of **SBA-15-Thia** was modified respect to the previous version reported in the Experimental Section of the Chapter 3 (section 8.1.2).

General procedure for the synthesis of material SBA-15-Thia: In a two-necked round-bottom flask 3-mercaptopropyl modified SBA-15 (1.0 g, SH loading 0.9 mmol/g, 0.9 mmol), bis-vinyl-thiazolium salt (3.69 eq.) ethanol (32.4 mL) and AIBN were placed. The suspension was degassed by bubbling nitrogen for 30 min. The reaction mixture was heated in an oil bath at 78 °C under nitrogen, and stirred for 20 h. After cooling to room temperature, the mixture was filtered and the solid washed with methanol in a Soxhlet system for 48 h. Then, the obtained material was dried in an oven at 40 °C overnight. Anal. found for **SBA-15-Thia** (%): N 3.19, C 28.17, H 3.88, S 6.85.

General procedure for the Synthesis of SBA-15-Thiazolidine-Pd: In a round-bottom flask were placed $PdCl_2$ (49.8 mg, 0.281 mmol), NaCl (312 mg, 5.342 mmol) and water (6.8 mL). The flask was heated at 80 °C until the $PdCl_2$ was dissolved. This clear orange solution was cooled at room temperature and added to a suspension of material **SBA-15-Thia** (250 mg) in water (2.25 mL). The suspension was stirred at room temperature for 20 h, then filtered under reduced pressure, washed with water and dried overnight under reduced pressure at room temperature. The material was suspended in anhydrous ethanol (6 mL) and to this suspension a solution of $NaBH_4$ (72 mg, 1.903 mmol, 7 equiv.) in anhydrous ethanol (6 mL) was added dropwise. The suspension turned black and was stirred at room temperature for 6 h, then filtered under reduced pressure, washed with water and ethanol and dried at room temperature.

Catalytic tests

General procedure for the Suzuki-Miyaura Reaction:[1] In a round-bottom flask, catalyst **SBA-15-Thiazolidine-Pd** (0.1 mol%, 1 mg), phenylboronic or 4-formylphenylboronic acid (1.1 mmol), K_2CO_3 (167 mg, 1.2 mmol), the aryl halide (1 mmol), ethanol (1.2 mL) and water (1.2 mL) were placed. The reaction mixture was stirred at 50 °C. After 19 h, the reaction mixture was cooled down, then water was added and the mixture extracted with dichloromethane (3 x 30 mL). The organic phase was dried with Na_2SO_4, filtered and concentrated under reduced pressure and the residue passed through a short silica pad (petroleum ether / ethyl acetate).

General procedure for the Heck Reaction:[2] To a round-bottom flask, catalyst **SBA-15-Thiazolidine-Pd** (0.1 mol%, 1 mg), alkene (1.5 mmol), aryl iodide (1 mmol), triethylamine (2 mmol) and DMF/H_2O (4 + 1) mL were added. The reaction mixture was heated at 90 °C for 16 h. Then, the reaction mixture was cooled at room temperature, diluted with water and extracted with dichloromethane (3 x 30 mL). The organic phase was dried with Na_2SO_4, evaporated under reduced pressure and the residue passed through a short silica pad (petroleum ether / ethyl acetate).

General recycling procedure for the Suzuki-Miyaura Reaction: In a round-bottom flask, catalyst **SBA-15-Thiazolidine-Pd** (0.1 mol%, 10 mg), 4-bromobenzaldehyde (10 mmol), phenylboronic acid (11 mmol), K_2CO_3 (12 mmol), ethanol (12 mL) and water (12 mL) were placed. The reaction mixture was stirred at 50 °C for 19 h. Then, it was allowed to cool down, filtered under reduced pressure and after extracted and purified as in the typical procedure for Suzuki reaction. The catalyst was washed with water, dichloromethane and dried at 40 °C overnight, to be subsequently reused in the next cycles.

General procedure for "hot filtration" and "room temperature" Suzuki-Miyaura Reaction: In a round-bottom flask, catalyst **SBA-15-Thiazolidine-Pd** (0.1 mol%, 1 mg), phenylboronic acid (138 mg, 1.1 mmol), K_2CO_3 (167 mg, 1.2 mmol), 3-bromoacetophenone (0.134 mL, 1 mmol), ethanol (1.2 mL) and water (1.2 mL) were placed. The reaction mixture was heated at 50 °C for 4 h to be subsequently filtered (in the case of hot filtration) or cooled at room temperature and then catalyst was separated from reaction mixture by means of a syringe filter. Then, the mixture was heated at 50 °C for 15 h. After, it was allowed to cool down, water was added and the mixture extracted with dichloromethane (3 x 30 mL). The organic phase was dried with Na_2SO_4, filtered and concentrated under pressure. The residue purified with a short plug of silica under vacuum using hexane/ethyl acetate as eluent.

8.2.3 References

For Suzuki and Heck compounds:

1. a) N. Mejias, R. Pleixats, A. Shafir, M. Medio-Simon, G. Asensio, Eur. J. Org. Chem. 2010, 5090-5099; b) Y. Li, X. Mi, M. Huang, R. Cai, Y. Wu, Tetrahedron 2012, 68, 8502-8508; c) D. Badone, M. Baroni, R. Cardamone, A. Ielmini, U. Guzzi, J. Org. Chem. 1997, 62, 7170-7173; d) L. Gattermann, Justus Liebigs Ann. Chem. 1906, 347, 347–386; e) N. Hoshiya, M. Shimoda, H. Yoshikawa, Y. Yamashita, S. Shuto, M. Arisawa, Journal of the American Chemical Society 2010, 132, 7270-7272; f) L. R. Moore, K. H. Shaughnessy, Organic Letters 2004, 6, 225-228; g) N. Kirai, Y. Yamamoto, Eur. J. Org. Chem. 2009,

1864-1867; h) J. L.Bolliger, C. M. Frech, Advanced Synthesis & Catalysis 2010, 352, 1075-1080; i) M. Kuriyama, R. Shimazawa, R. Shirai, Tetrahedron 2007, 63, 9393-9400; j) M. Planellas, R. Pleixats, A. Shafira, Advanced Synthesis & Catalysis 2012, 354, 651-662; k) M. Miura, T. Koike, T. Ishihara, S. Sakamoto, M. Okada, M. Ohta, S. Tsukamoto, Synthetic Communications 2007, 37, 667-674; l) I. Mutule, E. Suna, Tetrahedron 2005, 61, 11168-11176.
2. a) C. J. O'Brien, J. L. Tellez, Z. S. Nixon, L. J. Kang, A. L. Carter, S. R. Kunkel, K. C. Przeworski, G. A. Chass Angewandte Chemie Interantional Edition 2009, 48, 6836-6839; b) C. Huo, X. He, T. H. Chan J. Org. Chem. 2008, 73, 8583-8586; c) C. Petrucci, G. Strappaveccia, F. Giacalone, M. Gruttadauria, F. Pizzo, L. Vaccaro ACS Sustainable Chem. Eng. 2014, 2, 2813-2819; d) C. Pavia, F. Giacalone, L. A. Bivona, A. M. P. Salvo, C. Petrucci, G. Strappaveccia, L. Vaccaro, C. Aprile, M. Gruttadauria Journal of Molecular Catalysis A: Chemical 2014, 387, 57-62; e) V. R. Chintareddy, A. Ellern, J. G. Verkade J. Org. Chem. 2010, 75, 7166-7174; f) M. Shi, H.-X. Qian Tetrahedron 2005, 61, 4949-4955; g) C. Huo, X. He, T. H. Chan J. Org. Chem. 2008, 73, 8583-8586; h) V. R. Chintareddy, A. Ellern, J. G. Verkade J. Org. Chem. 2010, 75, 7166-7174; i) M. Erdéryi, A. Karlén, A. Gogoll, Chem. Eur. J. 2006, 12, 403-412; j) D.-J. Dong, H.-H. Li, S.-K. Tian, Journal of the American Chemical Society 2010, 132, 5018-5020; k) Y. Leng, F. Yang, K. Wei, Y. Wu Tetrahedron 2010, 66, 1244-1248.

8.3 Experimental Section Chapter 5

8.3.1 Materials and methods

1-methylimidazole, 4-vinylbenzylchloride, 1-vinylimidazole, $K_2S_2O_8$ potassium persulfate, biphenyl, toluene, styrene oxide (SO), epichlorohydrin (ECH), propylene oxide (PO) and glycidol (GLY) were purchased from Sigma Aldrich and used as received. 1,4-dibromo-pxylene was purchased from Fisher (ACROS Organics) and SWCNTs were purchased from Nanocyl (NC1100, 70+% C purity). Absolute ethanol was purchased from Fisher and chloroform from Roth. All the solvents were used without further purifications. ^{1}H NMR spectra and ^{13}C NMR spectra were recorded on a JEOL 400 and Bruker 500 spectrometers respectively. Combustion chemical analysis (C, H, N) were performed on a Thermo Finnigan-FlashEA 1112 apparatus. Transmission electron microscopy images were taken with a Philips TECNAI 10 instrument at 80-100 kV. Isothermal nitrogen adsorption was carried out at 77 K using a volumetric adsorption analyser (Micromeritics Tristar 3000) with a prior sample drying under vacuum at 120 °C.

8.3.2 Synthetic procedures

The procedures to prepare the salts **1-methyl-3-(4-vinylbenzyl)-imidazolium chloride** (**S-Imi**) and **1,4-bis(1-vinyl-imidazolium-1-methylbenzene) bromide** (**bV-Imi**) were similar to that reported in literature.[1,2]

General procedure for the synthesis of S-Imi-NT-1: In a two-necked round-bottom flask, the methyl-imidazolium chloride salt (500 mg, 2.19 mmol) was dissolved in 100 mL of Milli-Q water at room temperature. Pristine SWCNTs (130 mg) were added to this solution, which was then stirred for 24 h at room temperature. After 24 h, nitrogen was bubbled for 10 min and the mixture was heated to 65 °C. A solution of $K_2S_2O_8$ (150 mg) in 5 mL of Milli-Q water was added drop-wise under nitrogen and the mixture was then stirred for 48 h. After cooling to room temperature, the suspension was placed in an ultrasound bath for 1h, filtered and washed with water (30 mL). The resulting nanotubes were placed in a round-bottom flask with methanol (140 mL) and magnetically stirred at 60 °C overnight to remove the traces of adsorbed imidazolium salt. The product was filtered and dried in an oven at 60 °C. Anal. found for **S-Imi-NT-1** (%): N 2.31, C 82.09,

H 1.63. The percentage of imidazolium in the samples was calculated from the nitrogen content.

General procedure for the synthesis of bV-Imi-CNT-1: In a two-necked round-bottom flask, the bis-vinyl-imidazolium bromide salt (963 mg, 2.19 mmol) was dissolved in 150 mL of Milli-Q water at room temperature. Pristine SWCNTs (130 mg) were added to this solution, which was then stirred for 24 h at room temperature. After 24 h, nitrogen was bubbled for 10 min and the mixture was heated to 65 °C. A solution of $K_2S_2O_8$ (150 mg) in 5 mL of MilliQ water was added drop-wise under nitrogen and the mixture was then stirred for 48 h. After cooling to room temperature, the suspension was placed in an ultrasound bath for 1h, filtered and washed with water (30 mL). The resulting nanotubes were placed in a round bottom flask with methanol (140 mL) and magnetically stirred at 60 °C overnight to remove the traces of adsorbed imidazolium salt. The product was filtered and dried in an oven at 60 °C. Anal. found for **bV-Imi-NT-1** (%): N 0.68, C 89.56, H 0.65.

General procedure for the synthesis of bV-Imi-NT-2: In a two-necked round-bottom flask, the bis-vinylimidazolium bromide salt (963 mg, 2.19 mmol) was dissolved in 150 mL of absolute ethanol. The flask was heated to 45 °C to favour the dissolution of the salt. Pristine SWCNTs (130 mg) were added to this solution, which was then stirred for 24h at 45 °C. After 24 h, nitrogen was bubbled for 10 min and the mixture was heated to 80 °C. A solution of AIBN (150 mg) in 5 mL of absolute ethanol was added drop-wise under nitrogen and the mixture was then stirred for 48 h. After cooling to room temperature, the suspension was placed in an ultrasound bath for 1 h, filtered and washed with ethanol (30 mL). The resulting nanotubes were placed in a round-bottom flask with methanol (140 mL) and magnetically stirred at 60 °C overnight to remove the traces of adsorbed imidazolium salt. The product was filtered and dried in an oven at 60 °C. Combustion chemical analysis was performed on different batches of the material, giving the following range of values for **bV-Imi-NT-2** (%): N 6.15-7.31, C 65.49-60.15, H 3.50-3.20.

Catalytic tests

General procedure for the synthesis of cyclic carbonates: The catalytic tests were performed in a *Cambridge Design Bullfrog* batch reactor (Figure 1) with individual temperature control and mechanical overhead stirring, designed to operate at high temperature and pressures.

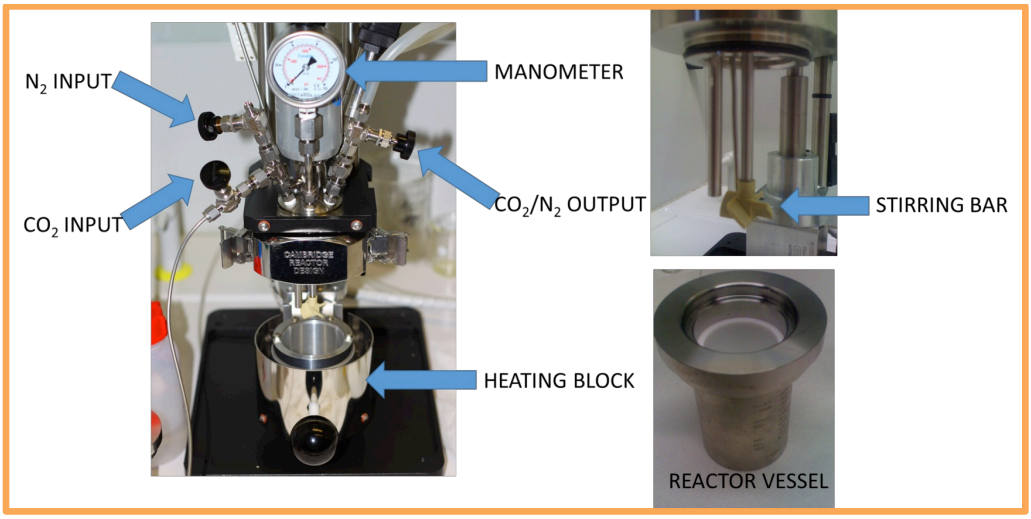

Figure 1. *Cambridge Design* 25 *Bullfrog* batch reactor used for the synthesis of cyclic carbonates.

The reactor was equipped with a Teflon liner, easily removable to facilitate work up of the reaction. In a typical experiment, the epoxide and the catalyst (100 mg or 200 mg) were first placed in an ultrasound bath for 30 min to favour the dispersion. The mixture was placed in a Teflon liner inside the reactor and biphenyl as GC internal standard was added. The reactor was closed and the mechanical stirring was kept constant at 500 rpm. The closed system was purged with N_2 (P= 4.0 bar) for 10 min and then filled with a CO_2 selected pressure depending on the final desired value. The temperature was gradually increased from room temperature to 150 °C (or 100 or 125 °C). Once the system reached the desired final temperature, the reaction was allowed to run for 3 h. After 3 h, the heating block was removed and the system cooled to room temperature. When the inner temperature was around 28 °C, the mechanical stirring was stopped and the slow depressurization of the reactor was carried out. At 0.5 bar pressure, the reactor block was opened and the collected reaction mixture was centrifuged at 4500 rpm during 5 min. The supernatant was removed and analysed by ^{1}H NMR spectroscopy using toluene-d_8 (SO, PO mixtures) or chloroform-d as solvents (ECH, GLY mixtures).

General procedure for recycling experiments of bV-Imi-NT-2: Recycling experiments were performed by removing the supernatant from the reaction mixture after a 5 min centrifugation step at 4500 rpm. Then, the catalyst was washed twice with toluene (30 mL) and twice with methanol (30 mL), placing each time the suspension in an ultrasound bath for 15 min to remove the reaction residues. After each washing step, the suspension was centrifuged at 4500 rpm at room temperature during 5 min. Finally, the catalyst was dried in an oven at 80 °C overnight before being reused.

8.3.3 References

1. B. Huber, L. Rossrucker, J. Sundermeyer, B. Roling, Solid State Ionics 2013, 247-248, 15-21.
2. C. Aprile, F. Giacalone, P. Agrigento, L. F. Liotta, J. A. Martens, P. P. Pescarmona, M. Gruttadauria, ChemSusChem 2011, 4, 1830-1837.

8.4 Experimental Section Chapter 6

8.4.1 Materials and methods

1-Methylimidazole, 3-chloropropanethiol, propanethiol, 2,2'azobisisobutyronitrile (AIBN), POSS-octavinyl, anhydrous toluene, styrene oxide (SO), anhydrous ethanol and isopropanol (^{i}PrOH) were purchased from Sigma Aldrich. Toluene, hexane, diethyl ether, methanol (MeOH), ethanol (EtOH), and dichloromethane (DCM) were purchased from Fisher and used without further purification. All of the liquid-state NMR experiments were conducted using 5 mm NMR tubes. When indicated, a J. Young valve tube was used to prevent solvent evaporation. ^{1}H NMR and ^{13}C NMR spectra were performed on a JEOL ECX-400 MHz spectrometer operating at 9.4 T (399.9 MHz for ^{1}H and 100.5 MHz for ^{13}C). Their chemical shifts were referenced to the ^{1}H residual signals and ^{13}C signals of the deuterated solvents. ^{29}Si NMR spectra were recorded on a Bruker Avance-500 spectrometer operating at 11.7 T (99.3 MHz for ^{29}Si). Liquid-state experiments were conducted at 298 K using a Bruker broadband probe, while solid-state MAS experiments were recorded at room temperature, using a 3.2 mm Chemagnetics probe and a spinning frequency of 8 kHz. IR absorption spectra were obtained with a Perkin-Elmer Spectrum II. Combustion chemical analysis (C, H, N, S) were performed on a Thermo Finnigan Flash-45 EA 1112 apparatus. Melting points were performed on a Büchi Melting Point B-545. Transmission electron microscopy images were taken with a PHILIPS TECNAI 10 at 80 eV.

8.4.2 Synthetic procedures

General procedure for synthesis of propyl-thio-ethyl-octasilsesquioxane (POSS-Me): POSS-octavinyl (300 mg, 0.47 mmol) was dissolved in anhydrous toluene (1.6 mL) under N_2 atmosphere. The radical initiator AIBN (30 mg, 0.18 mmol) was added to POSS-octavinyl solution and the reaction mixture was heated to 40 °C. Then the linker 1-propanethiol (380 µl, 4.19 mmol, 8.2 eq.) was slowly added to the mixture and the reaction was stirred for 17 h at 60 °C. After cooling the reaction at room temperature, the gel was dried under reduced pressure to give the **POSS-Me**.

POSS-Me. Transparent viscous gel. Yield: 99 %. ^{1}H NMR (400 MHz, $CDCl_3$) δ (ppm) = 2.61 (t, 16H, J = 8.5 Hz); 2.51 (t, 16H, J = 7.3 Hz); 1.62 (m, 16H); 0.99-1.05 (br, 40H, J =

8.7 Hz). ^{13}C NMR (100 MHz, $CDCl_3$) δ (ppm) = 34.2, 26.2, 23.1, 14.0, 13.4. MAS ^{29}Si NMR (99 MHz) δ (ppm) = - 68.

General procedure for synthesis of chloropropyl-thio-ethyl-octasilsesquioxane (POSS-Cl): POSS-octavinyl (1.0 g, 1.58 mmol) was dissolved in anhydrous toluene (5.5 mL) under N_2 atmosphere. The radical initiator AIBN (100 mg, 0.61 mmol) was added to POSS-octavinyl solution and the reaction mixture was heated to 40 °C. Then the linker 3-chloropropanethiol (1.32 mL, 13.55 mmol, 8.8 eq.) was slowly added to the mixture and the reaction was stirred for 13 h at 60 °C. After cooling the reaction at room temperature, the supernatant was removed and the gel was solubilized in dichloromethane (2.5 mL) and precipitated with hexane (5 x 25 mL) at 0 °C. Finally, the gel was dried under reduced pressure to give the **POSS-Cl**.

POSS-Cl. Transparent viscous gel. Yield: 99 %. ^{1}H NMR (400 MHz, $CDCl_3$) δ (ppm) = 3.66 (t, 16H, J = 6.2 Hz); 2.68 (t, 16H, J = 8.7 Hz); 2.63 (t, 16H, J = 8.7 Hz); 2.04 (m, 16H); 1.04 (t, 16H, J = 8.7 Hz). ^{13}C NMR (100 MHz, $CDCl_3$) δ (ppm) = 43.8, 32.4, 29.1, 26.3, 13.2. MAS ^{29}Si NMR (99 MHz) δ (ppm) = - 68. Anal. found for $C_{40}H_{80}Cl_8O_{12}S_8Si_8$ (%): C 32.09, H 5.28, S 16.27; calcd (%): C 31.65, H 5.31, S 16.90.

General procedure for synthesis of POSS imidazolium chloride (POSS-Imi): **POSS-Cl** (1.30 g, 0.861 mmol) was dissolved in anhydrous toluene (16 mL) under N_2 atmosphere and 1-methyl-imidazole (3.294 mL, 41.32 mmol, 48 equiv.) was slowly added to the **POSS-Cl** solution. The reaction was stirred for 48 h at 90 °C resulting in the precipitation of a brown solid. Then, the reaction mixture was cooled down and the supernatant removed. The solid was dissolved in methanol (2 mL) and was precipitated with hexane (3 x 20 mL) and diethyl ether (3 x 20 mL) using a centrifuge (20 °C, 4500 rpm, 5 min). The purified solid was dried under reduced pressure and with vacuum pump. Finally it was lyophilized overnight by dissolving it in milliQ water (2 mL) to give the **POSS-Imi**.

POSS-Imi. Brown viscous solid. Yield: 85 %. ^{1}H NMR (500 MHz, D_2O): δ (ppm) = 7.37 (d, 8H, J = 2.0 Hz); 7.31 (d, 8H, J = 2.0 Hz); 4.18 (t, 16H, J = 6.9 Hz); 3.75 (s, 24H); 2.54 (t, 16H, J = 8.9 Hz); 2.44 (t, 16H, J = 7.0 Hz); 2.03 (m, 16H); 0.86 (t, 16H, J = 7.0 Hz). ^{13}C NMR (125 MHz, D_2O) δ (ppm) = 135.7, 123.4, 121.8, 47.9, 35.4, 28.4, 26.5, 25.2, 12.6. MAS ^{29}Si NMR (99 MHz) δ (ppm) = - 60.7, -70.3. Anal. found for $C_{72}H_{128}Cl_8N_{16}O_{12}S_8Si_8$ (%): N 9.33, C 37.02, H 6.22, S 10.06; calcd (%): N 10.31, C 39.77, H 5.93, S 11.79.

General procedure to recover the catalyst (POSS-Imi): After the catalytic test (by using styrene oxide as starting material and ethanol absolute as solvent), the reaction mixture was dissolved in water (3 x 50 mL) and it was placed in a ultrasound bath for 5 minutes allowing the precipitation of the cyclic styrene carbonate. Then, the aqueous phase was extracted and dried under reduce pressure. The resulting residue was solubilized in methanol (2 mL) and precipitated at room temperature with toluene (3 x 20 mL) using a centrifuge (4500 rpm, 5 minutes). Finally, the purified solid was dried under reduced pressure to give the **POSS-Imi**.

General procedure to recover of the styrene glycol: After the catalytic test, the reaction mixture was dissolved in water (3 x 40 mL) and placed in an ultrasound bath for 5 minutes resulting in the precipitation of the cyclic carbonate. The aqueous phase was extracted and dried under reduced pressure. Then, the residue was dissolved in methanol (2 mL) and precipitated with toluene (3 x 20 mL) using a centrifuge (20 °C, 4500 rpm, 5 min). The purified solid was dried under reduced pressure to give the **styrene glycol**.

Styrene glycol. White powder. M. p. = 63 °C (theoretical 67.5 °C). ^{1}H NMR (400 MHz, DMSO-d_6) δ (ppm) = 7.24-7.39 (m, 5H), 5.27 (s, 1H), 4.77 (s, 1H), 4.58 (t, 1H, J = 6.0 Hz), 3.46 (d, 2H, J = 6.0 Hz). ^{13}C NMR (100 MHz, DMSO-d_6) δ (ppm) = 144.2, 128.6, 127.7, 127.1, 74.6, 68.3. Anal. found for $C_8H_{10}O_2$ (%): C 69.55, H 7.18; calcd (%): C 69.55, H 7.30.

Catalytic tests

For the synthesis of cyclic carbonates the reactor used for all tests is the same reported in the section 8.3.2, Figure 1. The general procedure to set up the reactor is similar to one reported in the section 8.3.2.

General procedure for synthesis of cyclic carbonates: All the catalytic tests were performed in a *Cambridge Design* 25 *Bullfrog* batch reactor (Figure 1, section 8.3.2) with individual temperature control and mechanical stirring, designed to operate at high temperature and pressures in the presence of different protic polar solvents (H_2O, MeOH, EtOH and ^{i}PrOH). In the general procedure, the catalyst (110 mg, 0.05 mmol) dissolved in protic polar solvent (1.50 mL) was added to the epoxide (0.210 mol) into the reactor vessel and connected to the heating block. The reaction mixture was mechanically stirred at 500

rpm and the system was purged with N_2 for 5 min before to filling the reactor with CO_2 until the required pressure was reached (ranged between 20 and 80 bar). The temperature was raised stepwise from room temperature to 100, or 125 or 150 °C. Once reached the desired temperature, the reaction was allowed to proceed during 3 h. After that, the temperature was fixed at 0 °C, the heating block was removed and the reactor was cooled down until the temperature of 28 °C was reached. The depressurization of the reactor was carried out slowly and the reaction mixture was recovered in a flask and analyzed by ^{1}H NMR. Conversion and selectivity were calculated via ^{1}H NMR.

8.5 Experimental Section Chapter 7

8.5.1 Materials and methods

All of the substrates and solvents were purchased from Sigma Aldrich and Ficher and used without further purification. Liquid state ^{1}H NMR and ^{13}C NMR spectroscopy were performed with a JEOL ECX-400 spectrometer, operating at 9.4 T (399.9 MHz for ^{1}H and 100.5 MHz for ^{13}C). Their chemical shifts were referenced to the ^{1}H residual signals and ^{13}C signals of the deuterated solvents. Liquids state ^{29}Si NMR spectra were recorded on a Bruker Avance-500 spectrometer operating at 11.7 T (99.3 MHz for ^{29}Si). Combustion chemical analysis (C, H, N) was performed on a Thermo Finnigan- FlashEA 1112 apparatus. IR absorption spectra were obtained with a Perkin.Elmer Spectrum II. Transmission electron microscopy images were taken with a PHILIPS TECNAI 10 instrument at 80 kV. Samples were dispersed in ethanol and deposited on a carbon coated copper grid. The X-ray photoelectron spectroscopy (XPS) analyses were performed with a Thermo Scientific K-Alpha spectrometer, equipped with a monochromatized Al anode (1486-6 eV): X-ray source: 12 kV, 1.8 mA; X-ray spot size: 200 mm. A flood gun (electrons and Ar ions at very low energy) was used to avoid possible charging effects. The analyzer was operated at constant pass energy (CAE) to ensure a constant energy resolution over the whole spectrum. The analyzer was operated at 200 eV pass energy for survey spectra, and at 40 eV for high-resolution individual spectra. Pressure in the chamber was in the range 10^{-7} mbar. Analyses of the peaks were performed with the software Thermo Avantage, based on non-linear least squares fitting program using a weighted sum of Lorentzian and Gaussian component curves after background subtraction according to Shirley and Sherwood. FWHM values were fixed for all the signals. All the biphenyl compounds synthesized are known molecules.[1]

8.5.2 Synthetic procedures

The strategy employed for the experimental part concerning the synthesis of **POSS-Imi** was modified respect to the previous version reported in the Experimental Section of the Chapter 6 (section 8.4.2).

General procedure for synthesis of chloropropyl-thio-ethyl-octasilsesquioxane (POSS-Cl): POSS-octavinyl (300 mg, 0.474 mmol) was added in anhydrous toluene (1.6 mL) under N_2 atmosphere. The radical initiator AIBN (30 mg, 0.183 mmol) was added to

POSS-octavinyl solution and the reaction mixture was heated to 40 °C. Then, the linker 3-chloropropanethiol (0.400 mL, 4.108 mmol, 8.67 eq.) was slowly added to the mixture and the reaction was stirred for 6 h at 60 °C. After cooling the reaction at room temperature, the supernatant was removed under reduced pressure and the gel was solubilized in dichloromethane (0.5 mL) and precipitated with hexane (3 x 25 mL) at 0 °C. Finally, the gel was dried under reduced pressure to give the **POSS-Cl**.

POSS-Cl. Transparent viscous gel. Yield: 99 %. ^{1}H NMR (400 MHz, $CDCl_3$) δ (ppm) = 3.66 (t, 16H, J = 6.2 Hz), 2.68 (t, 16H, J = 8.7 Hz), 2.63 (t, 16H, J = 8.7 Hz), 2.04 (m, 16H), 1.04 (t, 16H, J = 8.7 Hz). ^{13}C NMR (100 MHz, $CDCl_3$) δ (ppm) = 43.8, 32.4, 29.1, 26.3, 13.2. MAS ^{29}Si NMR (99 MHz) δ (ppm) = - 68. Anal. found for $C_{40}H_{80}Cl_8O_{12}S_8Si_8$ (%): C 32.09, H 5.28, S 16.27; calcd (%): C 31.65, H 5.31, S 16.90.

General procedure for synthesis of POSS imidazolium chloride (POSS-Imi): **POSS-Cl** (670 mg, 0.441 mmol) was dissolved in toluene (7.2 mL) and 1-methyl-imidazole (0.422 mL, 5.294 mmol, 12.00 eq.) was added to the **POSS-Cl** solution. The reaction was stirred for 4 days at 90 °C resulting in the precipitation of a brown gel. After this time, the reaction mixture was cooled down and the supernatant removed. The solid was washed with dichloromethane (6 x 20 mL) by stirring at room temperature and then, dried under reduced pressure. Finally, it was lyophilized overnight by dissolving it in milliQ water (2 mL) to give the **POSS-Imi**.

POSS-Imi. Brown viscous solid. Yield: 68 %. ^{1}H NMR (500 MHz, D_2O) δ (ppm) = 7.37 (d, 8H, J = 2.0 Hz), 7.31 (d, 8H, J = 2.0 Hz), 4.18 (t, 16H, J = 6.9 Hz), 3.75 (s, 24H); 2.54 (t, 16H, J = 8.9 Hz), 2.44 (t, 16H, J = 7.0 Hz), 2.03 (m, 16H), 0.86 (t, 16H, J = 7.0 Hz). ^{13}C NMR (125 MHz, D_2O) δ (ppm) = 135.7, 123.4, 121.8, 47.9, 35.4, 28.4, 26.5, 25.2, 12.6. MAS ^{29}Si NMR (99 MHz) δ (ppm) = - 60.7, - 70.3. Anal. found for $C_{72}H_{128}Cl_8N_{16}O_{12}S_8Si_8$ (%): N 9.32, C 34.54, H 6.28, S 9.47; calcd (%): N 10.31, C 39.77, H 5.93, S 11.79.

General procedure for synthesis of POSS imidazolium tetrachloropalladate (POSS-Imi-$PdCl_4$): In a round-bottom flask **POSS-Imi** (70.5 mg, 0.0324 mmol) was dissolved in water (1.0 mL). To this solution $PdCl_2$ was added (23.06 mg, 0.1300 mmol, ratio Imi/$PdCl_2$ is equal to 2:1) and the reaction mixture was heated at 80 °C for 1 h. Then, the orange mixture was cooled down and stirred at room temperature for 16 h. After this time, the supernatant was removed under reduced pressure to give the **POSS-Imi-$PdCl_4$**.

POSS-Imi-PdCl$_4$. Orange powder. Quantitative yield. ^{1}H-NMR (500 MHz, D_2O) δ (ppm) = 8.86 (8H), 7.59 (8H), 7.53 (8H), 4.42 (16H) 3.96 (24H) 3.01 (16H), 2.42 (16H), 2.24 (16H) 1.65 (16H). ^{13}C-NMR (100 MHz, D_2O) δ (ppm) = 136.3, 124.0, 122.3, 48.2, 35.6, 33.0, 32.1, 27.9, 13.2. Anal. found for $C_{72}H_{128}Cl_{16}N_{16}O_{12}Pd_4S_8Si_8$ (%): N 6.48, C 25.63, H 4.88, S 7.16; calcd (%): N 7.77, C 29.98, H 4.47, S 8.89.

General procedure for synthesis of 1-butyl-3-methylmidazolium tetrachloropalladate (bmim$_2$PdCl$_4$): An aqueous media solution of 1-butyl-3-methylimidazolium chloride (90.7 mg, 0.5209 mmol) was prepared in volumetric flask (2.0 mL). Then, in a round bottom-flask this solution (0.1302 mmol, 0.5 mL), and $PdCl_2$ (11.5 mg, 0.065 mmol) were added and heated at 80 °C for 1 h. Subsequently, the red mixture was cooled at room temperature and stirred for 16 h (as the procedure reported for the previous catalyst). Finally, the supernatant was removed under reduced pressure to give the **bmim$_2$PdCl$_4$**.

bmim$_2$PdCl$_4$. Red solid. Quantitative yield. ^{1}H NMR (400 MHz, CD_3OD) δ (ppm) = 9.02 (s, 2H), 7.72 (d, 2H, J = 2.0 Hz), 7.64 (d, 2H, J = 2.0 Hz), 4.31 (t, 4H, J = 8 Hz), 4.02 (s, 6H), 1.94 (m, 4H, J = 8 Hz), 1.45 (m, 4H, J = 8 Hz), 1.04 (t, 6H, J = 8 Hz). ^{13}C NMR (100 MHz, CD_3OD) δ (ppm) = 136.6, 123.7, 122.4, 49.4, 35.3, 31.8, 19.0, 12.3. Anal. found for $C_{16}H_{30}Cl_4N_4Pd$ (%): C 36.85, H 5.45, N 10.73; calcd (%): C 36.49, H 5.74, N 10.64.

General procedure for synthesis of propyl-thio-ethyloctasilsesquioxane palladium chloride (**POSS-Me-PdCl$_2$**): In a round-bottom flask **POSS-CH$_3$** (40.1 mg, 0.0323 mmol) and acetonitrile (5.0 mL) were added. To this turbid solution $PdCl_2$ was added (23.0 mg, 0.1300 mmol) and the reaction mixture was heated at 110°C for 21 h. The suspension turned yellow. Then, acetonitrile was added again (4 mL) and the reaction mixture was heated at 110 °C for 1 h. After this time, the yellow mixture was cooled down, filtered under reduce pressure and washed with acetonitrile (50 mL) in order to give a yellow powder (**POSS-Me-PdCl$_2$**).

Catalytic tests

General procedure for a Suzuki-Miyaura Reaction:[1] In a round-bottom flask, catalyst (0.16 or 0.08 mol%), phenylboronic acid (1.10 mmol), K_2CO_3 (2.10 mmol), aryl bromide (1.00 mmol), and water (1.0 mL) were placed. The reaction mixture was stirred at 100 °C. After 4 h, the reaction mixture was cooled down, then water was added and the mixture extracted with dichloromethane (3 x 30 mL). The organic phase was dried with Na_2SO_4,

filtered and concentrated under reduced pressure. The residue was passed through a short silica gel pad (petroleum ether / ethyl acetate).

Measurements of Pd nanoparticles.

After the Suzuki coupling reaction, the mixture was removed from the flask and the solid remained was dissolved in ethanol (2 mL) and ultrasonicated for 1 h at room temperature. Then, it was deposited on a carbon film copper grid, dried overnight and analyzed by transmission electron microscopy (TEM).

Measurements of Pd oxydation state.

After the Suzuki coupling reaction, the mixture was dried under vacuum. Then, the solid was deposited in a carbon film and analyzed by X-Ray photoelectron spectroscopy (XPS).

8.5.3 References

For Suzuki compunds:

1. a) N. Mejias, R. Pleixats, A. Shafir, M. Medio-Simon, G. Asensio, Eur. J. Org. Chem. 2010, 5090-5099; b) J. L.Bolliger, C. M. Frech, Advanced Synthesis & Catalysis 2010, 352, 1075-1080; c) Y. Li, X. Mi, M. Huang, R. Cai, Y. Wu, Tetrahedron 2012, 68, 8502-8508; d) D. Badone, M. Baroni, R. Cardamone, A. Ielmini, U. Guzzi, J. Org. Chem. 1997, 62, 7170-7173; e) Yoshiaki Nakao, Akhila K. Sahoo, Akira Yada, Jinshui Chen, Tamejiro Hiyama, Science and Technology of Advanced Materials 2006, 7, 536-543; f) L. R. Moore, K. H. Shaughnessy, Organic Letters 2004, 6, 225-228; g) N. Hoshiya, M. Shimoda, H. Yoshikawa, Y. Yamashita, S. Shuto, M. Arisawa, Journal of the American Chemical Society, 2010, 132, 7270-7272; h) L. Gattermann, Justus Liebigs Ann., Chemistry 1906, 347, 347-386.

Chapter 9

General conclusions and perspectives

Chapter 9

General conclusions and perspectives

9.1 General conclusions

In the last years, the industrial and academic interest for the development of new sustainable synthesis strategies increased dramatically. In this context, the design of novel materials and compounds that can be employed as catalytic systems able to reduce the cost and the environmental impact of the chemical processes gained a relevant importance.
The main objective of this doctoral project was the design of novel hybrid organic-inorganic systems based on thiazolium and imidazolium salts and their application as catalysts or support for catalysts in various and interesting reactions.

In the first section of this thesis (chapter 3, 4 and 5) a multilayered covalently supported thiazolium or imidazolium based mesoporous materials (SBA-15-Thia and SBA-15-Imi), a thiazolidine-palladium based material (SBA-15-Thiazolidine-Pd) and imidazolium functionalized carbon nanotubes (Imi-NT) were synthetized and completely characterized. All of these materials were employed in heterogeneous conditions. The determination of the structural properties of the materials was performed by means of a broad series of characterization techniques (elemental analysis, nitrogen physisorption, transmission electron microscopies, ^{1}H, ^{13}C and ^{29}Si nuclear magnetic resonance in the liquid or solid state, X-Ray photoelectron and Raman spectroscopy). Almost all of these materials showed very high percentage of catalytic sites, a good specific surface area and a homogeneous pore size distribution. These features rendered them promising materials for catalytic applications.
It is worth to be mentioned that we reported, for the first time, SBA-15-Thia and SBA-15-Imi materials as very active catalysts for the etherification reactions (chapter 3). They exhibited an excellent catalytic activity for the synthesis of ethers, especially the SBA-15-Thia, working in very low amount (0.056 %mol). The application of thiazolium-based catalyst embodies a novelty for the focus reaction. The most active material was used with a series of benzyl alcohols showing excellent performances, in term of both conversion and selectivity. Moreover, SBA-15-Thia displayed a good recyclability in the conversion of 1-

phenylethanol to bis(methylbenzyl)ether. In particular, this catalyst showed one of the highest productivity value reported in literature. A depth study of the influence of the gas phase was reported, highlighting the positive influence of the oxygen for the catalyzed reaction, probably regenerating the catalyst.

Motivated by these good results with the SBA-15-Thia, we decided to engage this material as support for palladium catalytic species (chapter 4). In this context, we took advantage of the multi-layer covalently thiazolium networks in order to obtain, in one-pot reaction, a highly cross-linked thiazolidine material, which acts as ligand for the palladium based catalyst. After the synthesis, this material was tested with success for Suzuki-Miyaura and Heck reactions. It is worth to note that there are very few examples in literature in which Pd^{II} species and palladium nanoparticles are stabilized and/or anchored by employing SN ligands. In particular, from the XPS investigations we highlighted the interaction S→Pd. The catalyst displayed good catalytic performances, working in only 0.1 % mol amount. Moreover, the good activity was maintained in multiple catalytic cycles confirming the recyclability of the solid.

The last materials tested in heterogeneous phase were represented by the mono and multi-layer imidazolium functionalized single walled carbon nanotubes (S-Imi-NT-1 and bV-Imi-NT-2, respectively, chapter 5). The functionalization was carried out by self-assembly and subsequent radical initiated polymerization, taking advantage from the high reactivity of the SWCNT C=C double bonds. It was demonstrated that both materials displayed good surface area and homogeneous pore size distribution, however lower percentage of organic functionalization was observed in the case of S-Imi-NT-1, probably due to the different synthetic approach. Whereas, bV-Imi-NT-2 showed an exceptional high degree of organic moiety, thanks to the highly cross-linked imidazolium networks. The materials displayed excellent catalytic activity for the reaction of CO_2 and epoxides to produce the corresponding cyclic carbonates as proved by the high turnover numbers (TON). Moreover, the best catalyst was tested in recycling experiments without loss of activity. Contrasting the bV-Imi-NT, S-Imi-NT material suffered of an important leaching of organic species in the reaction mixture, as confirmed by combustion elemental analysis of the material performed after the first cycle. It is important to highlight that the materials were employed without the use of any co-catalysts.

The second part of this doctoral project (chapter 6 and 7) was devoted to the design of new silsesquioxane based nanostructure functionalized with imidazolium chloride or

tetrachloropalladate, generally indicated as POSS-Imi and POSS-Imi-$PdCl_4$. The compounds were prepared starting from a commercial POSS and its functionalization with imidazolium moieties. The catalytic performances of these compounds were investigated in homogeneous conditions for selecting target reactions, as the conversion of carbon dioxide (POSS-Imi, chapter 6) and the Suzuki-Miyaura reaction (POSS-Imi-$PdCl_4$, chapter 7).

By employing several characterization techniques, it was highlighted the stability of the inorganic silsesquioxane core in the reaction conditions. This compound was tested for the first time for the conversion of CO_2 with epoxides into the cyclic carbonates, evidencing a good catalytic activity. Different conditions in term of amount of catalyst, temperature, pressure of CO_2 and solvents were optimized allowing excellent catalytic performances. In particular, the catalyst displayed improved catalytic performances respect to the un-supported 1-butyl-3-methylimidazolium chloride (bmimCl), evidenced by using styrene oxide and epichlorohydrin as substrate. The higher catalytic activity was ascribed to the proximity effect generated by the increased local concentration of imidazolium moieties surrounding the inorganic nanocage structure.

Finally, encouraged by the results reached with POSS-Imi, a novel class of silsesquioxanes-imidazolium tetrachloropalladate salt (POSS-Imi-$PdCl_4$) was easily prepared by reaction of a POSS-Imi with $PdCl_2$. This new compound was tested as pre-catalyst for Suzuki-Miyaura reaction in water and in very low amount (0.16 or 0.08 % mol), obtaining excellent yields of the products. It is worth to be underline that, as for the previous catalyst, it was demonstrated that the silsesquioxane nanostructure plays a positive role for the catalyzed reaction, through the comparison with the un-supported 1-butyl-3-methyl imidazolium tetrachloropalladate ($bmim_2PdCl_4$). Once again, the positive influence could be ascribed to the proximity effect created by the silsesquioxane core, which could generate a local environment in which the solubility of the substrates is higher respect to the water phases.

9.2 Perspectives

For almost all the materials and compounds synthesized during the development of this doctoral project, there are some aspects that render them promising systems to be further investigated for other applications.

An ambitious and future objective will be the application in flow conditions for both SBA-15-Thia and SBA-15-Thiazolidine-Pd. However, for this last material, the catalytic applications could be optimized in order to increase the performances of the material. Preliminary investigations with SBA-15-Thiazolidine-Pd were performed in order to study the catalytic activity for other C-C cross coupling reactions. It would be interesting to realize a thiazolium (or thiazolidine) based material supported onto magnetic particles, in order to have a major benefit because of the easier recover of the catalyst from the reaction mixture. Furthermore, the material SBA-15-Thia could be able to stabilize other metal catalysts, such as gold species, employed for further applications.

Imidazolium functionalized carbon nanotubes showed excellent catalytic activity for the conversion of carbon dioxide, and thanks to its properties, a future target could be its application in flow conditions. Because of the good results in term of productivity, this material could be interesting in view of possible industrial applications. However, the catalytic performances could be improved by changing the counter anion of the imidazolium moieties (iodide instead of bromide or chloride). It would be attractive to design a similar material able to capture the CO_2 and, by changing some parameters, it releases the carbon dioxide and catalyzes the conversion.

As before mentioned for the imidazolium carbon nanotubes, the catalytic activity of POSS-Imi could be enhanced by changing the counter anion. In addition, in order to increase the catalytic activity of the compound, it would be interesting to synthetize a new silsesquioxane nanostructure that contain some co-catalysts, such as Lewis acids. Because of POSS-Imi was recovered from the reaction mixture, next goal will be its reuse for CO_2 conversion. Concerning the characterization, in addition to usual techniques, a dynamic light scattering (DLS) would be ideal to confirm the presence of some nano-aggregates of POSS in solutions.

POSS-Imi-$PdCl_4$ showed very good results, however the performances could be still optimized in order to reach higher TON. In the future, its catalytic activity may be investigated for other C-C cross coupling reactions.

Annex A

Supporting informations

A.1 Supporting Information (SI) Chapter 3

Figure S1: Nitrogen adsorption/desorption measurements of **SBA-15-Thia**. Isotherm (a) and pore size distribution (b).

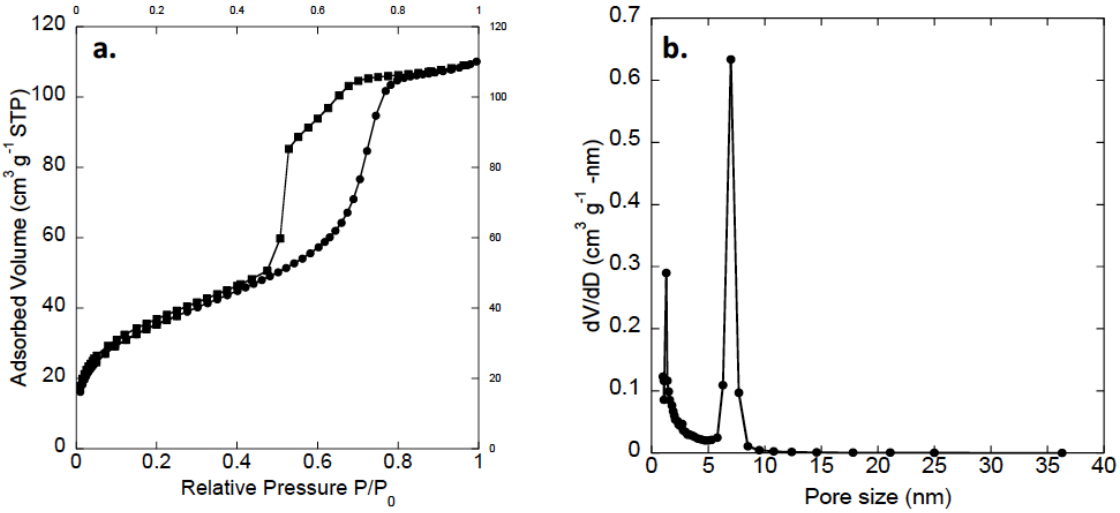

Figure S2: Isotherm nitrogen adsorption/desorption measurements of **SBA-15**

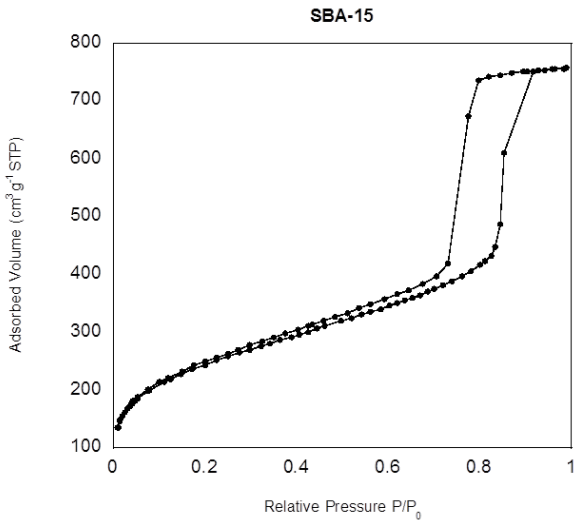

Figure S3: Isotherm nitrogen adsorption/desorption measurements of **SBA-15-SH**

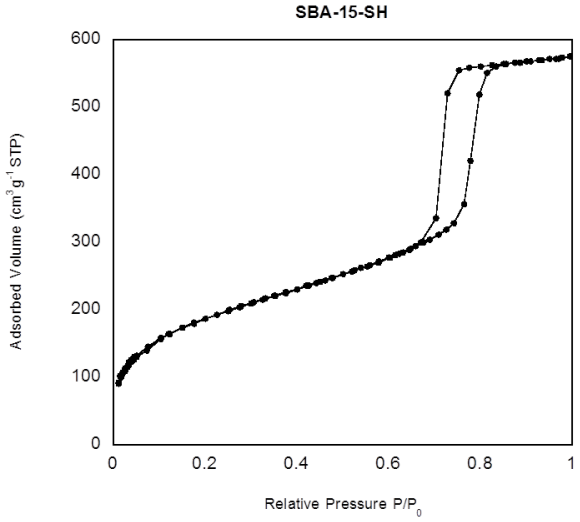

Figure S4: Isotherm nitrogen adsorption/desorption measurements of **SBA-15-Imi**

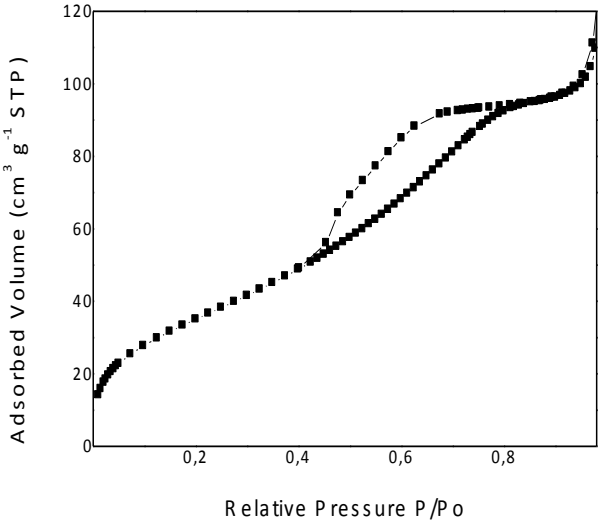

Figure S5: ^{1}H NMR spectrum of **1,4-Bis(5-methyl-4-vinyltiazolium-1-metylbenzene) bromide**

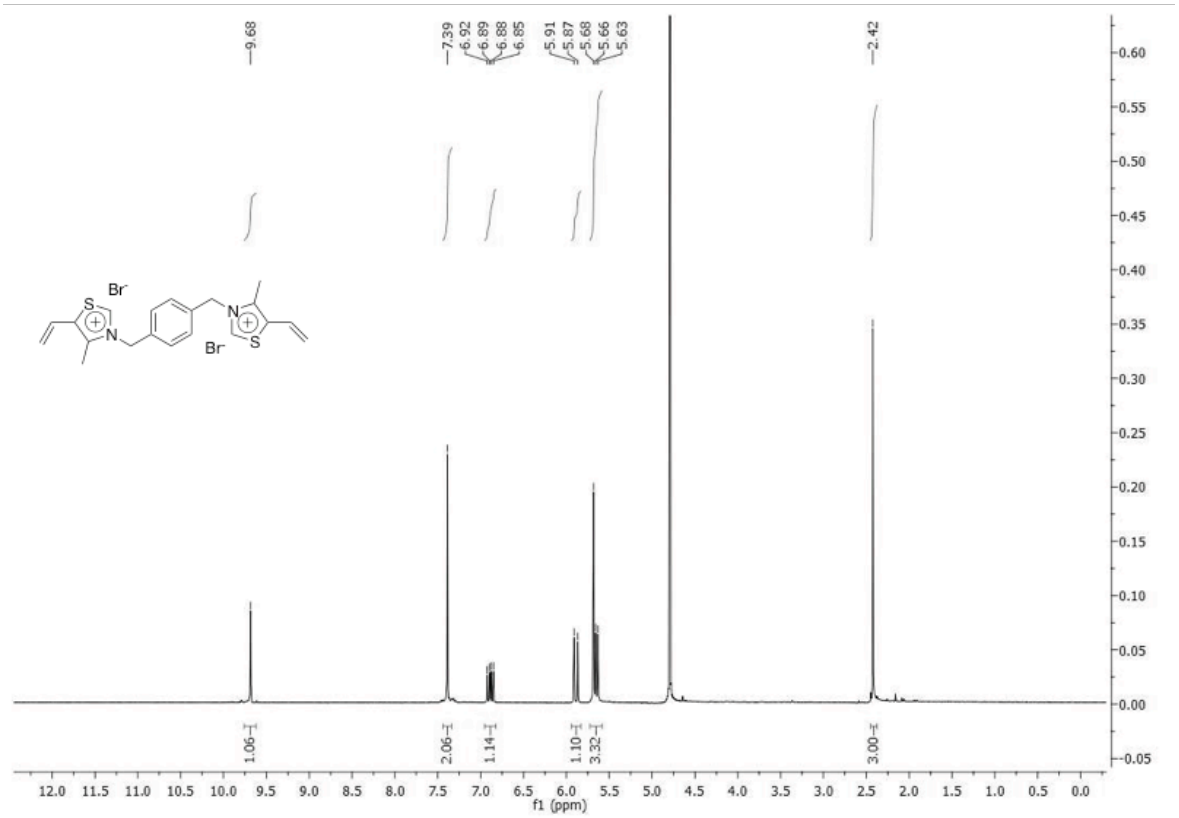

Figure S6: ^{13}C NMR spectrum of **1,4-Bis(5-methyl-4-vinyltiazolium-1-metylbenzene) bromide**

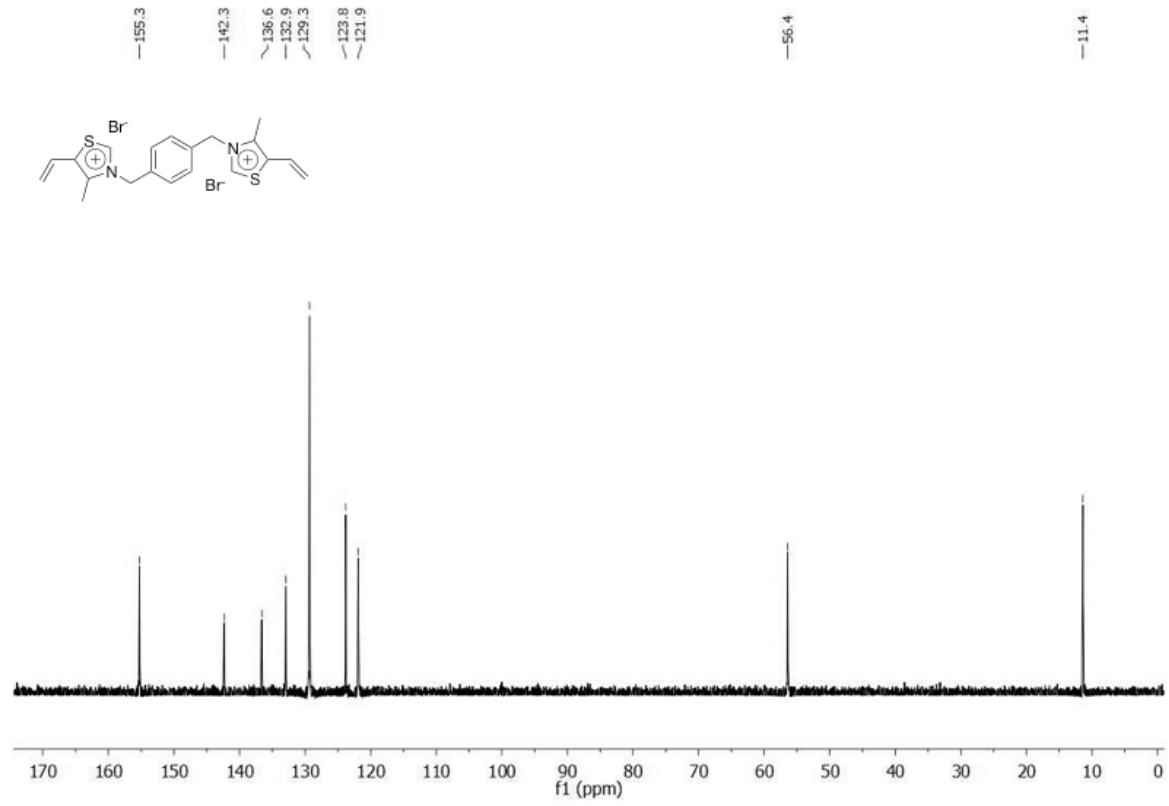

Figure S7: IR spectrum of **1,4-Bis(5-methyl-4-vinylthiazolium-1-methylbenzene) bromide**

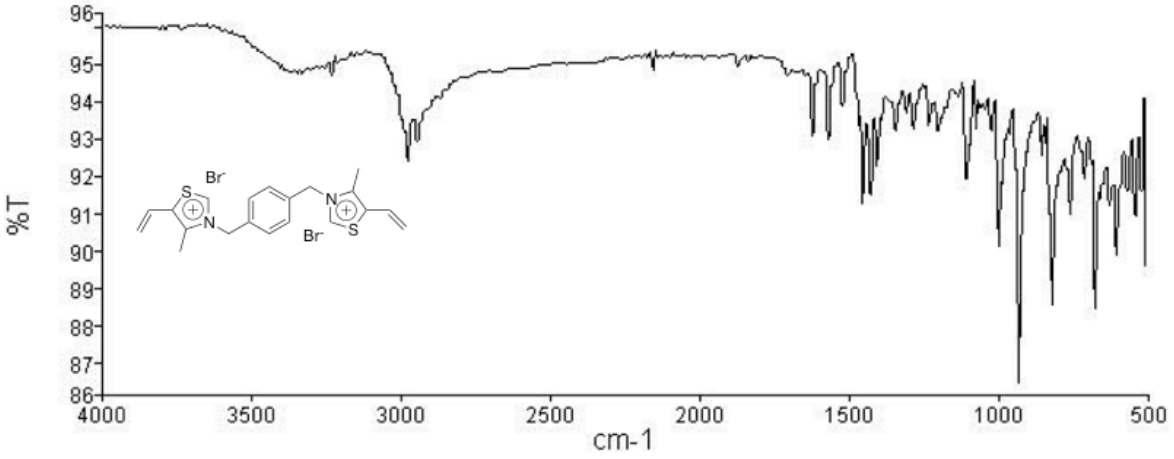

Figure S8: ^{1}H NMR of **Homo-Thia-H**

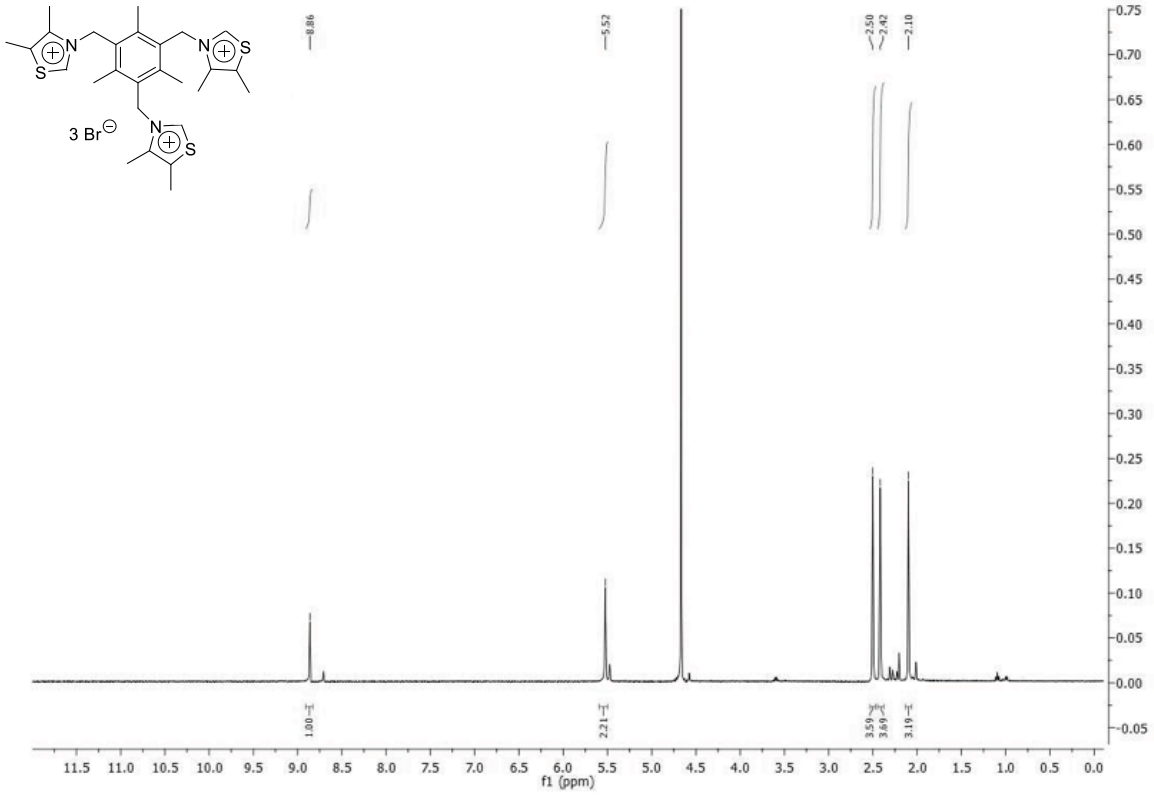

Figure S9: ^{13}C NMR of **Homo-Thia-H**

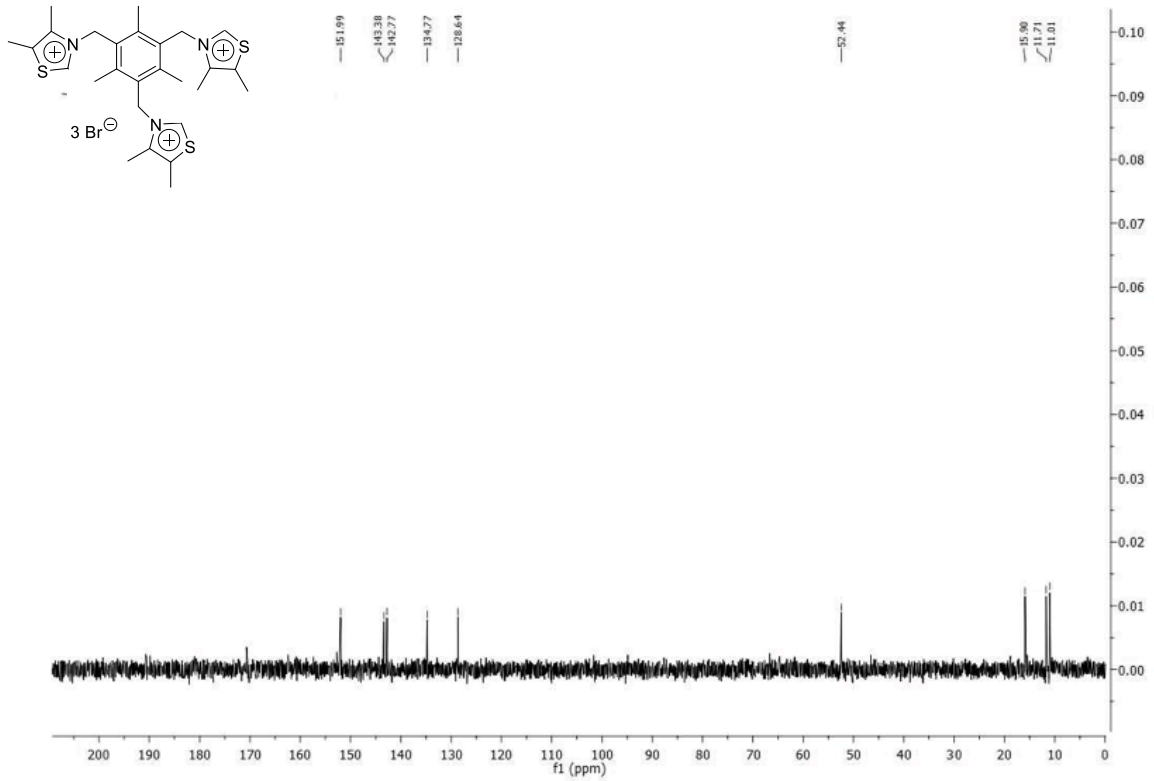

Figure S10: ^{1}H NMR of **Homo-Thia-Me**

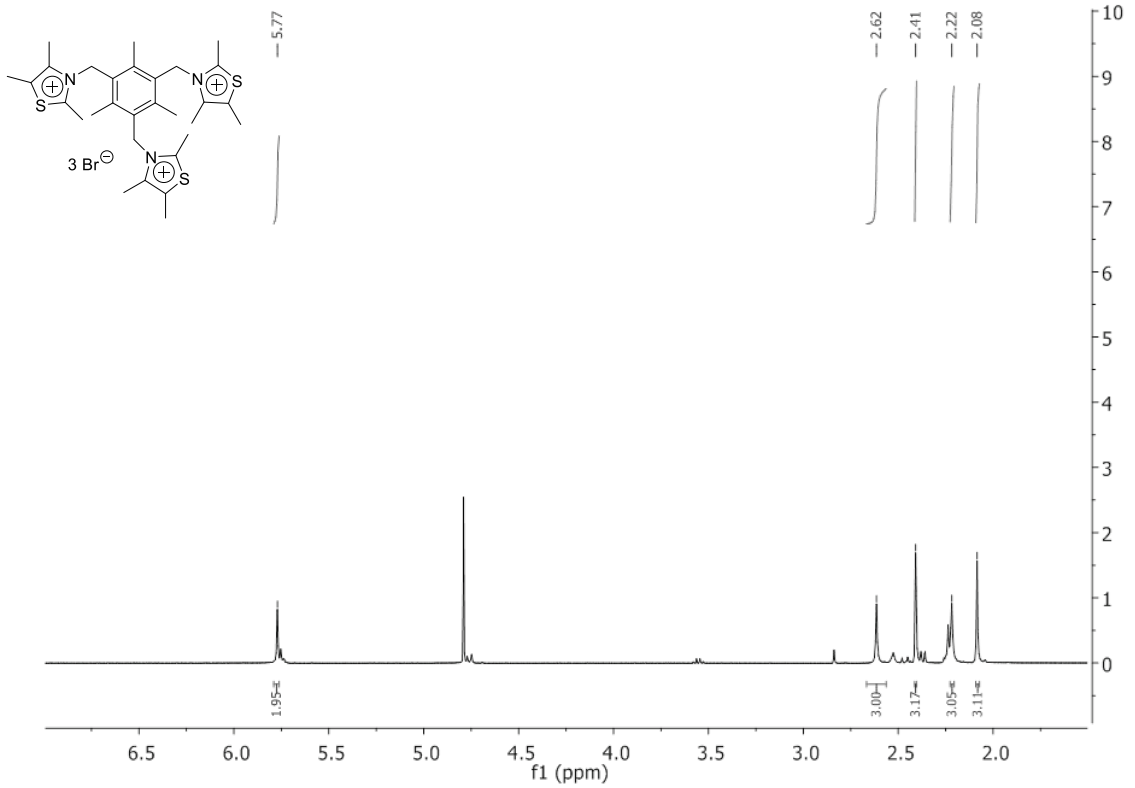

Figure S11: ^{13}C NMR of **Homo-Thia-Me**

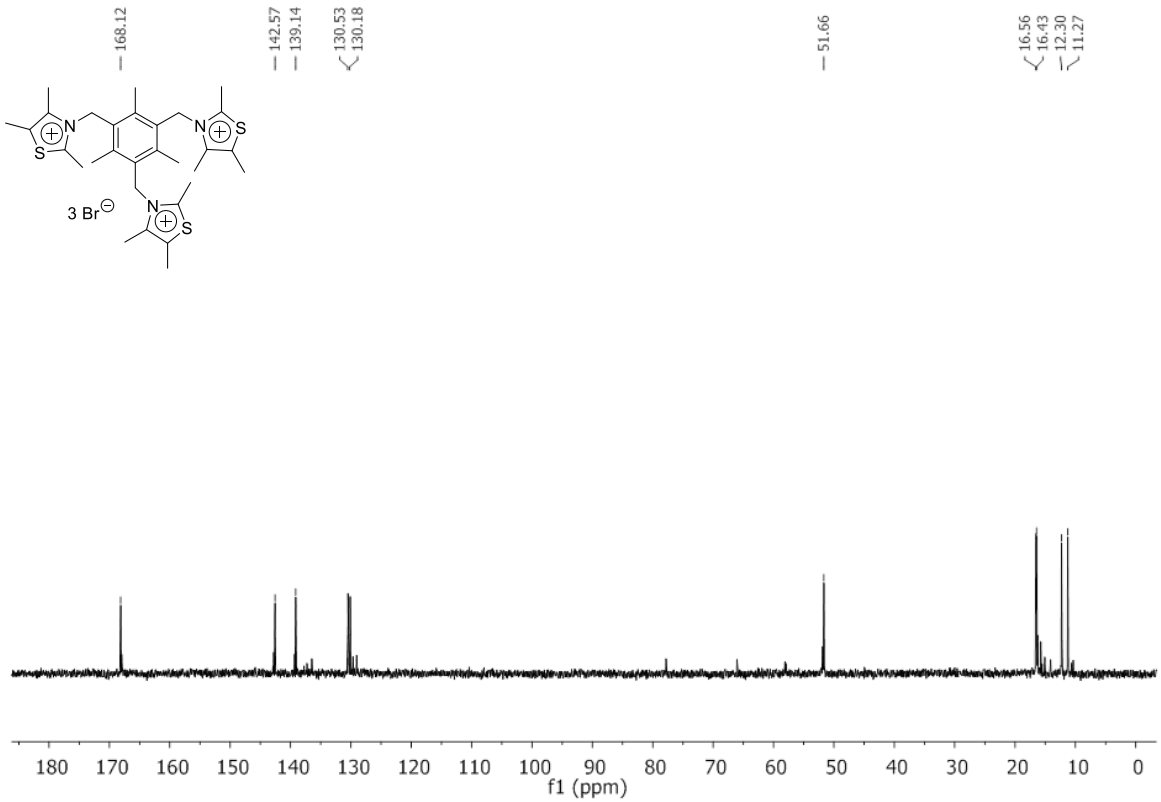

Figure S12: ^{1}H NMR of **Mono-Thia**

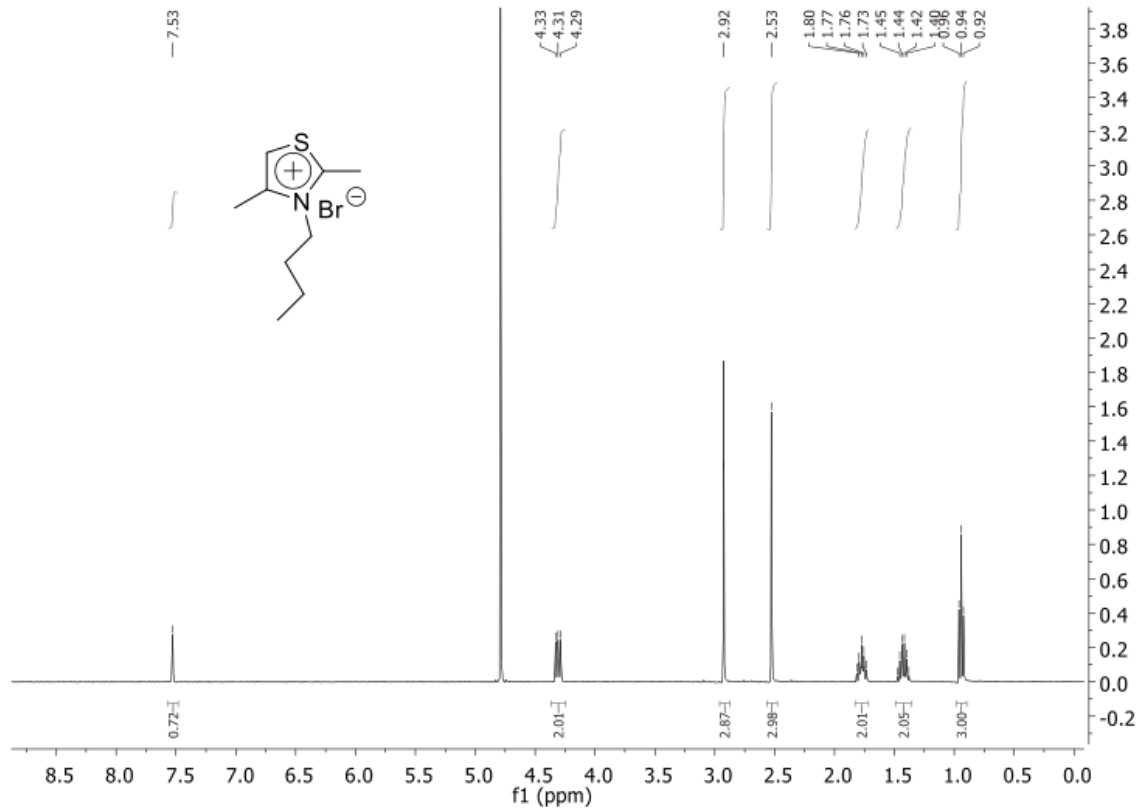

Figure S13: ^{13}C NMR of **Mono-Thia**

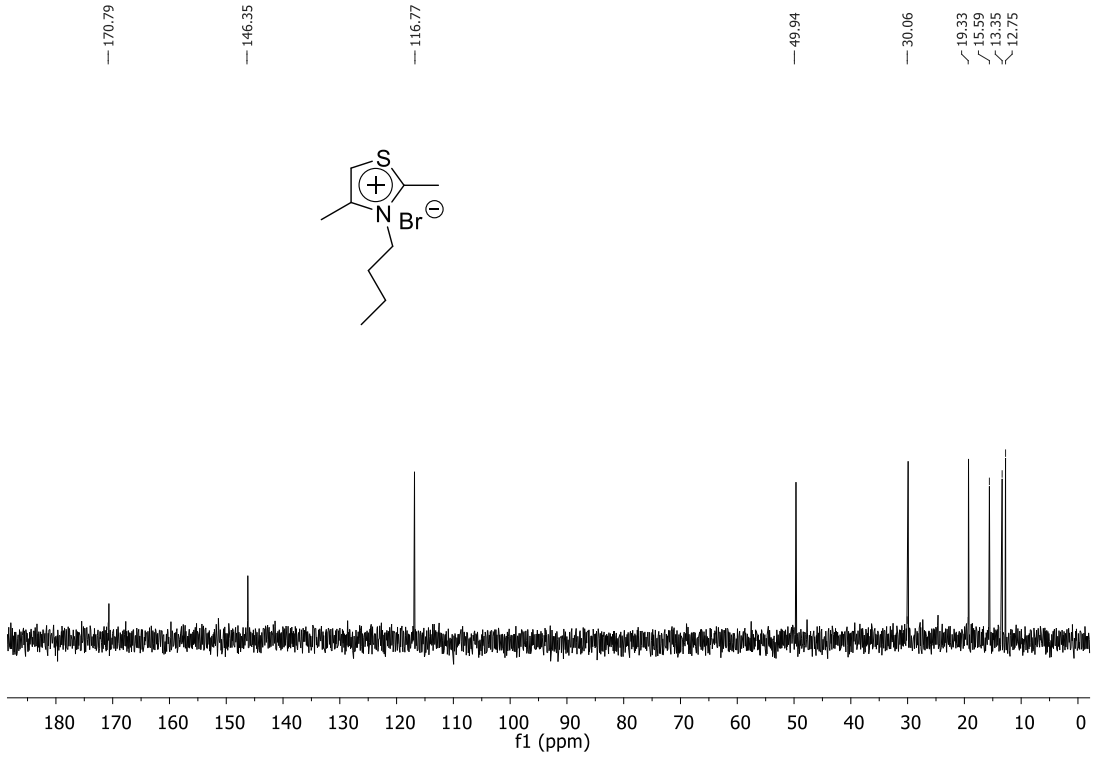

A.2 Supporting Information (SI) Chapter 4

Figures S1: Additional TEM images for the catalyst after the 3rd cycle.

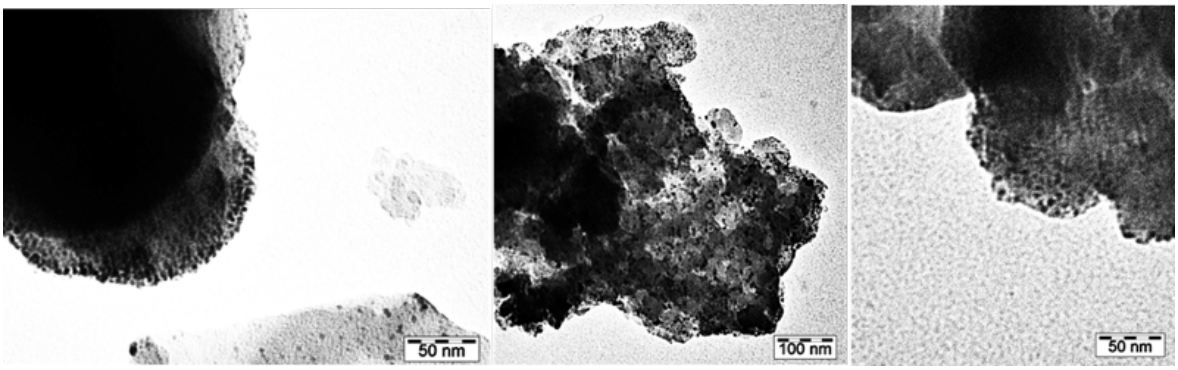

Figures S2: Images of "r.t. filtration" (see Table 4).

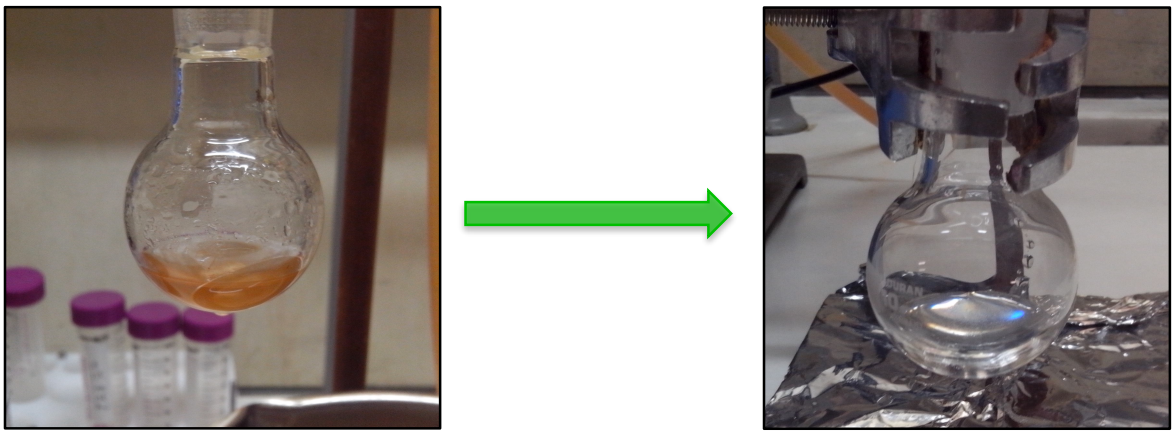

Measurement of Pd leaching.

The sample (1.3 mg) was dissolved in 2 mL of aqua regia and later mineralized by microwave heating for 30 minutes. Then, it was diluted with water 1:50 (v/v) and palladium concentration was measured by atomic absorption spectroscopy with a graphite furnace (AAS).

A.3 Supporting Information (SI) Chapter 6

Figure S1: ^{1}H NMR of **POSS-Cl**

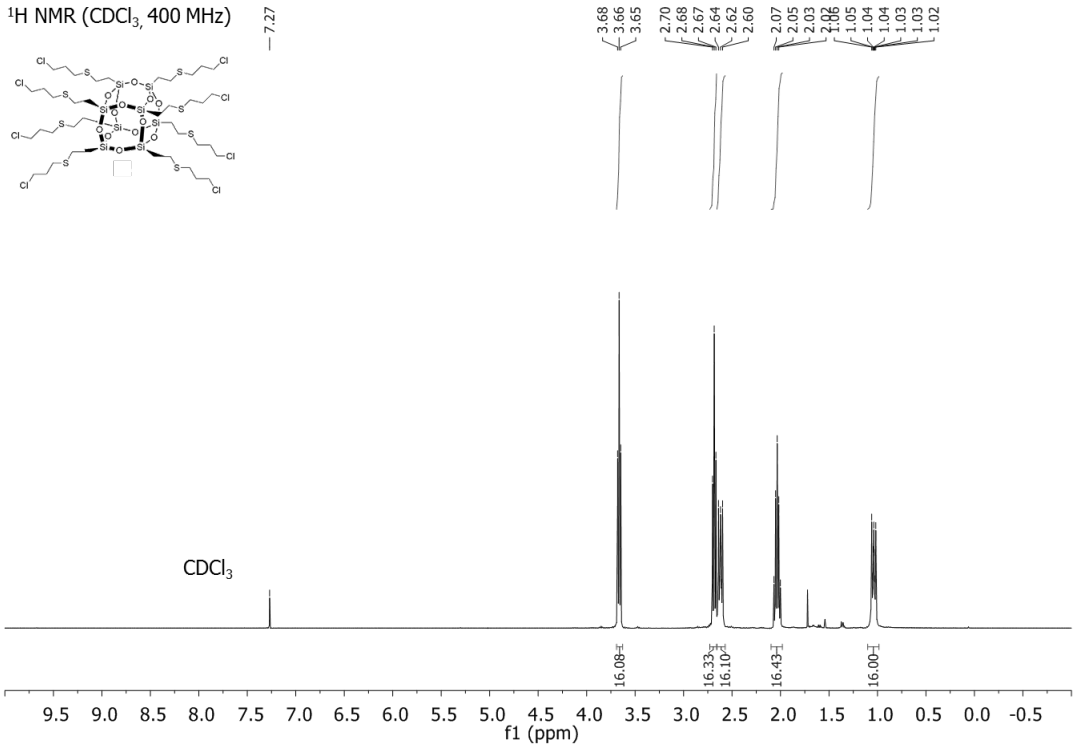

Figure S2: ^{13}C NMR of **POSS-Cl**

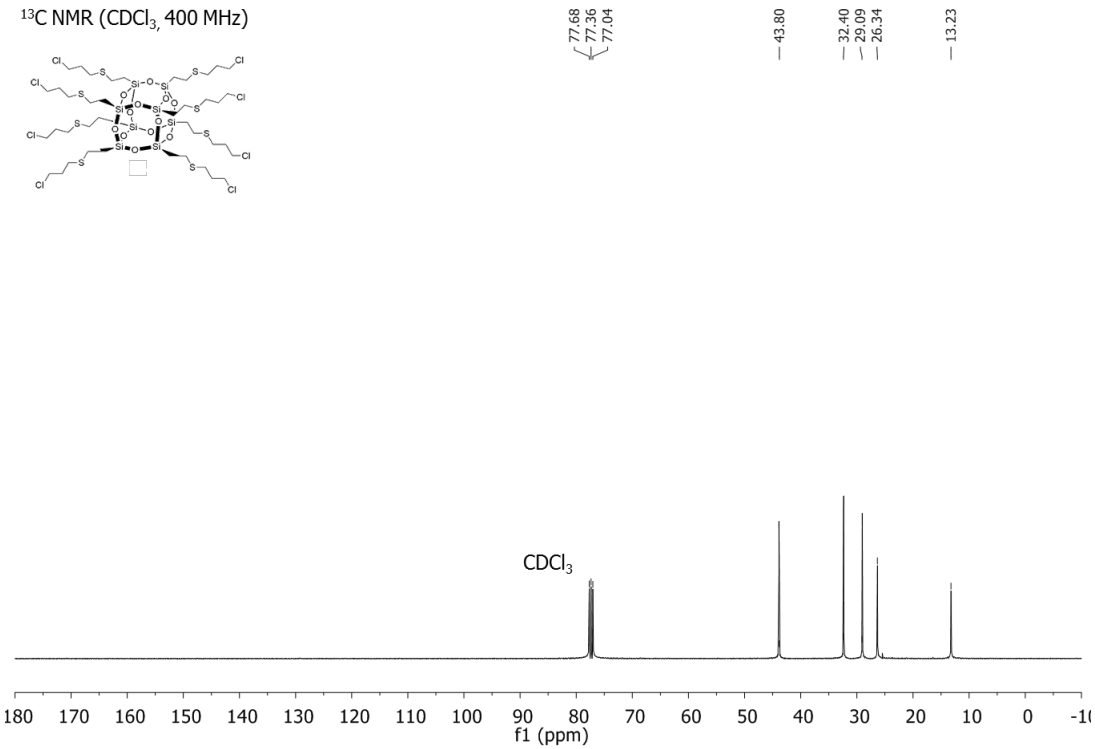

Figure S3: IR spectrum of **POSS-Cl**

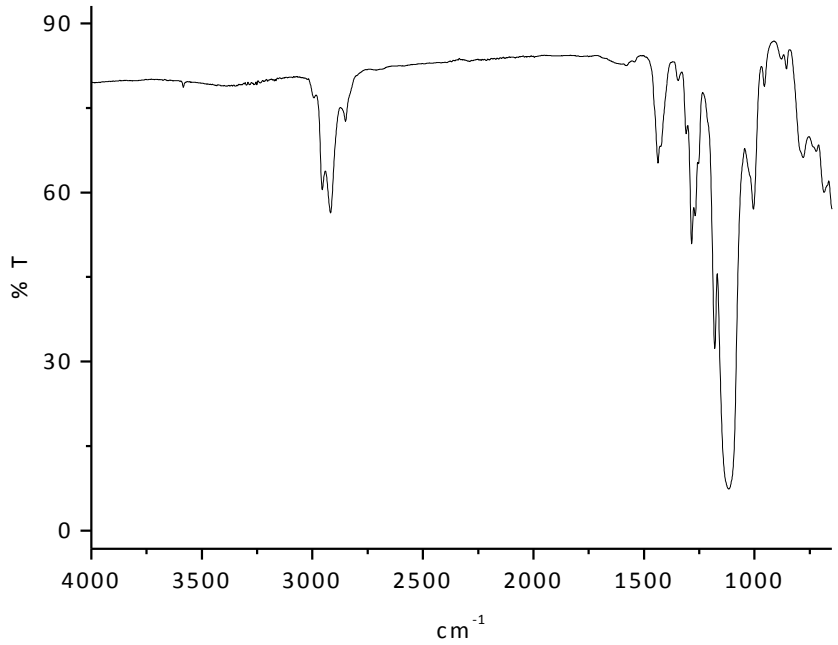

Figure S4: ^{1}H NMR of **POSS-Imi**

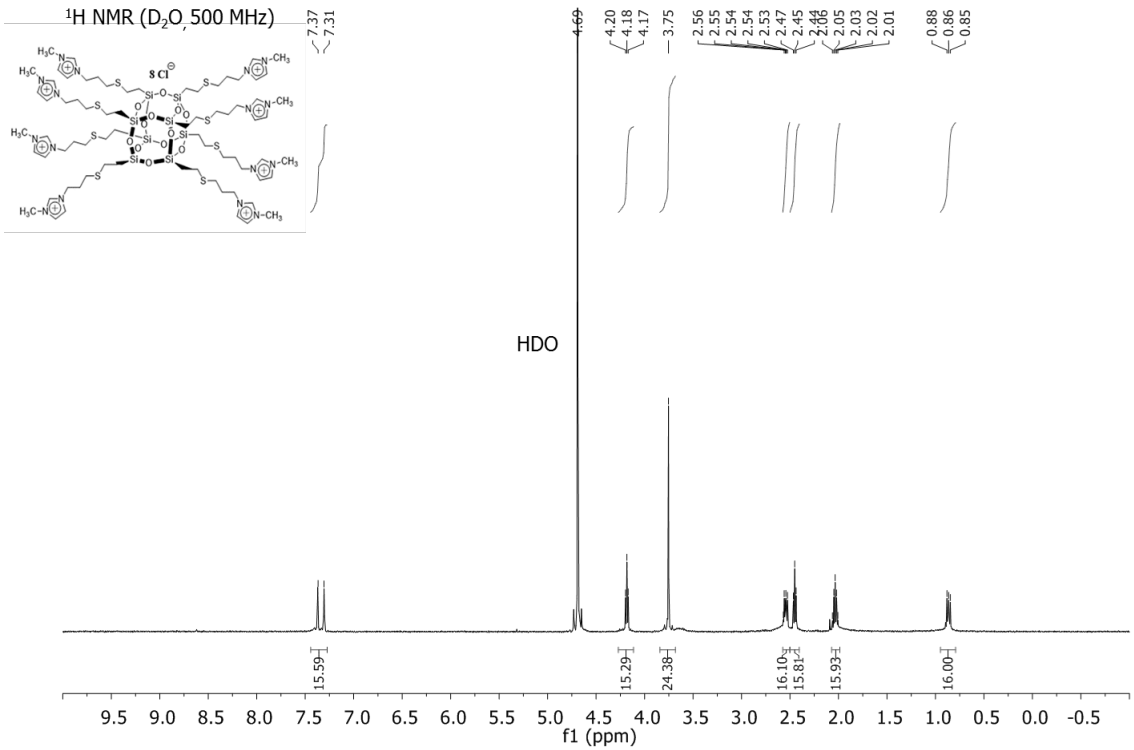

Figure S5: ^{13}C NMR of **POSS-Imi**

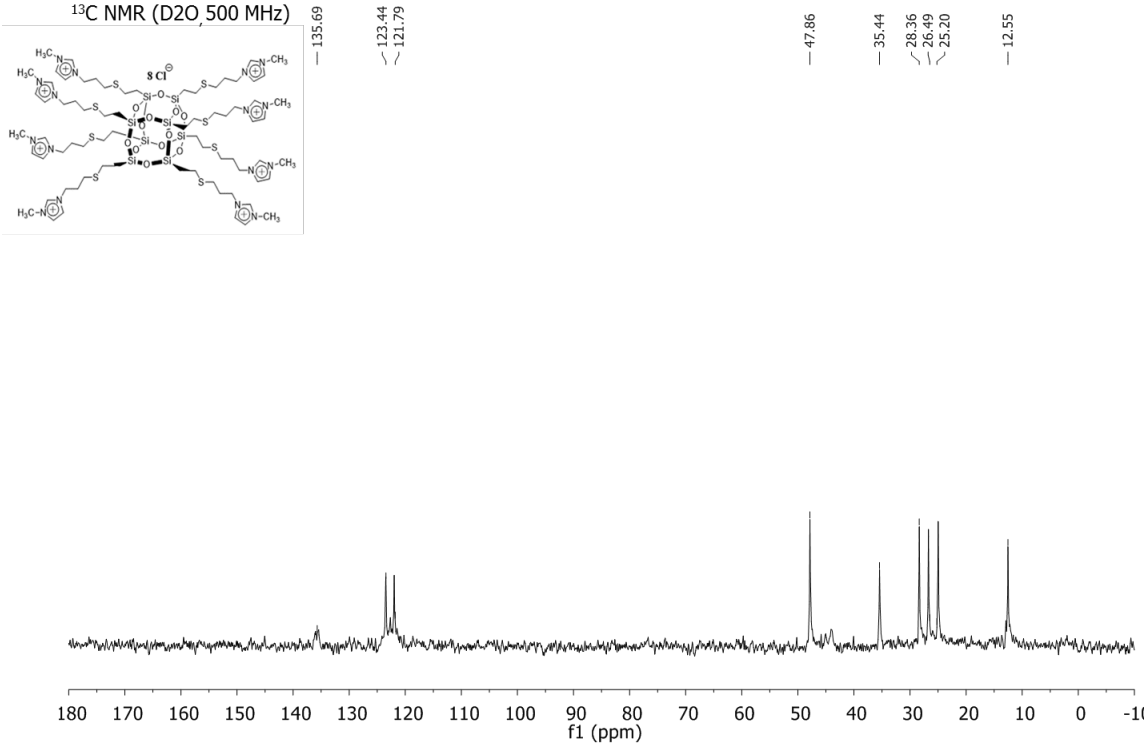

Figure S6: IR spectrum of **POSS-Imi**

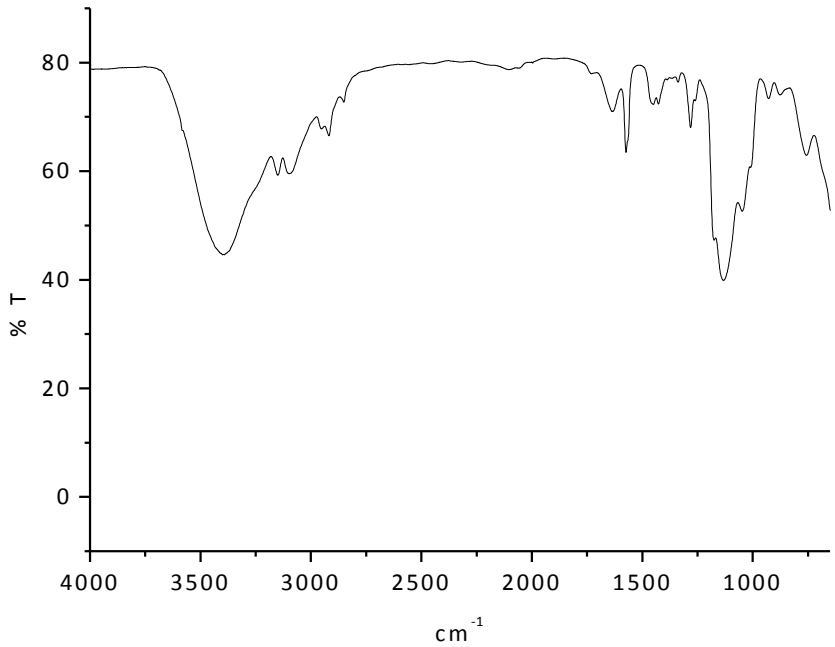

Figure S7: ^{1}H NMR of **POSS-CH$_3$**

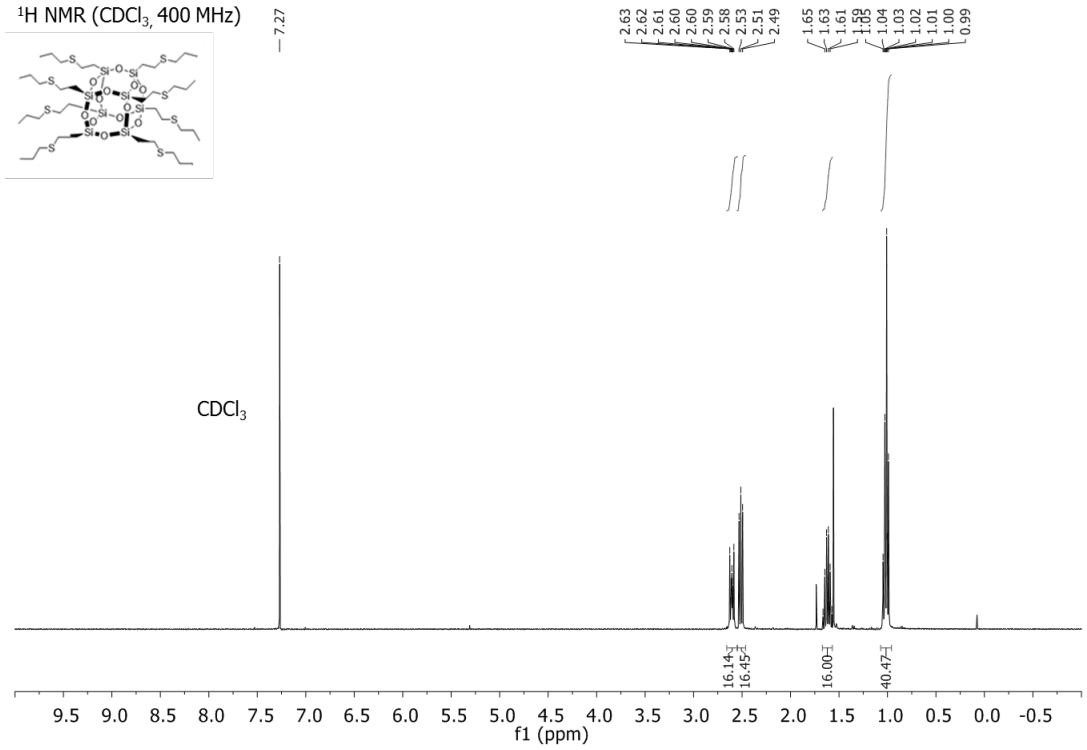

Figure S8: ^{13}C NMR of **POSS-CH$_3$**

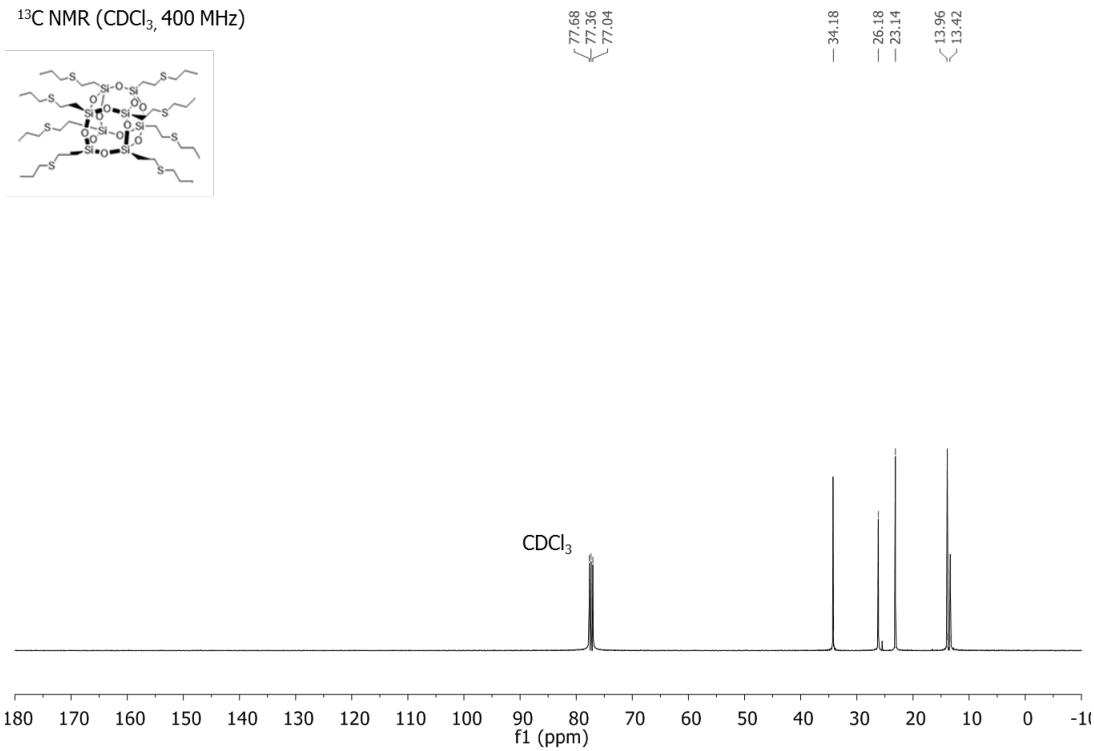

Figure S9: IR spectrum of **POSS-CH$_3$**

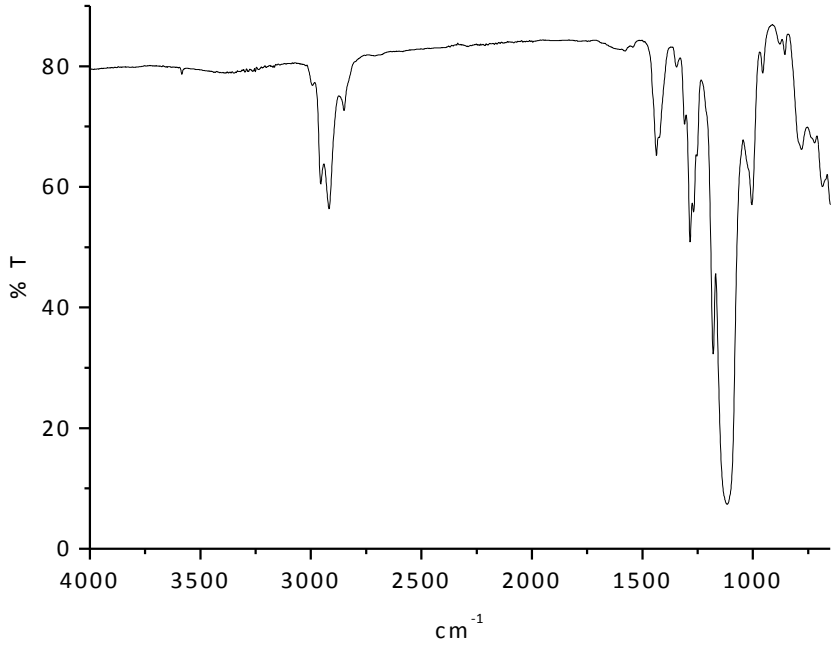

Figure S10: ^{29}Si NMR of **POSS-CH$_3$** in tol-d$_8$ (a), ^{29}Si NMR of **POSS-CH$_3$** in tol-d$_8$ after 48 h at 90 °C with 1-MeImi (24 eq.) (b), ^{29}Si NMR of **POSS-CH$_3$** in tol-d$_8$ after 48 h at 90 °C with bmim-Cl (8 eq.) (c).

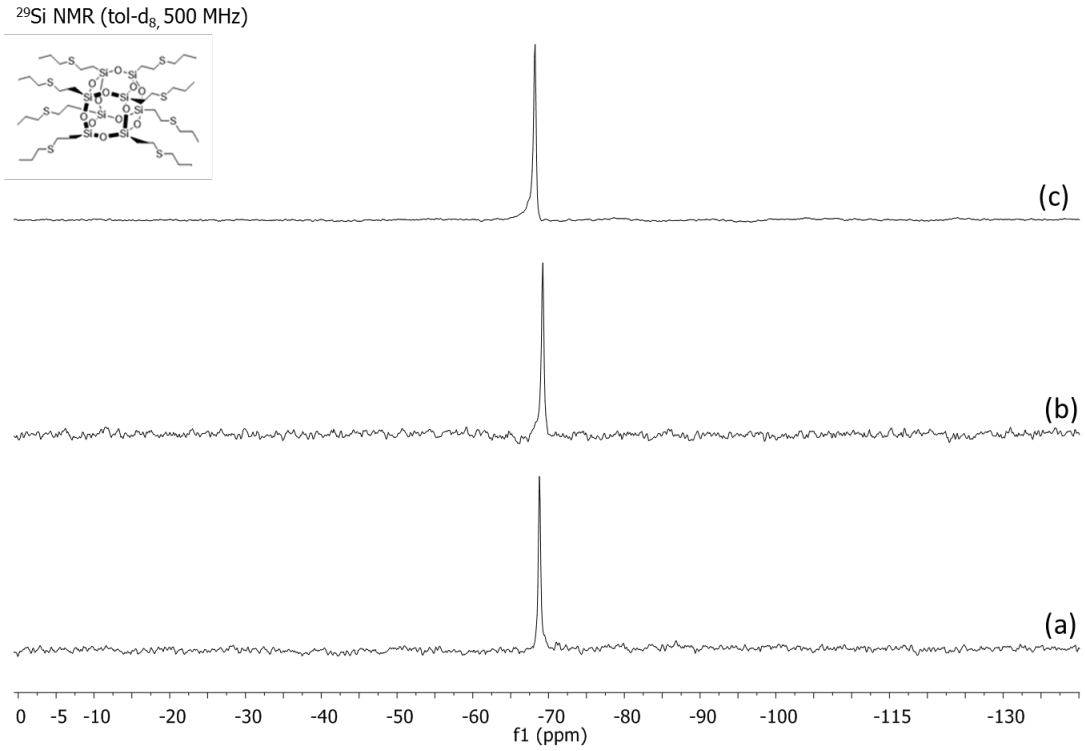

Figure S11: ^{1}H NMR of **styrene glycol**

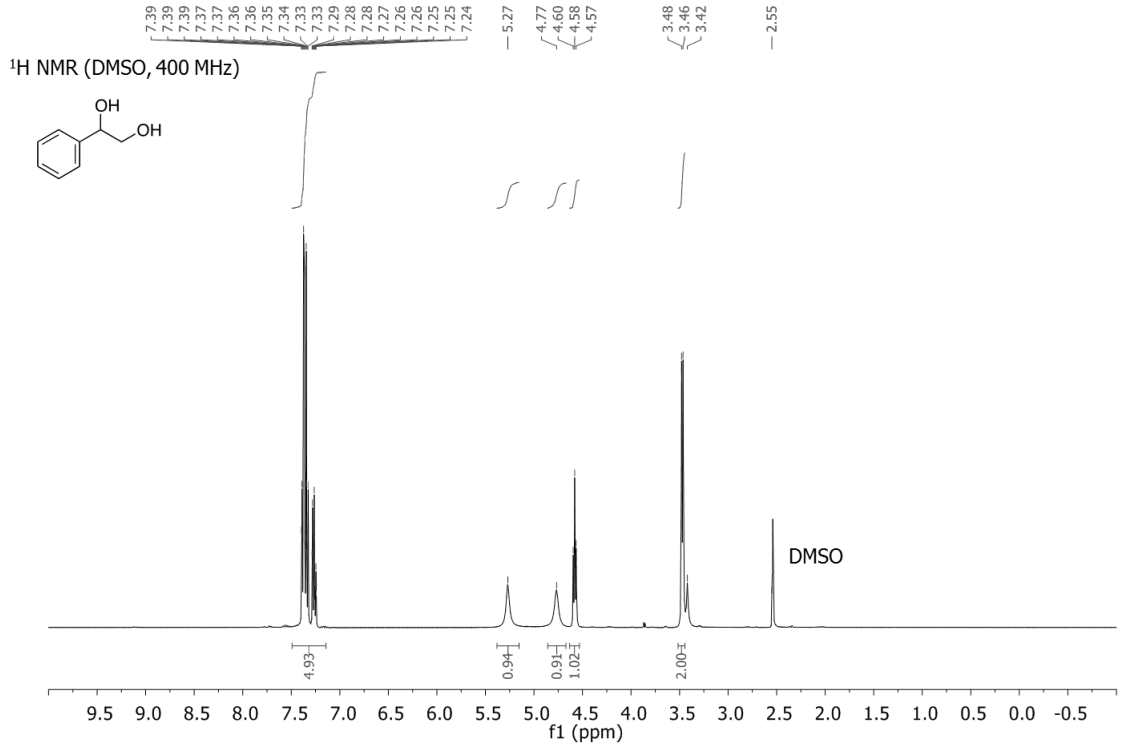

Figure S12: ^{13}C NMR of **styrene glycol**

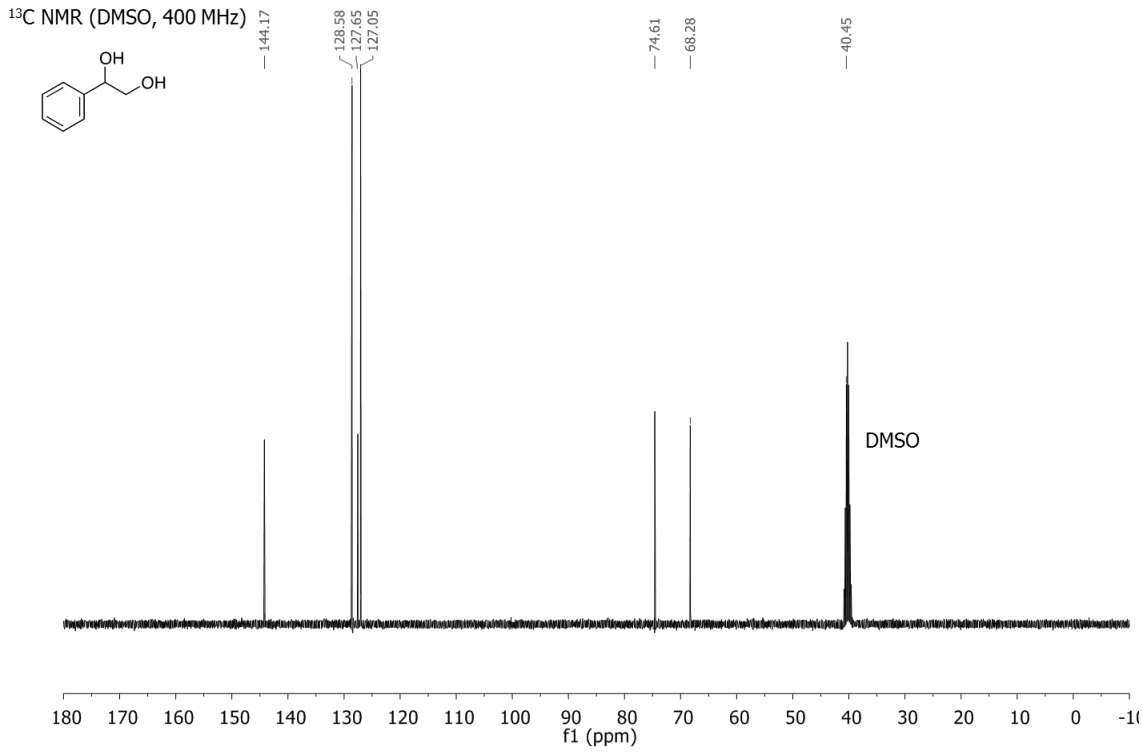

A.4 Supporting Information (SI) Chapter 7

The ^{1}H, ^{13}C and IR spectra of **POSS-Cl** and **POSS-Imi** are reported in the Supporting Information of the Chapter 6.

Figure S1: ^{1}H NMR spectrum of **POSS-Imi-PdCl$_4$**

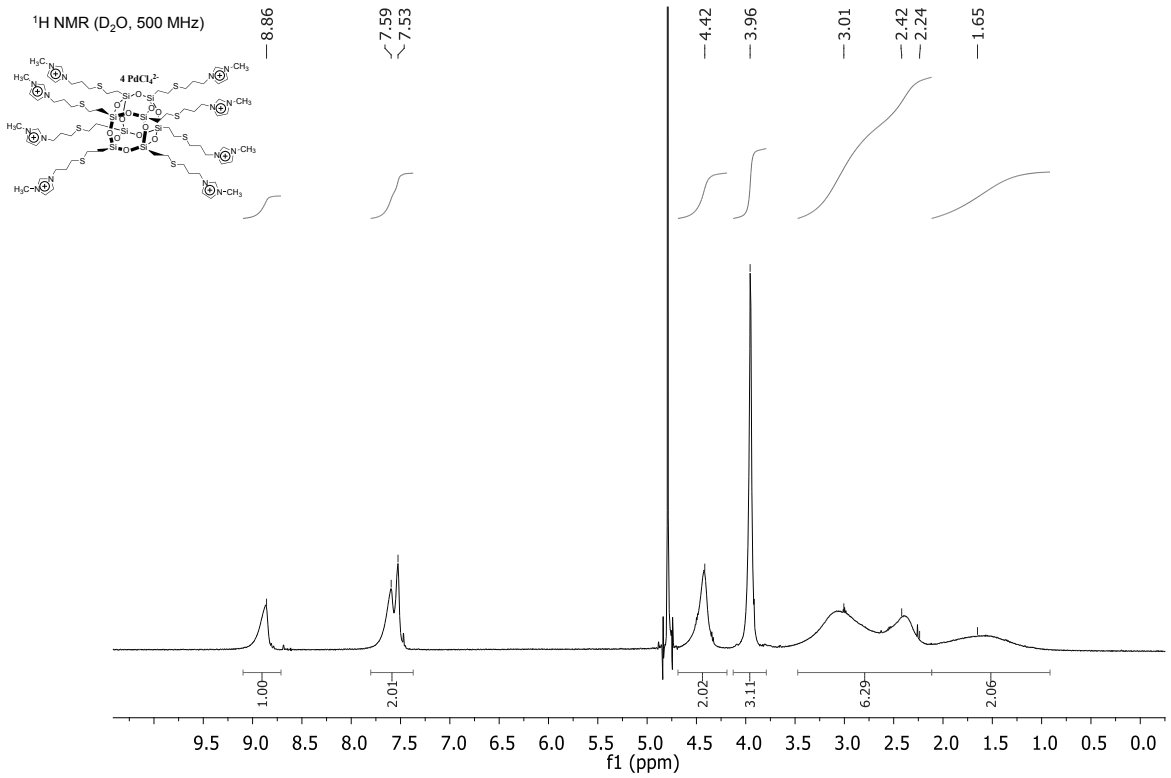

Figure S2: ^{13}C NMR spectrum of **POSS-Imi-PdCl$_4$**

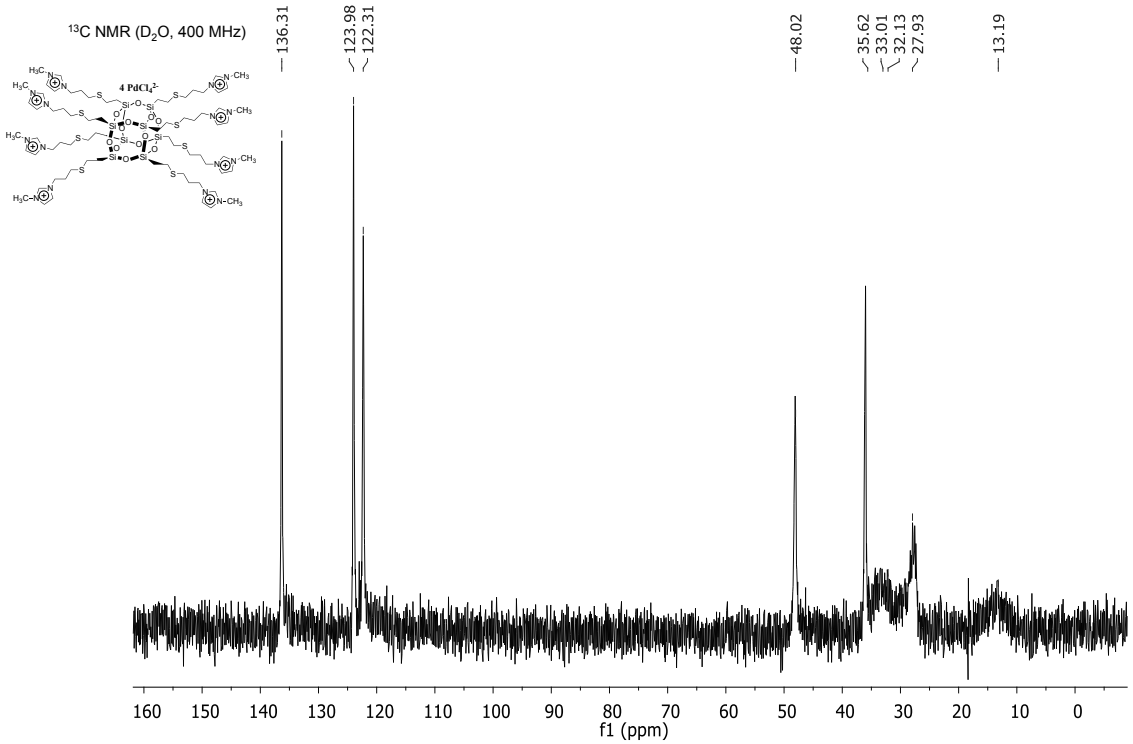

Figure S3: IR spectrum of **POSS-Imi-$PdCl_4$**

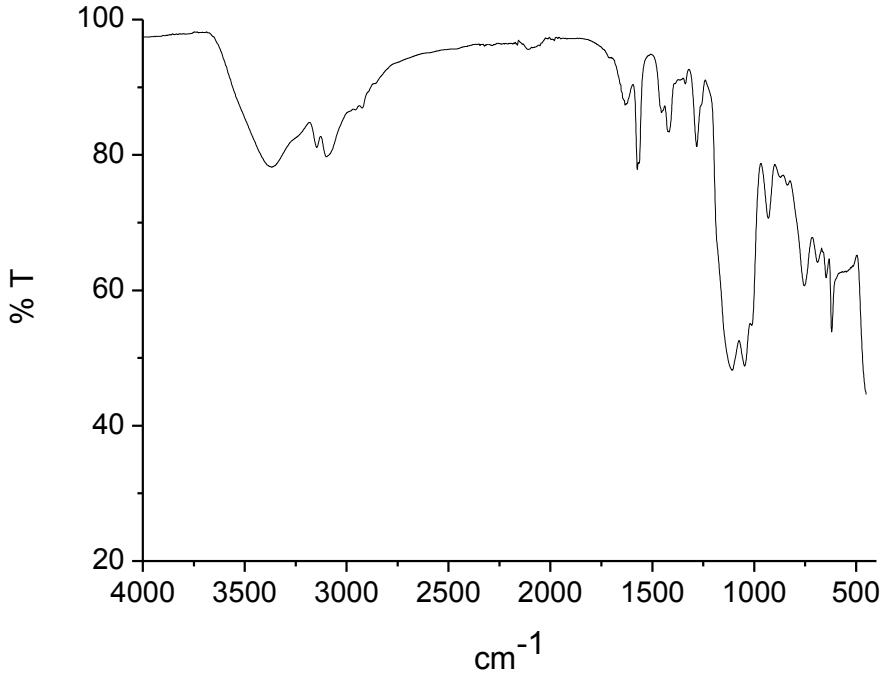

Figure S4: ^{1}H NMR spectrum of **$bmim_2PdCl_4$**

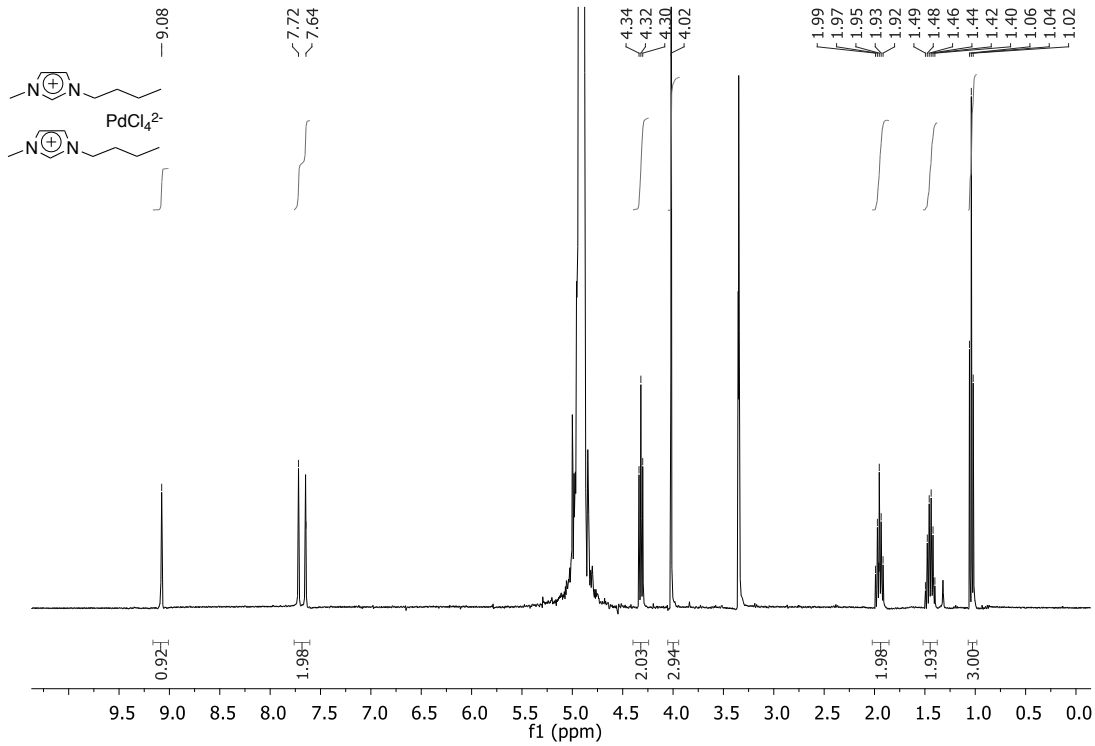

Figure S5: ^{13}C NMR spectrum of **$bmim_2PdCl_4$**

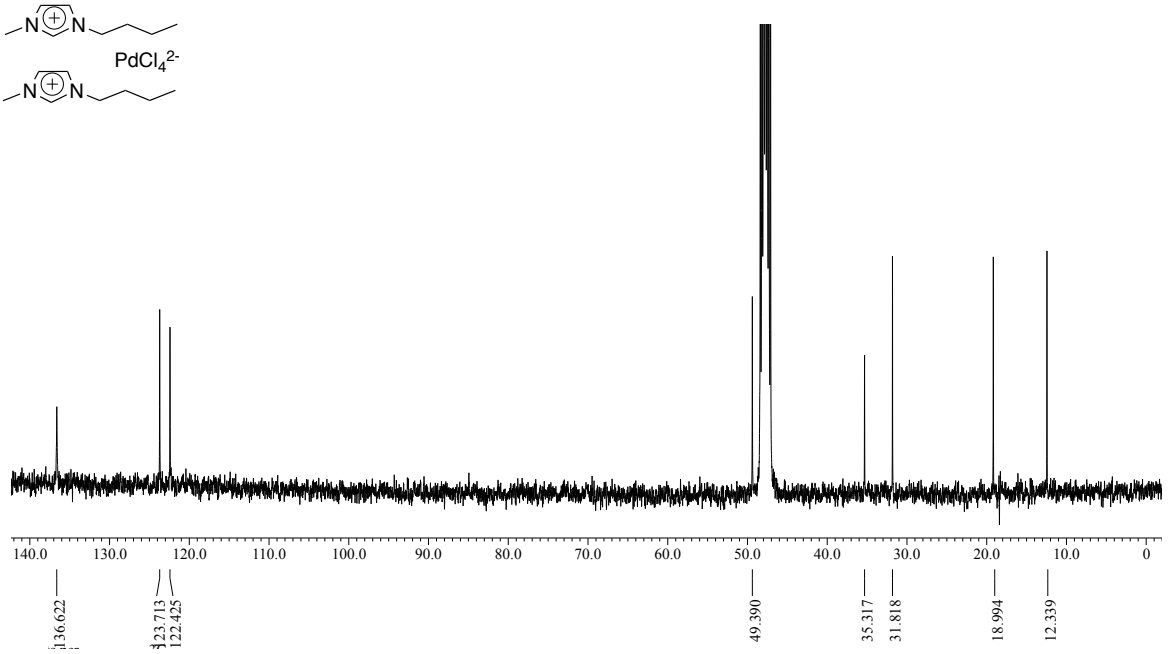

Figure S6: IR spectrum of **$bmim_2PdCl_4$**

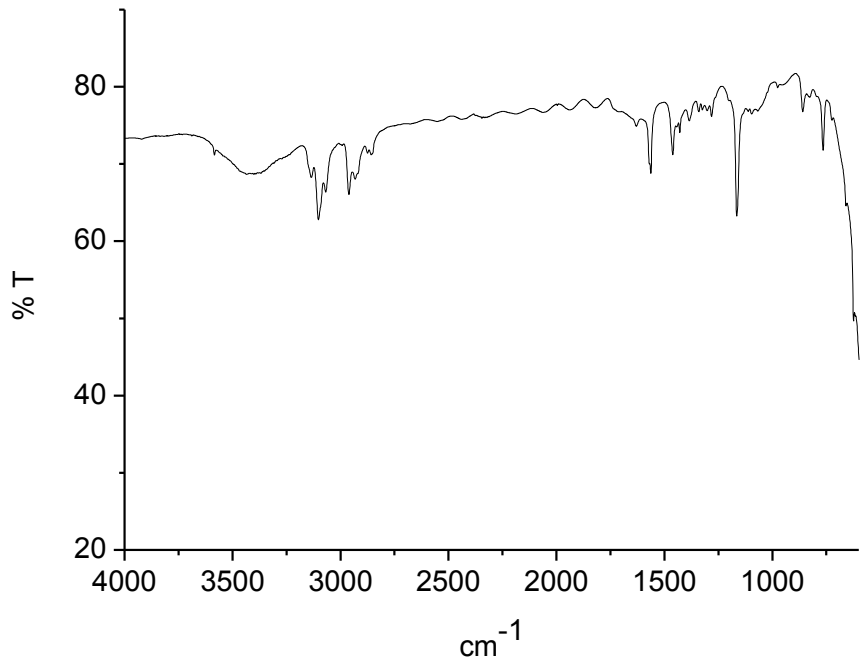

Annex B

List of publications and conferences

B.1 List of publications

This thesis is based on:

1. *Thiazolium-based catalysts for the etherification of benzylic alcohols under solvent-free conditions*
Advanced Synthesis & Catalysis 2015, 357, 800-810.
L. A. Bivona, F. Quertinmont, H.A. Beejapur, F. Giacalone, M. Buaki-Sogo, M. Gruttadauria,* C. Aprile*

* Corresponding authors

2. *Cross-linked Thiazolidine network as support for palladium: a new catalyst for Suzuki and Heck reactions*
ChemCatChem 2015, 7, 2526-2533.
L. A. Bivona, F. Giacalone, L. Vaccaro, C. Aprile,* M. Gruttadauria*

* Corresponding authors

3. *Bridging the gap between homogeneous and heterogeneous catalysis for the synthesis of cyclic carbonates: Imidazolium functionalized single wall carbon nanotubes*
Manuscript in preparation
M. Buaki-Sogo, A. Vivian, L. A. Bivona, M. Gruttadauria, H. Garcia, C. Aprile*

* Corresponding authors

4. *Polyhedral oligomeric silsesquioxane based catalyst for the efficient synthesis of cyclic carbonates*
Catalysis Science & Technology, 2015, 5, 5000-5007.
L. A. Bivona, O. Fichera, L. Fusaro, F. Giacalone, M. Buaki-Sogo,* M. Gruttadauria,* C. Aprile*

* Corresponding authors

5. *Imidazolium tetrachloropalladate based polyhedral oligomeric silsesquioxane: a new pre-catalyst for Suzuki coupling reactions*

Manuscript in preparation

L. A. Bivona, F. Giacalone, E. Lopis-Carbonell, M. Gruttadauria,* C. Aprile*

* Corresponding authors

1.2 Other publications

1. *Palladium Supported on Cross-Linked Imidazolium Network on Silica as Highly Sustainable Catalysts for the Suzuki Reaction under Flow Conditions*

Adv. Synth. Catal. 2013, 355, 2007-2018.

C. Pavia, E. Ballerini, L. A. Bivona, F. Giacalone, C. Aprile,* L. Vaccaro,* M. Gruttadauria*

* Corresponding authors

2. *Evidences of release and catch mechanism in the Heck reactioncatalyzed by palladium immobilized on highlycross-linked-supported imidazolium salts*

Journal of Molecular Catalysis A: Chemical 2014, 387, 57-62.

C. Pavia, F. Giacalone, L. A. Bivona, A. M. P. Salvo, C. Petrucci, G. Strappaveccia, L. Vaccaro, C. Aprile, M. Gruttadauria*

* Corresponding author

B.2 List of conferences, congress and schools

1. *Short Course on Nanostructures probed by intense particle beams (School), Leuven (Belgium) 15-19 April 2013*

Partecipation

2. *Second International Symposium on Advanced Complex Inorganic Nanomaterials (ACIN) Namur (Belgium), 15-19 July 2013*

Poster presentation: Palladium supported on cross-linked imidazolium network on silica as highly sustainable catalysts for the Suzuki reaction.

L. A. Bivona, F. Quertinmont, C. Pavia, F. Bellini, F. Giacalone, L. Vaccaro, C. Aprile, M. Gruttadauria

3. *Société Royale de Chimie (SRC) Congress – Namur – Octobre 2013*

Poster presentation: Synthesis and characterization of thiazolium based materials as multifunctional catalyst

F. Quertinmont, L. A. Bivona, C. Aprile, M.Gruttadauria

4. *6th ORCA (ORganoCAtalysis)-COST meeting, Palerme (Italy) 7-10 May 2014*

Partecipation (organization)

5. *6th ORCA (ORganoCAtalysis)-COST meeting, Palerme (Italy) 7-10 May 2014*

Oral Communication: Novel Thiazolium Based Heterogeneous Organocatalysts for Etherification Reactions

L. A. Bivona, F. Quertinmont, H. A. Beejapur, M. Buaki-Sogo, F. Giacalone, M. Gruttadauria, C. Aprile

6. *14th Anglo-Italian Meeting on Heterocyclic Chemistry, Windsor (England) 29 June – 1 July 2014*

Oral Communication: Thiazolium Salts as Catalysts for Etherification Reactions

L. A. Bivona, F. Quertinmont, H.A. Beejapur, F. Giacalone, M. Buaki-Sogo, M. Gruttadauria, C. Aprile

7. *Société Royale de Chimie (SRC) Congress – Namur – Octobre 2014*

Poster presentation: Novel Imidazolium Based Catalysts for the Chemical Fixation of Carbon Dioxide

O. Fichera, M. Buaki-Sogo, L.A. Bivona, C. Aprile

8. *Journées-Rencontres des Jeunes Chimistes, Namur (Belgium) 2 April 2015*

Oral Communication: Thiazolium-based catalysts for the etherification of benzylic alcohols under solvent-free conditions

L. A. Bivona, F. Quertinmont, H.A. Beejapur, F. Giacalone, M. Buaki-Sogo, M. Gruttadauria, C. Aprile

9. *Thirth International Symposium on Advanced Complex Inorganic Nanomaterials (ACIN) Namur (Belgium), 13-17 July 2015*

Poster presentation: Polyhedral Oligomeric Silsesquioxane Based Catalyst for the Efficient Synthesis of Cyclic Carbonates

L. A. Bivona, O. Fichera, L. Fusaro, F. Giacalone, M. Buaki-Sogo, M. Gruttadauria, C. Aprile

10. *EUROPACAT XII – Catalysis: Balance the use of fossil and renewable resources, Kazan (Russie) 30 August – 5 September 2015*

Poster presentations

10.1: Polyhedral Oligomeric Silsesquioxane Based Catalyst for the Efficient Synthesis of Cyclic Carbonates

L. A. Bivona, O. Fichera, L. Fusaro, F. Giacalone, M. Buaki-Sogo, M. Gruttadauria, C. Aprile

10.2: Thiazolium-based catalysts for the etherification of benzylic alcohols under solvent-free conditions

L. A. Bivona, F. Quertinmont, H.A. Beejapur, F. Giacalone, M. Buaki-Sogo, M. Gruttadauria, C. Aprile

11. *EUROPACAT XII – Catalysis: Balance the use of fossil and renewable resources, Kazan (Russie) 30 August – 5 September 2015*

Oral Communication: Novel Imidazolium Based Catalyst for the Chemical Fixation of Carbon Dioxide

L. A. Bivona, O. Fichera, L. Fusaro, F. Giacalone, M. Buaki-Sogo, M. Gruttadauria, C. Aprile

Partecipations in seminars, courses and supervisior of master students in the University of Namur and in the University of Palermo.